Republic of Iraq
Ministry of Higher Education
and Scientific Research
Babylon University / College of Engineering
Civil Engineering Department

Structural Behavior of Pre - Loaded Reinforced Concrete Columns Under Effect of Cyclic Fire Exposure

A Thesis
Submitted to the College of Engineering at the University of Babylon in Partial Fulfillment of the Requirements for the Degree of Master of Science in Engineering / Civil Engineering
(Structures)

By

Nuha Shakir Kadhum Al-awiady

Supervised by

Prof. Dr. Ammar Yasser Ali Al-janabi

2023 A.D. 1444 A.H.

بِسْمِ اللَّهِ الرَّحْمَٰنِ الرَّحِيمِ

قَالُوا سُبْحَانَكَ لَا عِلْمَ لَنَا إِلَّا مَا عَلَّمْتَنَا ۖ إِنَّكَ أَنْتَ الْعَلِيمُ الْحَكِيمُ ﴿٣٢﴾

صدق الله العلي العظيم

سورة البقرة (الآية 32)

Dedication:-

To the source of knowledge and wisdom, Muhammad and the family of Muhammad, the best prayers and peace be upon them

To the one who left me in body and did not leave me in spirit

To whose shadow was a home in the hardships of life

To whom I miss her joy in my joy

(My tender mother, may God have mercy on her soul)

To the one who taught me how to stand in front of the odds

To the meaning of friendliness and tenderness

To the one who wished to see me at this moment and did not see me

(My kind father, may God have mercy on him)

Researcher

Nuha Shakir Kadhim

Acknowledgments

In the name of God, the most gracious, the most merciful

All thanks and praise be to God who enabled me to accomplish this research work.

First, I would like to express my sincere gratitude to my supervising professor, **Dr. Ammar Yasser Ali**, for his insight, wisdom, and guidance. I really owe him.

I would like to thank the support staff of the Department of Civil Engineering at the University of Babylon for their assistance in daily matters throughout my postgraduate academic life. I also thank the technical staff of the structural laboratories for their assistance during the implementation of my pilot programmer.

I would like to thank the Directorate of Civil Defense / Babel Branch for providing us with the information

I would like to thank researcher (**Samah Adnan**) for constructed loading frame ,it is important part for study work

I would like to applaud the friendly support and assistance of my fellow graduate students who have made my overall experience more satisfying.

Finally, special thanks and gratitude to my family for their care and patience, and in particular: my parents and siblings who have been by my side throughout this entire endeavor. Without their love, encouragement and support I would not have been able to complete this academic achievement.

Nuha Shakir Kadhim

2023

Abstract

The purpose of this thesis is to investigate the structural behavior of eccentric pre-loaded reinforced concrete columns under exposure to cycles of burning , through evaluation of load –displacement response, ultimate load ,cracking load ,as well as cracking pattern and failure modes .

The experimental program included testing eighteen column specimens: fifteen columns were made of normal strength concrete ,and three columns were made of high strength concrete. One of column specimens was selected as a pilot column and seventeen columns were subdivided into five groups to study the effects of: (number of fire exposure cycles, temperate target for each cycle, time duration of each fire exposure cycle, eccentricity ratio of pre-load , longitudinal reinforcement ratio, type of concrete (high strength concrete (HSC) or normal strength concrete (NSC)), in addition to evaluation of adopted strengthening techniques by replacement the outer damaged shell of normal strength concrete (NSC) with Carbon Fiber Reinforcement Plastics (CFRP) laminates or utilizing Reactive Powder Concrete (RPC)). All the column specimens have same dimensions of cross section (150X150)mm and effective length (700) mm, and tested under eccentric load with eccentricity ratio, (e/h =0.5) through cyclic fire exposure.

From experimental results showed that the cracking and ultimate load capacity decrease with increasing number of cycles about (47)%,(56)% and (20)% ,(25)%, , for (two cycles and four cycles) respectively. The cracking and ultimate load capacity decrease with increasing temperature target from (400C˚ to 600C˚) of cycle about (74)% and (36)%, respectively for (four cycles), as well the cracking and ultimate load capacity decrease with

increase time duration of each fire exposure cycle (52)%, (63)% and (23) % ,(28)%, respectively for (one cycles and four cycles). while with the decreased eccentricity ratio (e/h) from(0.5 to 0), the ultimate load increasing about(83 to 86) % and (55 to 65)%, for (two cycles and four cycles) respectively.

Also, reducing longitudinal steel ratio lead to decrease, the cracking and ultimate load capacity about (53 to 67) % and (22 to 29)%, respectively for (two cycles and four cycles). For column specimens made of HSC, the cracking and ultimate load capacity increase about (60 to 72) % and (25 to 32)%, respectively for (two cycles and four cycles).

For repair of fire exposed column specimens by replacement the damaged external shell of (normal strength concrete (NSC) with Carbon Fiber Reinforcement Plastics (CRFP) laminate or Reactive Powder Concrete (RPC)) lead to an improvement in the cracking and ultimate load capacity ,about (36 and 63) % ,and (34 and 100)%, respectively when compared with the specimen control . That means that second method is more active and superior.

Numerical results were compared with the obtained experimental results in terms of load-deformation response, ultimate load, and cracking propagation. The results of the finite element model indicated reasonable agreement with the experimental results and the difference in the cracking and ultimate load of about (14.0)% and (3.2%) as average, respectively.

A parametric study included the effects of various parameters: the compressive strength of external RPC shell, and eccentricity ratio of post-fire load. With regard to the compressive strength of external RPC shell of

(200)MPa, the numerical results showed an obvious change in the performance where failure mode out the repaired region , as well as enhancement load and ultimate load about (1.75)%. Also, increasing eccentricity ratio (e/h) from (0.25 to 0.75),led to decreasing the ultimate load about (55, 25)%, respectively.

List of Contents

Subject	Page
Abstract	II
List of Contents	VII
List of Tables	XII
List of Figures	XIV
List of Plates	XVIII
Notation	XX
Abbreviations	XXIII
Chapter One: Introduction	
1.1 General	1
1.2 Column Definition	3
1.2.1Types of Columns in Building Construction	3
1.2.2 Behavior and Ultimate Strength of columns	4
1.2.3 Slenderness Ratio	5
1.2.4 Concrete Protective Cover	6
1.3 Column Behavior Under Fire Exposure	6
1.4 High-Strength Concrete	8
1.5 Repair and Strengthening of Fire-Damaged Reinforced Concrete	10
1.5.1 Reactive Powder Concrete (RPC)	10
1.5.1.1 Composition of Reactive Powder Concrete	12
1.5.1.2 Mechanical Performance and Durability of RPC	12
1.5.2 Fiber Reinforced Polymer (FRP)	13
1.6 Objective and aims the Present Work	16
1.7 Layout of the Thesis	18
Chapter Two: Literature Review	
2.1 Introduction	19
2.2 Studies on Behavior of Unloaded Fire Exposed RC Columns	20
2.3 Studies on Behavior of Pre-Loaded Fire Exposed RC Column	31
2.4 Studies on Strengthening of Fire Damaged Columns	47
2.5 Summary and Concluding Remarks	58
Chapter Three: Experimental Work	
3.1 Introduction	60
3.2 Test Program	60
3.2.1. Designation of Column Specimens	62

3.2.2 Description of Tested Columns	63
3.2.3. General description of specimen Groups	66
3.3 Properties of Construction Materials	68
3.3.1. Cement	69
3.3.2 Fine Aggregate (Sand).	70
3.3.3 Coarse Aggregate (Gravel)	71
3.3.4 Silica Fume	71
3.3.5 Steel Fibers	72
3.3.6 Admixture (Superplasticizer)	73
3.3.7 Steel Reinforcing bars	74
3.3.8 CFRP products	75
3.3.9 Epoxy Resin	76
3.3.10 Epoxy Adhesive	77
3.4 Concrete Mix Design	78
3.4.1 Normal Strength Concrete (NSC)	78
3.4.2 High Strength Concrete (HSC)	78
3.4.3 Reactive Powder Concrete (RPC)	79
3.4.4 Mixing Procedure	80
3.5 Preparation of Test Specimens	81
3.5.1 Molds Preparation	81
3.5.2 Casting Equipment	82
3.5.3 Casting procedure	84
3.5.4 Curing	86
3.6 Tests of Hardened Concrete	87
3.6.1 Destructive Tests	87
3.6.1.1 Compressive Strength Test	87
3.6.1.2 Modulus of Rupture (Flexural Strength) Test	87
3.6.1.3 Splitting Tensile Strength Test	88
3.6.2 Non-Destructive Test	90
3.7 Fire Flame Stove and Equipment	93
3.7.1 Brick Stove	95
3.7.2 Thermocouple	97
3.7.3 Digital Temperature Controller	99
3.7.4 Electrical Gas Regulator and Ignition-Burning System	100
3.7.5 Loading Frame	101
3.7.6 Hydraulic jacking	103
3.7.7 Load Cell	104

3.8 Drying of Specimens before Fire Exposure	105
3.9 Scenario of Fire Exposure	106
3.10 Scenario of Cyclic Fire Exposure	108
3.10. 1 One cycle of fire exposure with load (F2,F4).	109
3.10.2 Two cycles of fire exposure with load (F1)	109
3.10.3 Four cycles of fire exposure with load (F3, F5, F6)	109
3.11 Repair of The Fire Exposed Columns Specimens	111
3.12 Test Procedure and Instrumentations	117
3.12.1 Testing Machine	117
3.12.2 Download and Support Terms	118
3.12.3 Instrumentations	119
3.12.4 Test Setup	122
Chapter Four: Experimental Results and discussion	
4.1Introduction	124
4.2 Mechanical Properties of Control Specimens	124
4.2.1. Destructive Test Results	124
4.2.2 Non- Destructive Test Results	127
4.2.3 Evaluation of Concrete Mechanical Properties of columns	127
4.3 General Response of Tested Column Samples	131
4.3.1 Pilot Column	134
4.3.2 Test Results of Columns (Group I)	134
4.3.2.1 Control Column	134
4.3.2.2 Columns with Cyclic Fire Exposure	136
4.3.3 Test Results of Columns (Group II)	148
4.3.4 Test Results of Columns (Group III)	152
4.3.5 Test Results of Columns (Group IV)	157
4.3.6 Strengthened Specimens after Cyclic Fire Exposure (Group V)	163
4.4 Ductility Index	168
4.5 Stiffness Parameter	171
4.6 Crack Width and Cracking Pattern	173
4.7 Concrete Strains	175
4.8 Effect of Considered Variables	177
4.8.1 Number of Fire Exposure Cycles	177
4.8.2 Temperate target for each cycles	177
4.8.3 The time duration of each fire exposure cycles	178
4.8.4 Pre-load Eccentricity	178
4.8.5 Role of longitudinal the Steel Reinforcement Ratio for columns	179
4.8.6 Type of Concrete (HSC,NSC) for Columns	180
4.8.7 Evaluation of Adopted Strengthening Techniques	180

Chapter Five: Finite Element Analysis Method	
5.1 Introduction	182
5.2 Types of Element	183
5.3 Material Properties	184
5.4 Convergence Study	184
5.5 Modeling of Column Specimens	186
5.5.1 Elements and Assembly	186
5.5.2 Loading and Boundary Conditions	187
5.6 Numerical Analysis Results and Discussion	188
5.6.1 Numerical Results of Control Columns (Without Cyclic Fire Exposure)	192
5.6.2 Numerical Results of cyclic Fire Exposed Columns	196
5.6.3 Numerical Results of Strengthened Columns(GroupV)	210
5.7 Parametric Study	212
5.7.1 Compressive Strength of External RPC Shell	212
5.7.2 The Eccentricity of Post-Fire Load	214
5.7.3 Length of Column (Slenderness Ratio)	215
Chapter Six: Conclusion and Recommendations	
6.1 Introduction	217
6.2 Conclusions from Experimental Work	217
6.3 Conclusions from Analytical Study	222
6.4 Recommendations for Future Researches	223
References	
Appendix A	
Appendix B	
Appendix C	
Appendix D	

List of Tables

No.	Title of Table	Page
	Chapter One	
1-1	Main steps for producing reactive powder concrete	12
1-2	Comparison of RPC 200 and RPC 800	13
1-3	Comparison of HPC (80 MPa) and RPC 200	13
1-4	Durability of RPC compared to HPC	13
	Chapter Three	
3-1	Details of the tested columns Specimens.	62
3-2	Chemical properties of cement.	69
3-3	Cement Physical Properties.	70
3-4	Sieve analysis of sand	70
3-5	Physical and Chemical Properties of Fine Aggregate.	71
3-6	Sieve analysis of gravel	71
3-7	Results of Silica Fume Tests	72
3-8	Properties of The Steel Fibers.	73
3-9	Technical description of SikaViscocrete-5930	74
3-10	Properties of Reinforcement Steel Bars	75
3-11	Properties of Carbon Fiber Reinforcement Plastics Sheets (CFRP)	76
3-12	Technical properties of bonding materials	78
3-13	Proportions of Concrete Mixes (Normal Strength Concrete)	78
3-14	Proportions of Concrete Mixes (High Strength Concrete)	79
3-15	Proportions of Concrete Mixes (Reactive Powder Concrete)	80
	Chapter Four	
4-1	Mechanical properties of the control samples and hardened concrete	125-126
4-2	Mechanical properties of the control samples (RPC and NSC)	126
4-3	Experimental results of the tested column specimens	133
4-4	Ductility index of tested columns	169
4-5	Stiffness parameter of tested columns	171-172
4-6	Measured Crack Width of the Tested Columns	174
	Chapter Five	
5-1	Comparation of Numerical and Experimental Results for ultimate load ,cracking load and service displacement.	189-190
5-2	Numerical and Experimental results of the ductility index	190-191
	Appendix D	
D-1	the input data for concrete plasticity properties and CFRP material properties	D-8

List of Figures

No.	Title of Figure	Page
	Chapter One	
1-1	Types of reinforced concrete columns	4
1-2	Concrete column interaction diagram	5
1-3	Concrete protective cover	6
1-4	Stress-Strain Curves for Cylinders of Concrete Subjected to Uniaxial Compression	10
	Chapter Two	
2-1	Furnace construction and columns	23
2-2	Details of Reinforcement and Gradually Cooling for Column Samples	26
2-3	The full details of the stove and equipment	27
2-4	System installation in the furnace	28
2-5	Illustrates the Stove Equipment	29
2-6	Burning process	30
2-7	Different load eccentricities under 1-, 2-, and 3-face heating	32
2-8	load eccentricities under one face heating	33
2-9	Fire test setup configuration and design fire scenarios	42
2-10	The furnace and other equipment and The burner network with a steel box	45
2-11	Dimensions and reinforcing bars of specimens	48
	Chapter Three	
3-1	Designation Symbol of Tested Specimens	63
3-2	Geometry of column(side view and front view)	64
3-3	Dimension and Reinforcement Details of Tested Columns :a :for Groups(1,2,4 and 5),b: for (Group 3).	65
3-4	Details of Tested columns Fire Exposure	68
3-5	Details and Fabrication of Molds	81
3-6	Details of the Loading Frame with Stove	102
3-7	ASTM E119 Temperature Curve	108
3-8	Scenarios of Cyclic Exposure to Fire	110
	Chapter Four	
4-1	Effect of fire exposure and pre-load on mechanical properties of concrete column specimens.	129-130
4-2	The Load- displacement curves for specimen (C1).	135
4-3	The load-deflection curves for specimens (C1, C2, andC3).	137
4-4	The Load- displacement curves for specimen (C1, C4 and C5).	141

4-5	The Load- displacement curves for specimen (C_1, C_3 and C_5).	143
4-6	The Load- displacement curves for specimen (C_1, C_4 and C_6).	146
4-7	The Load- displacement curves for specimen (C_1 , C4 and C7).	147
4-8	The Load- displacement curves for specimens (C_2,and C_8).	149
4-9	The Load- displacement curves for specimen (C_2,and C_8).	151
4-10	The Load- displacement curves for specimen (C_1,and C_{10}).	153
4-11	The Load- displacement Curves for Specimen (C_2,C_{10} and C_{11}).	155
4-12	The Load- displacement Curves for Specimen ($C_{13,}$ C_{14} and C_{15})	158
4-13	The Load- displacement Curves for Specimen (C_1, C_4 andC_{16}).	165
4-14	The Load- displacement Curves for Specimen (C_1,C_4 andC_{17})	167
Chapter Five		
5-1	C3D8, T3D2 and S4R elements used to model by ABAQUS.	183
5-2	The considered meshes for the column specimens.	185
5-3	The convergence study.	185
5-4	modeling of column specimens	186-187
5-5	Representation (simulation) of applied loads and boundary conditions of modeled column.	188
5-6	The Load- displacement curves for specimen (C_1).	194
5-7	The Load- displacement curves for specimen (C_{10}).	194
5-8	The Load- displacement curves for specimen (C_{13}).	195
5-9	plastic strain and failure modes for control columns specimens (C_1,C_{10}, C_{13}).	195-196
5-10	The Load- displacement curves for specimen (C_2).	198
5-11	The Load- displacement curves for specimen (C_4).	198
5-12	The Load- displacement Curves for Specimen (C_3).	199
5-13	The Load- displacement Curves for Specimen (C_5).	199
5-14	plastic strain and failure modes for columns specimens (C_2,C_3,C_4, C_5)	200
5-15	The Load- displacement curves for specimen (C_6).	201
5-16	Damage Compression and failure modes for columns specimens ($C_3$and C_5)	202
5-17	The Load- displacement Curves for Specimen (C_7)	203
5-18	Damage Compression and failure modes for control column specimen (C_7).	203
5-19	The Load- displacement Curves for Specimen (C_8)	204
5-20	The Load- displacement Curves for Specimen (C_9)	205
5-21	Damage Compression and failure modes for columns specimens.	205
5-22	The Load- displacement Curves for Specimen (C11)	206

5-23	The Load- displacement Curves for Specimen (C_{12})	207
5-24	Damage Compression and failure modes for columns specimens (C_{11},C_{12}).	207
5-25	The Load- displacement Curves for Specimen (C_{14})	208
5-26	The Load- displacement Curves for Specimen (C_{15})	209
5-27	Damage Compression and failure modes for columns specimens (C_{14},C_{15}).	209
5-28	The Load- displacement Curves for Specimen (C_{16}).	211
5-29	The Load- displacement Curves for Specimen (C_{17}).	211
5-30	Damage Compression and failure modes for columns specimens (C_{16},C_{17})	212
5-31	The Load- displacement Curves for Specimen (C_{17})	213
5-32	Damage Compression and failure modes for column specimen (C_{17})	213
5-33	The Load- displacement Curves for Specimen (C_4)	214
5-34	Damage Compression and failure modes Different Eccentricity Ratio For (C_4)	164
5-35	The Load- displacement Curves different Slenderness Ratio for C_4.	216
5-36	Damage Compression and Failure Modes for Different Slenderness Ratio for C4	216
	Appendix A	
A-1	Cross-Section of Column (G1,G2,G4 ,G5)	A1
A-2	Cross-Section of Column (G3)	A2
A-3	Cross-Section of Corbel for Column	A11
	Appendix C	
C-1	Concrete Strain Distribution for Columns (C1)	C1
C-2	Concrete Strain Distribution for Columns (C2)	C1
C-3	Concrete Strain Distribution for Columns (C3)	C2
C-4	Concrete Strain Distribution for Columns (C4)	C2
C-5	Concrete Strain Distribution for Columns (C5)	C3
C-6	Concrete Strain Distribution for Columns (C6)	C3
C-7	Concrete Strain Distribution for Columns (C7)	C4
C-8	Concrete Strain Distribution for Columns (C8)	C4
C-9	Concrete Strain Distribution for Columns (C9)	C5
C-10	Concrete Strain Distribution for Columns (C10)	C5
C-11	Concrete Strain Distribution for Columns (C11)	C6
C-12	Concrete Strain Distribution for Columns (C12)	C6
C-13	Concrete Strain Distribution for Columns (C13)	C7
C-14	Concrete Strain Distribution for Columns (C14)	C7
C-15	Concrete Strain Distribution for Columns (C15)	C8
C-16	Concrete Strain Distribution for Columns (C16)	C8

C-17	Concrete Strain Distribution for Columns (C17)	C9
	Appendix D	
D-1	Yield surface in plane stress reproduced from	D2
D-2	Uniaxial tensile behavior of concrete	D3
D-3	Uniaxial compressive behavior of concrete reproduced	D3
D-4	Hyperbolic plastic flow rule reproduced	D5
D-5	+Stress-Strain Curves for Both Horizontally and Vertically Cast Prisms with and without Fiber Under Uniaxial Compression	D6

List of Plates

No.	Title of Plate	Page
	Chapter One	
1-1	Concrete column damaged by fire	8
1-2	Applications of Reactive Powder Concrete	11
1-3	Wet lay-up confining system	15
1-4	Confining system based on prefabricated FRP elements	16
1-5	Automated RC column wrapping	16
	Chapter Two	
2-1	burning process and load applied	46
2-2	FRP strengthened square RC column (a) before and (b) after fire testing	48
2-3	FRP wrapped and insulated concrete column (a) before fire test, and (b) immediately after fire test	49
2-4	(a) Columns before heating; (b) columns after heating	50
2-5	application of CFRP on column	51
2-6	Cross-sectional details of retrofitted column	56
2-7	Steps for repairing damaged RC column.	57
2-8	repairing damaged RC column	58
	Chapter Three	
3-1	Silica Fume	72
3-2	Micro Steel Fibers	73
3-3	SikaViscocrete-5930.	74
3-4	Testing Machine of Steel Reinforcing Bars	75
3-5	CFRP Laminates	76
3-6	Mixing Two Components of Epoxy Resin	77
3-7	Two components epoxy adhesive Nitobond EP.	77
3-8	Mixing equipment’s and specimens control	82
3-9	Preparation of Test Specimens	83-84
3-10	Stages of casting operation.	85
3-11	Curing of Columns and Control Specimens	86
3-12	The compressive strength test for cube.	87
3-13	The Flexural Strength Test (Modulus of Rupture).	88
3-14	The splitting tensile strength test.	89
3-15	Ultrasonic pulse transit time tester.	91
3-16	The full details of the stove and equipment	93
3-17	Details of the brick stove.	95
3-18	Burner network.	96

3-19	Stove cover.	96
3-20	Details Thermocouple Type (K).	98
3-21	Details of Gas Preparation	100
3-22	Digital temperature controller details	100
3-23	Electrical Gas Regulator	101
3-24	Hydraulic Jacking	103
3-25	load cell	105
3-26	Drying process before burning procedure.	106
3-27	Cracks and spalling of the fire exposed test with (30% Pu) pre-load.	111
3-28	Repairing of the damaged external shell	113-114
3-29	Measuring of concrete Strength by UPV ,and applying Epoxy Resin	115
3-30	Casting of New Concrete (RPC) and (NSC) for External Shell	116
3-31	Applying epoxy adhesive (Sikadur-330) and (CFRP) for column(C_{16})	116
3-32	Details of the Loading and Supports	118-119
3-33	Instruments used in testing columns.	120
3-34	Column Specimen through the testing procedure	124
	Chapter Four	
4-1	Failure mode and crack pattern of column specimen C_1.	135
4-2	Failure mode and crack pattern of column specimen C_2.	137
4-3	Failure mode and crack pattern of column specimen C_3.	139
4-4	Failure mode and crack pattern of column specimen C_4.	141
4-5	Failure mode and crack pattern of column specimen C_5.	143
4-6	Failure mode and crack pattern of column specimen C_6.	145
4-7	Failure mode and crack pattern of column specimen C_7.	148
4-8	Failure mode and crack pattern of column specimen C_8.	150
4-9	Failure mode and crack pattern of column specimen C_9.	152
4-10	Failure mode and crack pattern of column specimen C_{10}.	153
4-11	Failure mode and crack pattern of column specimen C_{11}.	155
4-12	Failure mode and crack pattern of column specimen C_{12}.	157
4-13	Failure mode and crack pattern of column specimen C_{13}.	159
4-14	Failure mode and crack pattern of column specimen C_{14}.	160
4-15	Failure mode and crack pattern of column specimen C_{15}.	162
4-16	Failure mode and crack pattern of column specimen C_{16}.	165
4-17	Failure mode and crack pattern of column specimen C_{17}.	168

Notation

The major symbols used in this thesis are listed below; the others are defined as they first appear.

Symbol	Definition	Unit
A_b	Area of reinforcement bar.	mm^2
A_c	Net area of concrete section.	mm^2
A_g	Gross area of concrete section.	mm^2
A_s	Area of longitudinal tension reinforcement.	mm^2
$A_s`$	Area of longitudinal compression reinforcement.	mm^2
A_{st}	Total area of longitudinal reinforcement.	mm^2
a	Depth of equivalent compression stress block.	mm
b	Width of compression face.	mm
d	Effective depth.	mm
e	Eccentricity of the axial load.	mm
E_C	Modulus of elasticity of concrete.	MPa
E_S	Modulus of elasticity of steel reinforcement	MPa
f_t	Tension strength of concrete.	MPa
$\tilde{f}_c$	Cylinder compressive strength of concrete.	MPa
f_{cu}	Cube concrete compressive strength.	MPa
f_r	Modulus of rupture of concrete	MPa
f_{sp}	Splitting tensile strength of concrete	MPa
f_y	Yield stress of reinforcement	MPa
h	Effective dimension of the column	mm
h_f	Top flange thickness of hollow core slab	mm
ℓ_d	Reinforcement development length	mm
P_{cr}	Applied load corresponding to initial crack	kN
P	Axial applied load	kN
P_u	Ultimate load	kN
V/S	Volume to surface ratio	mm
V_p	Direct ultrasonic velocity	mm/μs
β1	concrete stress-block factor controlling the block height	---
ϕ	ACI strength reduction factor	---
Φ	Diameter of reinforcement bars.	mm
ε_c	Strain of concrete.	---
$\varepsilon_c`$	Concrete compressive strain	---
ε_s	Strain of steel reinforcement.	---
μ	Ductility factor.	---

κ	Stiffness factor.	---
u	Poisson`s ratio.	
ρ	Reinforcement ratio.	
$\sigma_1, \sigma_2, \sigma_3$	Principal stresses	

Abbreviations

Symbol	Definition
ACI	American Concrete Institue.
ASTM	American Society for Testing and Materials
B.C.	Boundary Condition
BS	British Standard
CDP	Concrete Damage Plasticity
C3D8	Eight-node brick element with full integration
EC	Eurocode
E1	Eccentricity ratio
E2	Eccentricity ratio
EXP.	Experimental
Eq.	Equation
et al.	And others.
FEA	Finite Element Analysis
FEM	Finite Element Method
HSC	High strength concrete
IQS	Iraqi Specification
MPa	Mega Pascal (N/mm^2)
NSC	Normal Strength Concrete.
OPC	Ordinary Portland Cement.
Rebar	Reinforcing Bar
RC	Reinforced Concrete.
RPC	Reactive Powder Concrete.
T3D2	Two-node truss element
S4R	4-node shell element
U.P.V.	Ultrasonic Pulse Velocity
W/C	Water to Cement ratio
CFRP	Carbon Fiber Reinforcement Plastic

Chapter One

Introduction

Chapter One

Introduction

1.1 General:

The column is one of the oldest elements used in the construction process, and its forms and materials varied according to different ages and regions. The ancient Sumerians and Yemenis were the first to use columns in construction, and the column was made up of a bundle of reeds, and this style of columns is still used in this time. Also, stones were used in the formation of columns and gained wide fame around the world. The civilizations of the Middle East were famous for this style of columns, especially among the ancient Egyptians, Persians and others. Stone columns developed and flourished in Greece and pomegranate in a way large and featured columns several styles **(Abd wahid , 2019)**.

Now, Concrete column is considered to be an important structural element in reinforced concrete structure because it supports the structure and carry the loads to the foundation or supports, so each damage or failure occurs in the column might cause a partial or full failure of the structure by possibly chain action **(Kadhim et al,2019).** Mainly columns are responsible of bearing the axial load and for that they must be designed properly for high pressure.

The modern buildings should be provided resistance to different types of loading especially when exposing to high temperature. Always, structural engineering does not take into account the effect of high-temperature loading in the design of the structural elements. The effect of fire on structural members depends on different factors such as level of temperature , kind and distribution of fire, present of loading, the duration of exposure to

fire, the cooling method practice and ventilation system. In order to keep the human life and avoid the serviceability damage and collapse in the structure, the high temperature fire effects need to be considered in the design of the various main elements, such as columns, beams, slabs and shear walls **(Kadhim et al,2019).**

Concrete is widely used as a primary structural material in construction due to numerous advantages, such as strength, durability, ease of fabrication, and non-combustibility properties, it possesses over other construction materials. Concrete structural members, when used in buildings have to satisfy appropriate fire safety requirements specified in building codes **(ACI 216.1, 2007).** This is because fire represents one of the most severe an environmental conditions to which structures may be subjected; therefore, the provision of appropriate fire safety measures for structural members is an important aspect of building design. (**Adnan, 2020)**

In General ,the fire response of reinforced concrete (RC) members is influenced by the characteristics of constituent materials, namely, concrete and reinforcing steel. These include (a) thermal properties, (b) mechanical properties, (c)deformation properties, and (d)material specific characteristics such as spalling in concrete. The thermal properties determine the extent of heat transfer to the structural member, whereas the mechanical properties of constituent materials determine the extent of strength loss and stiffness deterioration of the member. The deformation properties, in conjunction with mechanical properties, determine the extent of deformations and strains in the structural member. In addition, spalling of concrete induced by fire can play a significant role in the fire performance of RC members **(Dwaikat and Kodur,2010,Kodur, 2014)**.

Fire safety for structural members are measured in terms of fire resistance which is the duration during which a structural member exhibits resistance with respect to structural integrity, stability, and temperature transmission**(Purkiss,2007 ,Buchanan,2001 andKodur,2014).**A structural member's fire resistance usually depends on the geometry of the structural member and the materials used in construction, load intensity, and fire exposure characteristics itself **(Kodur and Sultan, 1998), (Adnan ,2020).**

1.2 Column Definition

A column is any member that has a ratio of its length to a minimum lateral dimension equal to or greater than three and used primarily to support axial compressive load **(ACI-318, 2019).**

For example, a column might transfer loads from a ceiling, floor or roof slab or a beam, to a floor or foundations. Columns are typically constructed from materials such as stone, brick, block, concrete, timber, steel, and so on, which have a good compressive strength. The column is the most important part in concrete buildings.

1.2.1 Types of Columns in Building Construction

Columns are classified based on the several conditions which include **(Hamakareem, 2009)**: types of reinforcement, types of loading, slenderness ratio, shape, and construction material **(Adnan, 2020).**

a) **Tied Column:** Reinforced concrete is typically used to build this sort of column. Longitudinal reinforcement is confined to a small area of tightly spaced tie reinforcement. as indicated in Figure (1-1 a).
b) **Spiral Column:** The spiral column is also made of reinforced concrete. Longitudinal bars are restricted within closely spaced and constantly coiled spiral reinforcement in the form of column. Spiral

reinforcement provides lateral restrains (Poisson's effect) and delays axial load failure (ductile), see Figure (1-1 b).

c) **Composite column:** Acomposite column is one that has longitudinal reinforcement in the form of a structural steel section or pipe that has or does not have longitudinal bars. as shown in Figure (1-1 c). This type of column has a high strength and a tiny cross-section, as well as exceptional fire resistance.

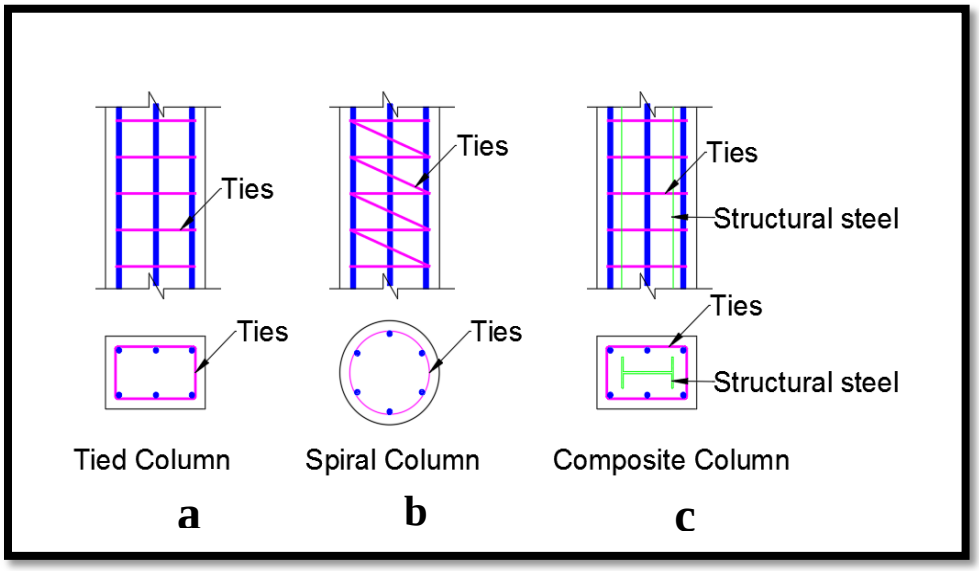

Figure (1-1): Types of reinforced concrete columns **(Krishna, 2017).**

1.2.2 Behavior and Ultimate Strength of columns

The ultimate eccentric load Pu and corresponding deflection are defined as the values at the peak of the experimental load–deflection curve **(Chen et.al,2009).** Eccentrically loaded columns are subject to moments, in addition to axial force. The moments can be converted to a load (P) and eccentricity (e_x)and (e_y) **(Al-Ansari and Afzal,2019)**. Fire resistance in normal strength concrete columns at large eccentricity increases by (47%) for close spacing of transverse reinforcement as compared to far spacing of transverse reinforcement (**Buch and Sharma,2019**).

In general, the column can be considered to be subject to either axial stress only, axial load plus uniaxial bending or axial load plus biaxial bending **(park and paulay ,2006)**. as shown in **figure(1-2)**

The nominal strength of the column at failure, consists of the role of the longitudinal bars with yield stress plus the concrete with stress of 0.85 fc̀ as reflected in the following equation: **(Nilson et.al, 2004)**.

$$\mathbf{P_n = 0.85 f_c' A_c + f_y A_{st}} \qquad \text{.....(1-1)}$$

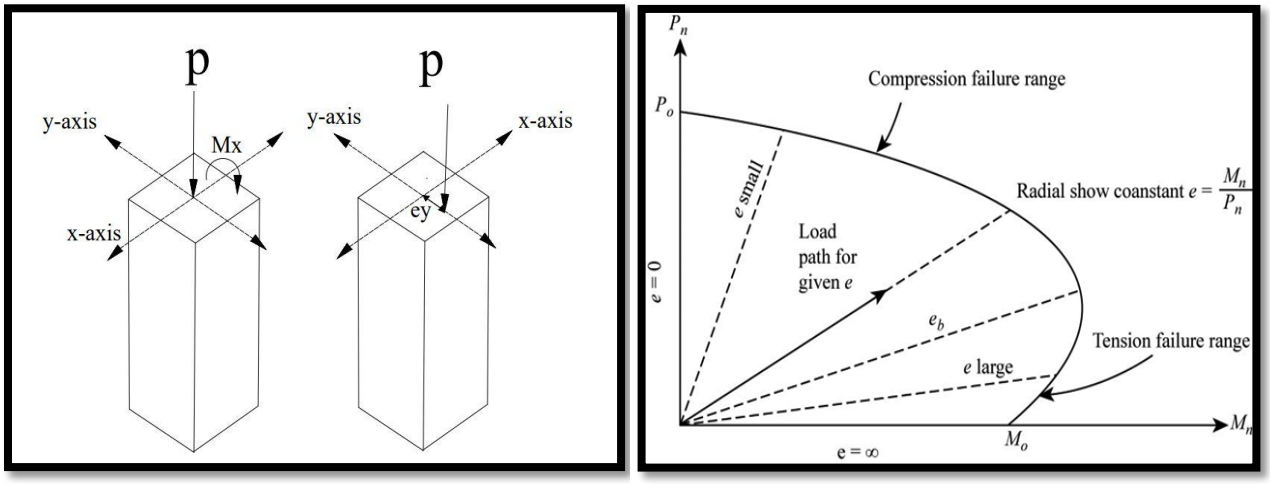

Figure (1-2): Concrete column interaction diagram **(Al-Ansari and Afzal, 2019) .**

1.2.3 Slenderness Ratio

Columns are categorized as short or tall depending on the proportions of their slenderness. The slenderness ratio is given by (kL/r) where (kL) is the effective length of the column and r is the radius of gyration. The proportion of the long column is greater than or equal to 22. While the proportion of the slenderness of the short column is less than 22, **(ACI code 318, 2019)**. According to **(BS 456, 2000),** if the column length is more than 12 times the lowest dimension of its cross section column, the column is classified as long column, while if the length of the column is less than or equal to 12 the

lowest dimension of its cross section, the column is classified a short column .

1.2.4 Concrete Protective Cover

concrete cover in reinforced concrete is the minimum distance between the surface of embedded reinforcing surface and the outer surface of the concrete **(ACI-318, 2019)**. as shown in figure**(1-3**). the reasons:

* To protect steel reinforcing bars from the environmental influences of prevent their wear.

***** To provide thermal insulation that protects the reinforcing bars from the fire.

* To give the reinforcing bars sufficient embedding to enable them to do so stressed without slipping.

* Prevent buckling of the reinforcing bars between the ties. (Hasan,2019)

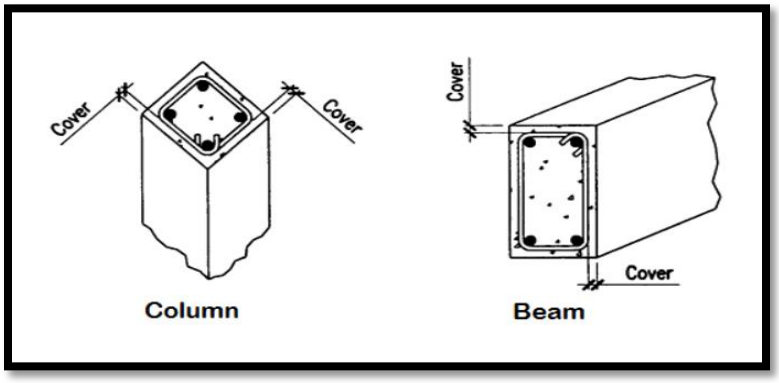

Figure (1-3): Concrete protective cover **(Hasan,2019**).

1.3 Column Behavior Under Fire Exposure

Generally, building codes require columns in tall buildings to have a fire rating of (1 to 4) hours depending on the building's usage and occupancy **(Wiley, 2002).** Poles made of (NSC) can provide required fire resistance without any external fire proof insulation **(Raut and Kodur, 2011).**when

exposure to fire, thermal gradients develop in the concrete cross section. With increasing temperatures, the moisture in the concrete turns into steam, the volumetric expansion of which leads to the compression of the pores. When these stresses, generated by mechanical and hydraulic mechanisms, overcome the tensile strength of concrete, the phenomenon of spalling occurs **(Mindeguia et. al, 2015)**.

Also in the event of a fire, the column may be exposed to fire from one, two, three sides or all four sides depending on the architecture and structural layout of the building. For example, a wall can act as a barrier in front of a column that exposes one, two, or three faces of the column to fire. On the other hand, a pillar can be placed in the middle of the room thus exposing the four sides of the pillar to fire. This leads to the development of thermal gradients that can lead to uniaxial (one side or three sides) or biaxial (two adjacent sides) shaft bending. Additional moments in the column reduce the load bearing capacity of the column and also cause additional deformations and thus reduced fire resistance. The fire type scenario has a significant influence on the development of self-restraining forces in reinforced concrete columns **(Kodur and Raut, 2012)**.

Concrete generally offers the best fire retardant properties of any type of building material. This excellent fire resistance is due to concrete as its constituent material (i.e. cement and aggregates) which, when chemically combined, forms an essentially inert material and has low thermal conductivity, high heat capacity and slower deterioration in strength with temperature. This slow rate of heat transfer and loss of strength is what enables concrete to serve as an effective fire shield not only between adjacent spaces but also to protect itself from fire damage. **(Kodur and Raut, 2012),Ada et. al 2018,** as shown in the **plate (1-1).**

Plate (1-1): Concrete column damaged by fire (**Ada et. al 2018**)

1.4 High-Strength Concrete

In recent years, the construction industry has shown significant interest in the use of high-strength concrete (HSC). This is due to the improvements in its structural performance such as high strength and the durability that it can provide, compared to traditional normal strength concrete (NSC). The use of high-strength concrete, which was previously in applications such as bridges, offshore structures and infrastructure projects, is becoming more popular in high-rise buildings. One of the major uses of HSC in buildings is for columns ,In buildings, HSC structural members are designed to satisfy the requirements of serviceability and safety limit states. One of the major Safety requirements in building design is the provision of appropriate fire safety measures for structural members **(Kodur,2000).**

In previous, high-strength—concrete that has a specified compressive strength for design of 6000 psi (41 MPa) or greater. The new value of 8000 psi (55 MPa) was selected because it represented a strength level at which special care is required for production and testing of the concrete and at which special structural design requirements may be needed ,as shown in **figure (1-4**). As technology progresses and the use of concrete with even higher compressive strengths evolves, it is likely that the definition of high strength concrete will continue to be revised**(ACI 363,2010)**.The engineer can build a smaller piece to carry the same loads as a larger one of regular strength concrete. As a result of the reduced dead weight, greater spans, and increased useable area of structures, this results in cost-effective construction (**Mahdi, 2016)**. Because it offers many advantages over traditional concrete, HSC has seen increasing use in recent years in prestressed concrete beams, bridges, high-rise constructions, and structural rehabilitation **(Aziz et.al ,2010)**.

Resistance is a property of a substance or collection of materials that is resistant to fire or protects against it; it is characterized by the ability to restrict fire or continue to perform a structural function, or both, when exposed to fire, as evidenced on structural elements of structures. the differences between normal-and high-strength concrete are less pronounced, Higher occurrences of explosive spalling of specimens were also observed above 572°F (300°C) by **(Phan and Carino, 2000), (Kodur, 2000)**.

Also studied the spalling characteristics of (HSC) subjected to fire and reported that spalling is not only influenced by concrete strength, but also concrete density, aggregate type, load intensity, reinforcement configuration, and layout. Experiments reported that the addition of synthetic fibers could improve HSC's resistance to spalling, although it is unclear how synthetic

fibers would affect the residual mechanical properties of the concrete after exposure to fire **(ACI 363R-10,2010)**.

In the present study the behavior and mechanical properties of (HSC)reinforced columns under effect of cyclic fire exposure will be investigated.

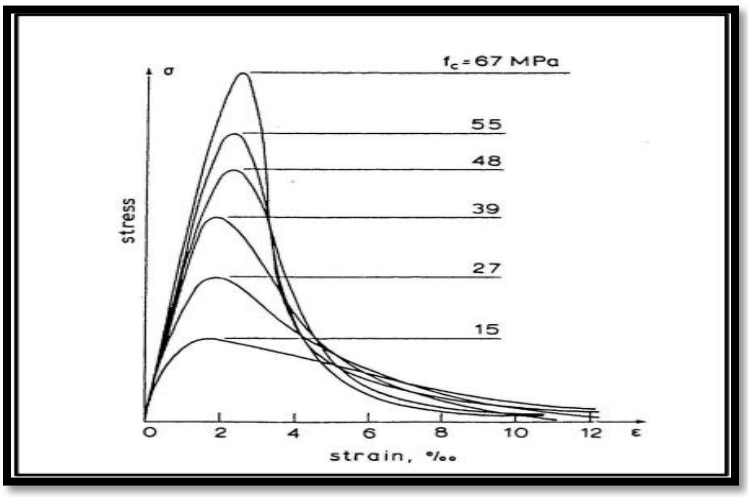

Figure (1-4): Stress-Strain Curves for Cylinders of Concrete Subjected to Uniaxial Compression **(Jiratatprasot 2003 , Mahdi 2016**)

1.5 Repair and Strengthening of Fire-Damaged Reinforced Concrete

Concrete structures may rarely collapse in fire incidents but fire induced damage to structural members is inevitable as a result of material degradation and thermal expansion. This requires certain repairing measures to be applied to restore the performance of post-fire members **(Jin Qiu et .al ,2021).**

1.5.1 Reactive Powder Concrete (RPC)

Reactive powder concrete (RPC), developed in late 1990S, has been known an advanced concrete-based composite with ultra-high strength and outstanding performance. From the advent of RPC, it has attracted attention from both academic and engineering fields, and has found wide application

in construction of municipal works, highways, bridges, hydraulic engineering, mining engineering, energy sources and military engineering, etc.**(Yang at el ,2011).**

(RPC) is a high strength and high ductility cementitious material formulated with advanced physical and mechanical properties. It consists of a special concrete in which the microstructure is optimized by the precise gradation of all particles in the mixture to achieve maximum density. It widely uses the pozzolanic properties of high purity silica fume and improves the chemistry of Portland cement to produce higher strength hydrates**.** Comparison of physical, mechanical, and durability properties of RPC and HPC (High Performance Concrete) shows that RPC has better strength (both compressive and flexural) and lower permeability compared to HPC. **Plate (1-2)** illustrates some of the applications of reactive crushed concrete.

Retrofitting of fire damaged structural components using RPC is the recent effective technique. This technique does not increase the deadweight of the members and the new members will have better fire resistance in the future than use carbon or glass fiber.

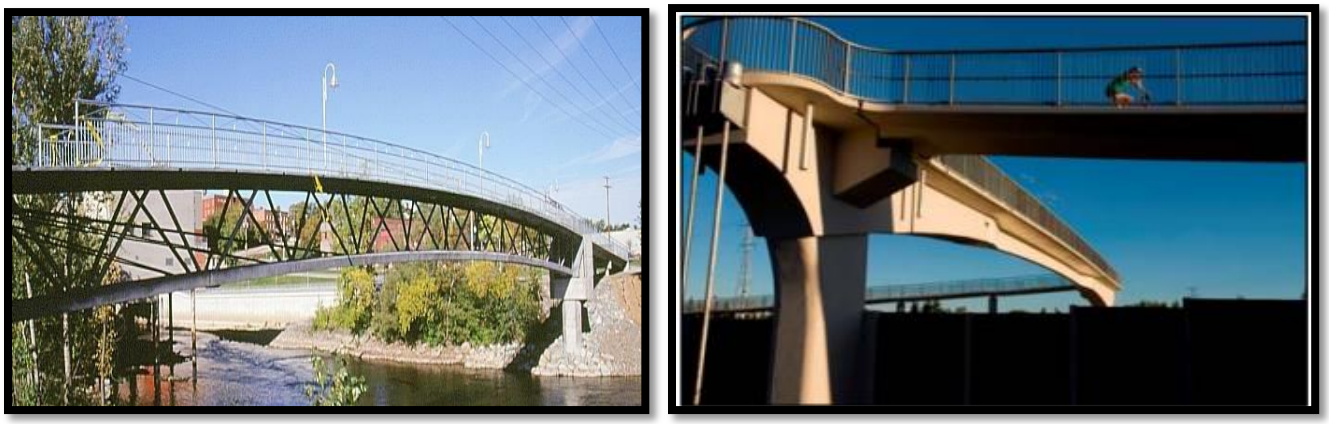

-Sherbrooke Pedestrian Bridge b-Glenmore/Legsby Pedestrian Bridge

Plate(1-2): Applications of Reactive Powder Concrete**(Seibert et. al 2019)**

1.5.1.1 Composition of Reactive Powder Concrete

RPC consists of very fine powders (cement, very fine aggregate (0.15-0.6) mm, low water-cement ratio), as well as other materials (silica fume, superplasticizer, fine steel fibers).The maximum particle size of the material (0.6) mm, optimization of dry fine powder packing must be managed to obtain a very dense matrix. Compressive strength of reactive powder concrete reaches (800) MPa. The main steps of producing reactive concrete powder can be summarized in **Table(1-1)**

Table(1-1): Main steps for producing Reactive Powder Concrete **(Maroliya, 2012).**

Steps	Reason
Elimination of coarse aggregate	Improve the homogeneity
Optimization of the granular mixture	Getting very dense matrix by improving the packing
Utilization of the Pozzolanic materials (Silica fume)	Lowering the anhydrate cement
Using superplasticizer	Reduce W/C ratio and improve the workability
Heat treatment after hardening	Improve the microstructure
Optional step	
Adding small size of steel fibers	Improve the ductility
Applying pressure before and during setting	More improving of compaction

1.5.1.2 Mechanical Performance and Durability of RPC

The RPC family includes two types of concrete, designated RPC 200 and RPC 800, which offer interesting implicit possibilities in different areas **(Alina at el, 2016)**. The mechanical properties of the two types of RPC are given in **Table (1-2).** The high bending strength of RPC is due to the addition of steel fibers**. Tables (1-3) , (1-4)** show typical mechanical

properties of RPC compared to conventional HPC with a pressure strength of 80 MPa **(Bickley,Mitchell 2001).**

Table (1-2): Comparison of RPC 200 and RPC 800 **(HDR Engineering Website1999)**

	RPC 200	**RPC 800**
Pre-setting pressurization	None	50 MPa
Heat-treating	20 to 90°C	250 to 400°C
Compressive strength (using quartz sand)	170 to 230 MPa	490 to 680 MPa
Compressive strength (using steel aggregate)		650 to 810 MPa
Flexural strength	30 to 60 MPa	45 to 141 MPa

Table (1-3): Comparison of HPC (80 MPa) and RPC 200 **(Matte and Moranville 1999).**

Property	**HPC (80 MPa)**	**RPC 200 C**
Compressive strength	80 MPa	200 MPa
Flexural strength	7 MPa	40 MPa
Modulus of Elasticity	40 GPa	60 GPa
Fracture Toughness	$<10^3$ J/m²	$30*10^3$ J/m²

Table (1-4): Durability of RPC compared to HPC (**Staquet and Espion 2000**)

Abrasive Wear	2.5 times lower
Water Absorption	7 times lower
lower Rate of Corrosion	8 times lower
Chloride ions diffusion	25 times lower

1.5.2 Fiber Reinforced Polymer (FRP)

Traditional materials and building techniques have traditionally been used to strengthen or retrofit existing concrete structures to withstand greater design loads, repair strength loss due to deterioration, correct design or

construction faults, or increase ductility. Traditional methods include externally bonded steel plates, steel or concrete jackets, and external post-tensioning to name. Fiber-reinforced polymers (FRPs) are composite materials comprised of fibers in a polymeric resin that have emerged as an alternative to traditional materials for repair and rehabilitation **(ACI 440.2R-08, 2008).**

In the present study ,CFRP laminates will be use to repaire post – fire damaged concrete column**s.**

There are different systems in this field **(Ciprian et.al, 2009):**

a)Wet lay-up systems: represents the most commonly used technique, in which unidirectional fiber sheets or woven fabric sheets are impregnated with resins and wrapped around columns, with the main fibers oriented in the hoop direction (**Hollaway and Teng,2008**). Installation on the concrete surface requires saturating resin, usually after a primer has been applied. Two different processes can be used to apply the fabric (a) the fabric can be applied directly into the resin which has been applied uniformly on to the concrete surface, (b) the fabric can be impregnated with the resin in a saturator machine and then applied wet to the sealed substrate. The wrapping can be realized continuously around the entire element or partially, using sheets of FRP disposed in spiral or in distinct sections. There can be applied variable number of layers (from same material or distinct ones), obtaining different thicknesses of the confining layer, depending on the required element strength, as shown in **Plate (1-3) (Cozmanciuc at. el, 2009).**

Plate (1-3): Wet lay-up confining system **(Cozmanciuc at. el, 2009).**

b) Systems based on prefabricated elements; are used, the jackets are fabricated in half circles or half rectangles and circles with a slit or in continuous rolls, so that they can be opened up and placed around columns ,as shown in **(Plate 1-4)**. This can be considered as technical most elaborated system, but the major problems emerge in the closure area of the composite layer because of insufficient over lapping **(Hollaway and Teng, 2008).**

c) Special automated wrapping systems: the FRP automated wrapping technique through winding of two or tape was first developed in Japan in the early 90s and a little later in the USA .The technique, as shown in (**Plate 1-5),** involves continuous winding of wet fibers under a slight angle around Columns by means of a robot. Key advantage of the technique, apart from good quality control, is the rapid installation **(Heiza et. al ,2014).**

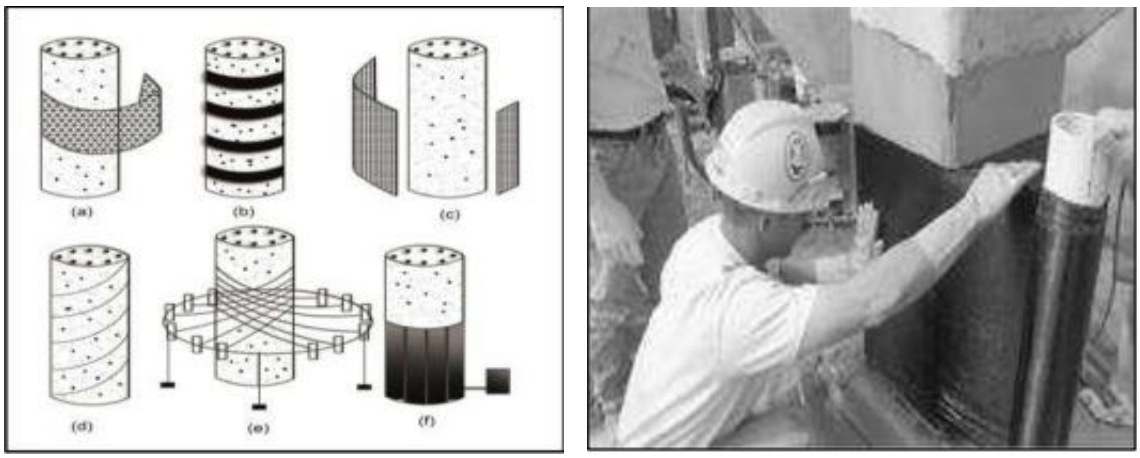

Plate 1-4: Confining system based on prefabricated FRP elements (Heiza et. al ,2014).

Plate 1-5: Automated RC column wrapping **(Hollaway and Teng, 2008)**.

1.6 Objective and aims the Present Work

The main objective of this research is the experimental and analytical study of the column behavior of pre-loaded reinforced concrete columns under exposure to cycles of burning , by knowing the extent of bearing concrete structures after exposure to more than one fire exposure. It included a number of aims:

1- All reinforced concrete columns are subjected to cycles of fire exposure with constant eccentric pre-loading on column.

2- Experimental study of the column behavior under effect of periodic burning that included a number of variables :

a- Effect of concentric and eccentric pre-loading on column through cyclic fire exposure.

b-Effect of scenario of cyclic fire exposure (time duration of each cycle ,number of cycles, target of temperature of each cycle).

c- Role of longitudinal steel reinforcement ratio.

d- Type of concrete (HSC , NSC) for columns .

3- Carry out practical methods for repairing and restoring the strength and performance of damaged (**RC)**. due to cycles of fire exposure and in its worst case with eccentric axial load, by:

a-Developing a hybrid concrete cross-section of (**RPC)** for the added outer shell and remaining (**NSC)** for the primary concrete core.

b-Utilizing **NSC** to compensate damaged outer shell and wrapping with **CFRP** laminates.

4-Evaluation of the structural performance of eccentric and concentric tested column after exposure to periodic burning of fire. through ultimate load, cracking pattern, failure mode and load deformation respone.

5-Evaluation the activity of proposed retrofitty methods for fire damaged columns through the ultimate load, cracking pattern, failure mode, vertical and lateral deformation.

6-Excute numerical analysis using a three-dimensional non-linear finite element througth utilizing (ABAQUS / Standard 6.14) to track and trace the total response of the tested columns, and compare the results with those obtained from experimental work.

7-Aparametric study of several important parameters that do not consider in the experimental program, such as:, the eccentric deviation of the applied load, the strength of the new shell (RPC) and slenderness ratio.

1.7 Layout of the Thesis

Chapter one: provides some basic information on RC column and fire exposure response. Impact on concrete structures, especially reinforced concrete columns. In addition to the general definitions that describe the types of concrete and a description of some of the properties and benefits of RPC, CFRP. It also provides a description of the importance, problem and objectives of the research, as well as the outline of the research.

Chapter Two: reviews a number of studies and scientific research that have been published on the effect of fire and cyclic behavior on reinforced concrete columns by accredited scholars and researchers.

Chapter three: defines the experimental program which included Characteristics of the materials used, concrete preparation, column samples, cyclic fire process, repair process, instrumentation, and sample testing after burning.

Chapter four: Review and discussion of experimental work results have been presented in this chapter.

Chapter five: through a analysis of the models by a computer program ABAQUS) in the F.E.M. and comparing results with those available from experimental work.

Chapter six (Conclusions and Recommendations):introduce the main conclusions from experimental and analytical works and recommendations drawn from the research work, as well as.

Chapter Two

Literature Review

Chapter two

Literature Review

2.1 Introduction

Fire accidents continue to occur despite the developments in the construction industry to avoid such cases. Therefore, studies that clarify structural and structural member performance under fire conditions are still required. According to the International association of Fire and Rescue Services **(Brushlinsky et al,2017),** 40% of fire accidents around the world during 2013 were defined as structural fires.

Moreover, in the USA, 494,000 structural fires were reported during 2014–2015. In England, 154,700 fire incidents were recorded, 28,200 of which were accidental dwelling fires. Therefore, the fire phenomenon should be understood and the performance of buildings under both ambient and fire conditions should be well assessed. This assessment can be conducted experimentally or with analytical and computational tools**(Arna'ot et al, 2017).**The behavior of reinforced concrete structures is better than that observed in small samples, as well as the behavior of larger structural elements better than those of smaller ones, as well as structural elements in dry environments, and with the age of concrete structures, their performance is better than those newly built and wet , athough the scenario of the burning concrete structure is very bleak and leaves strong negative impressions, in view of the engineering, the problem may be more aesthetic than structural. However, the structure must be checked by a qualified specialist, based on technical and experimental resources to correctly characterize the remaining

characteristics of the reinforced concrete structure (**Britez et al,2020**). We will discuss previous studies during the current century

2.2 Studies on Behavior of Unloaded Fire Exposed RC Columns:

Kodur and Grath ,(2003) In buildings, fire represents one of the most severe environmental conditions and, therefore, must be properly taken into account in the design of High Strength Concrete Structure (HSC) members. The increasing use of HSC in buildings has raised concerns about the behavior of this concrete in particular, high temperature spalling, as identified in studies by a number of laboratories, is a major concern.

In their paper, results from an experimental program for six columns for fire resistance of HSC poles are presented. Factors affecting the thermal and structural behavior of HSC concrete columns under fire conditions have been discussed, and results from this study indicate that the type of aggregate, concrete strength, load density, details and spacing between ties have an effect on the fire resistance performance of HSC columns. , the test results show that tie formation (bend ties at 135, ties and provide cross ties) and tie closer spacing significantly beneficial effect on the fire resistance of HSC columns. The presented results used to generate data about the fire resistance of HSC columns, and contribute to the identification of factors affecting the behavior of HSC columns

Kodur et al,(2003) presented, the results of fire resistance experiments on five types of reinforced concrete columns. Variables considered in the study include strength of concrete at NSC and HSC, aggregate type (siliceous and carbon aggregate), and fiber reinforcement (steel fibres, polypropylene).

Data from the study is used to determine the structural behavior of HSC columns at elevated temperatures. A comparison was made of the fire resistance performance of HSC columns with that of NSC columns and fiber-reinforced HSC columns. Factors affecting thermal and structural behavior of HSC concrete columns under fire conditions are discussed. The results show that the fire resistance of an NSC column is higher than that of a HSC column. The addition of polypropylene fibers and the use of carbonate aggregate improves fire resistance.

The behavior of high-performance concrete (HPC) columns exposed to fire is studied by **Kodur at el, (2004),**using a numerical model in the form of a computer program. Throug that, it was discussed the three steps of the columns, which are related to thermal and structural analysis in order to calculate fire resistance. The author proposes a simplified method for determining crushing under fire conditions. The use of a computer program to track the reaction of an HPC column from pre-loading through collapse due to fire has been demonstrated, and the numerical model employed in the software has been confirmed by comparing the computer program's predictions with full-scale fire resistance test results. Experiments on fire resistance on HPC poles are described in detail, as well as the findings. For any value of essential parameters including load, section dimensions, fiber reinforcement, column length, concrete strength, aggregate type, and fiber reinforcement, computer software may be utilized to forecast the fire resistance of HPC columns**.**

The response of the composite columns to the compressive load under the column, in which a non-uniform temperature distribution is carried out through Thickness was presented, by **Liu et al, (2006) ,** This irregular

temperature distribution can develop when one side of the structures is exposed to heat flow. In this paper, assume that this distribution is linear, which corresponds to the steady-state temperature profile due to thermal conductivity. The deterioration of the elastic properties with temperature is calculated using the experimental data of the elastic modulus. Moreover, the formula includes transverse shear and is first made for the general non-linear case and then is linearly shaped. Because of the irregular stiffness and the effect of the ensuing thermal moment, the structure behaves as an imperfect column and responds by bending rather than bending in the classic Euler sense (bifurcation). Another important effect of non-uniform temperature is that the neutral axis moves away from the centroid of the cross section, which results in another moment due to eccentric loading, which tends to bend the structure away from the heat source. Simple equations for column response are derived and results are presented for the skew change with heat flow, as well as for the combined effects of the applied load and heat flow. It was found that the thermal moment tends to bend the structure away from the heat source for small temperatures (small heat fluxes) but toward the heat source for large temperatures. On the contrary, the moment due to eccentric loading will always tend to bend the structure away from the heat source. The results indicate the combined effects of these moments and those of the axial constraint.

Wu et al ,(2010) The performance of 12 axially restricted RC columns for different shapes of cross- section, under fire conditions was recently completed at the South China University of Technology, as shown in **figure (2-1)**.The aim of the research is to study the effect of axial restriction on RC columns during the expansion and contraction phases. The RC columns were

all initially center-loaded and subjected to fire from all sides. Axial restraints were imposed at the top of the columns to simulate the restriction effect of the rest of the entire frame. Boundary conditions Columns were considered static - static for all tests. It was found that the restraint RC columns behave quite differently from the insulated ones.

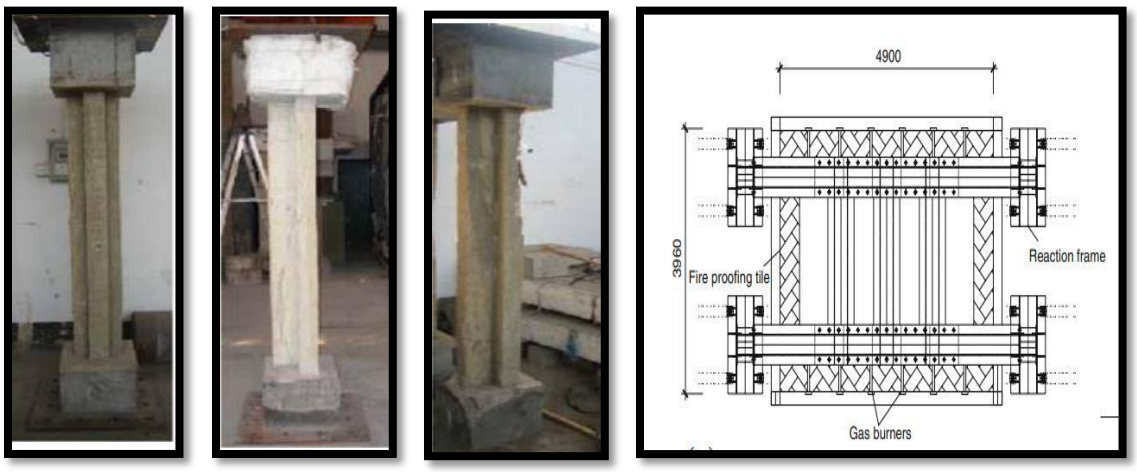

Figure(2-1): Furnace construction and columns **(Wu et al 2010)**

Junhua Li et al ,(2010) during the research, four samples of columns with a length of (1540)mm and dimensions of (250 * 420)mm for the corbel and (250 X 250)mm for the mid-section were studied, as the test data of three columns related to the mechanical properties of the eccentric columns of steel-reinforced concrete (SRC) after exposure to fire and one comparative test data were studied. The strain is distributed along the section height in the mid-span section of the eccentric columns prior to being loaded to (90%) of the final load bearing capacity. After exposure to fire, the bending stiffness and load bearing capacity of the samples are reduced compared to those at normal temperature. At various loading stages from initial loading to (80%) final strength, the bending stiffness of SRC eccentric columns and calculation values are shown The residual load bearing capacity of the

eccentric SRC columns after exposure to fire is about (69%) to (81%) of Those at room temperature after exposure to fire. With the same concrete strength and heating condition, the final strength of the samples decreases with increasing deflection.

Sadaoui et al ,(2013) The effect of fire on reinforced concrete (RC) columns was studied in this work. A finite element model is able to analyze the behavior of a constraint RC columns have been developed from pre-fire stages to collapse in fire to analyze RC structural elements exposed to normal or boundary fire conditions. The advantage of this procedure is The ability to consider the realistic constituent relationships of concrete and steel including a wide range of phenomena such as creep transient, plasticity, cracking, and deterioration of material properties, all within the framework of large displacements and small strains theory. Through the results of the parametric study, it was found that the fire parameters significantly affect the fire resistance of RC columns. As the load level has a great effect on the performance of RC poles in a real fire. An increase in the load level leads to a significant decrease in the fire resistance; the increase in the slenderness ratios and the eccentric eccentricity of the applied load leads to a significant decrease in the fire resistance due to the reduced bending stiffness of the slender columns, making them susceptible to torsion under axial restraint forces**.**

Bamonte and Monte,(2015) in the literature on concrete at high temperatures, some basic models have been proposed with the aim of simulating the structural behavior of reinforced concrete during heating, and a finite beam element algorithm has been developed in this context for thermomechanical calculations. Using four alternative foundation models

proposed in the literature on high-temperature concrete, a series of well-Documented thorough experiments on reinforced concrete columns exposed to standard fire (without cooling) were numerically simulated. The main aims are to emphasize the importance of some critical aspects of reinforced concrete members in hot conditions, such as second-order effects, transient and creeping strains (a), and to conduct a systematic comparison of numerical and experimental results in order to assess the reliability of both numerical modeling (b),and approved foundational forms for concrete (c),When transient and creeping strains, as well as second-order factors, are thoroughly evaluated, the results demonstrate that numerical modeling is generally in agreement with the experimental evidence.

Al-Gasham ,2016 the effect of high temperatures on the structural behavior of hollow reinforced concrete columns was studied in the research. Where they created sixteen square columns with dimensions (120 * 120) mm and a length of (600) mm,as shown in **figure (2-2).**The variables of the experiment were the cavity size and temperature. Twelve samples were hollow by extending a plastic tube (PVC) centrally along the sample. These samples were classified according to the diameter of the tube(25.4, 50.8, 76.2)mm. The remaining samples were of rigid section and collected in one group. Each group contains four models, three of which are exposed to different temperatures (300, 500, and 700)C°, and the fourth model is a source model that has not been exposed.to the fire. All columns were tested by applying a progressive axial compressive load on the model to the point of failure. For similar columns, the axial load capacity decreases with increasing fire temperature to(300-700)°C. The corresponding reductions were:(21.82%-52.73%) for solid columns, (20.00%-53.81%) for (25.4) mm hollow

columns, (26.67%-62.00%) for samples with a hollow size of (50.8) mm,and (18.18%-59.09%) for (76.2) mm hollow columns, respectively**.**

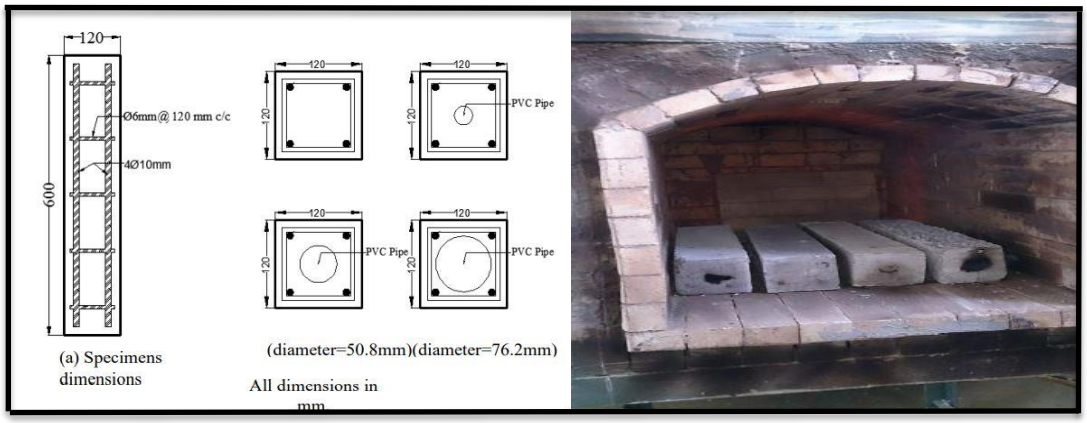

Figure(2-2): Details of Reinforcement and Gradually Cooling for Column Samples **(Al-Gasham ,2016).**

Abdulraheem and Kadhum, 2017 conducted a study on the behavior of centrally loaded reactive crushed concrete columns after exposure to fire, and there were two parts to the study. The first part is experimental work to ensure that the developed model is adequate while the second part is 3D element specific (FE) modeling of RPC columns with ABAQUS software using sequential thermal displacement analysis. It is also presented based on calculations of pore pressure in concrete.

The test results showed that the RPC columns lost about (39% -45%) of their bearing capacity after exposure to fire at (600°C) and a duration of one hour. It is shown that increasing the concrete cover and inserting the hardly side links improve the post-fire behavior of RPC columns. Moreover, the decrease in residual endurance increased dramatically with the increase in the number of exposure sides and the duration of the fire,as shown in **Figure (2-3).**

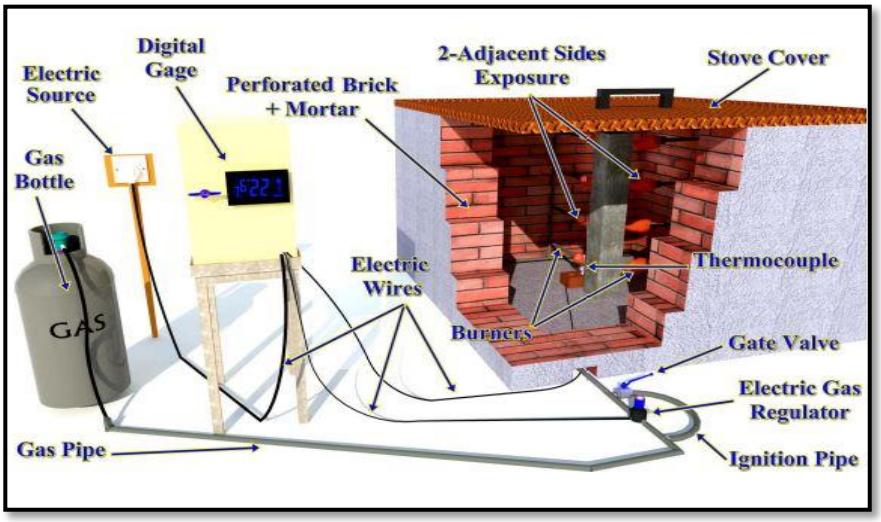

Figure(2-3): Details of the stove and equipment **(Abdulraheem and Kadhum, 2017)**

Gil et al, 2018 it aims to study the effect of three concrete mixtures, four coating thicknesses, and tar bars of longitudinal reinforcement on the splintering phenomenon exposed to the ISO 834 fire curve. The tested samples were representative of reinforced concrete columns from real buildings, with one side and two angles exposed to fire ,as shown in **Figure (2-4).**

Four liquefied petroleum gases heated vertical furnace was used. The burners are located on the side walls of the inner furnace chamber 2.5 m high, 2.5 m wide and 1.0 m long. All tests took 240 minutes and the maximum temperature inside the oven was around (1153)C˚. Concrete has been described from either axial compressive strength tests, water absorption by capillary pore measurement and mercury intrusion measurement, along with fire resistance tests in real-world samples. It was concluded that the diameter of the tape has no effect, because there is an effect of the mixture and thickness of the concrete cover.

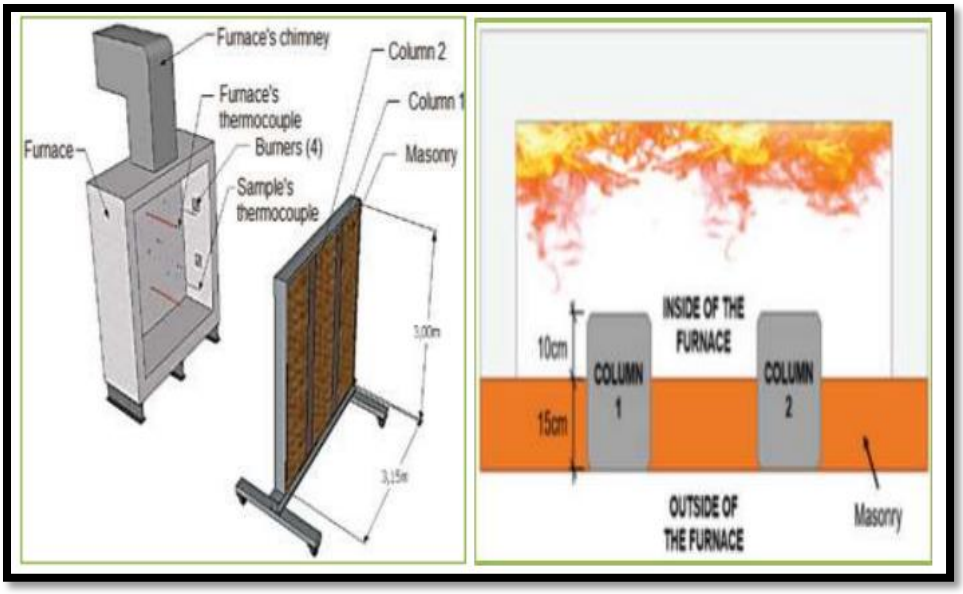

Figure (2-4): System Installation in the Furnace **(Gil and et al, 2018).**

Taha, 2018 an enlargement study was carried out on the behavior of reaction powder concrete (RPC) and normal strength concrete (NSC) columns exposed to a real four-sided fire flame, and the mechanical properties of RPC and NSC were tested at different ages of (3, 7, 28 and 56) days, after exposure For fire flame temperatures ranging from (25-500C°). The residual mechanical properties of the samples, load carrying capacity, axial and mid-height lateral displacement, plasticity index, crack pattern, fragmentation types, and failure method of RPC and NSC column samples exposed to a fire flame, were measured directly to complete the combustion period (before cooling).It was concluded that there was a decrease in the mechanical properties of the RPC samples after exposure to temperatures from 300-500°C. It was better than NSC. as shown in **Figure (2-5).**

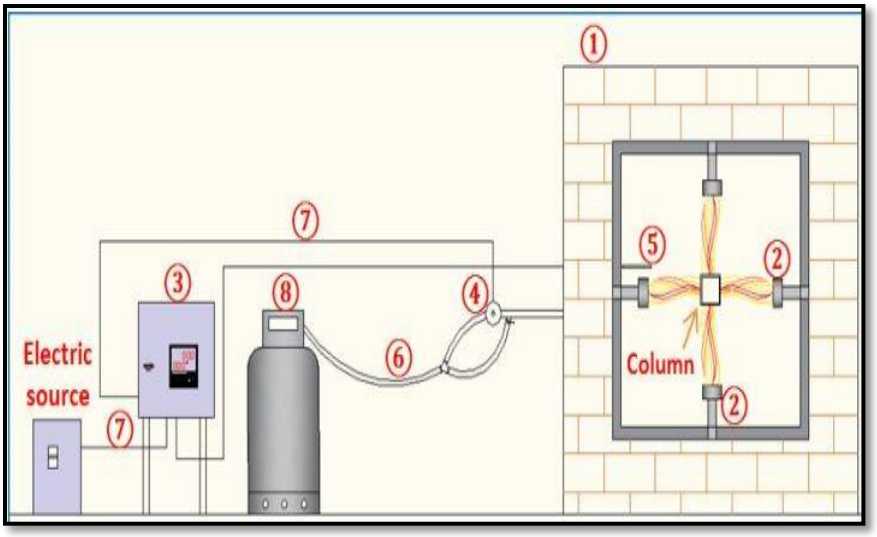

Figure (2-5): The Stove Equipment **(Taha, 2018).**

Shubbar and Alwash,2020 Presented an experimental study on the behavior of fiber-reinforced reactive powder concrete columns then Exposure to fire and improvements made to enhance the column's resistance to fire. This paper mainly aims to study the experimental behavior of the hybrid reinforced columns generated by reactive concrete powder (RPC) and exposed to unilateral fire flames and then subjected to eccentric load after cooling. The pilot study consists of testing sixteen RC poles distributed in four groups based on the variables used in the pilot study. All columns were under fire for different periods (1, 1.5, 2) hours, then after cooling they were tested under eccentric load. The main conclusion of this study is that the best fire resistance of the column was obtained when using a hybrid cross section (steel fiber concrete core with polypropylene fiber reactive concrete powder), as shown in **Figure (2 -6).**

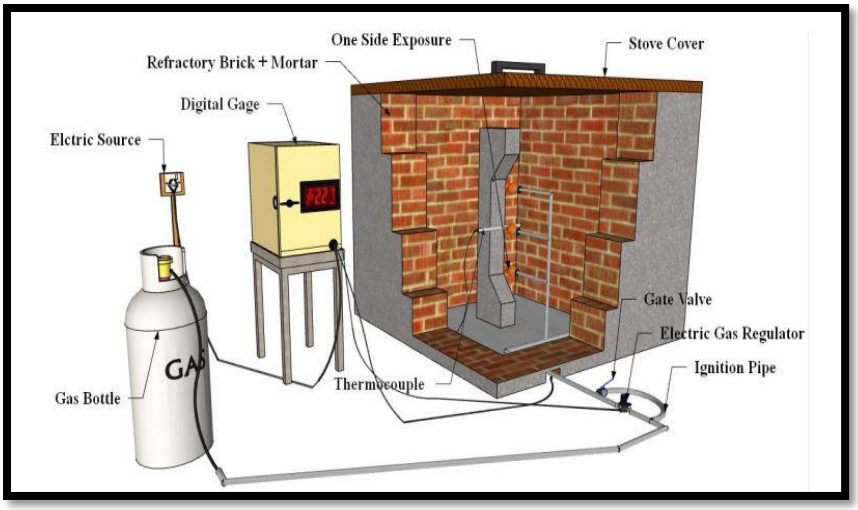

Figure (2 -6): Burning process (**Shubbar and Alwash,2019)**

Li et al ,(2021) proposed three-dimensional (3D) simulation model of a short RC column subjected to axial stress after being exposed to fire was created in this work. After high temperatures, the influence of depreciation of mechanical characteristics of steel bars and concrete materials was considered. The model also took into account the bonding and sliding behavior of the longitudinal steel bars with the concrete. The failure mode and mechanism of short RC columns were explored using the current simulation method. The impacts of the fire scenario and fire duration on the axial pressure performance of short RC shafts were also investigated. The average-scale numerical model is found to be capable of simulating the mechanical behavior of short RC columns under axial load. Furthermore, as the number of burning surfaces and the length of the fire rise, the final bearing capacity, axial compressive hardness, and ductility decrease, and the mechanical properties of short poles deteriorate more quickly.

2.3 Studies on Behavior of Pre-Loaded Fire Exposed RC Column:

Kodur et al , 2004 in their study of fire resistance results was conducted on five types of reinforced concrete columns. The variables taken into account during the study were the strength of concrete ,normal strength concrete (NSC) and High Strength Concrete (HSC), type of aggregate (silicic and carbon aggregate), and fiber reinforcement (steel and polypropylene). Higth srtrength concrete(HSC) and the fifth from (NSC), all columns were 3810 mm in length and 305 mm in square cross-section and five batches of concrete were used to manufacture the columns.

The tests were carried out by applying heat to the columns by placing them inside an oven specially designed to test the loaded columns. The final conditions of the columns were fixed for all tests, and the length exposed to fire was approximately (3 mm). Data from the study is used to determine the structural behavior of HSC columns at elevated temperatures. This data showed the following:

* The resistance of HSC columns to fire is lower than that of NSC columns.

* Presence of carbonate aggregates in HSC increases fire resistance.

* The addition of steel and polypropylene fibers in HSC can improve the ductility of HSC poles and increase their fire-bearing capacity.

Tan and Yao,2004 during the study a theoretical model for single-sided, second and third-sided RC heated columns was presented. It is based on the ACI method for column design at ambient temperature. With this method, the maximum load capacity of the RC columns corresponding to different

thermal boundary conditions can be directly determined Thus,the idea is to determine the deterioration of the properties of concrete and steel materials, as well as the movement of the neutral axis at a certain elevated temperature. Arising from 1, 2 or 3 exposures to fire, there are three potential deflection sites for the SP1 to P3d load, as shown in **Figure(2-7).** For design purposes. A large group of RC columns with different slack ratios, levels load, eccentricity, cross-sectional areas, and concrete strengths, concrete covers were analyzed by the proposed method and SAFIR finite element program. Omparisons of predictions are made between the proposed method and the finite element resltes.

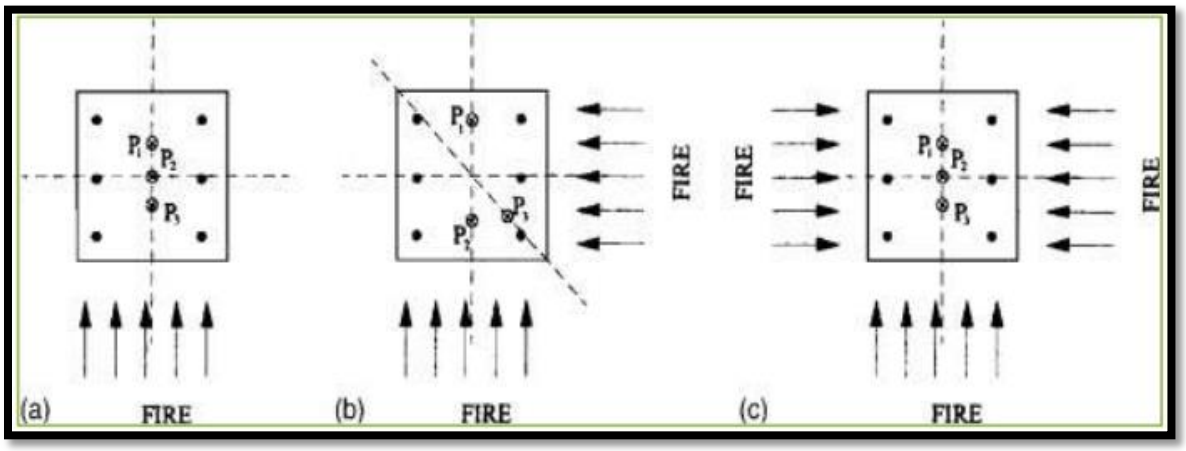

Figure (2-7): Different load eccentricities under 1-, 2-, and 3-face heating (**Tan and Yao, 2004)**

Tao Yu et al,2007,the behavior of reinforced concrete columns (SRCs) subjected to fire was studied using both experimental and numerical methods. At normal and high temperatures, twelve samples were evaluated. Following specific assumptions, a procedure was created to forecast the final temperature distribution and strength of fire-exposed SRC columns. The process used a hybrid finite-element and finite-difference method to

investigate the temperature distribution, and the procedure predicted the reactions of SRC columns under loads at both ambient and increased temperatures. We give some comparisons between the test data and the calculated results , as shown in **Figure. (2-8).**

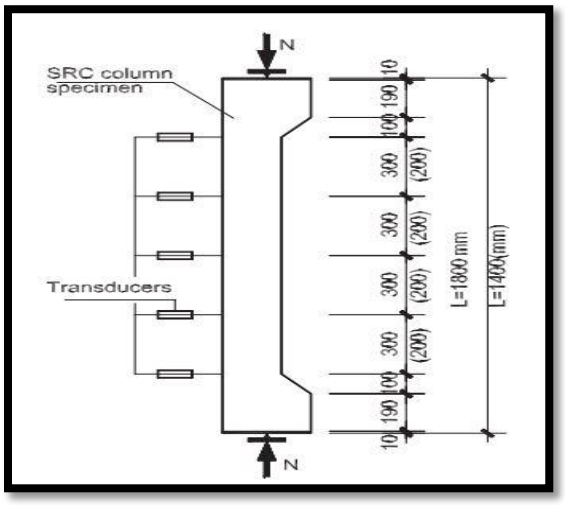

Figure (2-8): load eccentricities under one face heating (**Tao Yu et al,2007**)

Wu et al,(2007) the fire resistance of 480 square cross section normal strength concrete (NSC) columns and 480 high strength concrete (HSC) columns, made with siliceous aggregate, is presented in this paper. The variables considered in the study include concrete strength (NSC and HSC), dimensions of column cross section, axial load ratio, load eccentricity ratio (i.e., ratio of load eccentricity to dimension of column cross section), and steel ratio (i.e., ratio of longitudinal reinforcement to cross-sectional area of column). Explosive spalling of HSC exposed to fire is also considered approximately. Simulation results show that:(1) increasing the dimension of column cross section, reducing the axial load ratio, and reducing the load eccentricity ratio are all effective measures for improving the fire resistance of both NSC and HSC columns subjected to concentric axial load or

Eccentric axial load; (2) increasing the steel ratio has no significant influence on the fire resistance of concentrically loaded NSC and HSC columns, but has some positive effect on the fire resistance of eccentrically loaded NSC and HSC columns; (3) explosive spalling of HSC has a significant detrimental influence on the fire resistance of HSC columns. Based on simulation results, a simplified formula is empirically developed to enable determination of the fire resistance of both NSC and HSC columns, and is shown to be applicable to concrete columns with square cross-section.

Jau and Huang,(2008) in their study investigated the behavior of corner columns under axial loading, biaxial bending and un symmetrical fire loading. The number of test models was four columns with dimensions (300 X 450 X 2700). It was found that under a longitudinal stress ratio of 0.1, the residual strength ratios of the columns after fire loading appear: (a) 2 and 4 hour fire loads lead to residual strength ratios of 67% and 57% in particular; It results in a 10% reduction in residual strength as duration varies from 2 to 4 hours; (b) Reductions in the rebar ratio lead to lower residual strength ratios; and (c) an increase in the thickness of the conical cap results in decreased residual force ratios. It is also found that the temperature distribution across the cross section is unaffected by the thickness of the concrete cover and the proportion of steel. The remaining strengths can be used for future evaluation, repair and strengthening, and this study focused only on low-rise buildings with low axial load. Tall buildings are a different issue. It has high strength.

Chen et al ,(2009) The study was conducted on the effect of fire exposure time on the post-fire behavior of reinforced concrete columns. Nine full size

reinforced concrete columns (45 X 30 X 300cm) with two longitudinal reinforcement ratios (1.4% and 2.3%) were unstressed and exposed to 2 hours and 4 hours with fixed preload. After one month of cooling, the samples were tested in axial load with uniaxial or biaxial bending. The test results show that the residual load capacity decreases with the increase in the exposure time to fire. This deterioration in strength after increasing the exposure time can be slowed down by restoring the strength to the hot rolled reinforcing bars after cooling. In addition, the reduction in residual stiffness is higher than the maximum final load.

Martins and Rodrigues ,(2010) the behavior of reinforced concrete columns was studied with restricted thermal elongation exposed to fire, as the number of models was eleven columns with dimensions (160 X 160), (250 X 250) mm and a length of (3000) mm. The high temperatures caused by a fire overheated the thermal elongation of the structural elements,. It is therefore important to analyze the effect of thermal restriction on the behavior of fire-exposed reinforced concrete columns. Fire resistance tests were performed on reinforced concrete poles with constrained thermal elongation to study this phenomenon. The effect of several parameters tested on the behavior of columns exposed to fire, including longitudinal reinforcement ratio, column thinness, restraint level, load level and load anomaly, as the load level has a significant impact on the performance of RC poles in fire. With an increase in the load level, a significant decrease in fire resistance is observed. With a higher load level, explosive fragmentation is observed.

Martins and Rodrigues ,(2010) in this work. The parametric study looked at high-strength concrete columns with five different loading levels (0.2, 0.3,

0.4, 0.5 and 0.6) and two different heating rates, with a focus on explosive splintering. The second section of the study depicts a 3D finite element (FE) model of reinforced concrete columns under high temperature conditions. The concrete columns were modelled taking into account the embedded reinforcement and crack formation and propagation using the smeared cracks model, which allowed a nonlinear transient structural analysis to be conducted. The comparison of the results of the FE analysis and the tests performed showed a reasonable agreement and a divergence in some cases due to concrete spalling. An assessment of stresses generated in the high strength concrete columns under fire using the FE model is also presented in the paper. The evaluation shows that mechanical and thermal tensile stresses could reach up to 8.69 MPa, which is high enough to cause concrete spalling.

Xiaoyong and Kodur (2011) during their study, results from seven fire-resistant experiments on concrete-coated steel columns under standard fire exposure conditions are presented. Test parameters include column size, 3- and 4-sided fire exposure, load intensity, and eccentricity.The test data were used to study the effect of the above parameters on the thermal and structural response of concrete-coated steel columns. The test results show that columns have a higher fire resistance under 3-side heating than under 4-side heating. Also, the load ratio and the eccentric eccentricity of the load have a marked effect on the fire resistance of columns. In addition, concrete splintering reduces the fire resistance of columns.

Kodur and Raut ,(2012) due to biaxial bending produced by deflection in loads exposure to unilateral 2 or 3 sided fire, an uneven spalling that occurs when reinforced concrete (RC) columns are exposed to fire. When

measuring the fire resistance of RC poles in existing design regulations, the effect of such biaxial bending and sputtering is not taken into account. The effect of various parameters on the biaxial bending generated by fire in RC columns was investigated in this work through a series of numerical studies. The results of parametric research are used to create a simplified equation for determining the fire resistance of RC columns in biaxial bending situations. The suggested equation accounts for the effects of fire fragmentation, fire exposure on 1, 2, 3, or 4 sides, eccentric binary loading, and fire scenario design.The equation's validity is determined by comparing the equation's predictions to finite element analysis and test data. A numerical example illustrates the applicability of the proposed equation to the fire resistance design of RC poles.

Khaliq and Kodur,(2013) the test results for four columns with dimensions of a square cross-section of (203 * 203) mm and a length of 3300 mm for fire resistance on these columns were for fly ash, as the data obtained from the tests on high-strength fly ash concrete columns are compared with those of special With conventional high strength concrete (HSC) columns. The effect of concrete type, fire exposure scenario, fly ash, and fibers in the concrete mix on the fire performance of fly ash concrete columns was observed. The results of the fire resistance tests show that fly ash concrete poles exhibit a fire resistance almost similar to that of conventional HSC poles. Furthermore, the addition of polypropylene fibers reduce fire-induced spalling of high-strength fly ash concrete columns. the capacity to supply both heat and applied loads that are present in a typical structural member exposed to fire**.**

Bikhiet et al, (2014) included fire contributes greatly to the low strength of reinforced concrete columns. The aim of this study is to evaluate the behavior of columns exposed to fire under axial load and to evaluate the decrease in the pressure capacity of the column after fire. There were two parts to this study, the first part being the experimental investigation of fifteen columns Samples (150 X 150 X 1000) mm exposed, except for one sample for a fire (600 °C) for the oven. Columns have different firing durations equal to (0, 10, 15, and 20 minutes) respectively, which is equivalent to (0, 90, 135, and 180 minutes) respectively in the prototype scale. The second part is a theoretical analysis performed using the 3D nonlinear finite element program The main factors discussed were strength of concrete, duration of fire, level of applied loads, yield strength of longitudinal reinforcement, percentage of longitudinal reinforcement and diameters of bars. The comparison between the experimental results and the theoretical analysis showed that for the columns not exposed to fire, the first crack appeared at 80% of the column failure load while the first crack occurred at 50% of the column failure load for the columns exposed to fire.

Nguyen and Tan ,(2014) performed analytical and numerical analyzes in this study to investigate the additional axial forces caused by eccentrically loaded columns , a simplified analytical model is proposed to directly compute the so-called limiting forces owing to heat. Fire experiments on twelve samples of bonded concrete columns exposed to uniaxial and biaxial bending were undertaken at Nanyang Technological University to validate the model. The analytical and experimental results for the evolution of restraint strength were found to be in rather good agreement. As a result, the suggested model may be utilized to describe how axial restriction ratio,

deflection, initial load level, concrete strength, and uniaxial and biaxial bending affect the evolution of restricting forces. It's also clear that analyses based on material models that assumed transient concrete stress overstated the restraining forces that occur in bound RC columns during fire conditions.

El-Shaer,(2014) aimed in his study is to clarify the effect of high temperatures on the behavior of reinforced lightweight concrete columns made of lightweight expanded clay aggregate as a partial (by volume) replacement for normal weight aggregates.Two of the tested columns were exposed to a high temperature of 550°C, for 90 minutes, on four sides. The tested columns were heated using a constant concentric vertical load equal to 1/3 the final loads determined from the comparative control pole test (unheated).

The effects of several variables such as the type of concrete according to its weight, concrete grade and the effect of exposure time were studied numerically. The behavior of the tested columns was analyzed in terms of failure pattern, response to load strains, maximum carrying capacity, rigidity, and durability. Test results are analyzed to illustrate the effects of these studied variables on the tested lightweight concrete columns as well as the normal weight concrete columns.

Wang et al, (2015) natural fires, known as cabin fires, are responsible for carrying the fire in the cabin and are reduced once the fuel is burned. They are widely found and have important effects on concrete columns. In order to explain the mechanism of the combination of external loads and the effects of fire on concrete columns, an efficient and user-friendly method is required. As a first step in this study, a numerical cross-section method was

introduced to obtain interactive curves for columns exposed to fire. This method is then applied to analyze several cases with different thinness ratios. Moreover, different reinforcement ratios and thickness of concrete cover as well as eccentric loads are also considered. Finally, occupancy-specific fires were adopted to study the fire resistance of columns exposed to different natural fires, and tabular data was developed for columns exposed to natural fires.

Balaji et al, (2015) during their study, the elements that affect the firing rate of RC columns were investigated. Various parameters such as thermal limits, conditions, type of reinforcement, distribution of reinforcement, concrete for covering, type of aggregate and strength of concrete have a significant effect in changing the fire rate of columns, to study the influence of these factors. Parameters, columns of different cross-sections such as 300 x 300 mm, 400 x 400 mm are used. and 500 x 500 mm with a column length of 3000 mm.

*Axial capacitance and fire resistance decrease directly with thermal boundary conditions, and have the maximum effect on four-sided columns of fire exposure.

*Concrete cover has a significant impact on fire rating based on thermal criteria. The variance in fire rating based on thermal parameters is more pronounced for smaller cover thickness and on strength parameters for larger covers.

Zhang et al, (2016) during an experimental study of the post-fire behavior of five SRC columns under a combination of eccentric and axial loading, the cross-sectional size of all columns was 280 × 280 mm. The experiment

phenomena and mechanical response of SRC column samples were observed during the experiment, specifically loading, heating, cooling and post-fire loading. The residual load bearing capacity, failure modes and vertical deformation were studied. With the test program, the effects of factors such as load ratio, fire duration and steel ratio were studied**.** It turns out that the temperature delay effects become more pronounced with increasing depth from the hot surface. Some of the SRC column samples failed during the cooling phase. For the other samples, residual deformations were observed when the furnace temperature was decreased to ambient temperature. The effect of some variables including load percentage, fire duration and steel percentage on post fire loads is discussed. It can be concluded that the residual load bearing capacity of SRC poles decreases with increasing fire duration and load ratio, and increases with increasing steel percentage. Finally, a finite element analysis model is developed to simulate the behavior of the tested SRC columns**.**

Kodur et al ,(2017) carried out residual capacity tests on fire-damaged reinforced concrete (RC) columns**.** Two RC columns, first to structural loading and exposure to fire, as in a typical building, then loaded to failure upon cooling to ambient conditions. The column response including temperatures, deformations and fragmentation of the columns were monitored during the heating and cooling phases of fire exposure. When fully cooled, the fire-damaged columns were increasingly loaded until failing to assess residual capacity, as shown in **figure(2-9).** The results of these fire tests indicate that RC poles retain significant residual capacity after exposure to typical building fires. Moreover, the residual capacity of the RC columns, similar to that tested in this study, can reach 34% and 29%

of their nominal (untreated) capacity for a 90 min and 120 min fire exposure, respectively.

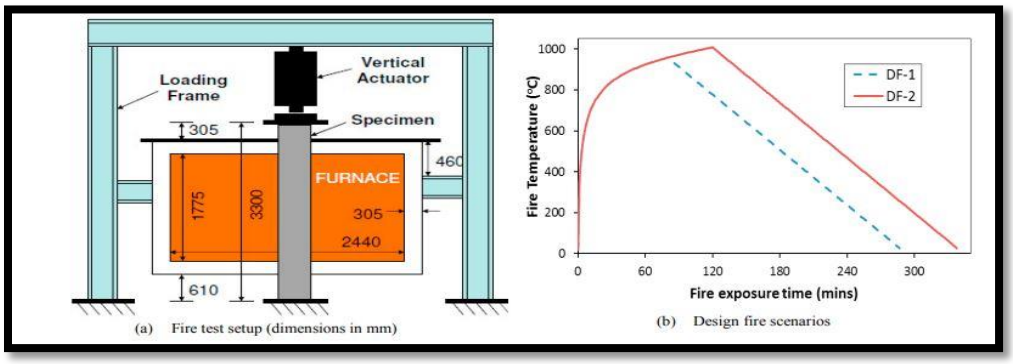

Figure (2-9): Fire test setup configuration and design fire scenarios (**Kodur et al ,2017)**

Aloglaa and Kodur,(2018) the impact of transient creep on the response of reinforced concrete columns under extreme fire exposure scenarios was investigated in this work. To investigate the effect of transient creep on RC columns under simultaneous loading and fire exposure, an ABAQUS 3D finite element model was created. The fire resistance study takes into account temperature-induced transient creep stresses in concrete and rebar, as well as property degradation in component materials, related materials, and geometric nonlinearities. The model is used to assess the impact of transient creep on the fire response of RC columns under various scenarios, including various fire exposures, loading levels, and the number of exposed sides. In a considerably shorter amount of time than a typical building fire. Asymmetric temperature gradients from one or three lateral fire exposures on a column can also amplify the effects of transitory creep, lowering fire resistance. Overall, the findings show that ignoring transitory creep might result in an underestimating of axial displacements and, as a result, an

overestimation of RC column fire resistance, especially when exposed to severe fire situations and at higher temperatures.

Buch and Sharma ,(2019) During the study eleven samples of RC poles were tested in the experiment, six of which were normal strength concrete poles (NSC0 to NSC5) and five high strength concrete poles (HSC0 to HSC4).And all the columns samples were 3150 mm high and all had a square cross-section of (300 X 300) mm. The experimental investigation is performed on 3.15 m column samples. Experimental results indicate that an increase in load deflection (from 20 mm to 40 mm) increases the amount of fragmentation resulting in an exponential decrease in fire resistance (by 43%). Fragmentation is restricted by the increase in the longitudinal bars, especially the center circumference bars, which contributes to an increase in fire resistance of 100% with a doubling of the number of longitudinal bars. Even reduction in transverse reinforcement spacing (from 300 mm to 150 mm) for eccentric loads It increases fire resistance by 123%. However, this advantage is limited by a greater amount of compression face fragmentation (400% more) under eccentric loads, which is seen to increase with reinforcement intensity. For explosively split high-strength columns, a further decrease in fire resistance occurs due to local softening of the longitudinal reinforcement due to early (10 min) and long (up to 58 min) deep fragmentation. The chances of bending the universal column element become more prevalent with the increase in the deflection in the load by about 40 mm. It was concluded that the spal ling levels change with the relative change in the reinforcement details with other parameters under eccentric loads.

Buch and Sharma,(**2019)** Samples were cast vertically in a specially designed frame. Their number was fourteen samples, the length of each column sample was 3.15 m in length of which 2.175 m was proposed to be in the fire zone and the cross section of each column was (300 X 300). And the fragmentation, especially the explosive detonation, has a great effect on the resistance of RC columns to fire. Increasing fragmentation from(15% to 80%) decreases fire resistance by 77%. Also, fragmentation increases by 375% with increasing column strength from 30 MPa to 60 MPa, and fragmentation increases by 750% with increasing eccentric load deviation from (0 mm to 40mm) in normal. Decrease in transverse reinforcement spacing from (300mm to 75mm)lead to increased fire resistance of 102% and 9% for high strength and normal strength RC column respectively.

Kadhim et al ,(2019) the main aim of this research is to investigate the response of the RC rectangular columns under loading simultaneously exposed to fire by using experimental study. The number of test columns were seventeenth columns. The dimension for these columns was 1600mm for length and 150mmx150mm for the cross-section. The columns were tested under axial load with two different types of eccentricity 60 mm 100mm, while the third type of loading is tested as a beam. The eccentric compression load was applied by using top and bottom cap with a column bracket. The eccentric load was applied simultaneously with fire. The test was performed under a high temperature of (400C˚, 600C˚, and 900C˚) on the side of a compression face. At each temperature burning, cooling by two techniques of cooling, and normal cooling (by open air) and fast cooling (by direct water). The experimental results show decreasing in ultimate load capacity with increasing of temperature burning, ultimate load, load-

deflection curve, strain profile, neutral axis, moment-curvature, and ductility. as shown **figure(2-10).**

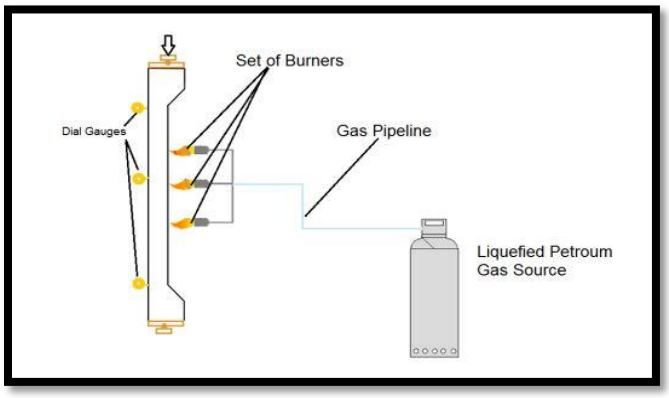

Figure(2-10): The furnace and other equipment and The burner network with a steel box **(Kadhim et al ,2019)**.

Adnan and Ali,(2020) presents the results of experimental and numerical studies of the fundamental response of normal strength concrete (NSC) columns under fire exposure with pre-concentric load. The present study aims to investigate experimentally the behavior of reinforced concrete columns exposed to fire flame with concentric axial load, post-fire behavior under the effect of axial eccentric load. Also, it aims to give a comprehensive account of the fire effects on the ductility and stiffness of these columns. The test results indicated that columns lost about (47.60-51.4) % of bearing capacity after exposure to fire at 500 ^{o}C with one hour. Moreover, increased decrease in residual bearing capacity significantly with increasing load level applied during fire exposure. Also, non-linear finite element (FE) analyses of postfire exposed RC columns with axially load using the ABAQUS computer program is discussed in this study.

Kadhum et al,(2021) the post-fire performance of the reactive powder concrete was investigated in this research. Two periods of time are spent exposing concrete columns to fire at various temperatures (300, 400, and 500 degrees Celsius) (30 and 60 minutes). Starting at 300 degrees Celsius, the RPC columns' residual strength falls as the temperature rises. According to the findings, explosive cleavage might occur in as little as 30 minutes of heating. Minor fragmentation always came first, then massive and severe fragmentation. There were two types of RPC degradation at 500°C: local column failure causes material damage (cracks) as well as overall damage. RPC is more prone to fire-induced fragmentation than NSC. This is most likely owing to RPC's low permeability and high density, which prevents water vapor from leaving at high temperatures, causing high pore pressure and spallation. At 500°C, pressure holes caused explosive fragmentation in RPC columns. Because the longitudinal reinforcement limits the column core and avoids fragmentation, the residual strength of reinforced RPC columns is larger than that of unreinforced RPC columns at high temperatures,as shown in **plate(2-1).**

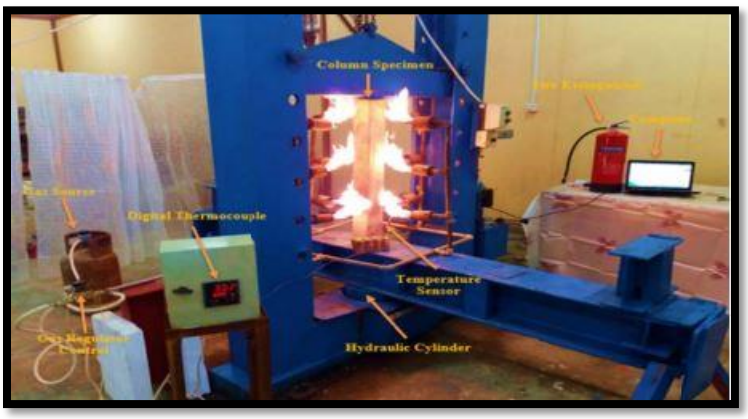

plate(2-1):burning process and load applied(**Kadhum et al,2021**)

2.4 Studies on Strengthening of Fire Damaged Columns:

Kodur et al, (2005) conducted large scale fire retardant experiments on two square columns of reinforced concrete (RC). The pilot program consisted of fire endurance tests on two full size square RC columns. One is unreinforced and the other is FRP coated and insulated. Both shafts were made with ordinary strength; and installed in a specialist test furnace designed to test the loaded columns under exposure to fire.

Data obtained during the experiments show that the fire behavior of insulated and FRP-coated concrete square columns, protected using a suitable fire protection system, is as good as the unreinforced RC columns. It has been demonstrated that satisfactory fire resistance ratings for FRP-coated square concrete columns can be obtained through careful design and by incorporating appropriate fire protection measures into the overall structural system. **Platel (2-2)** shows a square RC column coated with FRP before testing and just after failure. This data showed the following:

*The performance of FRP-reinforced shielded square RC poles at high temperatures can be similar or better than traditional RC poles.

* FRP Reinforced Square RC Poles are Fire-Protected The protection system discussed here is capable of causing fire ratings of 4 hours or more according to CAN/CSA-S101 and ASTM E-119 requirements, under full service loads

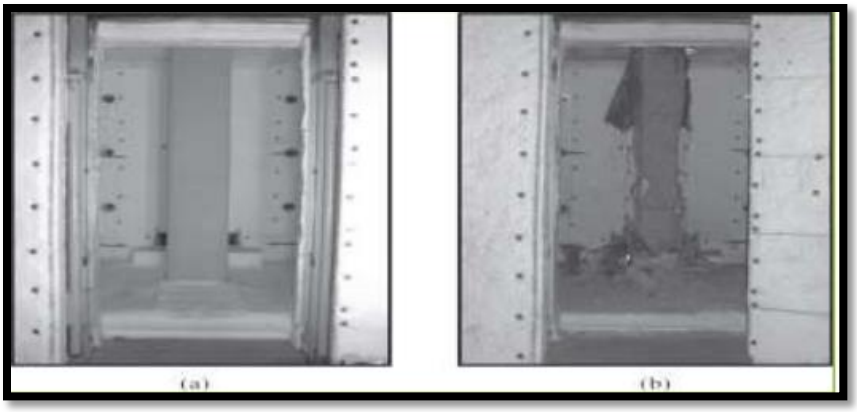

Plate (2-2): FRP strengthened square RC column (a) before and (b) after fire testing **(Kodur and et al, 2005).**

Lixian et al,(2009) an analytical model to calculate the strength of concrete columns is enhanced by the expansion of cross-sections after exposure to high temperatures. The calculated column temperatures and load capacities are compared with those measured. The eleven tested samples are illustrated in **Figure (2-11)**. The results indicated the ability of the analytical model to predict the temperatures and bearing capacities of the reinforced column with an accuracy suitable for structural practice. The model makes it possible to determine the bearing capacity of the booster column after exposure to high temperature for various values of important parameters.

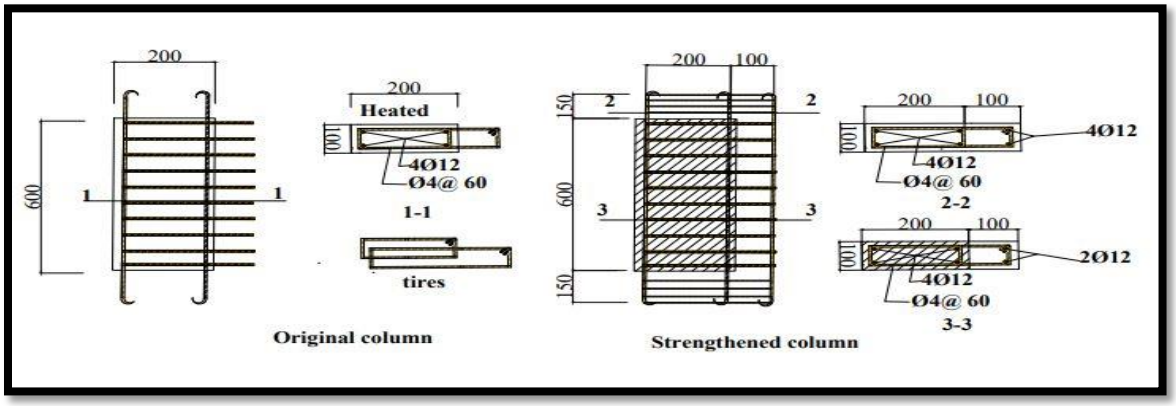

Figure (2-11): Dimensions and reinforcing bars of specimens (**Lixian and et al, 2009).**

Chowdhury,(2009) The results of a research project on the fire performance of FRP materials, fire absorbent and systems, and FRP coiled reinforced concrete columns are presented. The study's ultimate goal is to better understand the fire behavior of FRP materials and FRP reinforced concrete poles, as well as provide fire safety design advice and guidelines for these poles. The research study's aims were met using a combination of experimental and numerical examination. Both small-scale FRP material testing at elevated temperatures and thorough fire tests on FRP reinforced poles were part of the experimental study.

In order to simulate the behavior of unwrapped reinforced concrete and FRP of reinforced concrete with square or rectangular columns in fire, a numerical model was constructed. It was concluded that the numerical model may be utilized to assess the behavior of concrete axial compression members in fire after evaluating it against test data available in the literature.

Externally bonded FRP with a temperature somewhat lower than the resin matrix vitrification temperature can be utilized to reinforce concrete structural members in buildings if a complementary fire prevention system is provided via a FRP reinforcing system,as shown in **plate (2-3).**

Plate (2-3): FRP wrapped and insulated concrete column (a) before fire test, and (b) immediately after fire test (**Chowdhury,2009)**

Yaqub and Bailey, (2011) The efficiency of FRP for recovering heat-damaged circular concrete columns was presented as part of an experimental study. As shown in **plate (2-4),** six columns were simultaneously heated in an unstressed state, along with nine 100 mm cubes as control samples.

It was found that the bearing capacity of the columns after heating They can be restored to the original level or larger than those of unheated columns. However, it was shown that the effect of a single layer of glass or carbon-fiber-reinforced polymer on axial stiffness was not significant. The decrease in the residual stiffness of the heat-damaged column was greater than the decrease in the compressive strength. GFRP or CFRP is very effective in improving the compressive strength of fire damaged circular columns. This is because the subsequently heated columns became "soft" after heating and displayed more lateral expansion compared to the unheated columns.

Plate (2-4): (a) Columns before heating; (b) columns after heating **(Yaqub and Bailey, 2011)**

Chowdhury et al, (2012) Provided fire design suggestions and guidelines that are logical, comprehensive, and safe for these sorts of concrete members. This research resulted in the construction and partial validation of

a computational model capable of simulating the structural behavior of a short or thin column, loaded concentrically or eccentrically, unwrapped or coiled FRP, in both ambient and fire conditions. The structural element of the model's purpose is to determine the eccentric bearing columns failure stress at each time step during exposure to a certain user.

Waryosh et al ,(2012)the results of experimental tests on CFRP reinforced concrete columns subjected to axial load and bending torque are presented in this work. A total of twelve specimens with a square cross-section (120 mm x 120 mm) were constructed and tested until failure was achieved under eccentric pressure loading. The conical biceps samples were 1230 mm long in total. Concrete material type (normal and self-compacting), layer thickness (CFRP), and load deflection (eccentricity ratio/column depth 0.5 and 1) were used as test parameters. All samples are prepared and evaluated until they fail using eccentric pressure loading, as shown in **plate (2-5).** The effect of these factors on the columns' displacement and instantaneous bending behaviors, as well as the fluctuation of longitudinal stress on different sides, was investigated. In comparison to non-reinforced columns, reinforced columns performed significantly better, according to the study's findings**.**

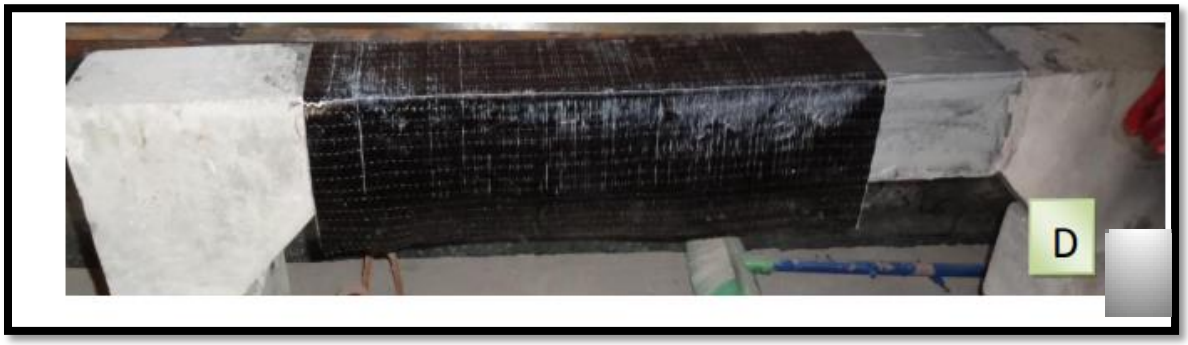

Plate (2-5):application of CFRP on column (**Waryosh at el,2012**)

Abdel-hafez et al, (2014) The major goal of this research is to investigate the behavior of CFRP reinforced concrete columns under axial load after being subjected to fire. Fourteen carbon fiber reinforced plastic columns with various protective layers were subjected to axial load and a temperature of 900°C for 30 minutes. It may be inferred that some protective materials have low thermal conductivity and good fire resistance, and that CFRP materials utilized with suitable fireproof insulation can endure high fire temperatures for more than 70 minutes under service loads .

Physical properties of concrete degrade as temperature rises,CFRP is placed on and around the specimens, and the hidden air is pushed out.

Al-Kamaki et al, (2014) investigated the trapping of concrete with fibre-reinforced polymer (FRP) composites, which can significantly improve its strength and ductility, and this study shows the residual confinement based on 10 identical circular RC columns with diameters of 204 x 750 mm, previously damaged by high temperatures and externally modified using fabrics CFRP, and then tested under axial stress. The RC columns were loaded during the heating and cooling stages, just like genuine structural elements in a fire.

The columns were subjected to a maximum load of 30% in the ambient environment during heating (up to 1000°C) and cooling before being treated with CFRP textiles and finally tested to failure. The findings suggest that CFRP fabric can be used to strengthen heat-damaged RC columns.

Kanaka et al, (2016) The compressive strength and stress-strain behavior of restricted concrete and fiberglass columns were investigated after they were

heated to high temperatures for up to four hours and then cooled to room temperature.

The findings revealed that the GFRP system is extremely effective at restoring the load bearing capacity of concrete columns that have been badly damaged by fire. Both fire-damaged poles and fiberglass are tested, with varying results Three types of concrete columns were tested for compressive strength, flexural strength, and heat radiation: normal columns, fire damaged columns, and fire damaged columns covered in fiberglass. The results demonstrated that stiffening is efficient for fire-damaged columns, restoring the strength and stiffness of the fire-damaged columns effectively..

Alhassnawi,(2018) investigated the influence of Carbon Fiber Reinforced Polymer (CFRP) on the post-fire reinforcement capacity of concrete columns (RC) exposed to fire. To complete this study, the investigation is divided into two parts. The first section is experimental work, which consists of fifteen tiny NSC columns that have been poured and tested. The variables analyzed are the number of lateral fire exposures based on the building plan (two opposite sides, three sides and four sides).The second portion is a three-dimensional finite element analysis utilizing the ABAQUS / standard 2014 computer application. It is decided to make a comparison between the test findings and the numerical modeling results. This analysis was utilized to look into additional key parametric studies for the fire-prone side that were not included in the experimental work, such as concrete cover, reinforcement ratio, eccentricity, and other situations.

The findings of this study revealed that there has been a rise in the number of an RC column's carrying capacity is reduced by a number of side

fire exposures. The effect of adding more reinforcement bars raises the final load of the control samples while increasing the load capacity loss of the columns exposed to fire. The fire-damaged columns' final load was increased after CFRP reinforcement. Because the exposed concrete surface and the carbon fiber-reinforced plastic have a poor connection, this percentage of improvement can be regarded low.

Zhao et al ,(2019) used a structural test to describe the mechanical behavior of the post-fire structure of a subway station. The fire has uncovered a large slab frame-post. The temperature on the sample surface was raised from room temperature to 530°C in 10 minutes, then maintained at that degree for 110 minutes before being cooled back to room temperature. After the concrete on the column peeled, the spaces were filled in and replaced with early strength concrete, which is a blend of early strength cement mortar and unique additives.

Following the repair of one of the fire-damaged columns, the reconstructed structure was subjected to a combination of static vertical and periodic lateral loads. The periodic pass test was used to determine how the post-fire construction would react mechanically under soil stresses and service loads. Damage builds up with increased cyclic loading until hull failure due to shear fracture of the repaired column. The hysterical episodes of the entire structure were thin, indicating that exposure to fire reduces energy dissipation. The results showed that the fire caused severe damage to the structure, which led to a decrease in the load bearing capacity, deformation capacity, and earthquake resistance.

Zhou and Wang,(2019) Over the last two decades, structural fires have wreaked havoc on buildings and destroyed property. As a result, there is a growing demand for structural elements to have post-fire repairs in order to improve their structural integrity. This research provides an up-to-date review of the repair of axial load fire-damaged reinforced concrete (RC) members. The impacts of loading method, physical dimension, and bonding behavior on the residual strength of members are investigated in this paper. Meanwhile, empirical experiments into the performance of fire-damaged RC members with axial load fixed with a concrete cover, steel jacket, and fibre-reinforced polymer (FRP) jacket are summarized. As a result, the FRP casing is a permanent fix; nevertheless, because FRP is sensitive to high temperatures, fire resistance must be supplied to the repaired column

Jxu at el,(2019) investigated The compressive behavior of high-strength circular reinforced concrete columns exposed to fire for (1-2) hours using an ISO834 standard fire curve, air-cooled, and then modified with two layers of transverse carbon fiber reinforced polymer (CFRP) wrapping is presented in this study. Five round RC poles (300mm x 1000mm) were used to assess the effects of fire duration and CFRP jacket efficacy. The load-displacement relationship, CFRP load-strain response, and failure mechanism were all looked at for the columns' compressive behavior. When the pillars were subjected to fire, they produced a significant temperature gradient. The maximum capacity and rigidity of the fire-damaged RC columns were lowered as a result of concrete deterioration at high temperatures, according to the test findings for the unprepared columns. Columns suffer more substantial damage as the firing duration is extended. Carbon fiber reinforced plastic jackets can successfully recover the hardness of fire-

damaged circular columns and improve their ultimate capacity, as shown in **plate (2-6).**

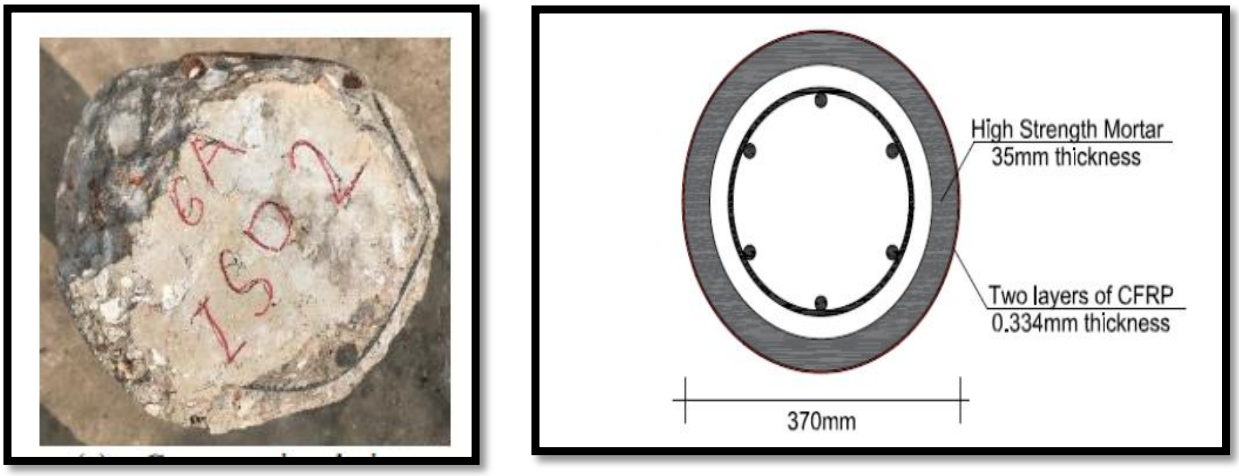

Plate (2-6): Cross-sectional details of retrofitted column (**Jxu at el,2019)**

Ali and Adnan ,(2020) presented an attempt to restore the main structural response characteristics of the damaged reinforced concrete column as a result of exposure to fire. When the building is exposed to fire, it will have an environmental and psychological impact on the community. The burning building is reinforced with environmentally friendly materials to return the building to its original size without alteration: cross-section or areas, operational function and specifications. This research showed that Reactive Powder Concrete (RPC) is effective in strengthening concrete columns to increase the load capacity and distortion. An experimental and numerical program was implemented to study the compressive strength, ductility and stiffness behavior of reinforced concrete columns after being heated to elevated temperatures (500°C) for one hour and cooled to room temperature. The results showed that RPC is very effective in enhancing the load bearing capacity of even the concrete columns that have been severely damaged by fire. The results show that the stiffening is effective for fire-damaged

columns, which can effectively restore the strength and stiffness of fire-damaged columns, as shown in **plate (2-7).**

Plate (2-7): Steps for repairing damaged RC column. **(Ali and Adnan,2020)**

Qiul at el ,2021 Studied the post-fire repairs in connection to various types of repair procedures (FRP, steel plates, enlarged concrete section) and structural members such as columns, beams, and slabs. The fire scenarios used in these research that caused damage are divided into three tiers based on the duration of the gas phase temperature exceeding 600°C. In terms of restoration methodologies and fire intensity levels, the effectiveness of the repair was summarized and compared in terms of the restored performance of the concrete structural members compared to the initial undamaged performance. The findings demonstrated that while recovering ultimate strength is possible, restoring stiffness is more challenging. Furthermore, the present fire loading scenarios used in post-fire repair studies are mainly effective, as shown in **plate (2-8).**

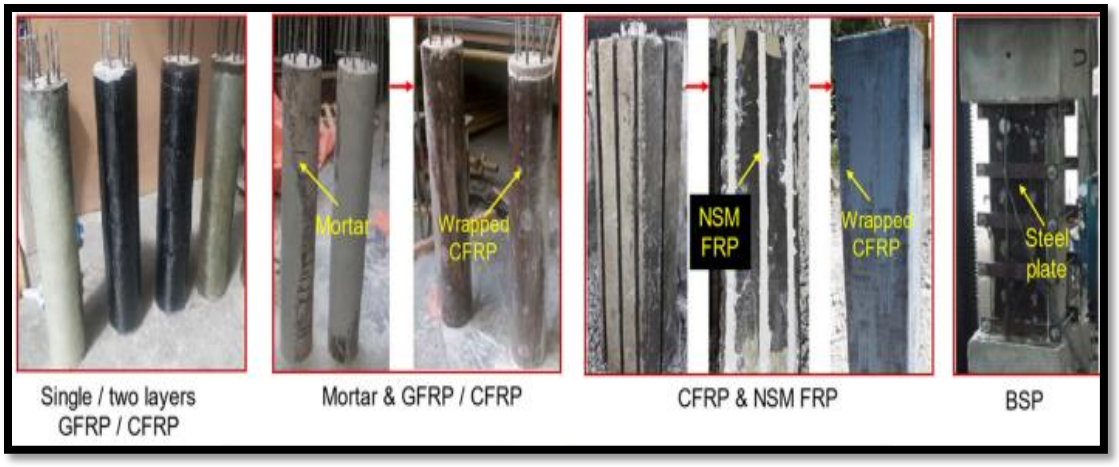

Plate (2-8): repairing damaged RC column**(Qiul at el ,2021)**

2.5 Summary and Concluding Remarks:

From the review of previous studies including scientific experiments of concrete columns exposed to high temperatures during fire, and the technical method for repairing and retrofitting of RC columns damaged by fire, The following conclusions can be summarized :

1- Decrease in ultimate bearing capacity, stiffness, ductility factor and energy dissipation capacity of RC columns after exposure to fire.

2-The Columns that subjected to cyclic side loading under constant axial load during burning resulted in significant degradation of the load-carrying capacity during the cooling phase.

3-The behavior of HSC columns at high temperatures is significantly different from that of NSC columns at the same temperature due to their coherent microstructure and low transmittance. The resistance of HSC columns to fire is lower than that of NSC columns, as it was observed that

HSC columns showed early fragmentation in the corners while no fragmentation occurred in NSC columns.

4- The authors concluded through their scientific research that the properties of the materials have a greater influence on the failure patterns of the concrete columns under effect of fire conditions

5-The ratios of the residual strength of the columns after loading with fire are shown: (a) Particular residual strength ratios are produced by exposure to the fire for two hours and four hours; It has a duration of 2 to 4 hours, which causes a decrease in residual strength; (b) The reduction in residual strength ratios is influenced by changes in the ratio of rebar; and (c) the residual force ratios decrease when the conical cap's thickness is increased.

6-The lack of research or studies that dealt with the behavior of reinforced concrete columns in the presence of axial loads and under the influence of cyclic fire exposure , so the present study deal with this type of fire exposure and many variables in this field .

7-There are also many studies that dealt with strengthening or repairing of columns exposed to the heat of fire, either by using FRP products or by increasing the damaging of the cross-section. This study includes restoring or repairing pre-loaded concrete columns exposed to fire by replacing the damaged outer shell using **RPC** or **NSC** with **CFRP** laminates.

Chapter Three
Experimental Work

Chapter Three

Experimental Work

3.1 Introduction

The main aim of this study is to investigate the structural behavior of concrete columns that have been subjected to periodic burning by looking of the number of cycles, amount of temperature target, fire duration, as well as the type of concrete (NSC and HSC).Then evaluating the serviceability and strength requirements of damaged fire exposed strength of columns after repairing . Details of the experimental program are described in this chapter. It outlines the research technique utilized to meet the first chapter's objectives, as well as the materials employed, mixing ratios, column sample preparation, the process of burning column samples, repair of the fire exposed columns, the process of burning column samples ,and the test procedure.

3.2 Test Program

The current experimental program included a series of tests on a variety of building materials, control specimens (cubes, cylinders), and eighteen reinforced concrete columns, one of which was used as a pilot.

The program was carried out in the laboratories University of Babylon Department of civil Engineering. The reinforced columns were made of either homogenous concrete (NSC or HSC) for fired columns or hybrid concrete (RPC and NSC) for repaired. **Table (3-1)** show the details of all column groups , where the program included the following objects:

1- Experimental study of the column behavior under effect of periodic burning that included a number of variables :

a-Effect of concentric and eccentric pre-loading on column through constant or cyclic fire exposure .

b-Effect of scenario of cyclic fire exposure (time duration of each cycles ,number of cycles, target of temperate of each cycle).

c- Role of longitudinal steel reinforcement ratio.

d-Type of concrete columns (HSC or NSC).

2-Introduce practical methods for repairing and restoring the strength and performance of damaged RC. due to exposure to cyclic fire ,by:

a-Developing a hybrid concrete cross section of RPC for the added outer shell and NSC for the primary concrete core.

b-Utilizing (NSC) to compensate damaged outer shell with (CFRP) laminates warps and NSC for the primary concrete core.

3-Evaluating of the structural performance of eccentric and concentric tested column through and after exposure to fire by ultimate strength, cracking pattern, failure mode, and load deformation response.

4-Evaluating the activity of proposed retrofitting methods for damaged columns through ultimate strength , cracking pattern, failure mode, vertical and lateral deformation.

Table(3-1): Details of Tested Columns Specimens *****

Group No.	Specimen Symbol (Ci)	Type of concrete	Steel Reinfo-rcement Ratio (ρi)	Eccentricity of pre - load (Ei)	Fire exposure History (Senario)(F)	Note
	PC	*N*	ρ_1	E_1	*F*	*Pilot*
Group1	$NC_1S_1E_1$	*N*	ρ_1	E_1	-	*control*
	$NC_2S_1E_1F_1$	*N*	ρ_1	E_1	F_1	
	$NC_3S_1E_1F_2$	*N*	ρ_1	E_1	F_2	
	$NC_4S_1E_1F_3$	*N*	ρ_1	E_1	F_3	
	$NC_5S_1E_1F_4$	*N*	ρ_1	E_1	F_4	
	$NC_6S_1E_1F_5$	*N*	ρ_1	E_1	F_5	
	$NC_7S_1E_1F_6$	*N*	ρ_1	E_1	F_6	
Group2	$NC_8S_1E_2F_1$	*N*	ρ_1	E_2	F_1	
	$NC_9S_1E_2F_3$	*N*	ρ_1	E_2	F_3	
Group3	$NC_{10}S_2E_1$	*N*	ρ_2	E_1	-	*control*
	$NC_{11}S_2E_1F_1$	*N*	ρ_2	E_1	F_1	
	$NC_{12}S_2E_1F_3$	*N*	ρ_2	E_1	F_3	
Group4	$HC_{13}S_1E_1$	*H*	ρ_1	E_1	-	*control*
	$HC_{14}S_1E_1F_1$	*H*	ρ_1	E_1	F_1	
	$HC_{15}S_1E_1F_3$	*H*	ρ_1	E_1	F_3	
Group5	$NC_{16}S_1E_1F_3R_1$	*N*	ρ_1	E_1	F_3	*Repaired(R1)*
	$NC_{17}S_1E_1F_3R_2$	*N*	ρ_1	E_1	F_3	*Repaired(R2)*

***** see **Fig (3-1)** for designation symbol.

3.2.1. Designation of Column Specimens

Each of these column models has its unique symbol to set it apart from the other samples, which include (the column number, type of concrete, number of fire exposure cycles, fire duration ,temperature target , eccentricity of pre-load deviation, steel reinforcement ratio, repairing technique scheme).

Where each symbol is referred in **Figure (3-1)** which illustrate the naming convention used to identify the column specimens.

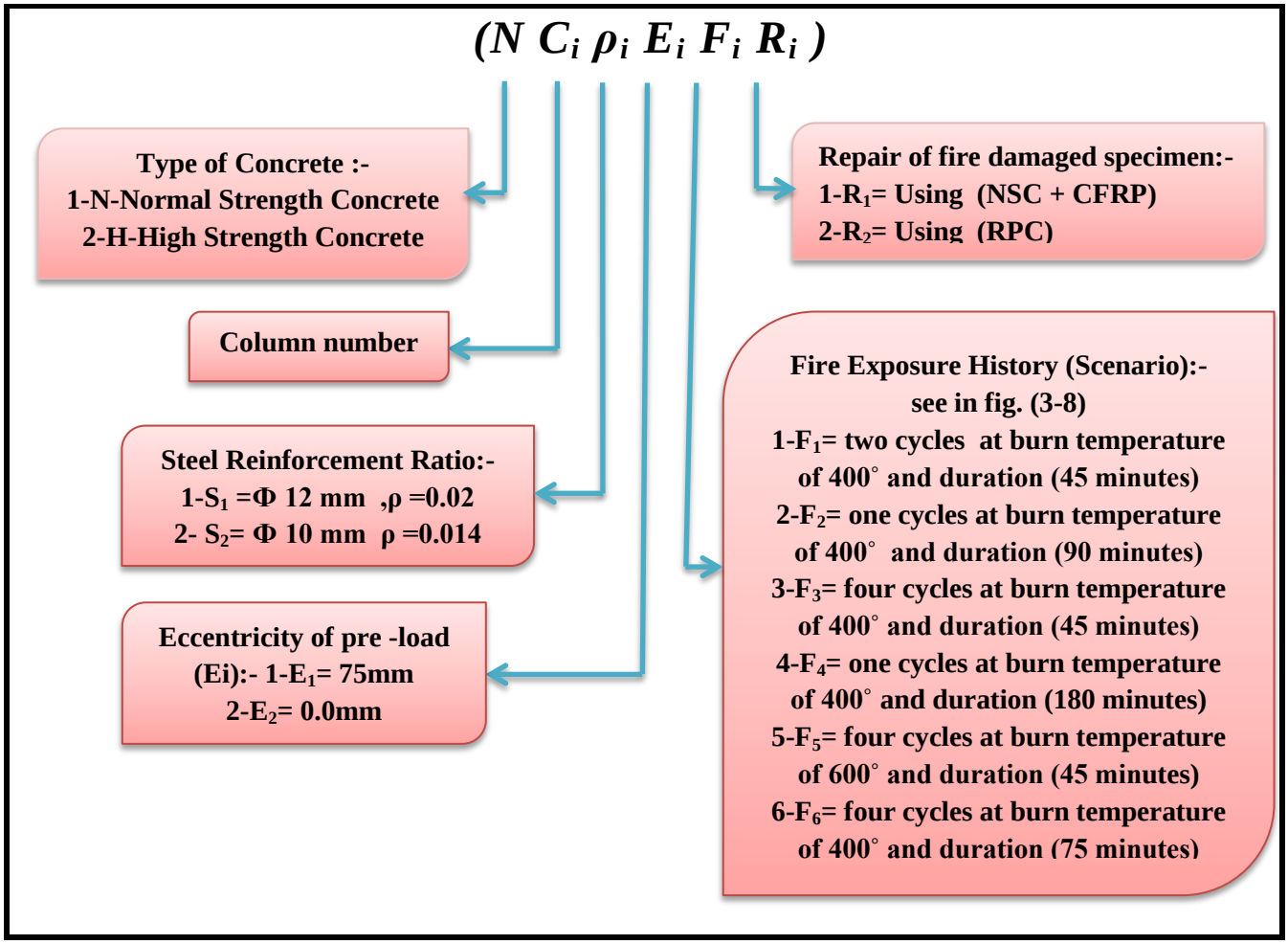

Figure (3-1): Designation Symbol of Tested Specimens

3.2.2 Description of the Tested Columns

The tested models have a constant shape and size. The cross-sections of these columns are square and total length of each column is (1300) mm . The middle cross-section of the column of dimensions (150 X 150) mm and length (700) mm, the corbel dimensions are (150 X 300 X 300) mm. The aim of the corbel is to apply the eccentric load through and after burning , as **shown in figure (3-2).** All columns, were reinforced with (4-Φ12 mm) deformed steel bars as longitudinal reinforcement (ρ = 0.02) and three columns reinforced with (4-Φ10 mm) deformed steel bars as longitudinal

reinforcement (ρ = 0.014), with a transverse concrete cover of thickness (25 mm). Steel ties of (Φ4 mm)and a distance of 100 mm (c / c) are also used in the columns. Fifteen columns are made of normal strength concrete (two columns were repaired after fire exposure),and three columns are made of high strength concrete. All columns and corbels have been designed according the specification **(ACI Code 318, 2019)**, as shown **Figures (3-3 (a, b)).**

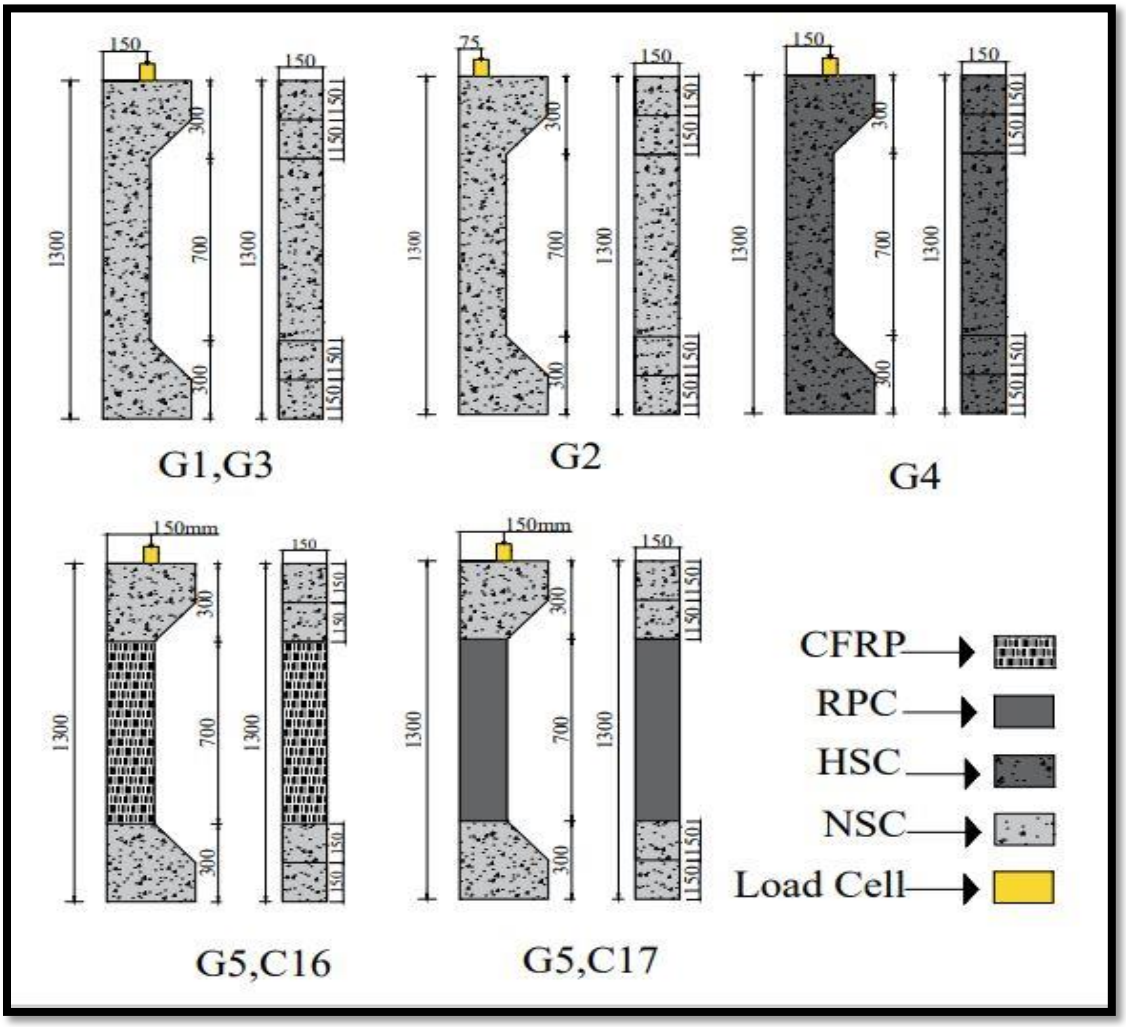

Figure (3-2): Geometry of Column(side view and front view) .

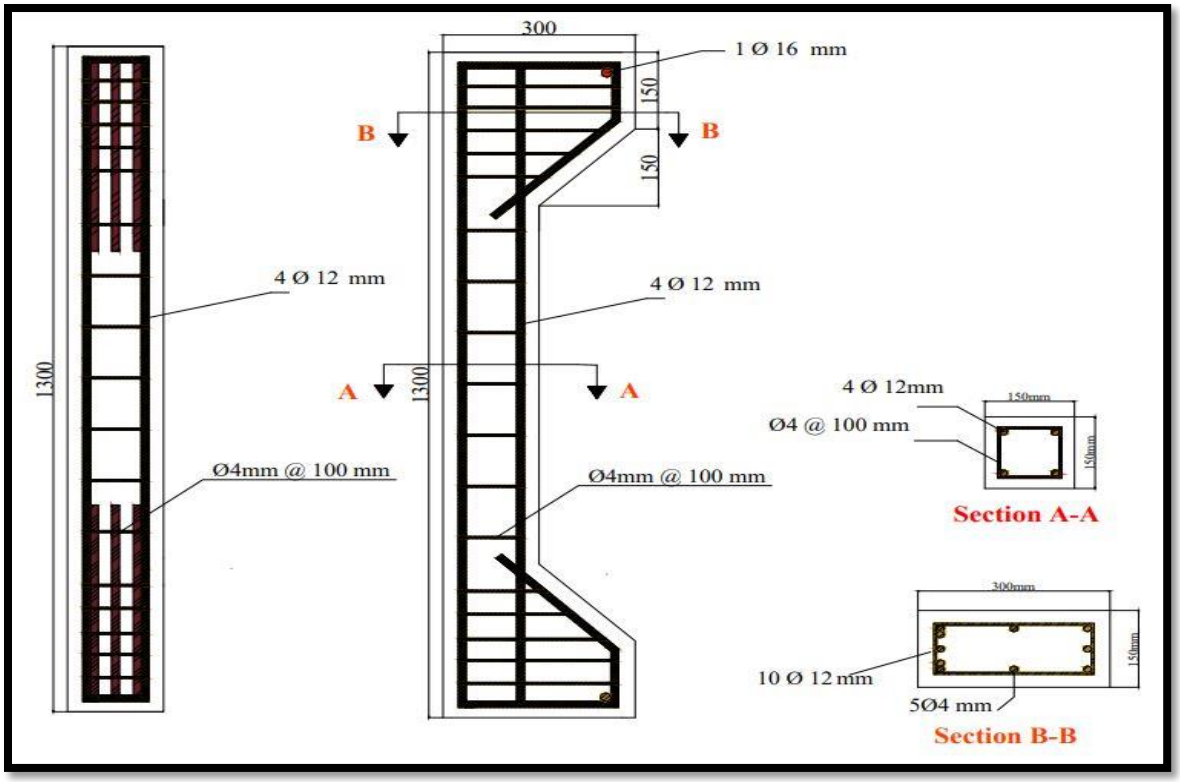
300
1 Ø 16 mm
150
150
B
B
4 Ø 12 mm
4 Ø 12 mm
1300
A
A
Ø4mm @ 100 mm
Ø4mm @ 100 mm
4 Ø 12mm
Ø4 @ 100 mm
Section A-A
300mm
10 Ø 12 mm
5Ø4 mm
Section B-B

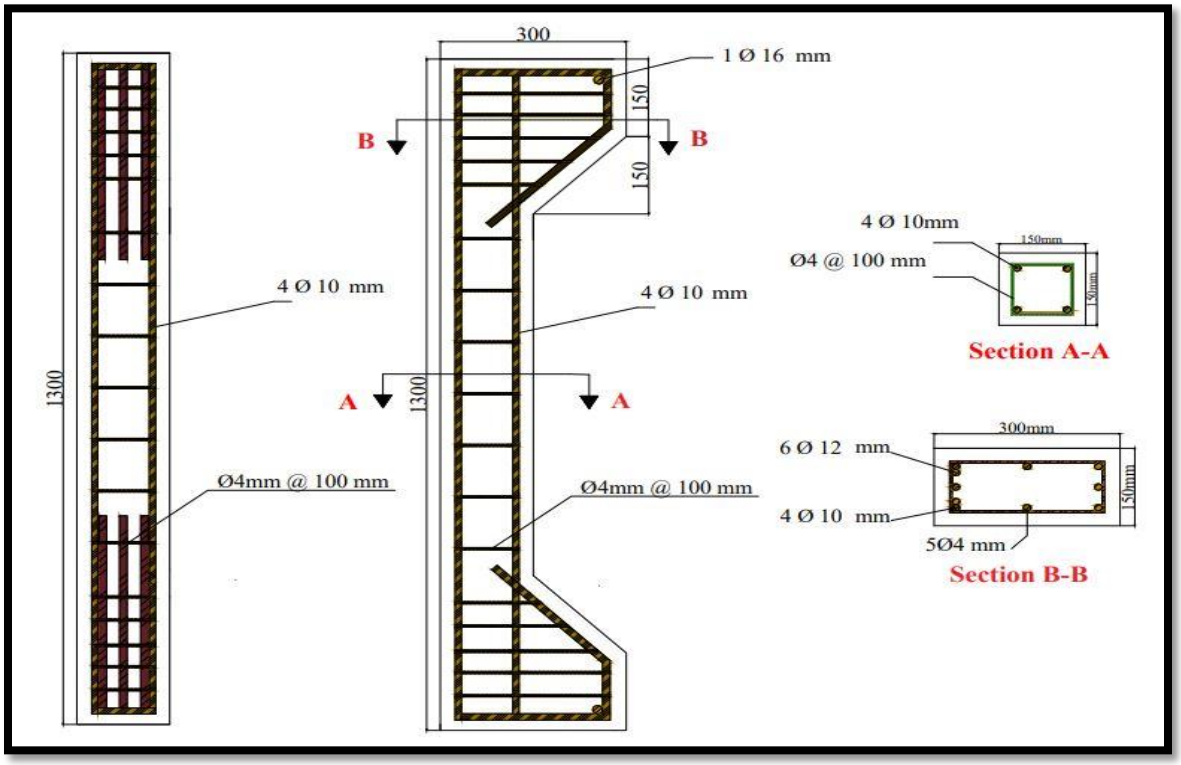
300
1 Ø 16 mm
150
150
B
B
4 Ø 10 mm
4 Ø 10 mm
1300
A
A
Ø4mm @ 100 mm
Ø4mm @ 100 mm
4 Ø 10mm
Ø4 @ 100 mm
Section A-A
300mm
6 Ø 12 mm
4 Ø 10 mm
5Ø4 mm
Section B-B

Figure (3-3

3.2.3. General description of specimen Groups

The current experimental program includes cast, burning and testing of (17) columns specimens divided into (5) groups in addition to pilot one, see in **Table(3-1)**details of flames for fire exposure and scenarios of cyclic burning for Fire Exposure, are shown in **Figures (3-4) and (3-8)**, respectively.

The first group consisted of seven columns (C_1 to C_7) to study the effect of fire exposure scenario. All other columns were subjected to pre-load (0.30Pu) with eccentricity (e=75mm) ,(e/h=0.5) through fire exposure, The first column (C_1) is a control in this group, and without exposure to fire, The remaining columns were subjected to cyclic burning with continuous loading (30%Pu).Column (C_2) was subjected to cyclic burning with temperature (400C˚) of two cycles (two day) and a duration of time heating (45 min) for each cycle. Column (C_3) was subjected to burning of one cycle with burning time (90 min) at temperature target (400C˚), while column (C_4) was subjected to periodic burning at a temperature of (400 C˚) of four cycles (four days) with burning time (45 min),for each cycle, while (C_5) was subjected to cyclic burning at a temperature of (400°C) of one cyclic with burning time (180 min). Column (C_6) was subjected to periodic burning at a temperature of (600°C) of four cycles (four day),and a duration of time heating (45 min) for each cycle, while the column (C_7) was subjected to a cycle of burning at a temperature of (400°C) of four cycles (four day), and a duration of time heating (75 min) ,see **Fig (3-8)** .

The second group consisted of two columns,(C_8,C_9) to study the effect of eccentricity ,and subjected to periodic burning with constant concentric pre-loading (30%Pu) (e=0), column (C_8) was subjected to cyclic burning of temperature of (400 C˚) of two cycles (two days), with burning time (45

min) for each cycle with pre-load(30%)Pu, while column (C_9) was subjected to periodic burning at a temperature of (400 C˚) of four cycles (four days) ,with continuous loading, with burning time (45 minutes),see **Fig (3-8).**

The third group to study the effect of a longitudinal steel ratio consisted of three columns (C_{10},C_{11},C_{12}) with ratio of steel reinforcement (0.014), (4-Φ10) mm , column (C_{10}) was a the sample control in this group, and without exposure to fire, while two other columns were subjected to periodic burning with continuous loading (30%Pu) of eccentricity (E=75),(e/h=0.5) at temperature (400C˚). Column (C_{11}) was subjected to cyclic burning of two cycles (two days) of burning time (45 min) for each cycle, while column (C_{12}) was subjected to cyclic burning of four cycles (four days) with a burning time (45 min) for each cycle, See Fig. (3-8).

The fourth to group study effect concrete type, consisted of three columns (C_{13}, C_{14}, C_{15}) consisting of high strength concrete and reinforcing steel ratio (ρ=0.02). The first column (C_{13}) is the control without exposure to fire, and other two columns are subjected to periodic burning at temperature target (400C˚), with continuous loading (30%Pu) and eccentricity (e=75) , (e/h=0.5). Column (C_{14}) is subjected to periodic burning with two cycles (two day) with a burning time (45 min) for each cycle, while the column (C_{15}) is subjected to periodic burning of four cycles (four days) with a burning time (45 min) for each cycle, See **Fig. (3-8).**

The fifth group consisted of two columns (C_{16} and C_{17}) made of normal strength concrete (NSC) with steel reinforcement ratio (ρ=0.02) (4-Φ12mm) that were subjected to periodic burning of four cycles with pre-loading at (30%Pu) and eccentricity (e=75) of temperature target (400C˚) and four

cycles (four day) with a burning time (45 min) for each cycle, and after cooling they were repaired and strengthened. (C16) was retrofitted through compensating the outer damaged shell by (NSC) with wrapping by (CFRP) laminates, while (C_{17}) was repaired with replacing the outer damaged shell by (RPC).

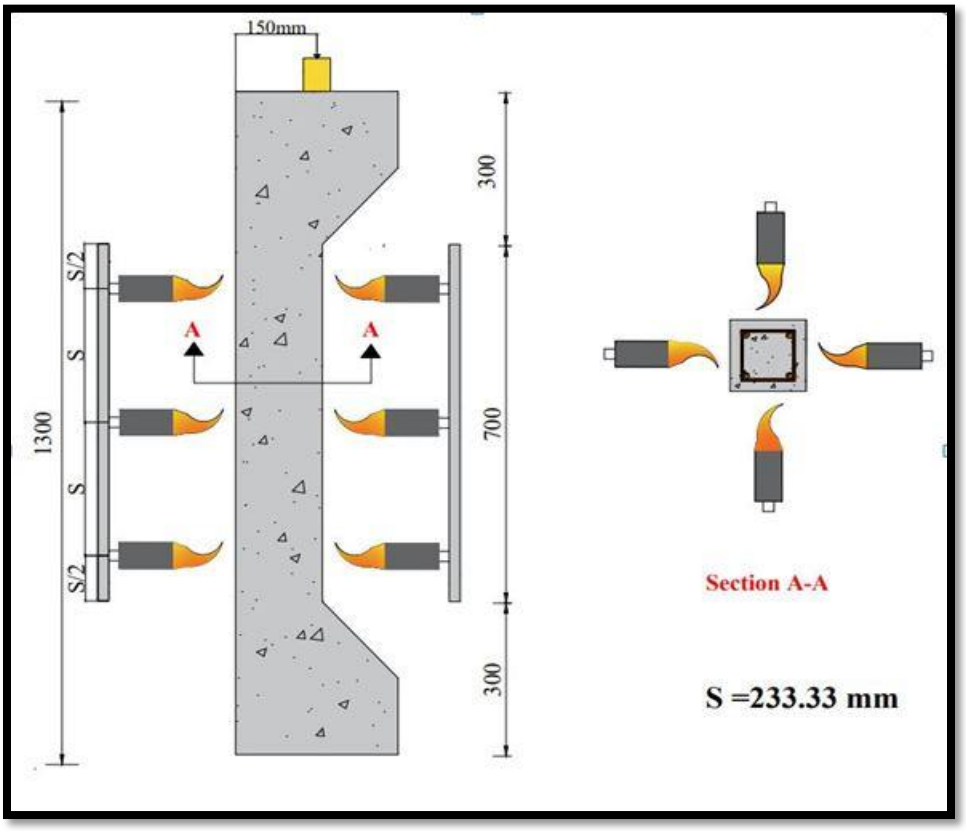

Figure (3-4) : Details of Tested columns Fire Exposure.

3.3 Properties of Construction Materials

It is imperative to know the properties and characteristics of constituent materials of concrete, which is a composite material made up of several different materials such as gravel, sand, water, cement, and admixtures. In order to ensure adequate production of concrete, stringent procedures adopted in materials selection, controlling and proportion of the whole

ingredient. Under this experimental investigation, the sources of materials, chemical compositions and physical properties of the materials that were used are described in detail, as illustrated below.

3.3.1 Cement

Throughout this investigation Ordinary Portland cement (type1) was used for casting all type of concrete (NSC,HSC and RPC) of the columns models and samples. The chemical and physical properties are listed ,in Tables **(3-2)(3-3).** these properties have been checked according to the **Iraqi specification No.5/1984** for ordinary Portland cement. The chemical and mechanical properties of the cement used have been tested in Construction Material and Environmental Laboratories at University of Babylon.

Table. (3-2): Chemical properties of cement

Chemical Test Results		
Oxide	Test Results	Limits of IQS No.5:1984
Lime CaO%	62.41	-------
Silica SiO2%	20.88	-------
Alumina Al2O3%	4.06	-------
Iron oxide Fe2O3%	5.40	-------
Magnesia MgO%	1.60	≤ 5%
Sulfate SO3(%)	1.19	≤2.5% if C3A < 5%
Loss of Ignition.(%) L.O.I	2.68	≤ 4 %
Total	98.22	-------
Free Lime (%)Free CaO	0.84	≤4%
Insoluble Residue.(%) I.R	0.56	≤ 1.50%
Lime Saturation Factor L.S.F	0.91	0.66 - 1.02
M.S%	2.21	-------
M.A%	0.75	-------
C3S%	53.57	-------
C2S%	19.45	≤ 3.5%
C3A%	1.62	-------
C4AF%	16.43	-------

Table (3-3): Cement Physical Properties

Oxide	Test Results	LimitsofIQSNo.5:1984
Setting time Initial (minute)Final (minute)	02:23 03:25	≥ 45 min ≤ 600 min
Fineness (m^2/kg)	326	≥ 250 M^2 /kg
Compressive strength (MPa)3 days	20.33	≥(15)Mpa
7days	28	≥(23)Mpa
Soundness (auto clave),(%)	0.22	≤(0.8)Mpa

3.3.2 Fine Aggregate (Sand).

Natural sand was used for the NSC,HSC and RPC mixes of this investigation. The fine aggregate used in NSC has (4.75mm) nominal maximum size with a rounded particle shape and smooth texture with a fineness modulus of (2.07). While for RPC natural sand was separated by sieving to get a maximum size between (150-600) μm. The fine aggregate grading is ,shown in Table (3-4) ,which conforms to the **Iraqi specification No. 45/1984** the physical and chemical properties of the fine aggregate, are listed in **Table (3-5)**. Fine aggregate has been tested at the University of Babylon in the Construction Material and Environmental Laboratories of the civil Engineering Department ,as shown in **Plate (3-2).**

Table (3-4): Sieve analysis of sand

Sieve size(mm)	Passing %	
	Sand (%)	Limit of IQS No. 45/1984 for GradeNo. (2)
10	100	100
4.75	99.8	90-100
2.36	83.80	75-100
1.18	63.60	55-90
0.6	40.22	35-59
0.3	10.47	8-30
0.15	4.40	0-10

Table (3-5): Physical and Chemical Properties of Fine Aggregate.

Property	Test Results	IQS No. 45/1984 forGrade No. (2)
Specific gravity	2.65	--------
Fineness modulus	2.07	--------
Materials finer than sieve 75 μm %	2.7	≤ 5
Sulfate content SO_3(%)	0.35	≤(0.5)

3.3.3 Coarse Aggregate (Gravel)

Rounded, well graded gravel of (14mm) maximum size from Badra quarry was used as a coarse aggregate in NSC. The gravel was passed from sieve size (14 mm) to separate the oversize and cleaned by water several times, after that, it was left to dry. The sieve analysis of aggregate satisfied the requirements of **Iraqi specification No.45/1984** as presented in Table(3-6), and shown in **Plate (3-3).**

Table (3-6): Sieve analysis of gravel

Sieve size(mm)	Passing Ratio (%)	
	Gravel	IQS NO.45/1984
14	100	90-100
10	83	50-85
5	2	0-10
2.36	0.60	--------

3.3.4 Silica Fume

MEYCO MS610 grey densified silica fume from BASF Chemical Company was used in RPC. Silica fume is an extremely fine powder, its particles are hundreds of times smaller than cement particles, always used in small percentage even as partial replacement of cement or as an additive to enhance concrete properties. Results of tests of silica fume used in this

experimental work are indicated in **Table (3-7),** and it conforms to the chemical **ASTM C1240-04** ,as shown in **Plate (3-1).**

Table (3-7): Results of Silica Fume Tests.

Oxide Composition	Oxide Content %	Limit of Specification Requirement ASTM C 1240
SiO_2	93.23	>85
Loss on Ignition (%)	1.38	<6.0
Specific surface (m^2/g)	22.15	>15
Absorption (%)	0.72	-----

Plate (3-1): Silica Fume.

3.3.5 Steel Fibers

The addition of fibers to the concrete mix constribte to reduce cracks, improve impact resistance, and increase overall concrete strength. This form of reinforced concrete is suitable for use in residential buildings as well as driveways to commercial parking lots. As indicated in **plate (3-2)**, a short straight copper-coated steel fiber with an aspect ratio of (65) was utilized, with parameters specified in **Table(3-8).**

Plate (3-2): Micro Steel Fibers.

Table (3-8): Properties of The Steel Fibers.*

Property	Specifications*
Type	WSF0213
Surface	Brass coated
Relative Density	7860 kg
Tensile Strength	Minimum 2300MPa
Modulus of Elasticity	203 GPa
Form	Straight
Melting Point	1500°C
Average Length	13 mm
Diameter	0.2mm±0.05mm
Aspect Ratio	65

*From Technical Report

3.3.6. Admixture (Superplasticizer)

sikaViscocrete-5930 (SP) is high range water reducing admixture (HRWRA) which was used in RPC. It is a third-generation superplasticizer (SP) and an aqueous solution of modified Polycarboxylic, as shown in **Plate (3-3)**. SikaViscocrete-5930 have not contained chlorides. Also it conformed to **ASTM C494-05, 2005** (type F and type G) and conformed to **BS EN 934 part 2, 2001**. It was used in current study by adding with mix water in (HSC and RPC). **Table (3-9)** shows the main properties of **Sika Viscocrete- 5930** from the manufacturer data sheet. 2009 .

Plate (3-3): SikaViscocrete-5930.

Table (3-9): Technical description of SikaViscocrete-5930.

Basis	Aqueous Solution of Modified polycarboxylate
Boiling	100°C
Hazardous decomposition products(Hazardous Reactions	No hazardous reactions known.
Odor	None
Appearance	Turbid liquid
Colour	Light yellow
Density	1.08 kg/It. ± 0.005
pH	7-9
Labeling	No hazard label required
Chloride content	None
Toxicity	Non-Toxic under relevant health and safety
Storage	Protected from direct sunlight and frost attemperatures between + 5°C and + 35°C.
Transport	Non-hazardous.

3.3.7 Steel Reinforcing bars

During this study, deformed steel reinforcing bars of Ukrainian regulation (**Φ12, Φ10,** and **Φ4**) mm were used. Reinforcing bars with a diameter of (**Φ12,Φ10**) mm were used as the main reinforcement for column and bracket, the bars with a diameter of (**Φ4**) mm was used for ties, indicated Table (3-10), gives the tensile test results for reinforcing bars according to **ASTM A615/A615M-15a, 2016**.The tensile test was carried out in the laboratories of the College of Materials Engineering, University of Babylon

,as shown in **plate (3-4)** and **Table (3-10).** Regarding the measurement of the actual diameter of the bar reinforcement, this examination was carried out in the health laboratory of the Civil Engineering Department, the University of Babylon.

Plate (3-4) :Testing of Steel Reinforcing Bars.

Table (3-10): Properties of Reinforcement Steel Bars

Nominal Diameter (mm)	Actual Diameter (mm)	Yield Stress (MPa)	Ultimate Stress (MPa)	Elongation%
4	3.92	690	760	4.44
10	9.97	613	704	8.33
12	11.84	600	680	11.76
16	15.89	589	670	14.63

3.3.8 CFRP products

The type of CFRP laminates used in this study is (**Sika Wrap Hex-230C**),as shown in **Plate (3-5).** When CFRP sheets are loaded in tension, they show no plastic behavior before rupture. The tensile behavior of CFRP

is characterized as a linearly elastic stress-strain relationship to failure, properties of the Sika Warp Hex-230C sheets and Sikadure-330 taken from manufacturer's specification (**Technical Data Sheet of Sika 2005**), as shown in **Table (3-11).**

Table (3-11): Properties of Carbon Fiber Reinforcement Plastics Sheets (CFRP)

Property	Amount
Thickness of layer (mm)	0.1375
Width of layer (mm)	400
Component fiber ultimate strength (Mpa)	4200
Component fiber elastic modulus (Mpa)	235000
Component fiber ultimate strain (%)	1.8

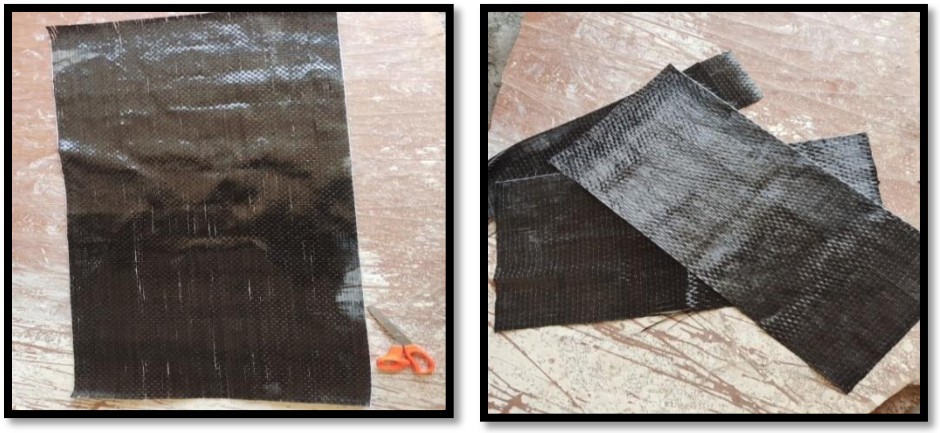

Plate (3-5) :CFRP Laminates

3.3.9 Epoxy Resin

Impregnating resin of type **Sikadur-330**, which is composed of two parts (Resin part A + Hardener part B) to mixing ratio (1:4) has been used in this study for the bonding of CFRP sheet, the properties of the bonding epoxy taken from manufacturer's specification (**Technical Data Sheet of Sika 2005**).as show in **Plate (3-6).**

Plate (3-6) : Mixing Two Components of Epoxy Resin

3.3.10 Epoxy Adhesive

Nitobond EP is the most suitable adhesive to bond two different types of concrete ,as shown in **Plate (3-7).** It is based on solvent-free epoxy resins containing pigments and fine fillers. It is supplied as a two-component material in pre-weighted quantities ready for on-site mixing ratio**(1:1.7)** and use. The 'base' component is white and the 'hardener' component is green, providing visual evidence that adequate mixing has been achieved. Its main properties as supplied by the manufacturer, are shown in **Table (3-12).**

Plate (3-7): Two Components Epoxy Adhesive Nitobond EP**.**

Table (3-12): Technical properties of bonding materials.*

Test method	Typical result
Compressive strength	≥50 N/mm^2
Water absorpation	≤ 0.2%
Slant shear	≥10 N/mm^2
Viscosity	4 ± 10 N/mm^2
Adhesive bond to concrete	≥1 N/mm^2 or substrate failure

*from manufacture (data sheet)

3.4 Concrete Mix Design

3.4.1 Normal strength concrete (NSC)

The mix of normal strength concrete was designed according to (**ACI- 211, Neville 2000)**. After several trial mixes, it was found that a mix of proportions (1:1.73:2.2) (by weight) cement, sand, gravel, respectively, and (0.49) water-cement ratio was appropriate for using to pour in all specimens. The trail mix has a 28-day for cubes (150*150*150)mm compressive strength of (31.79MPa). Mixture proportions are given in **Table (3-13).** Also, it was found from the trail mix that the admixture used in this study produced good workability and uniform mixing of concrete (no segregation).

Table (3-13): Proportions of Concrete Mixes (Normal Strength Concrete)

Experimental Materials	Mix1	Mix2
water/cement ratio	0.5	0.49
Cement (kg/m3)	391	423
Sand (kg/m3)	763	732
Gravel (kg/m3)	876	934
Water (kg/m3)	195.2	207
f c'u		39.98
f c' (28 days) MPa		31.79

f'c=0.8f'cu =0.8*39.98=31.79 MPa** ***Al-Mashhadany (2009)

3.4.2 High Strength Concrete (HSC)

Mix preparation and design for HSC are more important compared to NSC. Production of HSC requires careful selection of materials. Chemical

additives (superplasticizers) are necessary to improve the workability of mixtures with a low ratio (w / c). Therefore, many experimental mixtures were made during the early stage of the present work and some attempts were made at the rate of (3-5) cube (100*100)mm. The experimental mixtures were tested at ages (7 and 28 days). It was found from the trials on the experimental mixtures that the mixture presented in **Table (3-14)** mix of proportion (1: 1.25: 2) (by weight) (cement :sand: gravel) were good enough to give adequate strength (65.1 MPa at 28 days) and adequate workability. The superior plasticizer used gave sufficient mixing time and allowed the production of a uniform mixing of concrete without any separation.

Table (3-14) : Proportions of Concrete Mixes (High Strength Concrete)

No. of Mix										
Experimental Materials	1	2	3	4	5	6	7	8	9	10
Water/cement ratio	0.45	0.35	0.32	0.3	0.3	0.25	0.28	0.28	0.2	0.2
Water (kg/m3)	200	190	145	145	157	138	155	147	112	124
Cement (kg/m3)	445	500	454	484	525	550	550	525	500	550
Fine Aggregate(kg/m3)	680	478	780	650	656	670	720	656	671	720
Coarse aggregate(kg/m3)	1024	1178	1100	1200	1050	1060	1060	1050	1200	1060
Silica fume (kg/m3)	----	----	----	----		44	70	70	60	70
Superplasticizer(Kg/m3)	----	----	----	----	10.5	13.13	8.25	10.5	12.5	13.75
f c'u										79.35
f c'(28 days)MPa*0.82	40	43	43	52	49	57	54	55	58	65.1

F'c=0.82f'cu= 0.82* 79.35=65.1 MPa ***Al-Mashhadany (2009)***

3.4.3 Reactive Powder Concrete (RPC)

RPC has a higher priority for mix preparation and design than NSC and HSC. RPC manufacturing necessitates meticulous planning and material selection. To improve the workability of mixtures with a low (w / c) ratio, chemical additions (superplasticizers) are required. Experiments on the experimental mixes revealed that the 1:1.11 (cement: fine sand) (by weight)

mixture and use cubes (50*50)mm given in **Table (3-15)** provided sufficient strength (110 MPa in 28 days). as well as suitability for use.

Table (3-15) :Proportions of Concrete Mixes (Reactive Powder Concrete)

No. of Mix		
Experimental Materials	1	2
Water/cement ratio	0.18	0.16
Water (kg/m^3)	180	152
Cement (kg/m^3)	1000	950
Fine Aggregate(kg/m^3)	1000	1050
Coarse Aggregate(kg/m^3)	----	----
Silica fume (kg/m^3)	245	190
Steel Fibers (kg/m^3)	10	16
Superplasticizer (kg/m^3)	30	33.25
f'cu	92	110

***f'c =f'cu**

3.4.4 Mixing Procedure

The mixing procedure is important to obtain the required operability, and it was as follows:

1- All quantities of building materials were weighed and packed in clean containers before mixing. The inner surface of the mixer has been cleaned and moistened before applying the materials.

2-Mixing started by placing the dry ingredients (cement, sand and gravel) in the mixer, i.e. half the amount of gravel, half the amount of sand and all the cement, then the remaining two halves of sand and gravel were added respectively. The dry ingredients were mixed for 4 to 5 minutes (normal concrete), and (silica-Fume) was added to the mixture in the case of high-strength concrete. In the case of (RPC), the dry components (cement, fine sand) were mixed, then (silica-foam) and (steel fibers) were added to the

mixture.

3- Mixing the water with the mixture gradually added to the mixture. In the case of high-strength concrete, effective concrete, a quarter of the water was added to the mixture and all components were re-mixed for two minutes. The superplasticizer is then added to the remaining water before pouring it into the mixer. Then the fresh concrete was mixed for 3 minutes.

4- For steel fiber reinforced concrete, to avoid agglomeration and uniformly distribute the steel fibers, the required amount of steel fibers was uniformly added in the mix by hand with the mixer spraying. The mixing process was continued until a homogeneous concrete was obtained.

3.5 Preparation of test samples

3.5.1 Molds Preparation

Eighteen sample-casting plywood dies were designed and manufactured . The formwork that we required the required reinforcement (for the corbel and column) was placed inside the formwork and fixed in place and ensure that the form did not collapse while the concrete was being poured into it; The assembly of the template and the reinforcing mesh is shown in **figure (3-5).** Plastic spacers were used to ensure the main rails covered the edges.

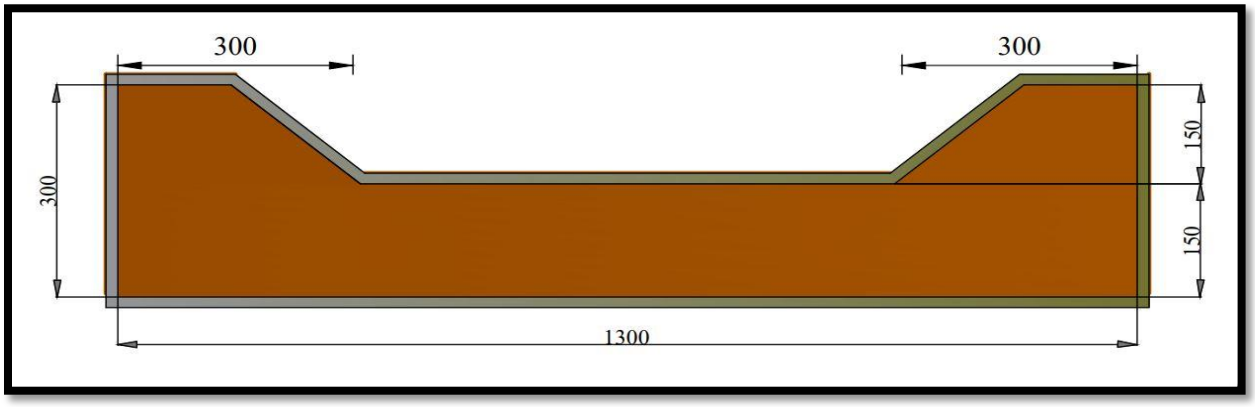

Figure (3-5): Details and Fabrication of Molds

3.5.2 Casting Equipment

In the present work, the concrete was mixed using a horizontal rotary mixer with a capacity of (0.1 m3), as shown in a **plate (3-8).** Two types of vibrators were used: a cylindrical vibrating table (external vibrator) consisting of a table dimension (0.75 m) made of a steel plate (0.60 m thick,) for pouring control samples, and a vibrator (internal vibrator) consisting of a steel poker (rod).), has a sloping column that is driven by a flexible driver (Vibration work mixing homogenizing inside the mold)for casting samples. The poker is made with a diameter (50 mm), a length (500 mm) with a semi-spherical edge (end). To determine the strength and other mechanical properties of concrete, sets of cylinders (150 x 300 mm), cubes (150 mm) for NSC, cylinders (100 x 200 mm), cubes (100 mm) for HSC, cylinders (100 x 200 mm), cubes (50 mm) for RPC, were prepared for each batch during concrete pouring. Preparation of test specimens ,as shown in a **plate (3-9).**

Plate (3-8): Mixing equipment's and specimens control

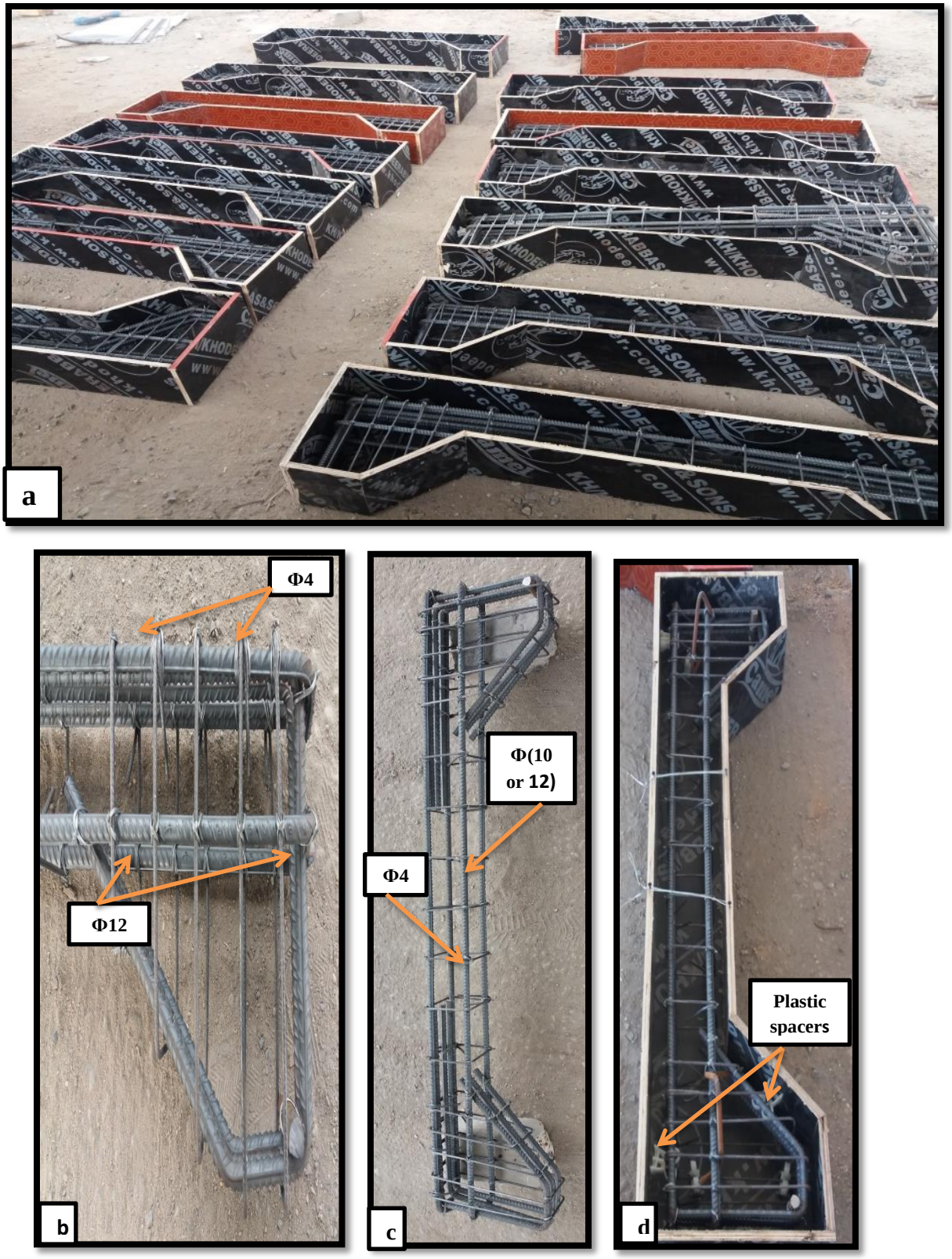

Plate (3-9): Preparation of Test Specimens**.**

Plate (3-9): Preparation of Test Specimens Continued.

(a) reparation of wood briquettes. (b) corbel reinforcement. (c) Processing of reinforcing steel molds. (d) Spacers Configuration.(e) Assembling the molds with reinforcing mesh horizontally. (f) Vibration apparatus.

3.5.3 Casting procedure

The samples were cast in the structural laboratory of the Civil Engineering Department at the University of Babylon. Prior to casting, the selection materials were prepared and weighed according to the volume of the mixture. Eighteen plywood molds were designed and manufactured for sample casting. The inner surfaces of the cube, and cylinder, are well cleaned and lubricated to avoid sticking to the concrete after hardening. Then each steel cage (for the column) is placed horizontally in wooden formwork and fixed in its proper place and horizontally; Assembling the mold and reinforcing mesh, as well. Plastic spacers were used to ensure that the main rails were covered by the columns, the typical technique of traditional concrete compaction for the cube, cylinder, and prism molds was followed. After the concrete is poured, all the molds are filled with concrete in one layer, by pressing and vibrating with an internal electric vibrator, the upper surface of the mold is smoothed using a hand trowel, as shown in the **plate (3-10).**

Plate (3-10): Stages of Casting Operation. : (a) Preparing the raw materials for the casting process .(b) Cast concrete in the mold Samples .(c)Vibrating the Concrete.(d) Casting Control Samples .(e) Leveling the surface of the mold with a trowel and Complete the casting process.

3.5.4 Curing

All samples were removed from their molds after (24) hours of casting, then agricultural nylon bags and jute bags were placed under the samples and these layers were wrapped over the samples and kept wet for up to 28 days. **Plate (3-11)** shows the treatment of test specimens.

Plate (3-11): Curing of Columns and Control Specimens: (a) Open the wooden mold for the columns. (b) The agricultural nylon brushes and the shawl cloth on top of it. (c) Put the molds over the nylon and cloth .(d) Spray the molds with water and cover them completely with the agricultural cloth and nylon.

3.6 Tests of hardened concrete samples

3.6.1 Destructive tests

3.6.1.1 Compressive strength test

The compressive strength test of concrete (**f'cu**) was carried out according to (**BS 1881- part 116:2000)**. A total of six cubes of size (150X150X150) mm for(NSC), (100X100X100) mm for (HSC) and (50X50X50) mm for (RPC) were tested using a hydraulic press with a maximum capacity of 2000 kN.as shown in a **plate (3-12)**. The load was applied continuously and gradually increased at a constant rate of (18 MPa) per minute until failure occurred.

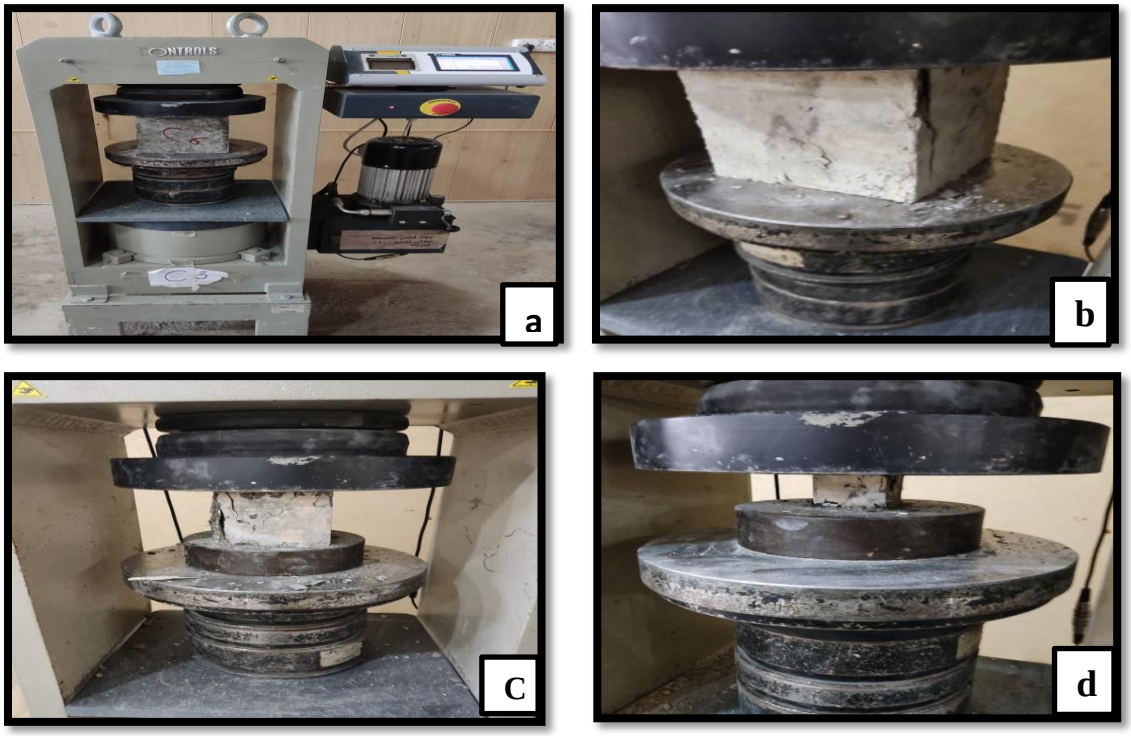

Plate (3-12): The compressive strength test cubes: (a)(b) for NSC. (c) for HSC. (d) for RPC.

3.6.1.2 Modulus of Rupture (Flexural Strength) Test

Prisms with dimensions (100×100×400) mm are tested according to **(ASTM C78, 2010)** procedure. The values of testing specimens was at 28-day,

shown in **Table (3-16),plate (3-13)** shows the modulus of rupture test. The modulus of rupture calculated from Equation .

fr=PL/bd2 …….(3-1)

Table (3-16): Modulus of Rupture Values

Specimens No.	Modulus of rupture (MPa)
1	4.62
2	4.65
3	4.8
Average value	4.7

plate (3-13) : The Flexural Strength Test (Modulus of Rupture).

3.6.1.3 Splitting Tensile Strength Test

The resistance was measured for the fission test according to **(ASTM C496, 2011).** A total of 6 cylinders (150 x 300) mm were tested for NSC, (100 x 200) mm for HSC and RPC. Two bearing strips of 3.0 mm thick, 300 mm long plywood were placed above and below the specimen to provide concentrated stress and a uniform load applied to the surface of the tested cylinder, as shown in the **plate (3-14)**, the capacitance of the test machine was 2000 kN and the load was loaded uniformly Continuous and without

shock until cylinder failure occurs. The expression for the split tension was calculated by the equation:

$$f_{st} = 2P/\pi LD \qquad \text{……(3-2)}$$

Where: ($\mathbf{f_{st}}$)is splitting tensile strength in N/mm^2,(P) is the applied compressive load in (N), (D) is the diameter of cylinder in(mm) and (L) is the length of cylinder in (mm).

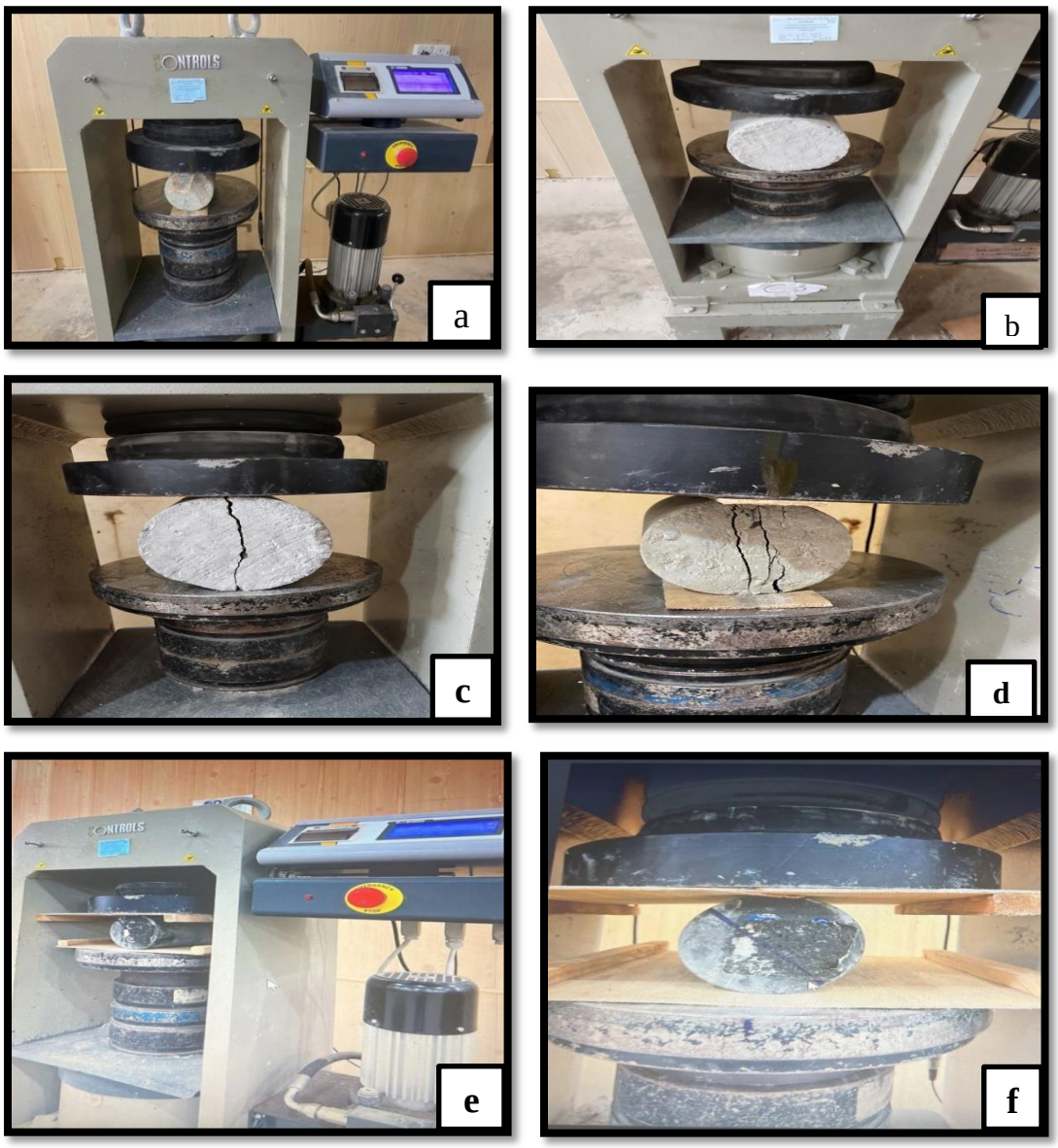

plate (3-14) : The Splitting Tensile Strength test ,(a)(b) For NSC. (c)(d) For HSC.(e)(f) for RPC.

3.6.2 Non-Destructive Test

The Ultrasonic Pulse Velocity UPV is a stress wave propagation method that …waves. The pulses are introduced into the concrete by a piezoelectric transducer and a similar transducer acts as a receiver to monitor the surface vibration caused by the arrival of the pulse **(Bissonnette et al 2018).** Ultrasonic Pulse Velocity (UPV) is one of the most common non-destructive methods used to evaluate concrete properties, All samples are tested by Direct Ultrasound Pulse Velocity (DUPV), to measure the wave velocity in concrete and the compressive strength of each sample (**Mohana,2020**). A timing circuit (t) is used to measure the time it takes for the pulse to travel from the transmitting to the receiving transducers during the materials path (L). The pulse velocity (V) is given by dividing path length (L) over transit time (t). The presence of low density or cracked concrete increases the travel time which results in a lower pulse velocity **(Camara et al ,2019).**

Ultrasonic pulse velocity technique is one of the most popular non-destructive techniques used in the assessment of concrete properties. However, it is very difficult to accurately evaluate the concrete compressive strength with this method since the ultrasonic pulse velocity values are affected by some factors, which do not necessarily influence the concrete compressive strength in the same way or to the same extent **(Trtnik et al, 2009).**

The factors affecting the strength-pulse velocity relationship are water/cement ratio (w/c), aggregate size, grading, type, and content, the concrete age, moisture condition, compaction, curing temperature, path length, and level of stress **(Malhotra and Carino2004).**

Ultrasonic Pulse transit times were measured by the direct transmission method. This test was carried out according to **(ASTM C597, 2009)**. The Ultrasonic Pulse velocity test was applied to the NSC RC column after burning. A portable ultrasonic concrete tester known as (TICO) 54 kHz was used for this purpose, as shown in **plate (3-15).** Calibration of the concrete tester was done before testing to check the accuracy of the transit time measurements. This was achieved by the calibration of the reference bar. A thin layer of grease was applied on the surface to act as a couplet and to prevent the dissipation of transmitted energy.

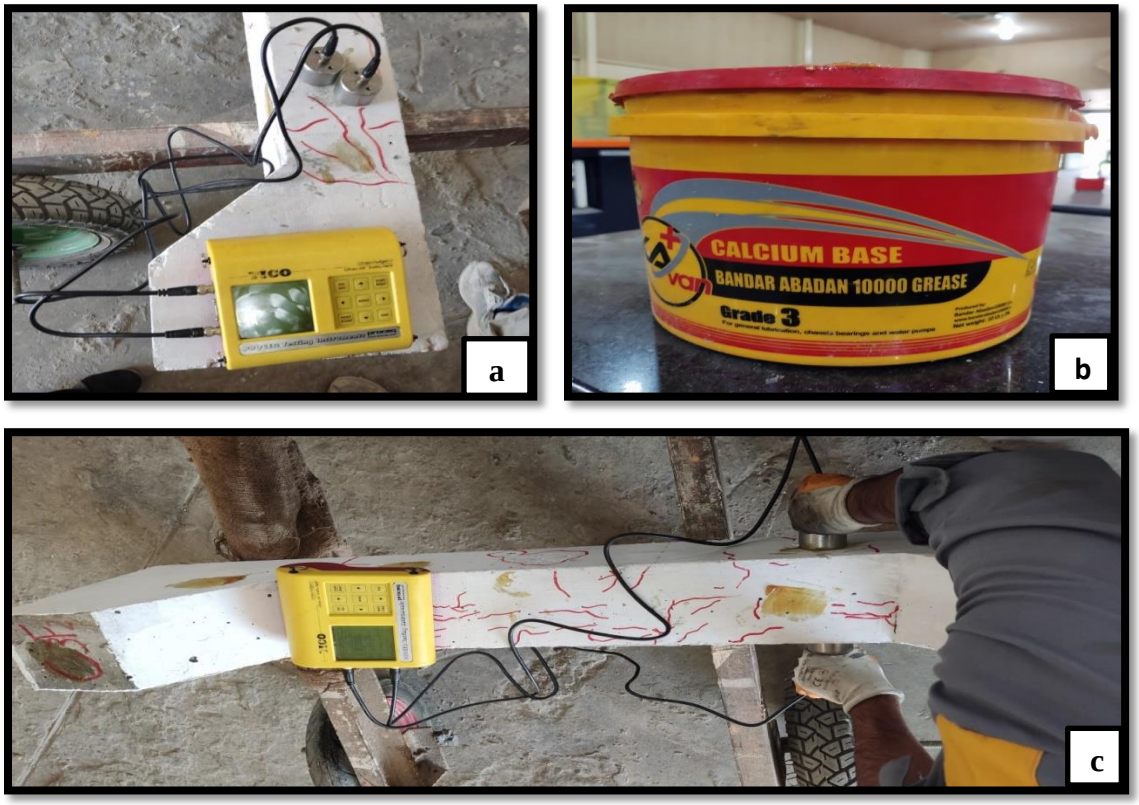

Plate (3-15): Ultrasonic Pulse transit Time Tester:(a) UPV device. (b) The grease was used . (C) Procedure of the test.

The evaluation of concrete compressive strength is usually based on empirical relations between strength and non-destructive parameters.

Numerous data and the correlation relationships between concrete compression strength (S) and Ultrasonic pulse velocity (Vp) of concrete have been proposed and presented. The most popular formula is **(Trtnik, et.al, 2009).**

$$S = a \exp(b\,Vp) \qquad \ldots\ldots(3\text{-}3)$$

Where (**a)** and **(b)** are empirical parameters determined by the least squares method.

In estimation, of the strength of in-situ concrete strength from pulse velocity measurements, an empirical relationship must be established on test specimens in the laboratory. In practice, it is generally agreed that there is no unique relationship between concrete strength and Ultrasonic pulse velocity. There exist factors that may affect one parameter only leading to the existence of different relationships. Locally **(Raouf and Samurai-1999)** developed an experimental relationship to estimate concrete compressive strength using rebound numbers, which was adopted by many researchers in this field **(Alhassnawi, 2018 and Al-Obaidi, 2019)**and it was utilized in the present research.

$$S = 2.8 \exp(0.58\,Vp) \qquad \ldots\ldots(3\text{-}4)$$

V: Ultrasonic pulse velocity, in **(mm/µs)**

S: concrete compression strength, in **(MPa)**

3.7 Fire Flame Stove and Equipment

The primary purpose of the flame burner is to raise the temperature of the concrete models to the desired level and maintain that temperature for the appropriate time. The following equipment is used in the burning process to manage the fire exposure with axial pre-load:

1. Brick stove.

2. Network methane burners.

3. Thermocouple.

4. Digital temperature controller.

5. Electrical network.

6. Two Gas bottle.

7. Gas connections and pipelines.

8. Stove steel cover.

9. Loading Frame.

10. Hydraulic jacking.

11. Load Cell

The complete version of the stove and equipment was developed, including the pre-loading frame system, as shown in a **plate (3-16):**

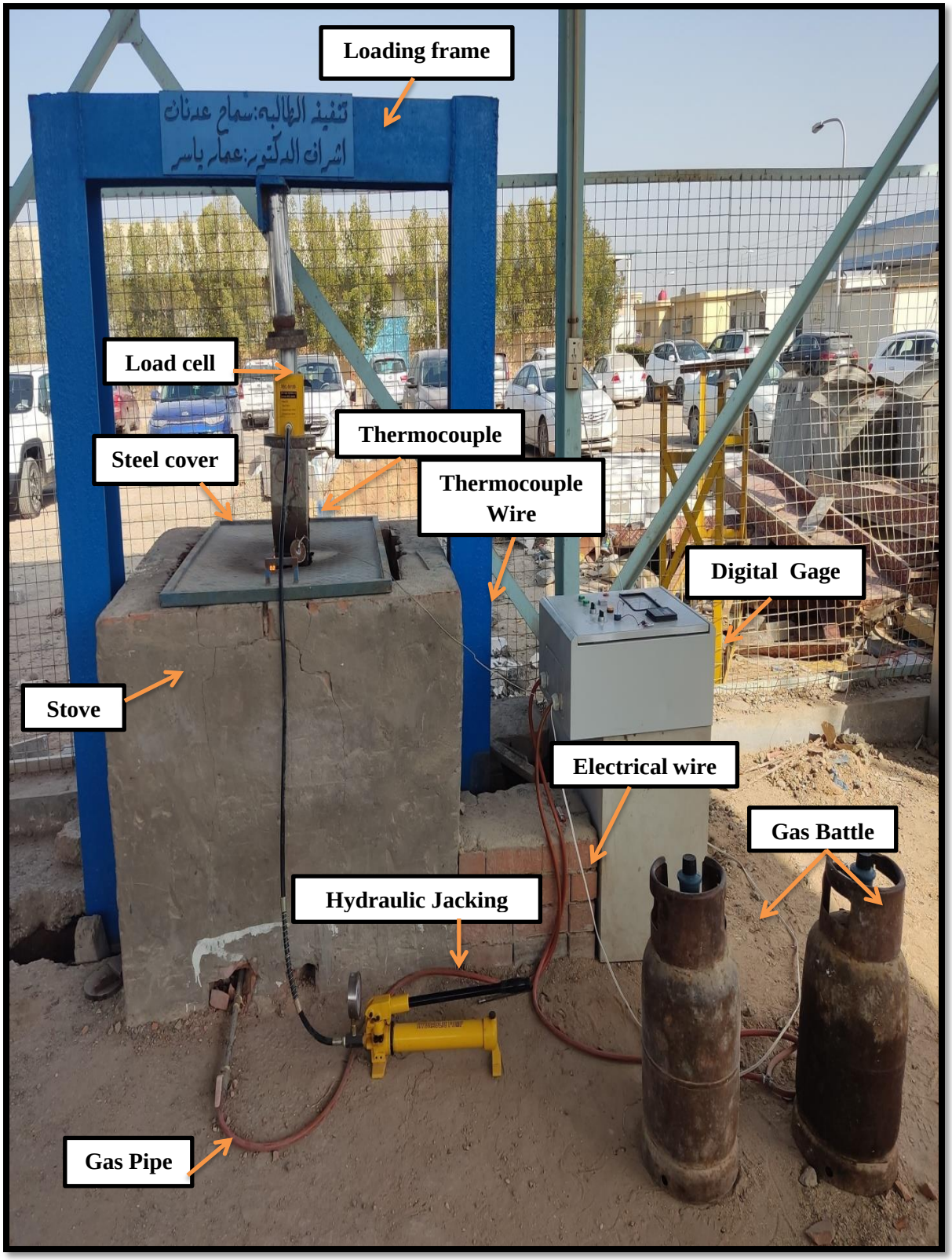

plate (3-16): The full details of the stove and equipment

3.7.1 Brick Stove

The stove dimensions (1400 x 1400 x 1100) mm (length, breadth, and height, respectively) and has a wall thickness of 250 mm on all sides **(Abdul Rahim and Kazem, 2017)**. The main structure is made up of perforated bricks and mortar with a small hole to allow fresh oxygen to the burners.

The burner network consists of twelve methane burners set in four vertical lines on each side of the exposure (3 methane burners on each side) and evenly spaced along the shaft, all of which are connected by a single pipeline network to manage the gas discharge. In addition, it is linked to the electronic control system. The purpose of flame bars is to imitate the heating situation in a real fire**.**

The outside and inside views of the stove for the fire exposure test , are shown in **Plate (3-17)** and **(3-18).**

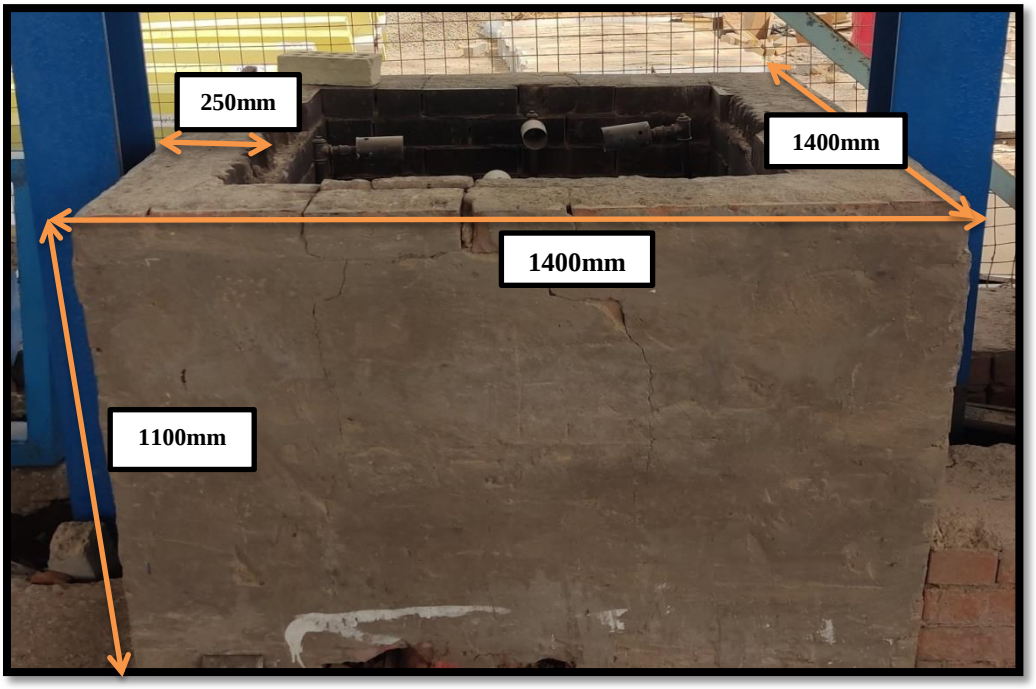

Plate (3-17): Details of the Brick stove.

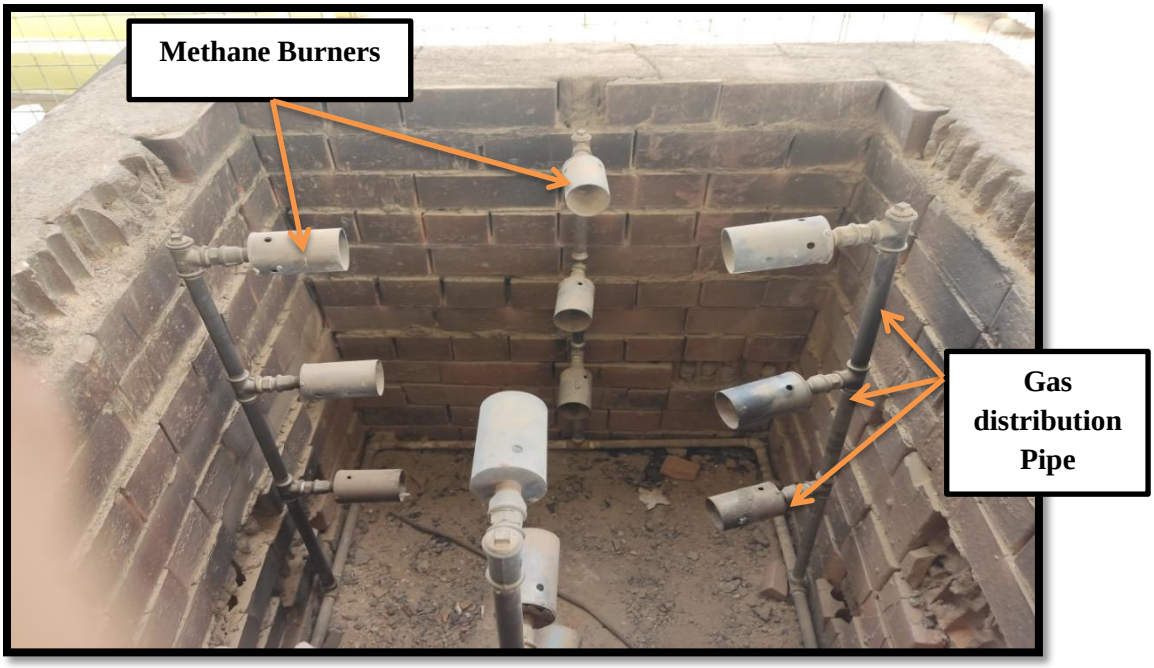

Plate (3-18): Burner Network.

The stove cover is made of an insulator plate with 8 mm thickness to keep the temperature consistent. Because the column is higher than the stove, The cover must be cut and a hole made in the center to allow the column to pass through as shown in the **plate (3-19).**

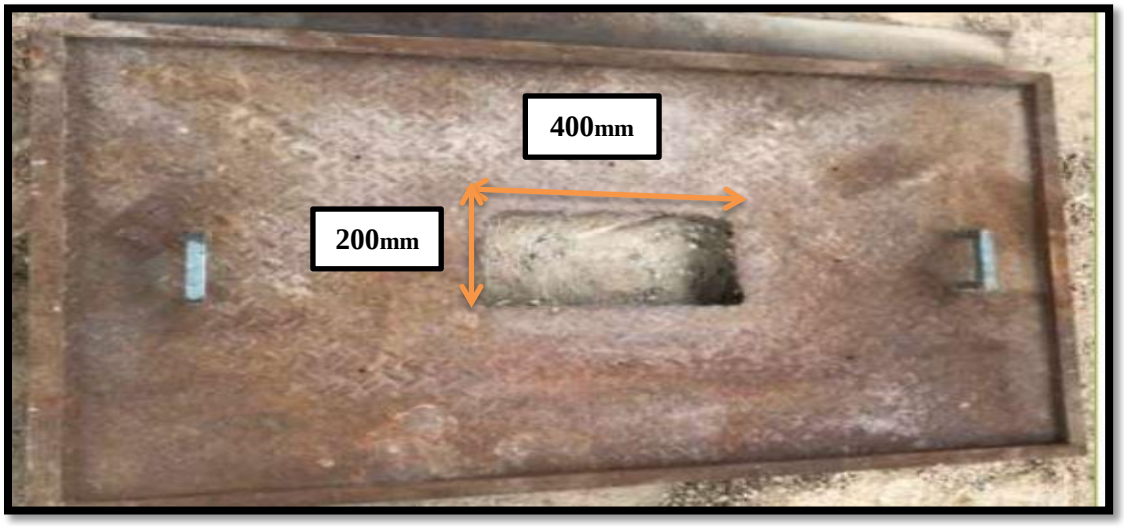

Plate (3-19): Stove cover.

3.7.2 Thermocouple

A thermocouple is a sensor used to measure temperature and consists of two wire legs made from different metals inside a metal tube. The wires legs are welded together at one end, creating a junction, as shown in **Figures (3-5).** When the junction experiences a temperature change, a voltage is created, and this voltage can be interpreted to measure temperature. Thermocouples are widely used in science and industry. Applications include temperature measurement for kilns, gas turbine exhaust, diesel engines, and other industrial processes. Thermocouples are also used in homes, offices, and businesses as temperature sensors in thermostats, and also as flame sensors in safety devices for gas-powered appliances **(Ghimire, 2017)**. There are several types of thermocouples such as types (B, E, J, K, N, R, S, and T) **(Webster, 2000).**

The wide temperature range, low cost, and high tolerance of both oxidizing and inert atmospheres make Type K the most widely used thermocouple type. To avoid hysteresis effects, no part of the wire of a type K thermocouple should be used at lower temperatures once it has been used at temperatures above about (150 °C)

Type K Thermocouples (Nickel-Chromium / Nickel-Aluminum) was used in the present study, it is the most common type of thermocouple, it's inexpensive, accurate, reliable, and has a wide temperature range **(Ramsden, 2000)**, see **plate (3-20).**

Typical applications for these mineral insulated Type-K thermocouple probes include heat exchangers, power stations, brick, and cement kilns, heat treatment and annealing furnaces, thermostats, food thermometers, vehicle

Diagnostics and in laboratories. These thermocouples are particularly suitable for high pressure and vacuum applications, and able to withstand high levels of vibration.

Type K Mineral Insulated Thermocouple Sensor with probe length and diameter of 200mm and 4mm respectively is adopted in this study. The cable length is 5000mm and the maximum temperature that could be detected is 1200℃.

Thermocouple usually connected to a thermometer or data logger or any other thermocouple-capable device (digital gage used in this investigation) by a thermal-insulated electric wire to resist high temperatures during burning. Thermal couples will be connected to the digital gage through the openings on the sides of the furnace.

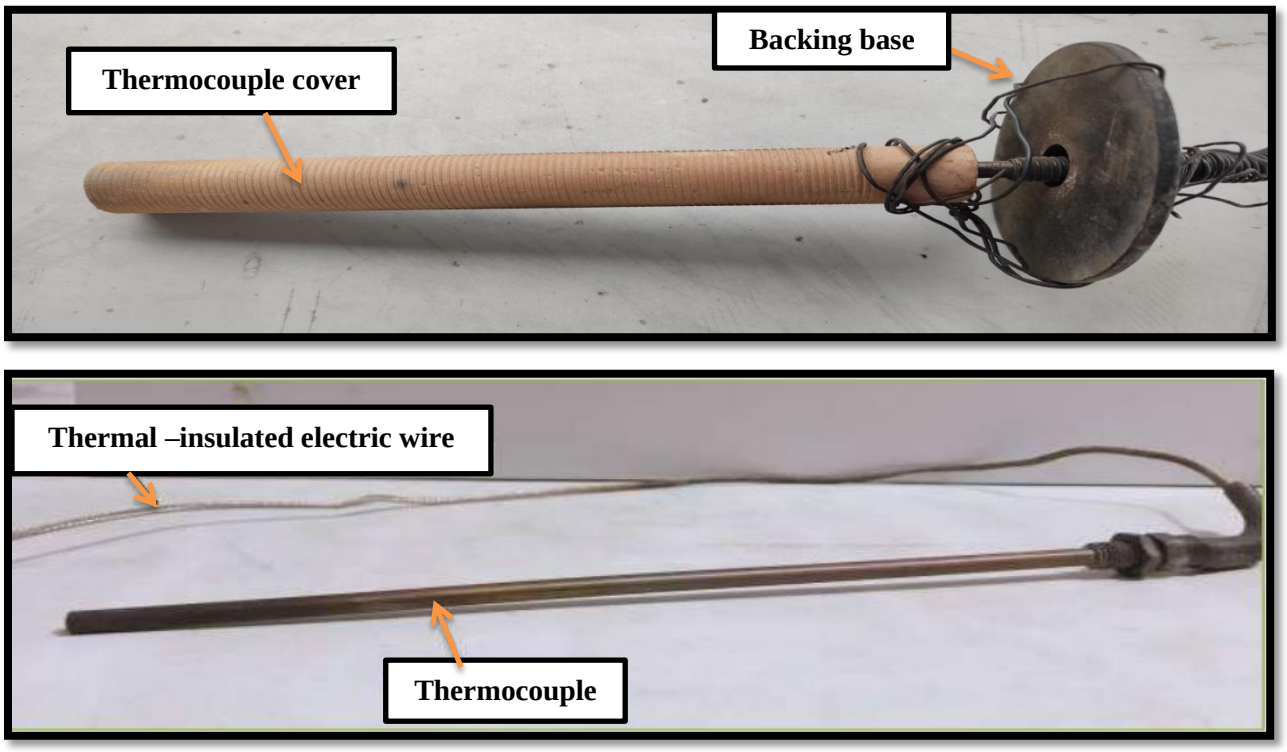

Plate (3-20): Details Thermocouple Type (K).

3.7.3 Digital Temperature Controller

It is an electrical electronic device that provides temperature control inside the oven by controlling the amount of gas that feeds the oven by an electronic gas regulator inside the system to be opened and closed according to the temperature measured inside the oven by the sensor after installing the oven, the temperature required by the user.

It also consists of two external gas regulators, each one connected to a gas bottle to keep the temperature constant inside the oven (that is, if the gas runs out in the first bottle, the gas is opened directly from the other bottle, and thus the temperature is maintained stable and constant), as shown in the **plates (3-21)(3-22).**

At first, the manual external gas valve is opened before the electricity is turned on to open the burners; The flames in the burners are controlled by this electronic valve to maintain the presence of the required flame inside the burners. Then electricity is turned on to start combustion, with the electronic regulator feeding the furnace with the amount of gas necessary for ignition. If the temperature inside the furnace is greater than the desired temperature value, the control gas supply is turned off (the electronic gas regulator is turned off). If the temperature inside the oven is lower than the required temperature value, the control feed is activated (the electronic regulator gas is turned on) .Displays the digital temperature control unit through a small screen that shows the required temperature for the oven, the reading represents the upper reading as the current temperature while the lower reading is installed in the device, which maintains a constant temperature inside the oven.

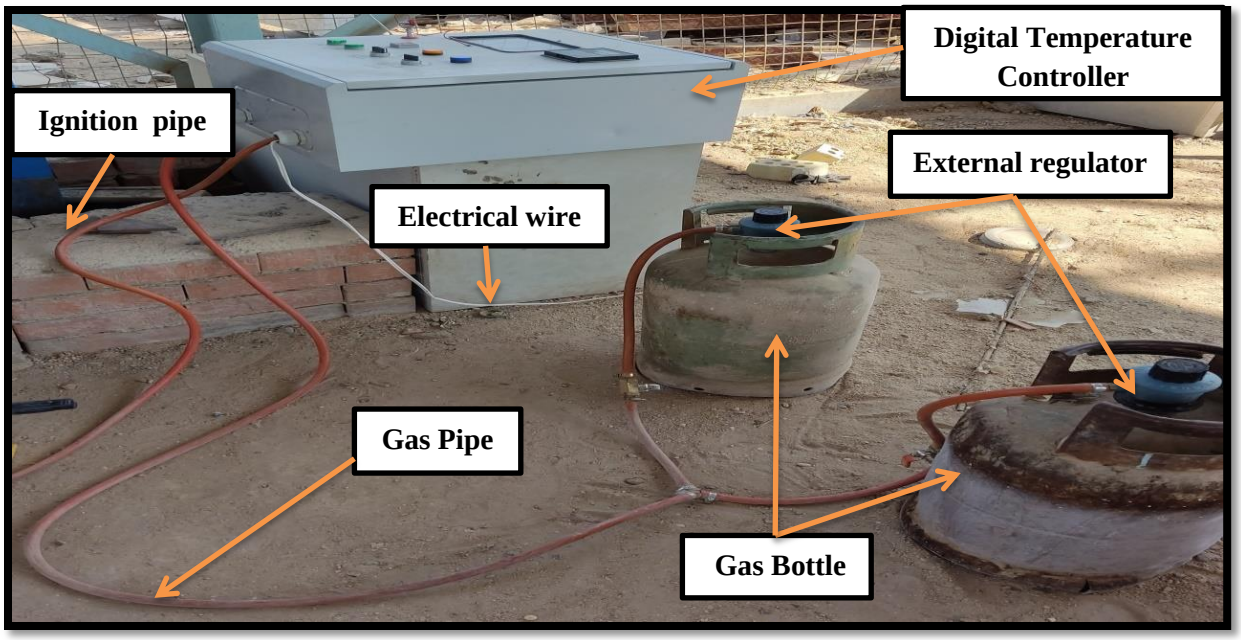

Plate (3-21): Details of Gas Preparation

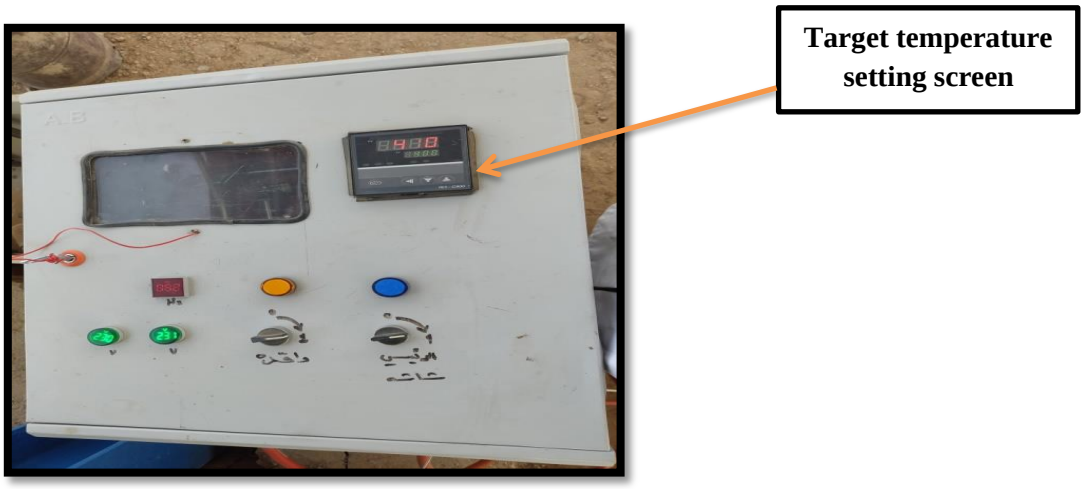

Plate (3-22): Digital temperature controller details.

5.7.4 Electric Gas Regulator and Ignition Burner System

The gas regulator is an electronic valve designed to provide a purpose Fast and accurate gas flow to the burner, the electricity is turned on and the sensor is installed inside the oven before the gas opening process, then the gas is opened and the burners are turned on by an external burner. The flames in the burners are controlled by an electronic valve inside the system

that maintains the presence of the flame inside the burners according to the temperature required for burning. The regulator feeds the furnace with the amount of gas necessary for ignition through the electronic system. Where the heat is gradually raised to the required combustion temperature inside the furnace, The gas flow controlled by the valve electronically (i.e. stopping any increase in feeding) maintaining the uniformity of the gas inside the oven and keeping the burners fire. when the temperature inside the furnace falls below the required temperature value, it will open electronically and thus continue in this way until the end of the combustion process, and the combustion process is deactivated by (the external regulating gas is turned off),**plate(3-23)** shows the electrical gas regulator.

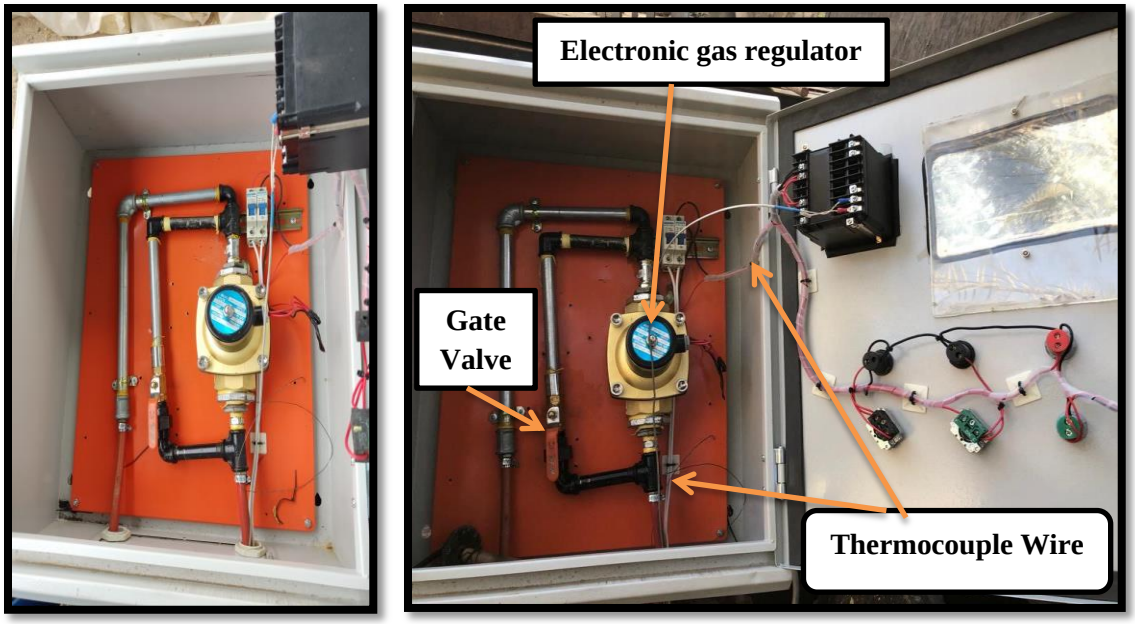

Plate (3-23): Electrical Gas Regulator.

3.7.5 Loading Frame

This design was implemented for its importance and prominent role in the loading process through the exposure stage of fire ,which was constructed by

(**samah adnan**). It can, in turn, give a clear visualization of buildings or columns loaded during combustion, as it consists of the first section of rolled steel with a section (I-shape) especially to provide preload while the column is exposed to fire. This frame in Figure (3-6) consists of two separate parts, the upper part being three parts welded together like an inverted letter (U), welded into the middle of the horizontal centerpiece a steel tube to provide a load centered on the column while the lower part is a single piece placed Under the base of the stove and at the end of this part some holes are used to connect the pieces through screws.

The function of this frame is to load the columns during the firing process using the hydraulic jack.

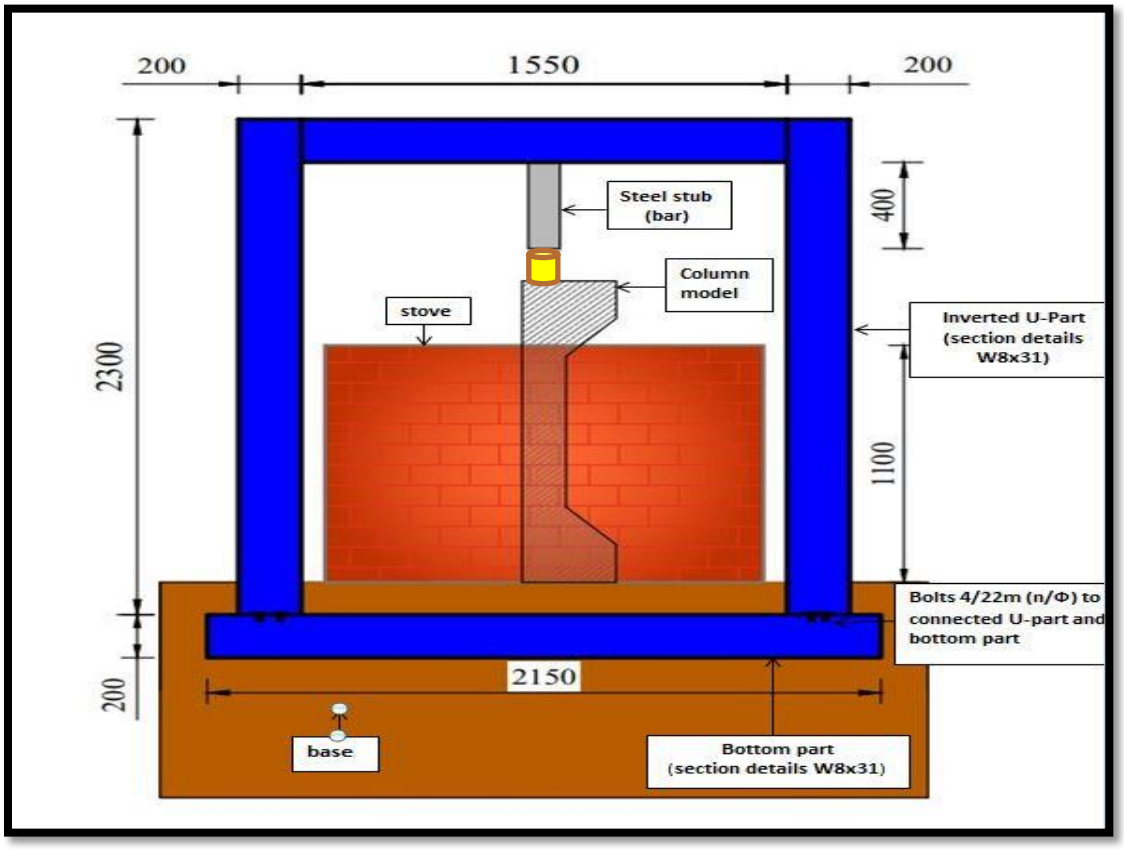

Figure (3-6): Details of the Loading Frame with Stove (all dimensions in mm).

3.7.6 Hydraulic jacking

A hydraulic jack is a mechanical arrangement that uses the power of fluids for operation. With a hydraulic jack, one can easily lift heavy loads using a small applied force. Normally, this lifting device uses a hydraulic cylinder for applying initial power.

Hydraulic jack working is based on Pascal's principle. That is, the pressure applied to a fluid stored in a container will be distributed equally in all directions., as shown in the **plate (3-24).** Oil is used since it is self-lubricating and stable. When the plunger pulls back, it draws oil out of the reservoir through a suction check valve into the pump chamber. When the plunger moves forward, it pushes the oil through a discharge check valve into the cylinder.The capacity of the hydraulic jack used in this study is about 50 Tons.

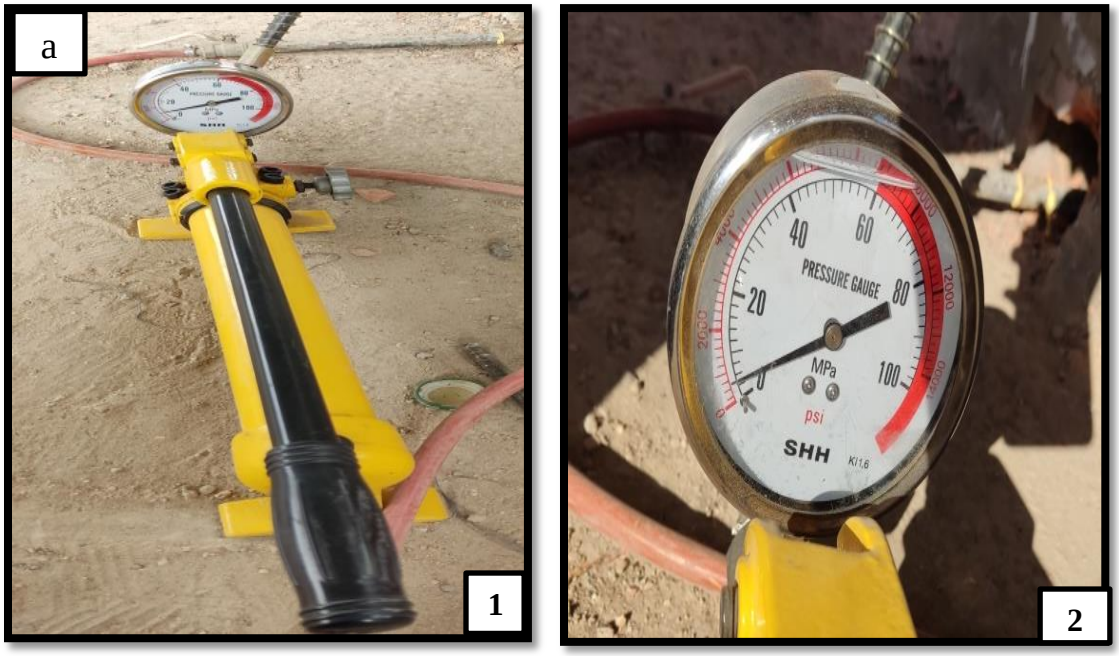

Plate (3-24): a:Hydraulic Jacking ,b: Hydraulic Jacking Burning with applied Load.

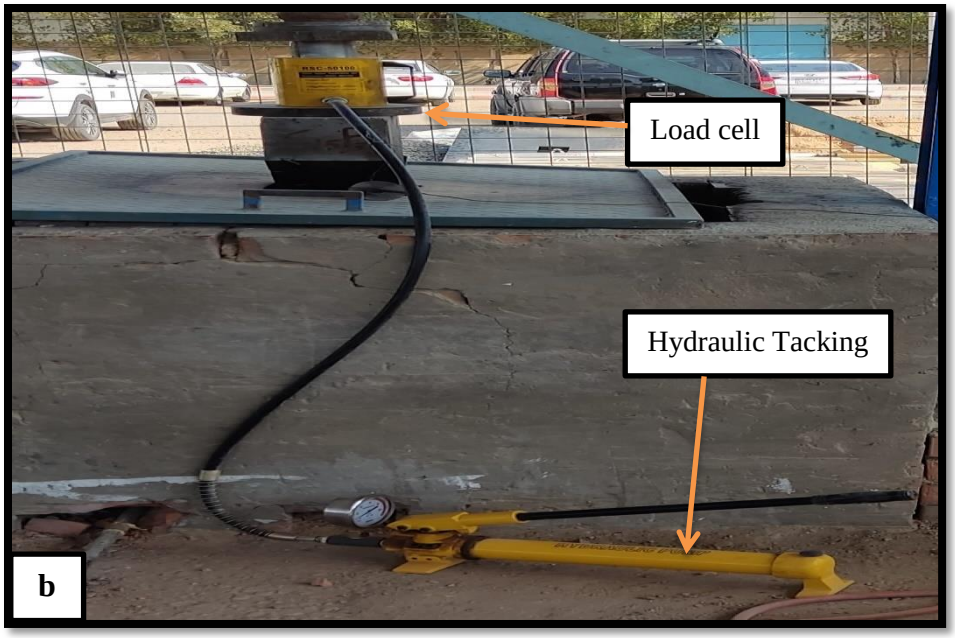

Plate (3-24): Continues.

3.7.7 Load Cell

A load cell is a type of transducer, specifically a force transducer. It converts a force such as tension, compression, pressure, or torque into an electrical signal that can be measured and standardized. As the force applied to the load cell increases, the electrical signal changes proportionally **.**

Hydraulic Jack Working is based on Pascal's principle. That is, the pressure applied to a fluid stored in a container will be distributed equally in all directions.

The hydraulic load cell uses a conventional piston and cylinder arrangement with the piston placed in a thin elastic diaphragm, as shown in **Plate (3-25).** The piston doesn't actually come in contact with the load cell. Mechanical stops are placed to prevent over strain of the diaphragm when the loads exceed a certain limit. The load cell is completely filled with oil.

When the load is applied to the piston, the movement of the piston and the diaphragm results in an increase in oil pressure. This pressure is then transmitted to a hydraulic pressure gauge via a high pressure hose **(Deglandon, Kathy, 2016)**. The gauge's Bourdon tube senses the pressure and registers it on the dial. Because this sensor has no electrical components, it is ideal for use in hazardous areas.

Plate (3-25): Load Cell

3.8 Drying of Specimens before Fire Exposure

After completing the process of ripening the columns within (28) days, during which the samples are completely saturated with water, When structural concrete elements are exposed to fire directly, it is possible, that sudden explosive spalling of the concrete takes place when free water, (water that is not employed for hydration reaction and remained unused in concrete) in concrete is changed to steam because of concrete exposure to fire, and if the steam is not released in concrete then it causes explosive spalling.

The concrete cover protecting the reinforcement will be removed due to explosive splintering and therefore the steel bars will be exposed to fire. This weakens the reinforcing bars and reduces the final load-bearing capacity of the reinforced concrete element. It is therefore essential to take precautions **(Hamakareem, 2009)**. Therefore, before starting the burning process, the columns were dried at a temperature of (90-100) for about an hour ,as shown in **the plate (3-26) (3-27),** to avoid the occurrence of explosive cracks, and left to cool to room temperature (25) ℃ for one day and then proceeded to the next day of burning

Plate (3-26): Drying Process before Burning Procedure

3.9 Scenario of Fire Exposure

After drying was completed (after 1 day), the burning procedure have been applied. The samples were burned with a direct fire flame by a grid of

methane burners inside a brick burner to the target temperature. The burning process was carried out through the following steps:

1. After the burner was equipped with all connections, the column was carefully moved to the combustion place and carefully installed inside the burner making sure that the loading was eccentric or concentric. (about 30% Pu)

2. The concrete samples (columns) were placed symmetrically towards the methane burners at the same distance from each burner line, from all sides of the sample.

3.Pre-loading: A predetermined axial pressure load, eccentric and concentric loading, is applied to the samples. Since the installed samples were higher than the hearth chamber, the height of the sample exposed to fire was (700) mm. A loading crane with a capacity of (50) tons located on top of the stove was used to loading the column with the required (30%) pre-load.

4. Combustion temperature rise stage: the gas valve is opened and the burners are ignited by an external burner, and the measured temperature is gradually increased to the required level while maintaining the stability of the applied pre-load.

5. Constant temperature during the burning process: Through the electric electronic gas system, the temperature is controlled by regulating the gas flow. When the target temperature is reached, the gas-electronic system stops the increase in the gas flow to the burners until the desired temperature drops, so the gas will open and is electronically adjusted so that the target temperature remains constant, the target temperature was measured with a thermocouple placed in contact direct with fire flame.

6.After each fire exposure cycle for duration (45 or 75) min, the column remains inside the oven to cool while the loading continues to be fixed and shed until the next day, then the column burns again, and so the column remains inside. A state of cooling and burning until the end of the periodic burning period (four days, two days, or one day), and on each burning day, after the completion of the one-day burning (cycle) the gas valve is completely closed. After the periodic burning is completed, the samples are left to cool are carried out on thermal gloves, and taken out of the oven to a location. The heating method inside the burner was controlled to simulate the (**ASTM E119)** temperature curve, as shown in **Figure (3-7).**

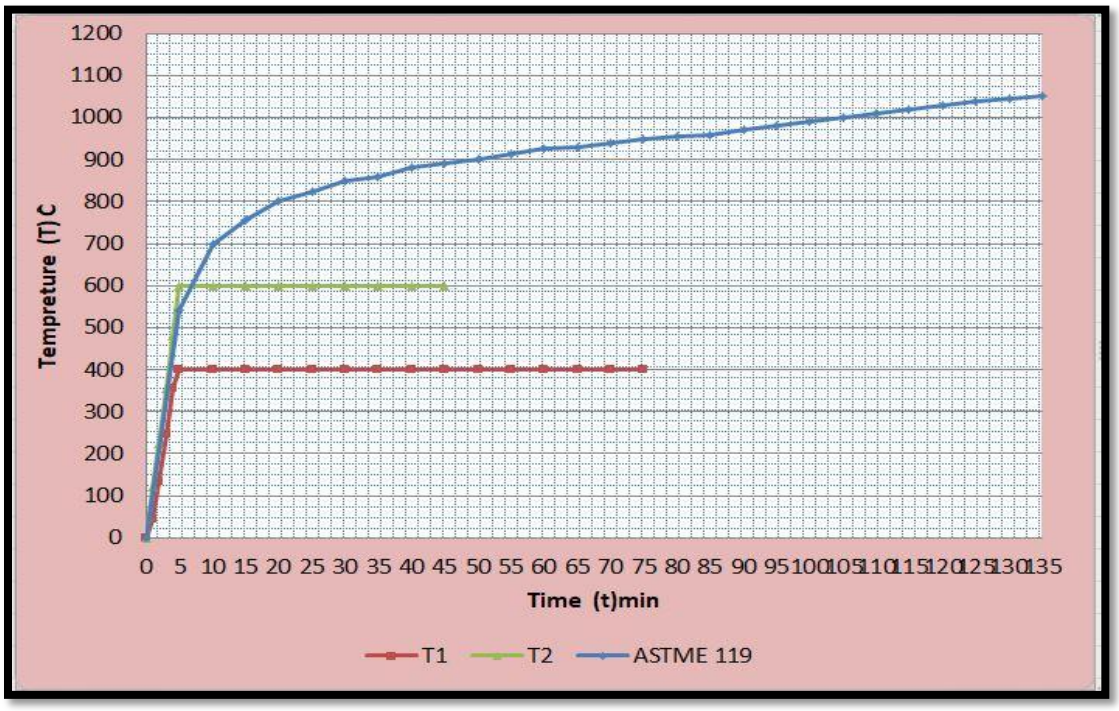

Figure (3-7): ASTM E119 Temperature Curve

3.10 Scenario of Cyclic Fire Exposure

To investigate the effect of the cyclic burning on column response, three scenarios of cyclic exposure to fire as shown in **Figure (3-8).**:

1-One cycle of fire exposure with load (30% of Pu).

2-Two cycles of fire exposure with load (30% of Pu)

3-Four cycles of fire exposure with load (30% of Pu)

3.10.1 One cycle of fire exposure with load (F2,F4).

This consists of two columns (C_3 and C_5), column(C_3) was burned with load (30%Pu=77 KN) at a temperature of (400C) for (90)min, the column(C_5) was burned with load (30%Pu=77 KN) and at a temperature of (400C) for (180) min, see in **Figure (3-8 b,d).**

3.10.2 Two cycles of fire exposure with load (F1)

This consisted of four columns (C_2, C_8, C_{11}, and C_{14}), which were placed inside the burner and the applied load was gradually increased up to (0.30 %Pu)at a temperature (400 C˚) for two cycles (two days) and burning time (45)mm), see in **Figure (3-8 a).**

3.10.3 Four cycles of fire exposure with load (F3, F5, F6)

This consisted of four columns (C_4, C_6, C_7, C_9, C_{12}, C_{15}, C_{16}, and C_{17}), which were placed inside the burner and the applied load was gradually increased up to (0.30 %Pu)at temperature(400C˚) or (600C˚) and burning time (45 or 75)min through four cycles(four days), see in **Figure (3-8 c,e,f).** This load was applied to these columns using a hydraulic lifting system designed for this study

*Notice that the duration of each fire exposure cycle is about one day, including the time of burning, (45 min,75 min), and then cooling to a temperature of the room for end of the day.

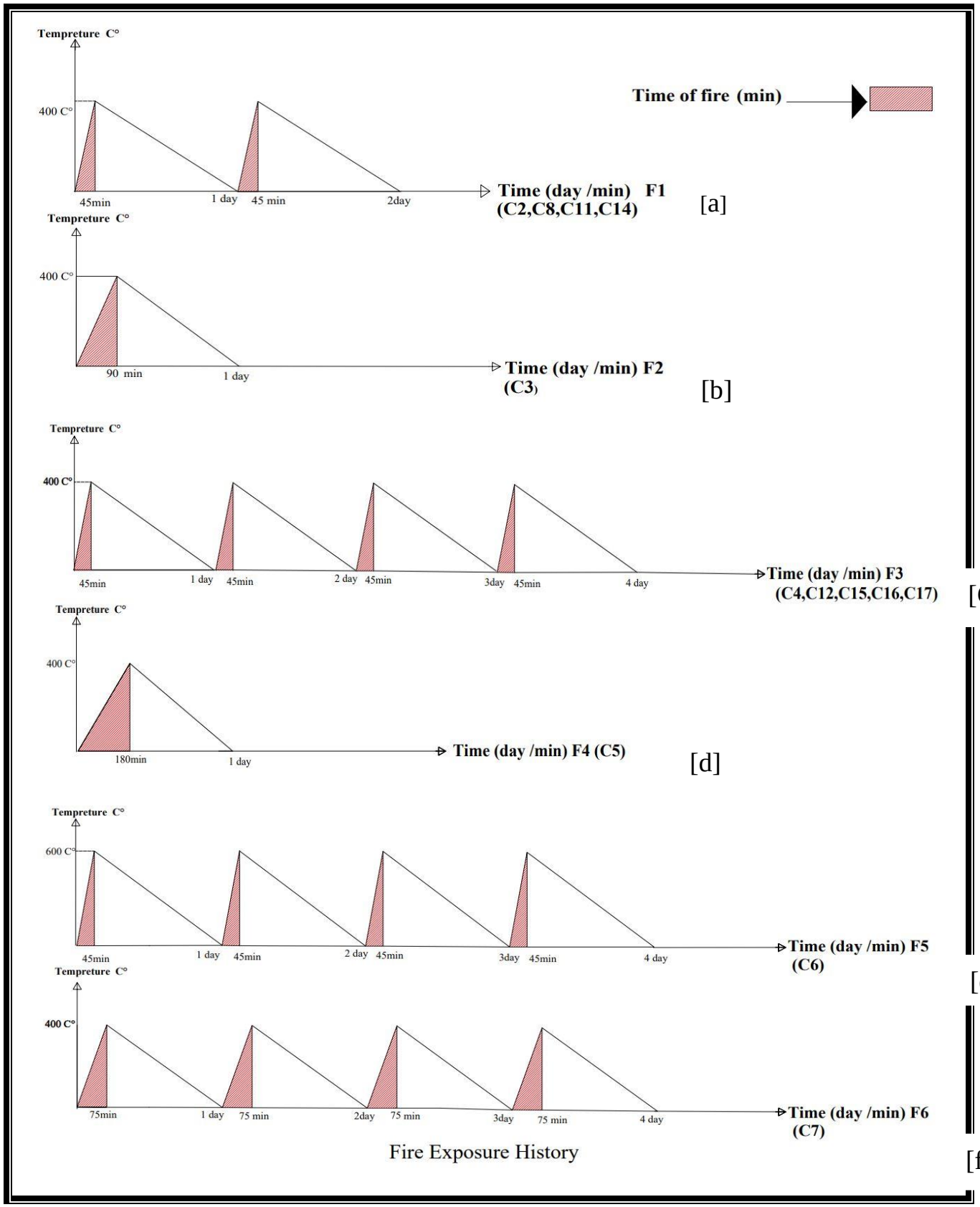

Figure (3-8):Scenarios of Cyclic Exposure to Fire .

Plate (3-27): Cracks and Spalling of the Fire exposed test with (30% Pu) Pre-load.

3.11 Repairing of Damaged Fire Exposed Columns

The structural treatment of the damaged columns due to cyclic fire exposure (C_{16} and C_{17}) included the following items:

1. Removing the outer damaged concrete shell from the columns, up to expose the longitudinal reinforcing steel. The manual method (hand tools such as hammer and nail)was used carefully and without using mechanical methods to avoid generating a dynamic vibration force that leads to the weakness of the damaged members and thus decrease in resistance, as shown in **plate (3-28)**

2. Shear (U) connectors (Φ 4 mm in diameter) installed horizontally on each side of the four stirrups to provide the connection between the old concrete core and the new shell (RPC)(C_{17}) or NSC (C_{16}), as shown in **Plate (3-29**).

3- Removing the excess dust from the columns resulting from the peeling process by means of water currents and rehabilitating the surface to receive the binder

4-Measuring the resistance of fired concrete using an ultrasonic pulse velocity (UPV) as shown in **plate (3-30).**

5-The epoxy resin was prepared by mixing the two components (the base and the hardener). Care must be taken to ensure that Nitobond EP is thoroughly mixed. The 'hardener' and 'base' components must be stirred separately before mixing to disperse any settling. The full contents of the "hardener" tin should be poured into the "basic" tin and the two substances mixed well using a suitable slow-speed drill and mixing paddle for 2 minutes until a completely uniform color is obtained. see **plate (3-33).**

6- About (90)min before the RPC or NSC pour, the broken surface of the old concrete is coated (after cleaning) with Nitobond EP to achieve the bonding between the old and new concrete, see **plate (3-33).**

7- Pour new concrete using Reactive Concrete Powder (RPC) or (NSC), as shown in **plate (3-34).**

8-After (28 days) of completing the ritroftening process for column(C_{16}) (CFRP) laminates are applied according to the following steps: see **plate (3-34).**

a- cut the carbon fiber reinforced plastic panels to the required length and the concrete surface was cleaned to remove any contamination.

b- Prepare epoxy adhesive (A, B) (Sicador 330) and mix them in the ratio (4:1) in succession until the color becomes homogeneous, Apply epoxy to the column with a layer (1.5 mm) thick carbon-fiber-reinforced plastic sheet.

c- Next, a Carbon Fiber Reinforced Plastic (CFRP) sheet is fixed to the surface of the columns on the epoxy-coated area and pressed by a plastic roller to hold it causing the epoxy to be pushed out from the sides of the sheet. Excess epoxy is removed from the sides of the carbon fiber-reinforced plastic sheets.

d- Finally, the columns are ready for testing after curing for a period of (7 days) at a laboratory temperature of 25°C.

a. Removing of the External Concrete Shell.

b. Fastening of Shear Connectors for Damaged Columns. continue

Plate (3-28): Repairing of the Damaged External Shell.

c. fastening of shear connectors for damaged columns.

Plate (3-28):continue.

Plate (3-29): Measuring of Concrete Strength by UPV ,and applying Epoxy Resin.

Plate (3-29): continue.

Plate(3-30): Casting of New Concrete (RPC) or (NSC) for External Shell.

Plate (3-31): Applying Epoxy adhesive (Sikadur-330) and (CFRP) for Column (C_{16})

3.12 Test Procedure and Instrumentations

3.12.1 Testing Machine

The hydraulic universal test machine was used to test the burned columns and repaired columns as well as the control specimens, as shown in **Figures (3-9).** The test machine has an ability of (650 kN) available in the Laboratory of Civil Engineering Department of Engineering College at Babylon University.

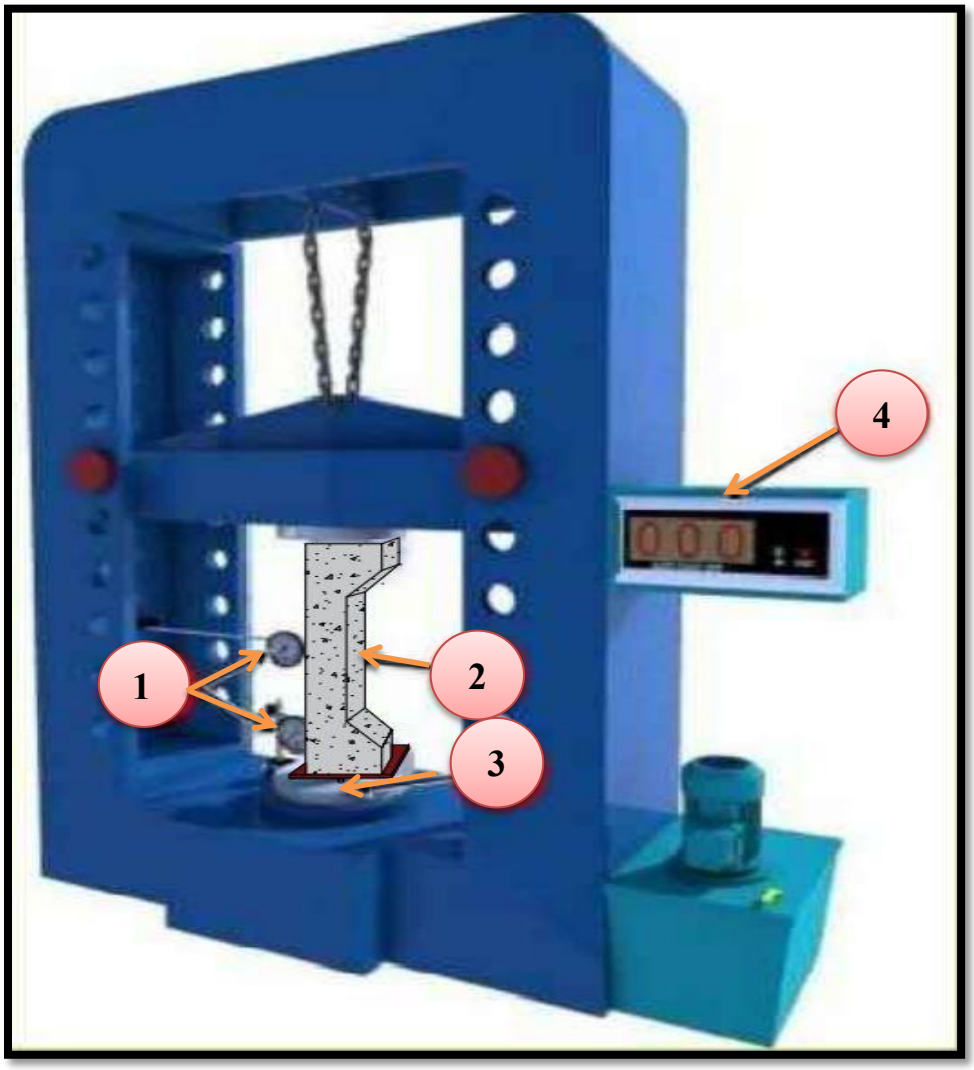

1-Dail gage 2-column Specimen 3- Load Cell 4-Output Device

figure (3-9): Electro-Hydraulic Testing Machine used for Testing Columns.

3.12.2 Download and Support Terms

All columns are pivot-supported, lateral unrestricted columns and tested to failure. Two bearing plates with dimensions (400 x 250 x 10) mm were used in the supports and bearing points to avoid local crushing in the concrete. To control the position of the load, rods of 25 mm diameter were welded to the load plate and the distance required for loading represented the axially of the load. Two deviations were made in this study E_1 = 75 mm and E_2 = 0 mm. **Plates (3-35**) shows details of the supports used in the test.

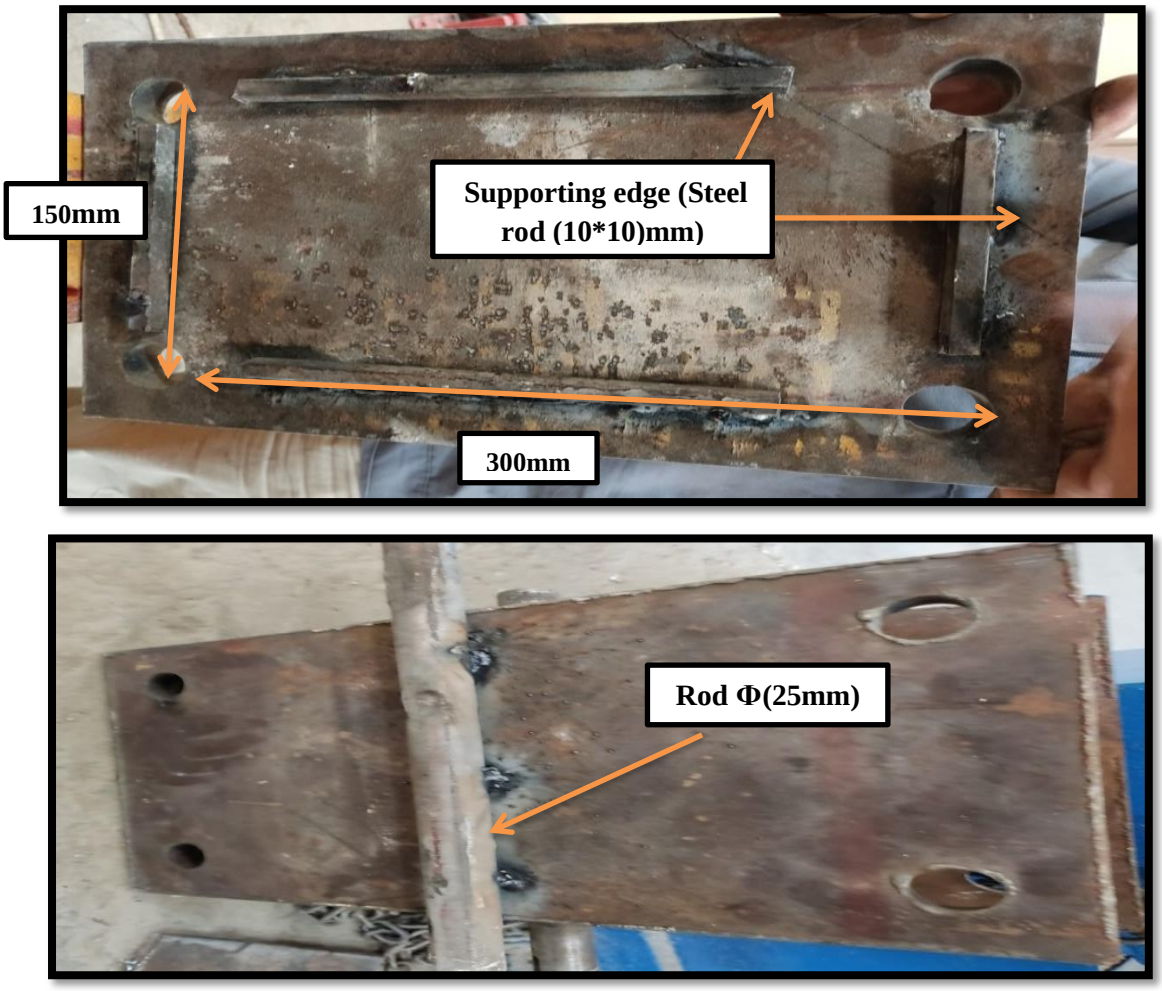

Plate (3-32): Details of the Loading and Supports

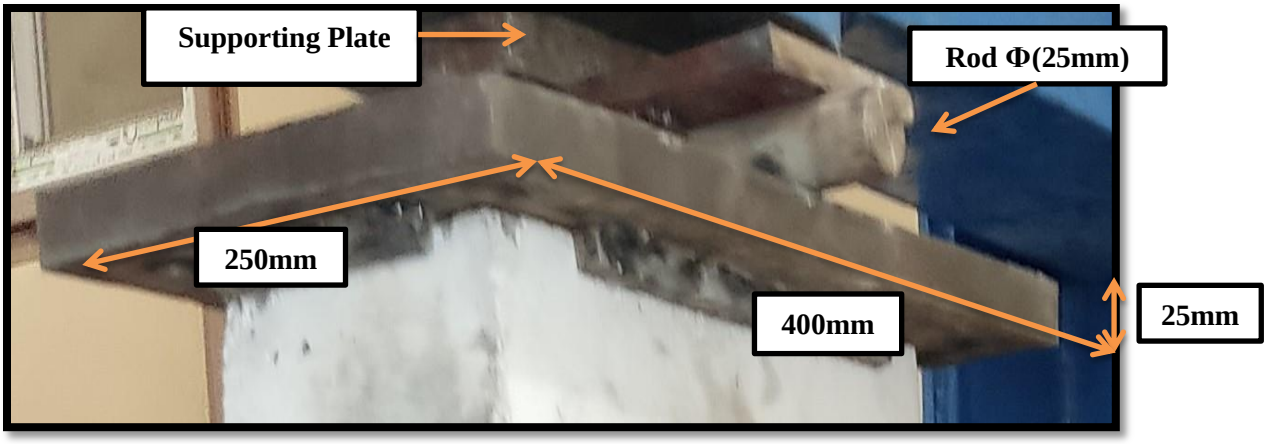

Plate (3-32): continue

3.12.3 Instrumentations

The structural behavior of concrete columns was measured using devices at each stage of loading. The associated lateral deflection, axial deformation, and concrete strain at mid-height, as well as the first crack load, were recorded during each loading step. The tests were followed until failure and the final load was recorded, as well as the width of the cracks at the first incision and the service load. The devices used in the tests are, shown in a **plate (3-36)** as follow:

1- Contact precision measuring devices 0.01 mm were used to measure the lateral deflection and axial deformation.

2-A mechanical expansion gauge with removal points was used to measure concrete strains.

3-Use webcam cameras during the test to record the load and read the demand metrics at the same time by connecting it to a computer.

4- An optical micrometer with an accuracy of (0.005mm) was used to measure the crack width of all column samples.

The positions of the dial gauges and the demic discs are illustrated in **Figure (3-10).**

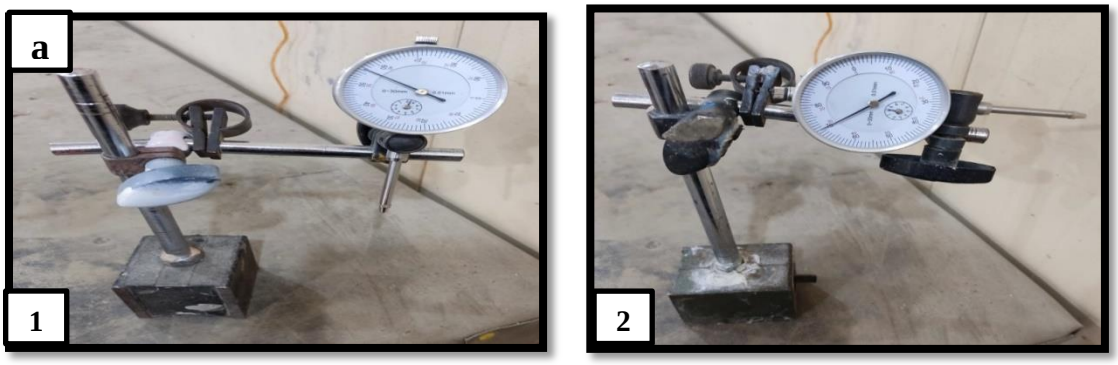

(a) Dial gages(1,2).

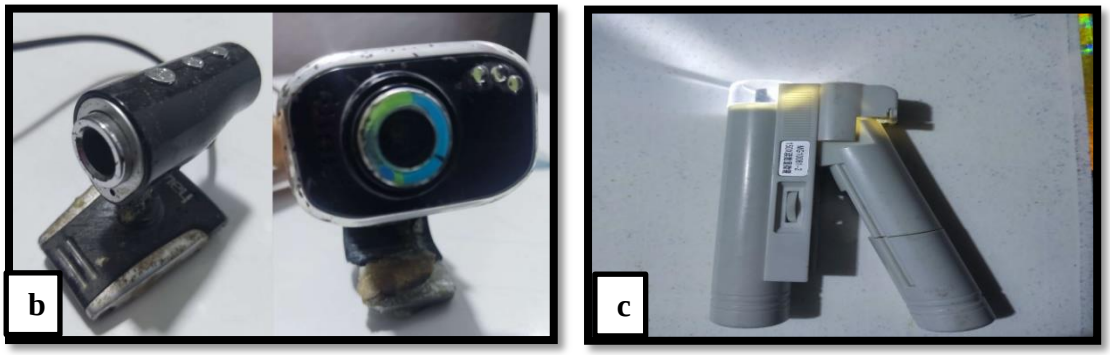

(b) Webcam cameras. (c) Crack meter.

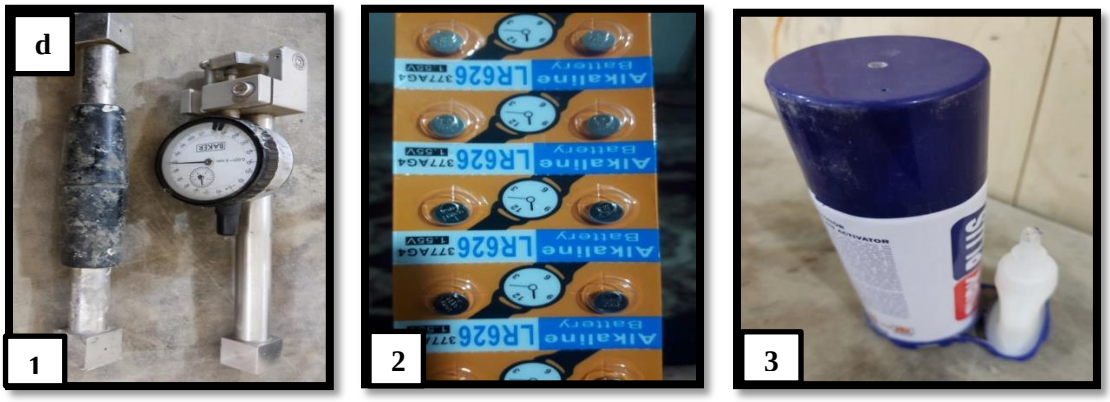

(c) : (1): Mechanical extensometer. (2): demic discs. (3): adhesive demic discs .

Plate (3-33): Instruments used in testing columns.

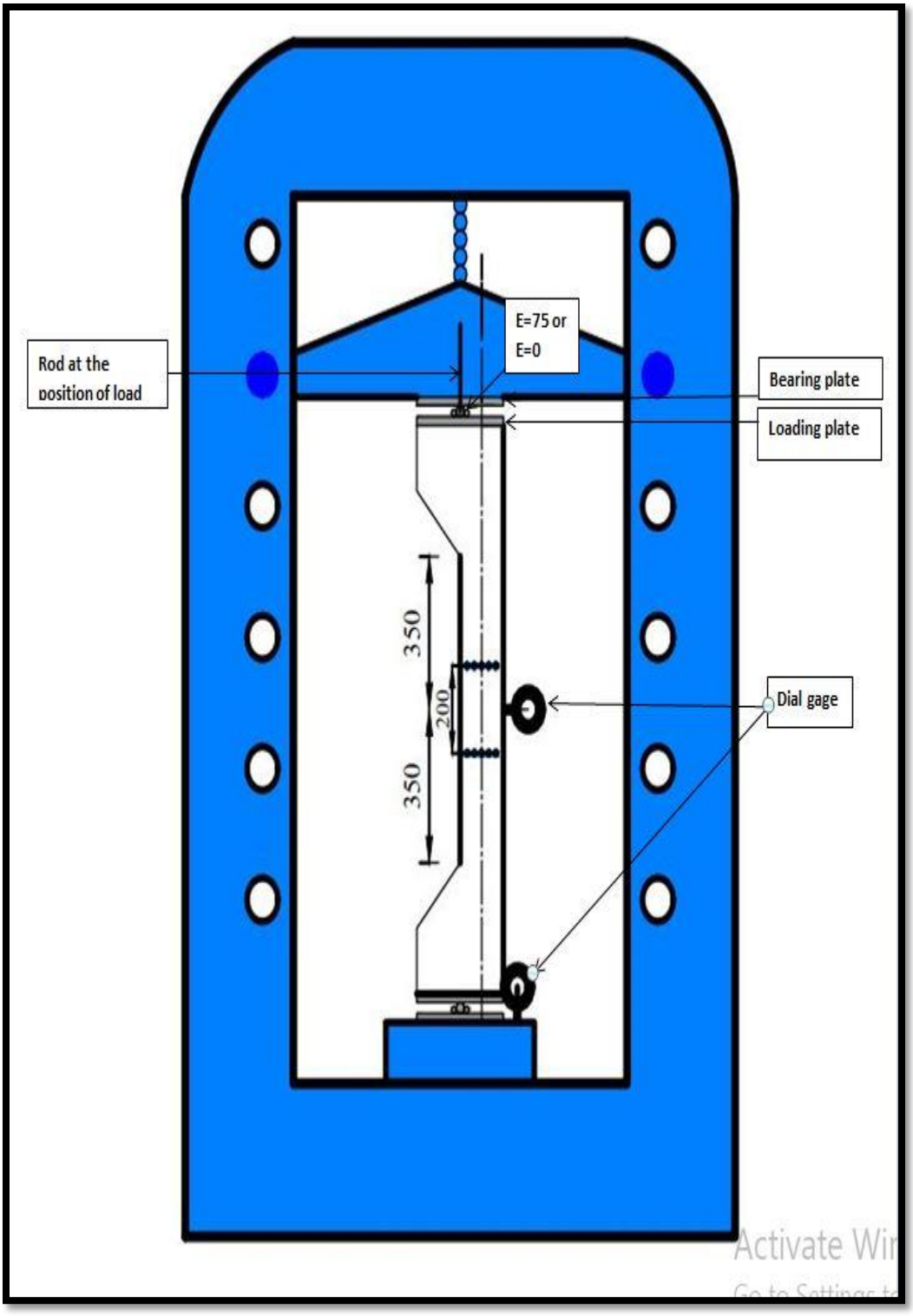

Figure (3-10): Loading System for the Column under loading.

3.12.4 Test Setup

Through testing the columns specimen, the main characteristics of their structural behavior at each step of the loading such as crushing load and final load, strain in offset failure mode, and concrete were recorded. The measurements that were recorded during the tests were as follows:

1- The applied axial load was done by the test machine of a capacity of 650 kN, and the load gain was 20 kN for each stage of the load.

2- For eccentric and concentric loaded columns, the lateral deflection and axial deformation were recorded using a dial gauge with an accuracy of 0.01 mm, and lateral displacement measurements were taken on the tensile side of the column at mid-height and a distance of 350 mm above. Below average height.

3 -Concrete strains were measured with a mechanical stress meter With an accuracy of (0.001) mm. Five pairs of dimes discs of medium column height, i.e., at a distance of (350)mm, are distributed, to monitor the concrete stress at the specified loading level for each column sample.

4-At the specified loading level the crack occurs and its width is measured by the crack meter as well as cracks and other loads causing it to be detected and marked on the tested column. the test Sample procedures are shown in a **plate (3-34).**

Plate (3-34): Column Specimen through the testing procedure.

Chapter Four
Experimental Results and Discussion

Chapter Four

Experimental Results and Discussion

4.1 Introduction

In this chapter, the test results of the experimental program described in chapter three will be presented and discussed. The main purpose is to investigate experimentally the behavior of reinforced concrete columns (NSC, HSC) exposed to periodic fire flame with axial load (eccentric load, concentric load), as well as the behavior of post periodic fire under the influence of axial eccentric load, as well as the restored properties of the structural response of concrete columns that were, repaired and strengthened after damaged due to periodic fire exposure.

Evaluation and comparison of the behavior of all column samples will be based on: residual mechanical properties, residual load capacity, axial and lateral displacements versus load, ductility and hardness index, cracking pattern, types of spalling, failure modes, and strain of concrete at the mid-height of column.

4.2 Mechanical Properties of Control Specimens

The results of destructive tests conducted on the control samples of hardened concrete to specify their mechanical properties without fire exposure. Also, the result of the nondestructive test to estimate the mechanical properties of the damaged concrete columns after fire exposure will be presented.

4.2.1 Destructive Test Results

After completing of the curing period, several destructive tests are performed on the control samples (cubes and cylinders) to determine the mechanical properties of hardened concrete (NSC or HSC)for all column samples prior to fire exposure . Each value was calculated using the average

of three samples, as illustrated in **Table (4-1)**, as well as expected cylinder compressive strength (f́c).

In addition, the results of the destructive test of control sample cubes and cylinders to determine the mechanical properties of the hardened (RPC or NSC) of the outer shell provided for the repaired column samples. Also, according to the equation **(Wong,2013),** the expected compressive strength of the cylinder (f́c) is shown in **Table (4-2):**

Table (4-1): Mechanical properties of the control samples and hardened concrete

Group No.	Specimen	Strength of cubes fcu' (MPa)	Compressive strength fc' (MPa)		Splitting Tensile Strength f_{sp} (MPa)		Modulus of Elasticity Ec(GPa)**	
			Before fire exposure	After fire exposure	Before fire exposure	After fire exposure*	Before fire exposure*	After fire exposure
Group1	$NC_1S_1E_1$	40.79	32.63	____	4.64	_____	26.85	_____
	$NC_2S_1E_1F_1$	39.31	31.45	12.43	4.27	2.08	26.36	16.57
	$NC_3S_1E_1F_2$	39.31	31.45	14.37	4.27	2.24	26.36	17.82
	$NC_4S_1E_1F_3$	38.31	30.65	10.67	4.19	1.93	26.02	15.35
	$NC_5S_1E_1F_4$	38.31	30.65	9.11	4.19	1.78	26.02	14.19
	$NC_6S_1E_1F_5$	39.59	31.67	6.57	4.47	1.51	26.45	12.05
	$NC_7S_1E_1F_6$	39.59	31.67	8.32	4.47	1.70	26.45	13.56
Group2	$NC_8S_1E_2F_1$	39.03	31.22	16.17	4.11	2.37	26.26	18.90
	$NC_9S_1E_2F_3$	39.31	31.45	13.99	4.27	2.20	26.36	17.50
Group3	$NC_{10}S_2E_1$	41.38	33.1	_____	4.81	_____	27.04	_____
	$NC_{11}S_2E_1F_1$	40.79	32.63	11.86	4.64	2.03	26.85	16.19
	$NC_{12}S_2E_1F_3$	39.31	31.45	9.87	4.27	1.85	26.36	14.77

	Table (4-1) Continue.							
Group4	$HC_{13}S_1E_1$	79.76	65.4	_____	6.96	_____	33.75	_____
	$HC_{14}S_1E_1F_1$	78.77	64.59	22.7	6.31	2.81	33.58	22.72
	$HC_{15}S_1E_1F_3$	79.51	65.2	19.12	6.82	2.58	33.71	21.42
Group5	$NC_{16}S_1E_1F_3R_1$	39.59	31.67	10.2 (25.12)	4.47	1.88 (2.96)	26.45 (23.56)	15.01
	$NC_{17}S_1E_1F_3R_2$	39.31	31.45	9.87 (23.57)	4.27	1.85 (2.86)	26.36 (22.82)	14.77

() Ultrasonic pulse velocity test results of brackets.

$f'_{c\,(NSC)} = 0.8\ fcu$ *Al-Mashhadany (2009)* …… (4-1)

$f'_{c\,(HSC)} = 0.82\ fcu$ *Al-Mashhadany (2009)* …... (4-2)

$f'_{c\,(RPC)} = f\ cu$ *Al-Khazragy (2016)* ..... (4-3)

$*fsp_{(NSC,HSC)} = 0.59\sqrt{fc'}\ (MPa)$ *according to (ACI 318-19)* …... (4-4)

$**\ Ec_{(NSC)} = 4700\sqrt{fc'}\ (MPa)$ *according to (ACI 318-19)* ..... (4-5)

$**Ec_{(HSC)} = 3320\sqrt{fc'} + 6900(MPa)$ *according to (ACI 363R-11)* …. (4-6)

Table (4-2): Mechanical properties of the control samples (RPC and NSC)

Specimen	*Compressivestrength fc' (MPa)*	*Splitting TensileStrength fcp (MPa)*	*Modulus of Elasticity Ec(GPa)**
$NC_{16}S_1E_1F_3R_1$	110	10.17	43.42
$NC_{17}S_1E_1F_3R_2$	32.61	4.61	26.84

$*Ec_{(RPC)} = 4140\sqrt{fc'}\ (MPa)$ *according to (Adheem)* ….. (4-7)

4.2.2 Non- Destructive Test Results

- **Ultrasonic Pulse Velocity**

A non-destructive test (ultrasonic pulse velocity test) is performed on all columns, with or without repair, to estimate the mechanical properties of concrete column samples after fire exposure. The measured pulse velocity in concrete can be affected by many factors, including the nature of the concrete surface (smooth or rough) temperature of the specimen, moisture conditions, age of the specimen, and the presence of steel reinforcement **(Trtnik, and et.al.2009).**

For sample columns that had been subjected to fire, ultrasound pulse velocity tests were provided, To minimize the expected error in any measured results, the average values of two different sites free of reinforcement and on opposite axes were averaged in each column sample after cyclic fire exposure. The ultrasonic pulse velocity results of compressive strength for all column specimens after fire exposure are presented in **Table (4-1).**

4.2.3 Evaluation of Concrete Mechanical Properties of columns

The result of the **Table (4-1)** showed the effect of periodic burning that included some variables on the mechanical properties of columns concrete. These variables can be described as follows:

- **Effect of number of fire-exposure cycles**

From comparison with to control sample column(C_1), the columns (**C_2** and **C_3)** and (**C_2** and **C_4**) have a decrease in the compressive strength about (14 and 8)% with an increase in the number of burning cycles. Also, there is

degradation in splitting tensile strength and modulus of elasticity about (7 and 8) %, and (7 and 8)%, respectively ,as shown in **Figures (4-1 a ,b, c).**

- **Effect the time duration of each fire exposure cycle**

From comparison to the columns compared to the control sample column(C_1), Comparison the columns (C_3 and C_5) (one cycle) and (C_4 and C_7) (four cycles),that is a decrease in the compressive strength with increasing time duration cyclic, about (37 and 22) %,respectively. There is, also decreased in splitting tensile strength and modulus of elasticity from about (21 and 12)%, and (21 and 12)%, respectively, as shown in **Figures (4-1 a, b, c)**.

- **Effect of temperate target of each fire cycle**

column (C_6) with compared column (C_4),experiences an increase in the target of cycles fire exposure during burning, resulting in a decrease in compressive strength about (39) %. Split tensile strength and modulus of elasticity , also decreased about (22)% and (22)% , respectively for (four cycle), as shown in **Figures (4-1a,b,c).**

- **Effect the Eccentricity of pre-load**

From comparison between samples (**C_8** and **C_9**) with concentric pre-load ,and samples(**C_2** and **C_4**) with eccentric pre-load through the cyclic fire, there is a increase in the compressive strength, splitting tensile strength, and modulus of elasticity during the periodic fire exposure of the samples about (24 and 23) % , (13 and 12)% and (13 and 12)%, respectively for (two cycle and four cycle), respectively, as shown in **Figures (4-1 a, b, c).**

➢ **Role of longitudinal Steel Reinforcement Ratio**

Comparing specimens ($\mathbf{C_{11}}$ and $\mathbf{C_{12}}$) to ($\mathbf{C_2}$ and $\mathbf{C_4}$) with the lowest longitudinal steel reinforcement , compressive strength, splitting tensile strength, and modulus of elasticity decrease by (5 and 8)% , (2 and 4)%, and (2 and 4)%, respectively, for (two cycle and four cycle), respectively, as shown in **Figures (4-1 a, b, c).**

➢ **Type of concrete (HSC) for columns**

Comparison between samples ($\mathbf{C_{15}}$,$\mathbf{C_{14}}$ and $\mathbf{C_{15}}$) which were made of high-strength concrete, through the periodic fire exposure there is a decrease in the compressive strength, splitting tensile strength and modulus of elasticity of the samples about (64 and 73)%, (59 and 64)%,and (32 and 38)%, respectively, for (two cycle and four cycle) , respectively, shown in **Figure (4-1a,b, C).**

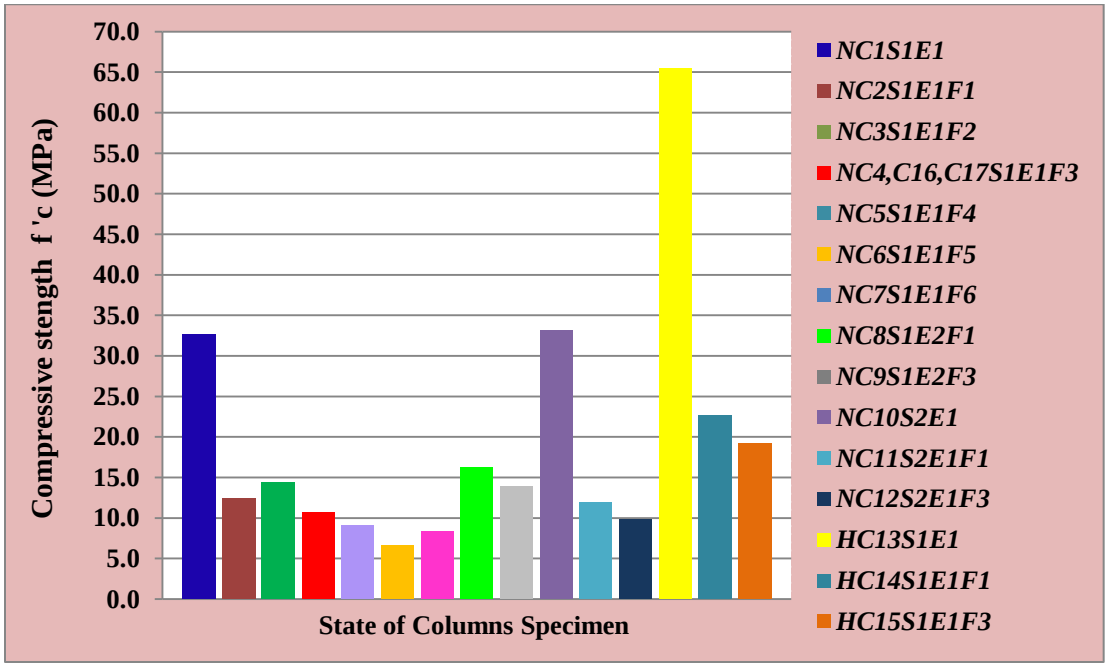

Figure (4-1a) Effect compressive strength.

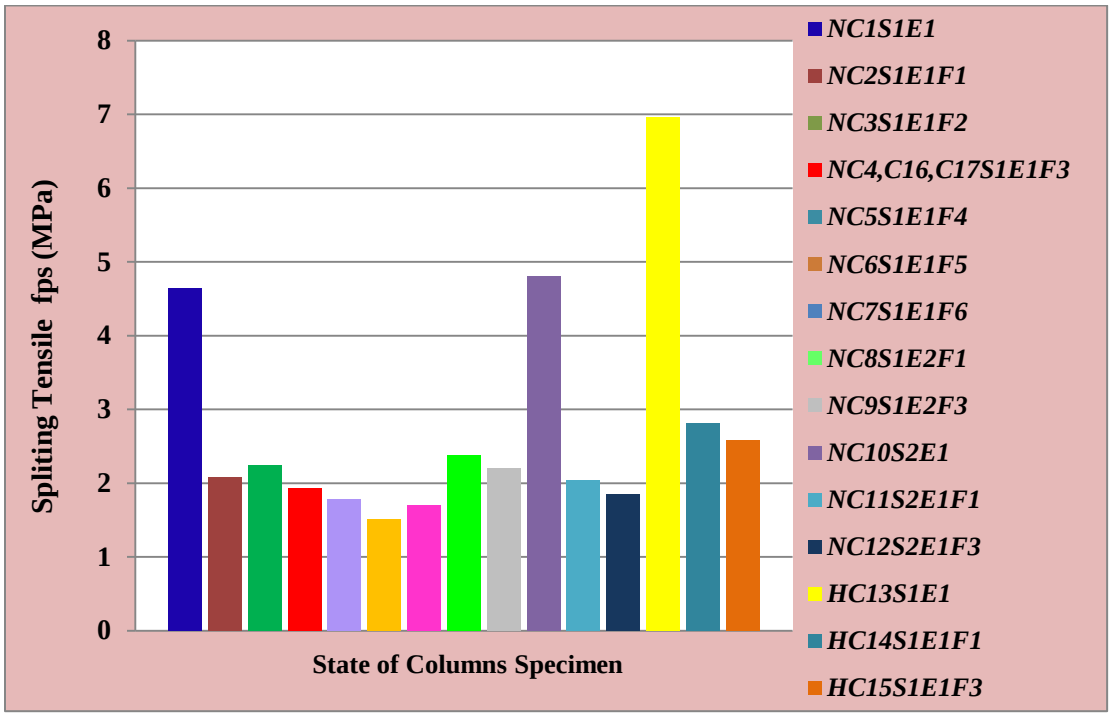

Figure (4-1b) : Effect splitting tensile strength.

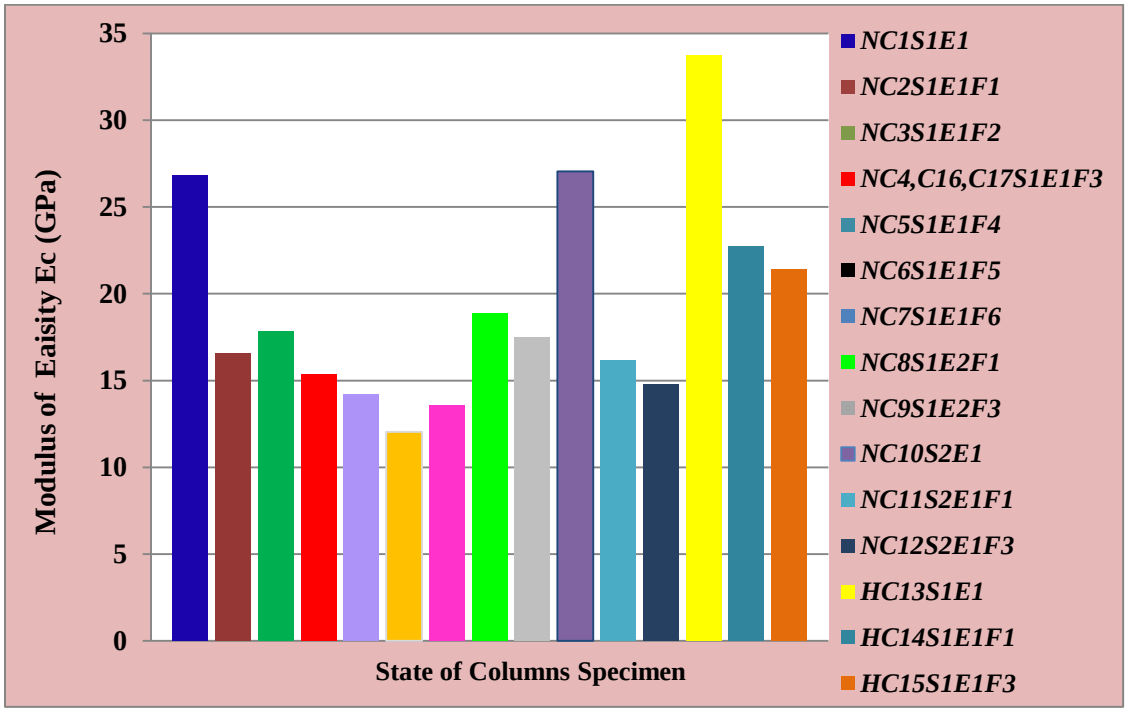

Figure (4-1c) Effect the Modulus of Elasticity.

Figure (4-1): Effect of Fire Exposure with Pre-Load on Mechanical Properties of Concrete Column Specimens.

4.3 General Response of Tested Column Samples

The results of the control samples without fire exposure , pre-loaded samples with cyclic fire exposure at a rate (one cycle, two cycles, and four cycles) and retrofit samples after cyclic fire exposure are summarized in **Table (4-3).**The main experimental results in test are included of cracking load, ultimate load, axial displacement, lateral displacement, and failure mode .

In the early stages of loading ,after completing fire exposure scenarios the reinforced concrete columns are free of any cracks, and the first visible crack is a horizontal crack that appeared on the tensile side at and around the mid-height of the column samples with a load value called the first crack load ($\mathbf{P_{cr}}$).As the applied load increases, the cracks spread in different positions on the tension side and begin to spread until the ultimate stage where spalling occurred followed by failure**. Plates (4-1) to (4-17),** show the cracking pattern and failure mode of the tested columns.

The control samples (C_1, C_{10}, and C_{13}) that were not exposed to fire showed a significant difference in cracking, ultimate load, axial deformation of the axial load, and lateral displacement when compared to samples exposed to periodic fire. The cracking load and ultimate load were lower and the deformation was greater for samples (C_3 and C_5) exposed to fire for one cycle than for samples (C_2, C_{11}, and C_{14}) exposed to burning for two cycles. Additionally, samples exposed to periodic burning for four cycles (C_4, C_{15}, C_{16}, and C_{17}), The cracking load and ultimate load were lower and the greater deformation, when increased the target temperature for sample (C_6). Also, The sample(C_7) was periodically burned for a longer duration.

It was noted that the samples (C_8, C_9) with concentric loaded during exposure to cyclic burning, and there is a significant in cracking and ultimate load compared to samples that were eccentrically loaded during exposure to cyclic burning with the same number of cycles (C_2 and C_4),where cracking load, and the ultimate load was more, in addition to lesser .

Also, for the samples (C_{16} and C_{17}) that were retrofitting and strengthening ((NSC with CFRP) and RPC), respectively, have improvement the cracking load and the ultimate load compared with of samples subjected to periodic burning at a rate of (four cycles (C_4) and control (C_1)).

In general, load versus average lateral deflection of mid-height, and load versus axial deformation behavior include ,and three important phases: non-cracked elastic, cracked elastic, and ultimate stages. The first was a straight segment at the load-displacement curve, and the second was about a non-linear part with slope changing with increasing longitudinal and lateral displacement (the cracked elastic part), the third was also the non-linear part but with characteristics showing a slight increase in load results versus greater axial deformation and lateral deflection (representing plastic or ultimate stage). Figure **(4-2) to (4-17)** show the response of the load - axial displacement and the response of the load -lateral displacement at mid-height of the tested columns.

Table (4-3): Experimental Results of the Tested Column Specimens.

Group	Specimen Symbol (C_i)	Cracking Load Pcr (kN)	Ultimate Load P_u (kN)	Displacement at service Load Δ_s (mm)		Failure Model
				Axial	Lateral	
Group1	$NC_1S_1E_1$	80	261	4.78	4.06	Gradual compression failure at bottom height
	$NC_2S_1E_1F_1$	39	203	5.11	5.23	Gradual compression failure at mid height
	$NC_3S_1E_1F_2$	48	215	4.99	4.65	Gradual compression failure at mid height
	$NC_4S_1E_1F_3$	32	190	5.41	5.84	Gradual compression failure at bottom height
	$NC_5S_1E_1F_4$	29	187	6.83	7.04	Compression failure with the crushing or spalling of concrete at mid height
	$NC_6S_1E_1F_5$	21	166	7.58	8.76	Compression failure with the crushing or spalling of concrete at last height
	$NC_7S_1E_1F_6$	27	185	7.41	8.52	Compression failure with the crushing or spalling of concrete at last height
Group2	$NC_8S_1E_2F_1$	200	454	7.75	3.31	Shear failure at the top of the column
	$NC_9S_1E_2F_3$	180	438	8.92	3.89	Shear failure at the top of the column
Group3	$NC_{10}S_2E_1$	62	230	4.43	4.75	Tension and compression failure with spalling of concrete
	$NC_{11}S_2E_1F_1$	28	179	5.22	5.91	Tension and compression failure with spalling of concrete
	$NC_{12}S_2E_1F_3$	20	163	5.43	6.17	Tension and compression failure with spalling of concrete
Group4	$HC_{13}S_1E_1$	103	425	6.57	5.24	Brittle tension and sudden spalling of the cover
	$HC_{14}S_1E_1F_1$	52	323	7.12	7.31	Brittle tension and sudden spalling of the cover
	$HC_{15}S_1E_1F_3$	36	291	7.38	7.93	Brittle tension and sudden spalling of the cover
Group5	$NC_{16}S_1E_1F_3R_1$	50	254	6.32	5.1	Crushing failure in concrete and rupture CFRP
	$NC_{17}S_1E_1F_3R_2$	87	380	6.16	6.56	Shear failure at the bracket

***Δs**= displacement at service load (Ps =0.65 Pu) **(Al-Haddad,2016).**

4.3.1 Pilot column

This column was installed to ensure sufficient force was applied during the burning process, as it was tested under eccentric axial load (77 kN), as well as to verify the test system and loading instruments suitable for post-fire exposure testing. It was subjected to periodic burning for two days and with a period time (1 hour) of burning temperature (500C˚),The first crack that show at mid-height column ,at a load of (20 kN). The failure happened on the compression side suddenly at load (158 kN).

4.3.2 Test Results of Columns (Group I)

the group includes samples (C_1 to C_7) which were made of (NSC) for reinforced with (4 Φ12 mm) steel bars ,and ties (Φ4 mm) is spacing of (100 mm) and pre-loading (30% Pu=77KN) with concentric (E=75 mm or e/h= 0.5).

4.3.2.1 Control Column ($NC_1S_1E_1$)

This specimen is made from normal concrete and not exposed to fire .The first visible crack is horizontal and appeared on the tension side of mid-height column at axial load (80 kN). The failure happened on the compression side suddenly at load (261 kN) with spalling of the external shell , as shown in **Plate (4-1).**The load axial displacement and the load lateral displacement curve ,are illustrated in **Figure (4-2).**

Plate (4-1): Failure mode and crack pattern of column specimen ($\mathbf{C_1}$)

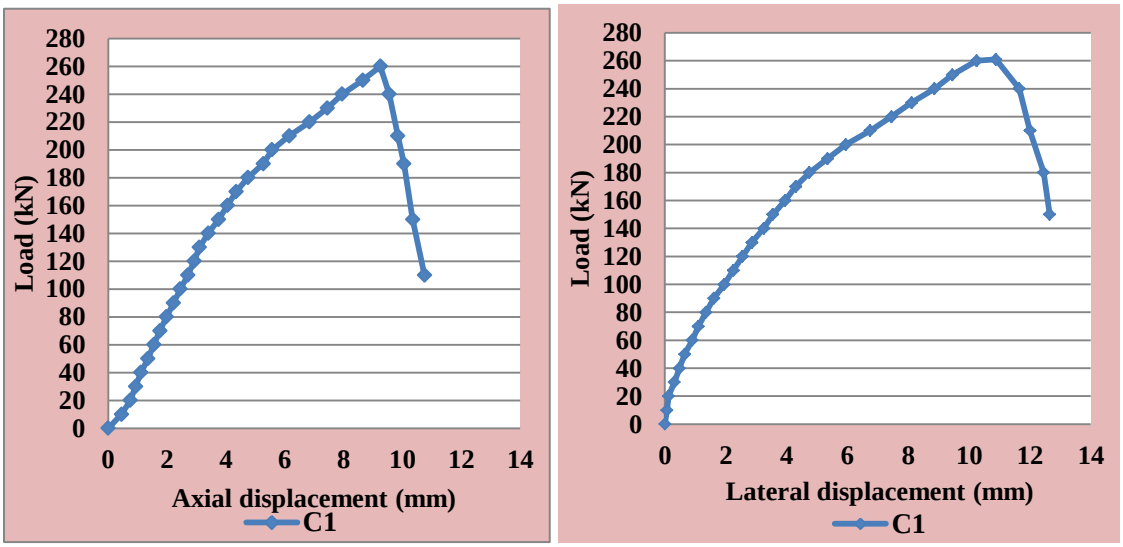

Figure (4-2): The Load- displacement Curves for Specimen (C_1).

4.3.2.2 Columns with Cyclic Fire Exposure

These samples were (C_2,C_3,C_4,C_5,C_6 and C_7) exposed to different cyclic fire scenarios with pre-loading.

- **Specimen($NC_2S_1E_1F_1$)**

This sample was subjected to periodic burning of temperature (400°C) and rate of two cycles and with a time duration (45 min) per cycle (day),

In the first day of burning, after (15 min) of firing the appearance of cracks on the left south side at the top of the column and the appearance of fragmentation in the left northern corner. In the second day after the passage of (24) hours after burning the first day of the column and while keeping the loading constant on the column.

In the second day of burning, fire was shed on the column with stable loading (30%Pu) .The cracks were in a state of increasing spread throughout the column.

After cooling and remove the pre-loading, the column was tested up to failure :the first visible crack is the horizontal crack that appeared on the tensile side at and about mid-column height at the axial load (39 kN). The failure on the compression side occurred suddenly at loading (203 kN) with the outer shell fragmenting, as shown in **Plate (4-2).** The axial load deformation and the lateral load displacement curve ,are illustrated in **Figure (4-3).**

Comparison with the control specimen (C_1), there is a decrease in the cracking load by about (51) % .Also, there was a decrease in the ultimate capacity of about (22) %, as shown in **Table (4-3**).

Plate (4-2): Failure mode and crack pattern of column specimen (C_2).

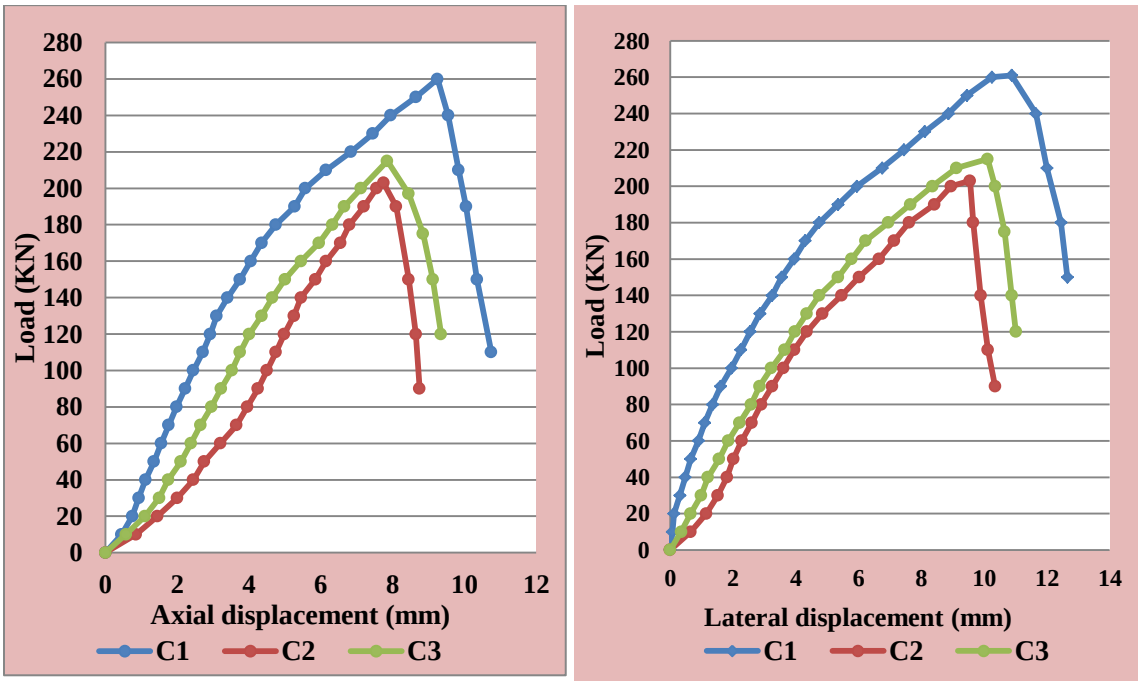

Figure (4-3): The Load-Displacement Curves for Specimens **(C_1,C_2, C_3)**

- **Specimen $NC_3S_1E_1F_2$**

The sample was subjected to periodic burning at a temperature of (400C°) with rate of one cycle and a period time (90 min). which is the total burning time of specimen C_2 .

When preparing the column and setting the fire (with keep of pre-loading (30%P)) and after (15 min) of fire on the column, we see the appearance of capillary cracks on the right and left south side below the column, and (30min) of burning we see fragmentation on the right north side, mid-height column and the spread of capillary cracks in all sides After the passage of (1 hour) of burning, the appearance of capillary cracks on all sides of the column increased.

After Colling to room temperature, the column was tested under static load: the first visible crack is the horizontal crack that appeared on the tensile side at and about mid- height column of load about (48 kN). The failure on the compression side occurred suddenly at loading (215 kN) with the outer shell fragmentation, as shown in **Plate (4-3).** The load axial deformation and the load lateral displacement curve are illustrated in **figure (4-3).**

Comparison with the control specimen (C_1) decrease in the cracking load and ultimate capacity about (40 and18) % ,respectively ,also; comparison with specimen (C_2), there is an increase in the cracking load and ultimate capacity about (19 and 6) %, respectively, as listed **Table (4-3).**

Plate (4-3): Failure mode and crack pattern of column specimen (C_3).

- **Specimen $NC_4S_1E_1F_3$**

This sample was exposed to four fire cycles (4 days) with a period (45 min) per cycle (day), and temperature of target (400 °c) .

First day: after (15) minutes of burning, capillary cracks on the right south side and left (bottom of the column), and after (30 min) fragmentation developed at the right northern corner of the column.

In the second day: we notice that cracks may increase in length and depth on the column. then we do the burning process for same time duration (45 min) , the occurrence of along column.

In the third day: we notice the column and before burning an increase in cracks on the right north side and right south side, deterioration of concrete, then we do the burning process for (45min) monitoring, we notice that spalling occurs on the left north side (mid height) and the right southern side (mid height) and after the end of the period, the column is left to cool for (24 hours) while maintaining constant loading on the column during cooling.

In the fourth day: Before burning, noticed an increase in the deterioration in the concrete and an increase in the width of the cracks spread on all sides of the column, then do the burning process and continuous monitoring and after (45) minutes of burning we turn off the fire, raise the load and let it cool Inside the oven, then lift out of the oven to cool on site.

For post-fire testing: the first visible crack is the horizontal crack that appeared on the tensile side at mid-height column at load (32 kN).The failure on the compression side occurred suddenly at loading (190 kN) with the outer shell fragmentation, as shown in **Plate (4-4).** The load axial deformation and the load lateral displacement curve, are illustrated **in figure (4-4).**

Comparison with the control specimen (C_1), there is a decrease in the cracking load of about (60) % also, there was a decrease in the ultimate capacity of about (27) %, as shown in **Table (4-3).**

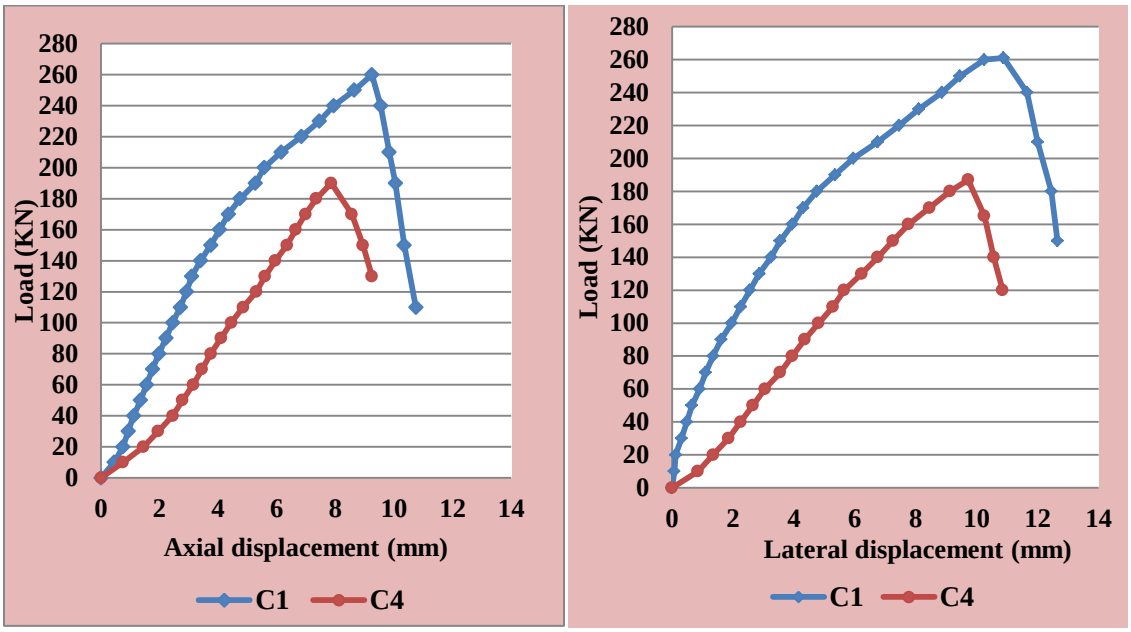

Figure (4-4): The Load-Displacement Curves for Specimens (C_1, C_4)

Plate (4-4): Failure Mode and Crack Pattern of Column Specimen (C_4).

- **Specimen $NC_5S_1E_1F_4$**

This sample is subjected to one fire cycle of temperature of (400C˚),at time duration (180)min. which is total time burning of column (C_4).

The day burning: After preparing the column and setting the fire (with keep of loading) and continuous monitoring. After (15 min) of burning, we notice the appearance of thin cracks on the left-south side in the middle of the column.

For post–fire test: the first visible crack was a horizontal crack that appeared on the tension side at and about the mid-height column at load (29 kN). The failure on the compression side occurred suddenly at load (187kN) with the outer shell fragmentation, as shown in **Plate (4-5)**. The load axial deformation and the load lateral displacement curve, are illustrated in **figure (4-5)** .

Comparison with control specimen (C_1), there is a decrease in the cracking load and ultimate capacity about (64% and 29%), respectively, comparison with specimen (C_3) there is a decrease in the cracking load and ultimate capacity about (40% and 13%), respectively; also, comparison with specimen (C_4) there is a decrease in the cracking load and ultimate capacity about (9%)and(2)%, respectively ,as shown in **Table (4-3).**

Plate (4-5): Failure Mode and Crack Pattern of Column Specimen (C_5).

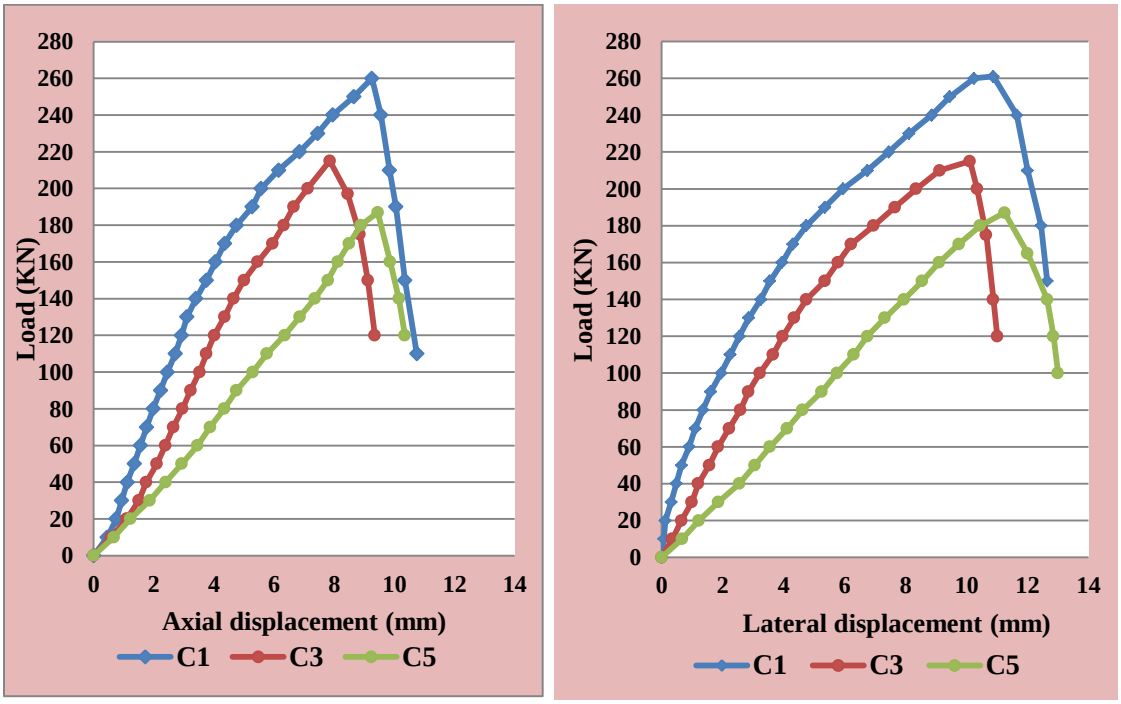

Figure (4-5): The Load- displacement Curves for Specimen (C_1,C_3 **and** C_5).

- **Specimen $NC_6S_1E_1F_5$**

This sample (C_6) was made of ordinary concrete and subjected to periodic fire at a rate of four cycles and with a time (45 min) per cycle (day) under the influence of pre- loading (30%Pu), and temperature of (600°C).

In the first day of periodic burning: after (20 min) of burning, capillary cracks appeared along the left north side, after the combustion period is over, the column is allowed to cool for (24) hours while maintaining constant loading on the column during the cooling period.

In the second day: noticed that cracks may increase in length and width on the column, through the burning process, through burning process for time (45) min , the cracks spread in all sides of the column, then it is cooled for (24) hours while maintaining constant loading on the column during the cooling period as well.

In the third day: notice the column and before combustion an increase in cracks on the right-north side and the right-south side, and deterioration of concrete, through burning process for time (45 min) with continuous monitoring, and after the end of the period, the column is left to cool for (24) hours ,while Load on the column during cooling

In the fourth day: after (20) min of burning process , we notice that fragmentation occurred in the north-south right corner (top height column) and after completion of burning turn off the fire, raise the load and leave it to cool inside the oven, then raise it outside the oven to cool inside the laboratory.

For post-fire test: the first visible crack is the horizontal crack that appeared on the tensile side and about mid-height at load (21 kN). The failure on the compression side occurred suddenly at loading (166 kN) with the outer shell fragmentation, as shown in **Plate (4-6**). The load axial deformation and the load lateral displacement curve, are illustrated in **figure (4-6).**

Comparison with control specimen (C_1) and specimen(C_4),there is a decrease in the cracking load and the ultimate capacity about(74%) and (37)%, respectively; also, for specimen comparison (C_4) there is a decrease in the cracking load and the ultimate capacity about (35%) and(13%), respectively, as illustrated in **Table(4-3).**

Plate (4-6): Failure Mode and Crack Pattern of Column Specimen (**C_6**).

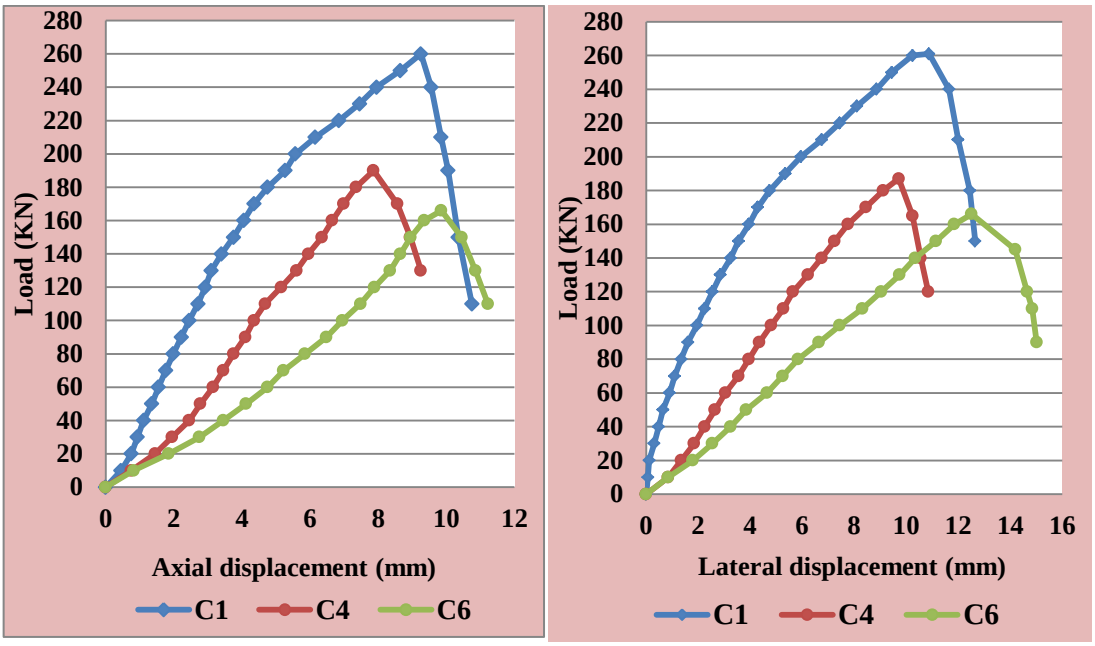

Figure (4-6): The Load- displacement Curves for Specimen (**C_1,C_4 and C_6**).

- **Specimen ($NC_7S_1E_1F_6$)**

This sample was subjected to periodic fire of four cycles with temperature target (400C˚) and time duration (75 min) per cycle (day).

In the first day: after preparing the column and setting the fire (with keep of loading),and after (20min) of burning, capillary cracks appeared along the side The left north, the column is allowed to cool for (24 hours) while maintaining constant loading on the column during the cooling period.

In the second day: then we do the burning process for some time (45min), we note the increased spread of cracks in all sides of the column, while maintaining constant loading on the column during the cooling.

In the third day: then we do the burning process for (45min) and continuous monitoring, and after the end of the period, the column is left to cool for (24 hours) while maintaining its stability. Loading on the column during cooling.

In the fourth day: then do the burning process and continuous monitoring (20 min) we notice that fragmentation occurred in the north-south right corner (top height column) and after finishing the process of burning, We turn off the fire, raise the load and leave it to cool inside the oven, then raise it outside the oven to cool inside a location.

For post-fire testing: the first visible crack is the horizontal crack that appeared on the tensile side at and about mid-height column of load (27 kN). The failure on the compression side occurred suddenly at loading (185 kN) with the outer shell fragmentation, as shown in **Plate (4-7).**The load- axial deformation and the load- lateral displacement curve ,are illustrated in **figure (4-7).**

Comparison with control specimen (C_1) and there is a decrease in the cracking load and the ultimate capacity about (66% and 29%) ,respectively; also, comparison with specimen (C_4),there is a decrease in of about (16%) and (3)% respectively, as listed in **Table(4-3).**

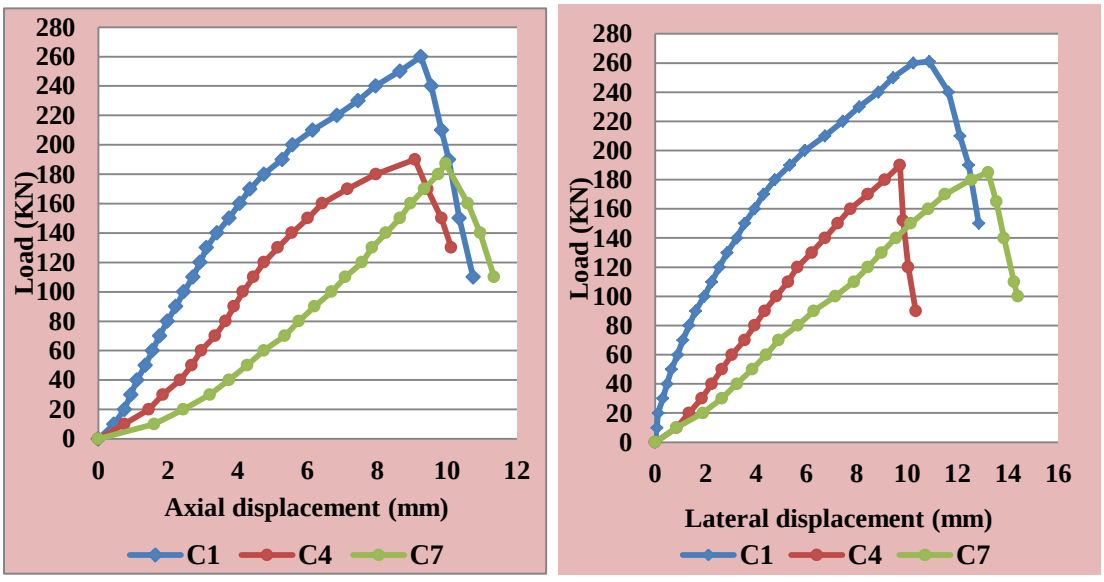

Figure (4-7): The Load- displacement Curves for Specimen (C_1,C_4 andC_7).

Plate (4-7): Failure Mode and Crack Pattern of Column Specimen (**C_7**).

4.3.3 Test Results of Columns (Group II)

These samples (C_8 and C_9) were made of normal concrete reinforced with (4 Φ12) mm steel bars as longitudinal reinforcement, and ties (Φ4 mm) of spacing (100 mm),pre-loading (30% Pu=163KN) with concentric (E = 0 mm or e/h = 0).The samples were exposed to periodic firing at a temperature (400°C) of rate (two cycles and four cycles),respectively, with a period time (45)min per cycle (day).

- **Specimen ($NC_8S_1E_2F_1$)**

This sample was subjected to periodic fire at a temperature (400°C) of rate two cycles and a period time (45 min) per cycle (day).

In the first day of periodic burning: after preparing the column and making a fire (with constant loading) and continuous monitoring. After (15 minutes) of burning, we noticed the appearance of thin cracks on the left south side at the top and middle of the column.

In the second day of burning: After turning on the furnace and starting combustion, after (15 min), increase the number of lattice cracks along the north side and the right and left the south.

For post - fire testing: the first visible crack is the horizontal crack that appeared on the tensile side at and about mid-column height at the axial load (200 kN). The failure on the compression side occurred suddenly at loading (454 kN) with the outer shell fragmenting, as shown in **Plate (4-8).** The load -axial displacement and the load - lateral displacement curve ,are illustrated **Figures (4-8).**

Comparison with the control specimen (C_2) of eccentric pre-load, there is an increase in the cracking load of about (80%) and there is an increase in the ultimate capacity of about (55 %) . as shown in **Table (4-3).**

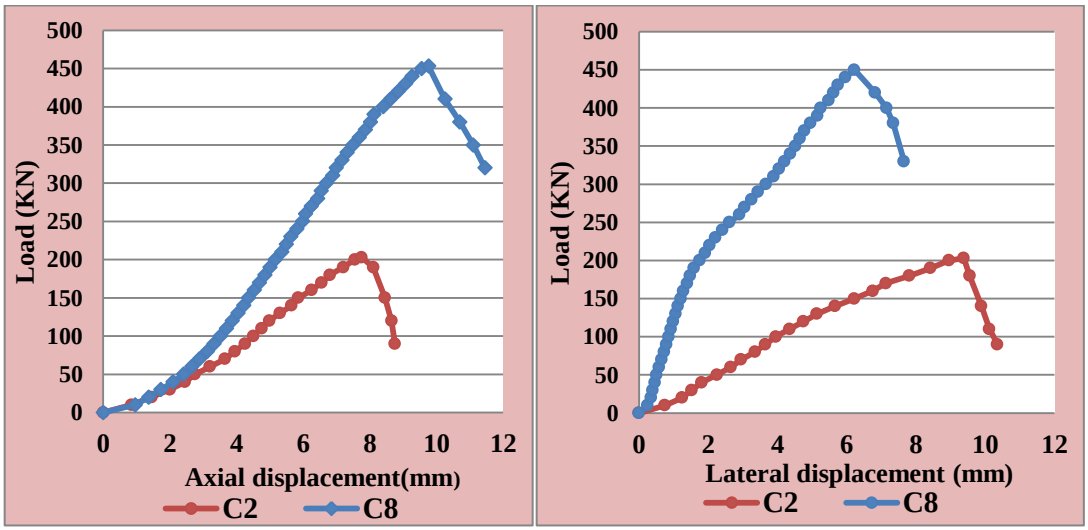

Figure (4-8): The Load- displacement Curves for Specimen (**C_2 and C_8**).

Plate (4-8): Failure Mode and Crack Pattern of Column Specimen (C_8)

- **Specimen $NC_9S_1E_2F_3$**

This sample was made of normal concrete and subjected to periodic burning at a temperature of (400 °C) and rate of four cycles with a period time (45 min) per cycle (four days).

In the first day of periodic burning: after (25min)of burning, we noticed the appearance of thin cracks on the left-south side in the top of the column and the mid-height.

In the second day of burning: turning on the furnace and start combustion, after (20min) of burning , increase the number of thin cracks along the north side and the right and left south sides.

In the third day of burning: after the end of the burning period we noticed an increasing in the number and width of cracks .The column was left to cool for (24 hours), and keep constant load on the column during cooling.

In the fourth day: before burning, oticed the deterioration of the concrete and the increase of capillary cracks spread on all sides of the column. After (45min) of burning, we turn off the fire, raise the load and let it cool inside the oven, then lift it outside the oven to cool inside the laboratory.

At post-fire test: the first visible crack was the horizontal crack that appeared on the tensile side at mid height about of load (180 kN). The failure on the compression side occurred suddenly of load (438 kN) with the outer shell fragmentation, as shown in **Plate (4-9).** The axial load deformation and the load lateral displacement curve ,are illustrated in **Figures (4-9)**

Compared with the control specimen(C_4) of eccentric pre-load, there was an increase in the cracking load of about (83%) and there was an increase in the ultimate capacity of about (56 %), as listed in **Table (4-3).**

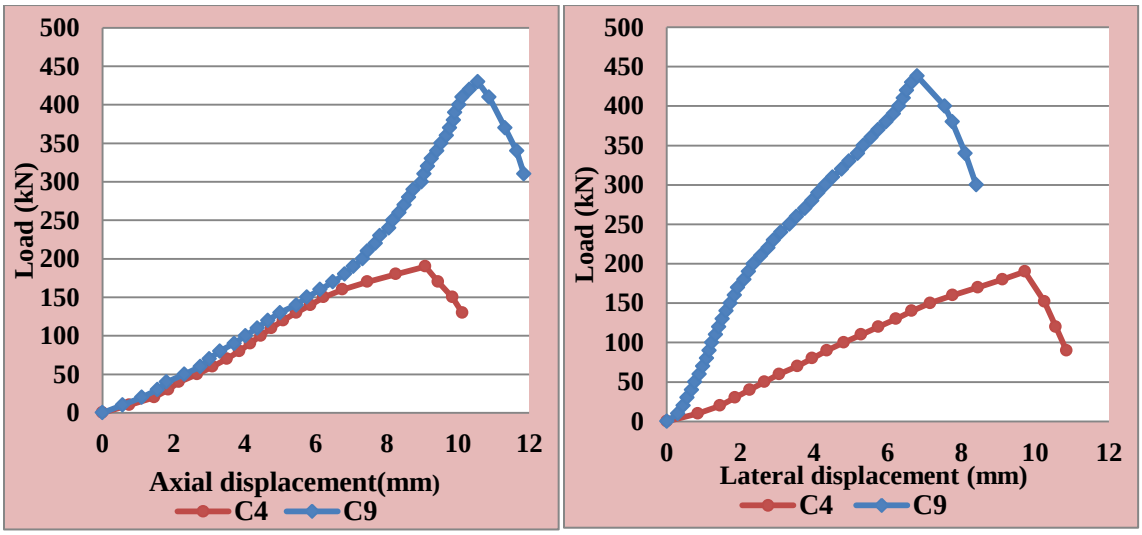

Figure (4-9): The Load- displacement Curves for Specimen (**C_4 and C_9**).

Plate (4-9): Failure Mode and Crack Pattern of Column Specimen (C_9)

4.3.4 Test Results of Columns (Group III)

These samples(C_{10}, $C_{11}$and C_{12}) were made of normal concrete reinforced with (4 Φ10 mm) steel bars, and ties (Φ4 mm) of spacing (100 mm), pre-loading (30% Pu=68 KN) and eccentricity (E = 75mm or e/h = 0.5).The samples (C_{10}) without burning while (C_{11}) and(C_{12}) were exposed to periodic firing at a temperature (400°C) of rate (two cycles and four cycles) respectively, with a period time (45) min per cycle (day).

- **Control Columns($NC_{10}S_2E_1$)**

This specimen was made from normal concrete and not exposed to fire. The first visible crack was a horizontal crack that appeared on the tension side at and around the mid-height of the column at load (62 kN). The failure happened on the compression side suddenly at load (230 kN) with spalling

of the external shell, as shown in **Plate (4-10).** The load- axial deformation and the load-lateral displacement curve ,are illustrated in **Figures (4-10).**

Comparison with the control specimen (C_1),there is a decrease in the cracking load of about (23)% and there was a decrease in the ultimate capacity of about (12 %) ,which is approximately near to difference between C_1 and C_2 ,as listed in **Table (4-3)**.

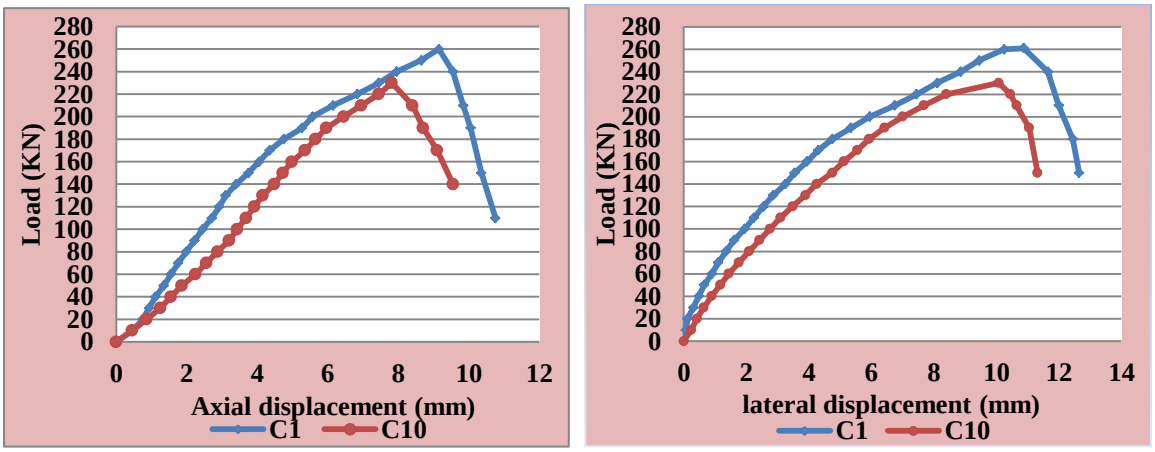

Figure (4-10): The Load- displacement Curves for Specimen (**C_{10} and C_1**).

Plate (4-10): Failure Mode and Crack Pattern of Column Specimen (C_{10}).

- **Specimen (*$NC_{11}S_2E_1F_1$*)**

This sample was made of normal concrete and subjected to periodic firing at a temperature of (400 C˚) of two cycles and with a period (45 min) per cycle (day).

In the first day of periodic burning: after (15min) of burning, we noticed the appearance of thin cracks on the left southern side at the middle and top of the column and the left northern side at the top and middle of the column. These cracks continue to spread until the expiration of the burning period.

In the second day: noticed that cracks increased after the cooling period of the column. Then turning on the furnace and starting the burning, after (30 min) we see the appearance of fragmentation on the side left south (bottom column), in addition to the cracks previously scattered on all sides of the column.

At post-fire test: the first visible crack was the horizontal crack that appeared on the tensile side at and about mid height column of load (30 kN). The failure on the compression side occurred suddenly at loading (179 kN) with the crushing. as shown in **Figures (4-11)** and **plate (4-11)**

Comparison with the control specimen (C_{10}),there is a decrease in the cracking load of about (58)% and there was a decrease in the ultimate capacity of about (22 %) ,which is approximately near to difference between C_1 and C_2 ,as listed in **Table (4-3).**

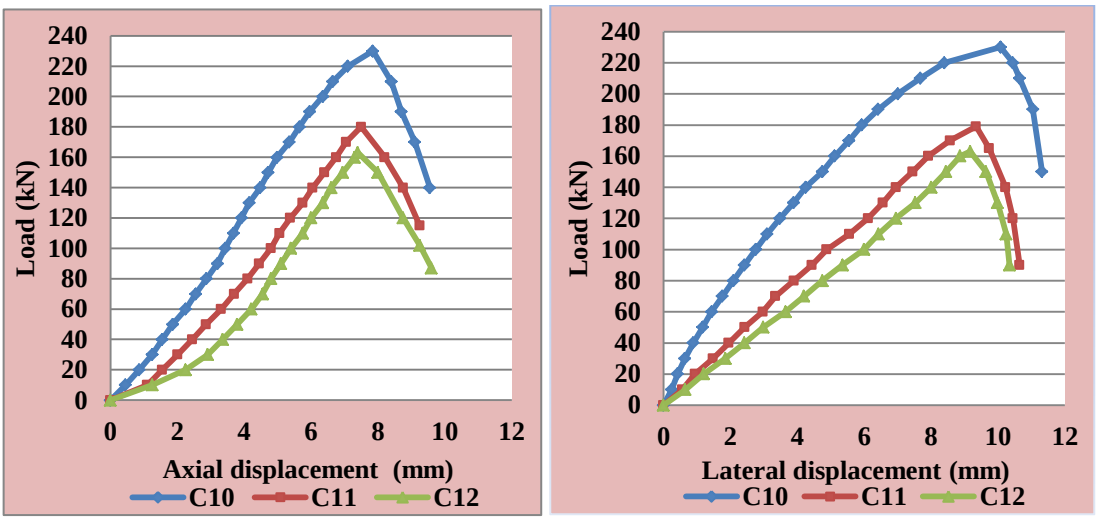

Figure (4-11): The Load-displacement Curves for Specimen (**C_{10},C_{11} and C_{12}**).

Plate (4-11): Failure Mode and Crack Pattern of Column Specimen (**C_{11}**)

- **Specimen (*$NC_{12}S_2E_1F_3$*)**

This sample was made of ordinary concrete and subjected to periodic burning of four cycles with temperature (400°C) and period (45 min) per cycle (day).

In the first day of periodic burning: after (20 min) of burning, noticed the appearance of thin cracks on the left south side and right in the middle, the top of the column and the left north side at the top of the column. These cracks continued to spread until the burn period was over.

In the second day: after (24) hours of burning on the first day, noticed required load, and cracks increased in number after the cooling period of the column. After turning on the furnace and start burning, after (25 minutes) we see the beginning of fragmentation on the left north side (bottom of the column), in addition to cracks spreading on the right side of the column, cracks appearing above and below the column to the right southern side.

In the third day of consuming: After 24 hours, observed an increase in cracks on the north-right and right-south sides as well as spalling of concrete. After 45 minutes of burning and continuous monitoring, the column was left to cool for(24 hours) with constant loading on it during cooling.

In the fourth day: In the fourth day: before burning, notice an additional deterioration of the concrete and an increase in cracks scattered on all sides of the column (right side, left side north, right side, left side south), and then we do the burning process. After (45) minutes of burning, we turn off the fire, raise the load and leave it to cool inside the oven , then raise it outside the oven to cool inside the laboratory .

For post-fire test: the first visible crack is the horizontal crack that appeared on the tensile side at and about mid-height at the axial load (20 kN). The failure on the compression side occurred suddenly at loading (163

kN) with the outer shell fragmentation, as shown in **plate (4-12)**, and **Figure(4-11).**

Comparison with the control specimen (C_{10}) and specimen (C_4), there is a decrease in the cracking load of about (76 %) and there was a decrease in the ultimate capacity of about (29%) which is approximately near to difference between C_1 and C_4 ,as listed in **Table (4-3).**

Plate (4-12): Failure Mode and Crack Pattern of Column Specimen (**C_{12}**).

4.3.5 Test Results of Columns (Group IV)

The samples (C_{13},$C_{14}$and C_{15}) was made of High Strength concrete reinforced with (4 Φ12 mm) steel bars longitudinal reinforcement, ties (Φ4mm)of spacing (100 mm),and pre-loading (30% Pu=109 KN) with eccentricity (E= 75mm and e/h = 0.5).The sample (C_{13}) without burning while (C_{14}) and

(C15) were exposed to periodic firing at a temperature (400°C) of rate (two cycle and four cycle) respectively, with a period time (45 min) per cycle.

- **Control Columns($HC_{13}S_1E_1$)**

This specimen was made from High Strength concrete and not exposed to fire, The first visible crack was a horizontal crack that appeared on the tension side and around mid-height of the column at load (130 kN). The failure happened on the compression side suddenly at load (425 kN) with spalling of the external shell, as shown in **Plate (4-13).** The load axial deformation and the load lateral displacement curve are illustrated in **figure (4-13).**

Comparison with the control specimen (C_1), there is a increase in the cracking load of about (39 %) and there was a decrease in the ultimate capacity of about (39%).The failure type this specimen brittle tension and sudden spalling of the cover ,while (C_1) gradual compression failure at quarter height.

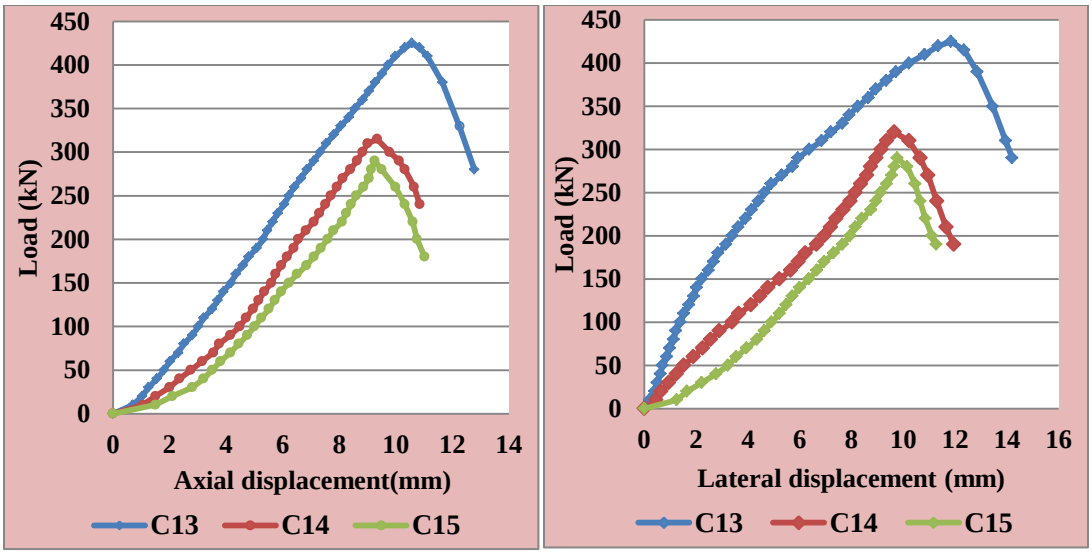

Figure (4-12): The Load- displacement Curves for Specimen (C_{13},C_{14} **and** C_{15}).

Plate (4-13): Failure Mode and Crack Pattern of Column Specimen ($\mathbf{C_{13}}$)

- **Specimen ($\mathbf{HC_{14}S_1E_1F_1}$)**

This sample was made of high-strength concrete and subjected to periodic burning at temperature (400°C), for two cycles with a period of time (45 min) per cycle.

In the first day of periodic burning: after (20 min) of burning, noticed the appearance of thin cracks on the left and right south side at the top of the column and the left north side at the bottom of the column ,and the right north side at the mid height of the column. These cracks will continue to spread until the burn period was over.

In the second day: After (24) hours of cooling the column from burning for the first day, noticed an increase in the number of cracks. After turning on the furnace and starting combustion, after(20min) notice the appearance of fragmentation in the north-right corner and the right-north-south corner

(top of the column), and the occurrence of fragmentation on the right-south side (middle of the column), in addition to the spread of cracks in all sides of the column. after (45 min) minutes of burning we turn off the fire, raise the load and leave it to cool inside the oven, then raise it outside the oven to cool inside the laboratory.

For post-fire test: The first visible crack was a horizontal crack that appeared on the tensile side at and about mid-column height at the axial load (52kN). The failure on the compression side occurred suddenly at loading (323kN) with the outer shell fragmentation, as shown in **plate (4-14)** .

Compared with the control specimen (C_{13}), there is the decrease in the cracking load of about(60)% and a decrease in the ultimate capacity of about (25)% , as shown in **Figures (4-13**)and **Table (4-3),**which is (51 and 22) % then difference between C_1 and C_2 is more .

Plate (4-14): Failure Mode and Crack Pattern of Column Specimen (C_{14})

- **Specimen ($HC_{15}S_1E_1F_3$)**

The sample was made of HSC and subjected to periodic burning at a temperature of (400 °C) at a rate of four cycles and with a period time (45min) per cycle .

In the first day of periodic burning: after (25 min) of burning, notice that fragmentation occurred on the left south side (bottom of the column), and cracks appeared on the right southern side and the left north side (middle of the column). These cracks was continue to spread until the burn period is over.

In the second day: after (24 hours) of burning on the first day, noticed the cracks increased in number after the cooling period of the column. After turning on the furnace and starting burning, after (15 min), spalling occurring on the right north side (upper column), in addition to capillary cracks spreading on the north side of the mid-column.

In the third day of burning :after (24 hours) of burning on the first day, noticed the column and before burning an increase in cracks on the north-right side and the right-south side and the deterioration of concrete, then do the burning process for (45min) accurate and continuous monitoring, note the spread of cracks on the right south side (top and mid height of the column) and left (top and mid height of the column) , and after the burning period ends, the column is left to cool for (24 hours) while maintaining a constant load on the column during cooling.

In the fourth day, before burning, notice a deterioration of the concrete and an increase in cracks scattered on all sides of the column (right and left side in the north, right and left side in the south), and then we do the burning

process. after (25 min) we notice the fragmentation of the right northern corner near the right southern side, and after (45min) of burning turn off the fire, raise the load and leave it to cool inside the oven.

For post-fire test: The first visible crack was a horizontal crack that appeared on the tensile side at mid-height column of load (36 kN). The failure on the compression side occurred suddenly at loading (291 kN) with the outer shell spalling, as shown in **plate (4-15)**and **Figure (4-13).**

Compared with the control specimen (C_{13}), there is a decrease in the cracking load of about (72)% and there was a decrease in the ultimate capacity of about (32)% , as listed in **Table (4-3).** which is (60 and 27)% for cracking load and ultimate capacity then difference between C_1 and C_4 is more .

Plate (4-15): Failure Mode and Crack Pattern of Column Specimen C_{15}

4.3.6 Strengthened Specimens after Cyclic Fire Exposure(Group V)

The specimens(C_{16} and C_{17}), were same to (C_4) in detail and burning process made from normal concrete, and reinforced with (4Φ12mm) steel bars as longitudinal reinforcement and ties (Φ 4mm) of spacing (100 mm) with pre-load (30%Pu) of eccentricity (E=75 mm and e/h= 0.3). The specimens were strengthened and retrofit after being exposed to periodic burning of four cycles at temperature (400C˚),specimen(C_{16}) that made from the normal concrete for core and strengthened by new external shell (NSC with CFRP laminate), while (C_{17}) made from the normal concrete core and strengthened by only new external shell of (RPC), in attempt to restore the missed strength and serviceability requirements.

- **Specimens ($NC_{16}S_1E_1F_3R_1$)**

This column was exposed to fire for a scenario of four cycles and a period (45 min) per cycle pre-loading (30%Pu). After (25 min), of burning capillary cracks appeared on the top of the right and left north side, top of the left south side, and such cracks spread along the column throughout the burning period. After the burning period ends, the column leaves cooling for (24) hours while keeping the loading on the column during the cooling period.

In the second day: before burning, noticed that the cracks are increasing in their spread on the column, then do the burning process time (45) minutes and remain in a state of continuous monitoring of the column crack propagation. cool for 24 hours while keeping the loading constant on the column during the cooling period as well.

In the third day: noticed an increase in cracks on the right north side and the right south side and the deterioration of the concrete. Then do the

burning process for (45 min) and continuous monitoring, and note the appearance of fragmentation on the left northern side (mid height of the column) and after the end of the period leaves the column to cool for (24) hours Keeping constant loading on the column during cooling.

In the fourth day: before burning, notice a further deterioration of the concrete and an increase in cracks spread on all sides of the column (the right and left north side, the right and left south side), then do the burning process for cycle and continuous monitoring and after (45) minutes of burning we turn off the fire and lift the load and let it cool inside the oven. Then raise out of the oven to be cooled for a day or two, then we removed the outer crust of the columns and carry out the treatment process and apply all the steps and pour the normal concrete. Then do the strengthening process for the column with carbon fiber (CFRP) laminates of width (50)mm ,as illustrated in experimental program .

For post –repair test: the first visible crack was the longitudinal crack that appeared at the center of the corbel at load (50 kN). The failure occurred gradually compression load (254 kN) on side near of the corbel and shell spalling at mid- height, as shown in **plate (4-16).**

Comparison with specimen (C_4), there is increase the cracking load of about (36)%, and there is increase in the ultimate capacity of about (34)%, as shown in **Figures (4-14).**on the other hand, compassion with control specimen (C_1) it have approximately same ultimate load.

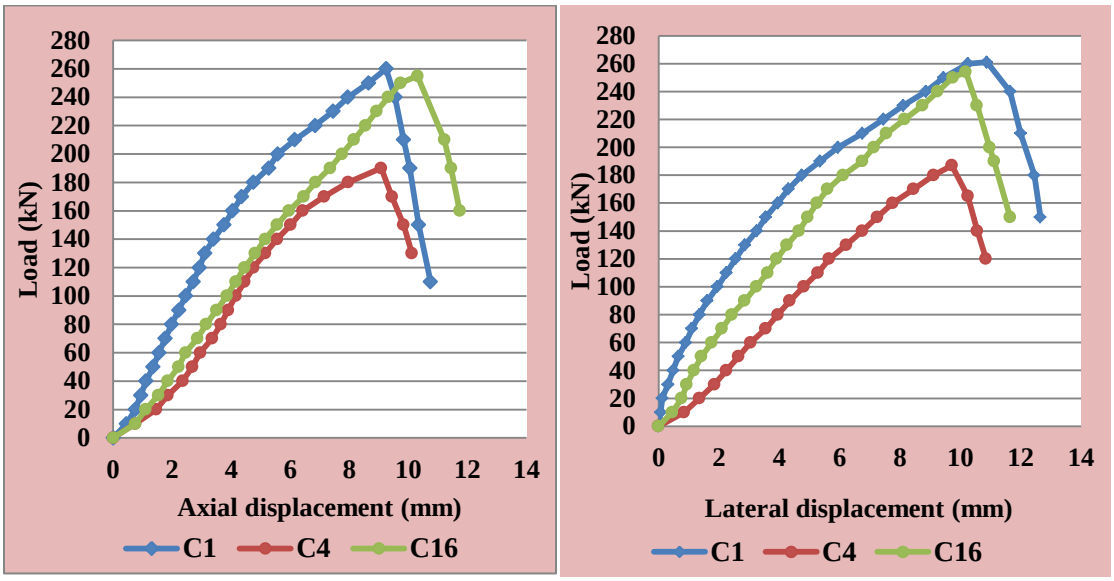

Figure(4-13): The Load- displacement Curves for Specimen(**C_1,C_4 andC_{16}**).

Plate (4-16): Failure Mode and Crack Pattern of Strengthened Column Specimen (**C_{16}**).

- **$NC_{17}S_1E_1F_3R_2$**

The column was exposed to fire of four cycles with a period (45min) and influence of continuous pre-loading (30% Pu).

In the first day: after (20 min) of burning, capillary cracks appeared in the upper right south side and left, and these cracks are increasingly spread along the column throughout the combustion period. after the burning period is over, the column was left to cool for (24) hours while keeping the loading constant on the column during the cooling period.

In the second day: of this day and before burning, noticed that the cracks we increased in their number and width on the column. Then we burn for time (45) minutes and we remain in a state of continuous monitoring of the column and the location of the cracks. Cool for (24) hours while maintaining constant loading on the column during the cooling period.

In the third day: noticed the column and before combustion an increase in cracks on the right north side and the right south side and the deterioration of the concrete, then we do the burning process for (45) minutes and continuous monitoring, and we note the occurrence of fragmentation on the right southern side (top and middle of the column) and in the northern side of (mid-height) and after the end of the period, the column was left to cool for (24) hours while keeping constant loading on the column during cooling.

In the fourth day: before burning, noticed a further deterioration of the concrete and an increase in cracks scattered on all sides of the column (right side, left side north, right side, and left side south), then we do the burning process, and after (45) minutes of burning, we turn off the fire, raise the load and leave it to cool inside the oven, and raise from oven to cool, then we

removed the outer damaged shell of the columns and do the strengthening process illustrated previously in experimental program .

For post–repair test: The first visible crack was the longitudinal that appeared at load (87 kN). The failure occurred gradually upon load (380 kN) on the top column and near the corbel in compression mode outside the strengthened region , as shown in **plates (4-17).**

Comparison with the specimen (C4), there is an increase in the cracking load of about (63)% and an increase in the ultimate capacity of about (100)%, as shown in **Figures (4-16)**. comparison with control specimen (C_1) it have more cracking load ultimate load about (9 and 46)% , respectively addition compression and curve (C_1,C_{16},C_{17}) and find for that specimen (C_{17}) giving the good rustle from C_{16}.

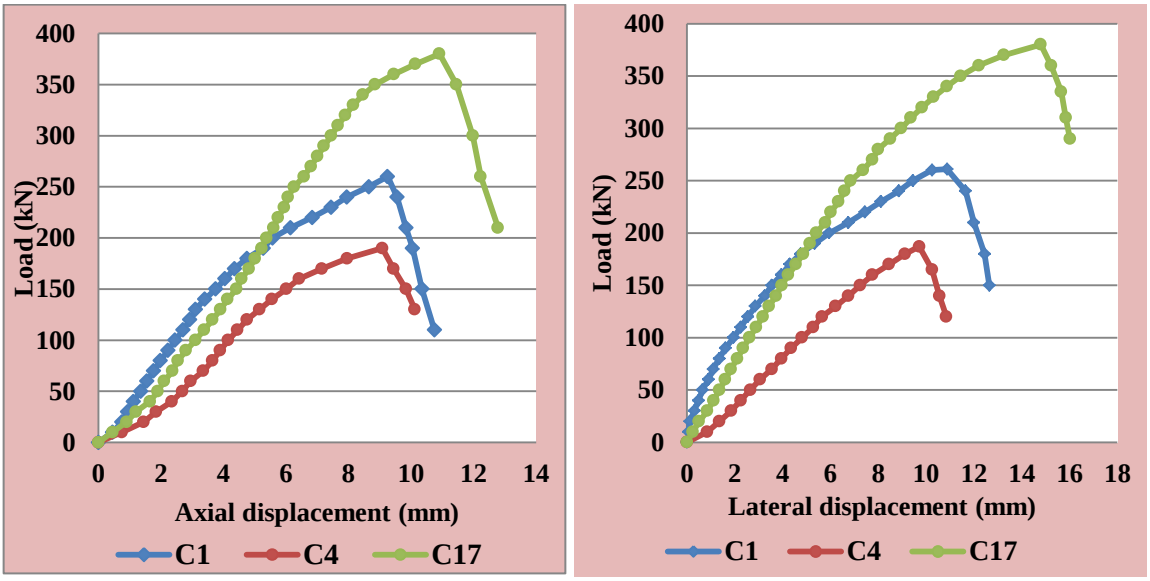

Figure (4-14): The Load- displacement Curves for Specimen (C_1,C_4 and C_{17}).

Plate (4-17): Failure Mode and Crack Pattern of Strengthened Column Specimen (C_{17})

4.4 Ductility Index

The ductility index is defined as the ratio of deflection at ultimate load to the deflection at the yielding of the tensile reinforcement **(Al-Haddad,2016).** Also, ductility is defined as the energy absorbed through materials up to the failure that has been completed. In the current study, ductility ratios are assessed according to the vertical or lateral displacement at maximum load divided by vertical or lateral displacement at the service load (approximately 65% of ultimate load)**(Al-Haddad,2016**), as listed in **Table (4-4).**

Table (4-4): Ductility index of tested columns.

Group No.	Specimen Symbol (Ci)	Service displacement Δs (mm)*		Ultimate displacement Δu(mm)		Ductility ratio $\mu = (\frac{\Delta u}{\Delta s})$	
		Axial	Lateral	Axial	Lateral	Axial	Lateral
Group 1	$NC_1S_1E_1$	4.78	4.06	9.1	10.99	1.90	2.71
	$NC_2S_1E_1F_1$	5.11	5.23	7.61	9.65	1.49	1.85
	$NC_3S_1E_1F_2$	4.99	4.65	7.85	10.11	1.57	2.17
	$NC_4S_1E_1F_3$	5.41	5.84	7.72	9.72	1.43	1.66
	$NC_5S_1E_1F_4$	6.83	7.04	9.45	11.28	1.38	1.60
	$NC_6S_1E_1F_5$	7.58	8.76	9.86	12.32	1.30	1.41
	$NC_7S_1E_1F_6$	7.41	8.52	9.94	13.22	1.34	1.55
Group 2	$NC_8S_1E_2F_1$	7.75	3.31	9.61	6.22	1.24	1.88
	$NC_9S_1E_2F_3$	8.92	3.89	10.32	6.85	1.16	1.76
Group 3	$NC_{10}S_2E_1$	4.43	4.75	7.81	10.85	1.76	2.28
	$NC_{11}S_2E_1F_1$	5.22	5.91	7.52	9.47	1.44	1.60
	$NC_{12}S_2E_1F_3$	5.43	6.17	7.31	9.03	1.35	1.46
Group 4	$HC_{13}S_1E_1$	6.57	5.24	10.53	10.68	1.60	2.04
	$HC_{14}S_1E_1F_1$	7.12	7.31	8.92	9.57	1.25	1.31
	$HC_{15}S_1E_1F_3$	7.38	7.93	8.33	9.31	1.13	1.17
Group5	$NC_{16}S_1E_1F_3R_1$	6.32	5.1	10.57	10.78	1.67	2.11
	$NC_{17}S_1E_1F_3R_2$	6.16	6.56	10.97	14.86	1.78	2.27

***Δs**= displacement at service load (Ps =0.65 Pu) **(Al-Haddad,2016).**

In general, for the first group: the specimens exposure cyclic fire for specific variables that leading to decrease in ductility ratio (axial or lateral) displacement that showing by for specimens (C_2 to C_3) (C_2 to C_4) and (C_4 to

C_5) about (6 ,4 and 3) % or (18, 11and 4)%, for (number fire exposure cycles), respectively. For specimen (C_4 to C_6) , ductility ratio in the (axial or lateral) displacement is decreased about (9 or 16) %, for (highest intensity temperature), respectively. While the specimens (C_3 to C_5) and (C_4 to C_7) ductility ratio in the (axial or lateral) displacement is decreased about (12 and 6)% or (26 and 7)%, for (longest duration burning), respectively.

In the second group of the specimens (C_8, C_9)with concentric (e=0),with completed (C_2 , C_4) with eccentric (e=75mm)the ductility decreases in the (axial) or increases in (lateral) displacement, about (17 and 19)% or (5 and 6) %, respectively.

The third group samples (C_{11}, C_{12}) to control (C_{10}) with reinforcement (0.014) during exposure to periodic burning, completed (C_2, C_4) with reinforcement (0.02) , the ductility ratio the (axial or lateral) decreasing about (4 and 5)% or (10 and 12), respectively ,for (two cycles and four cycles) ,respectively.

The fourth group samples (C_{14}, C_{15}) with control column(C_{13}) The samples were made from high strength concrete, , the ductility ratio for the axial and lateral displacements about (22 and 30)%,or (36 and 43)%, respectively.

The fifth group was the retrofitting and strengthening columns (C_{16}, C_{17}), were retrofitted of ((NSC with CFRP) and RPC), respectively, for (C_{16}) with compared the sample (C_1) ,the ductility ratio (axial or lateral) decreased (13 or 22) % , respectively. And with comported the sample (C_4) the stiffness(axial or lateral) increased about (16) % or (27)%, respectively, while sample (C_{17}) with compared the sample (C_1) , the ductility ratio (axial or lateral) is improvement and increased about (6)% or (17)%, respectively.

And with compared the sample (C_4) , the ductility ratio (axial or lateral) increased about (25)% or (36) % , respectively. Also, the ductility ratios for all tested columns, as shown in **Table (4-4),** all cyclic burning variables (number of cycles, burning intensity, cycle time, type of reinforcement, and type of concrete) have an effect on the behavior of columns for ductility.

4.5 Stiffness Parameter

Stiffness is defined as the load required for producing unit deformation in the member. The slope of the secant drawn to the load-deflection curve at a load of (0.75) times the ultimate load can be utilized as stiffness criteria (**Muthuswamy and Thirugnanam , 2014)**. The stiffness was calculated and compared with the reference column of each group ,as illustrated in **Table (4-5).**

Table (4-5): Stiffness parameter of tested columns.

Group No.	Specimen Symbol (Ci)	0.75Pu (KN)	Deflection at 0.75Pu(mm)		Stiffness t(KN/mm)	
			Axial	Lateral	Axial	Lateral
Group 1	$NC_1S_1E_1$	195.75	5.47	6.05	35.79	32.36
	$NC_2S_1E_1F_1$	152.25	5.69	6.47	26.76	23.53
	$NC_3S_1E_1F_2$	161.25	5.23	6.15	30.83	26.22
	$NC_4S_1E_1F_3$	142.5	6.13	7.02	23.25	20.30
	$NC_5S_1E_1F_4$	140.25	7.21	8.18	19.45	17.15
	$NC_6S_1E_1F_5$	124.5	8.35	9.32	14.91	13.36
	$NC_7S_1E_1F_6$	138.75	8.11	9.12	17.11	15.21
Group 2	$NC_8S_1E_2F_1$	340.5	8.67	4.37	39.27	77.92
	$NC_9S_1E_2F_3$	324	9.81	5.13	33.03	63.16
Group 3	$NC_{10}S_2E_1$	172.5	5.44	5.91	31.71	29.19
	$NC_{11}S_2E_1F_1$	134.25	6.08	7.03	22.08	19.10
	$NC_{12}S_2E_1F_3$	122.25	6.33	7.36	19.31	16.61

Table (4-1) Continue.						
Group 4	$HC_{13}S_1E_1$	318.75	7.24	7.95	44.03	40.09
	$HC_{14}S_1E_1F_1$	237	7.65	8.66	30.98	27.37
	$HC_{15}S_1E_1F_3$	217.5	8.05	8.99	27.02	24.19
Group5	$NC_{16}S_1E_1F_3R_1$	190.5	6.56	6.74	29.04	28.26
	$NC_{17}S_1E_1F_3R_2$	285	7.61	8.23	37.45	34.63

It can be seen that the stiffness after periodic burning with the load applied to the columns deteriorated significantly, the first group reduced the stiffness with the increase in the number of cycles for samples (C_2 to C_3),(C_2 to C_4) and (C_4 to C_5),the decrease in the stiffness (axial or lateral) about (10)% ,(11)%and (17) % or, (13)% ,(14)% and (16) % ,respectively, the stiffness ,also is reduced due to the increasing time periodic burning of cycle for (C_5 to C_3)and (C_7 to C_4) about (36)% and (27)% ,or (34)% and (25)% ,respectively .The stiffness in (axial or lateral) for sample (C_6 to C_4) was reduced by increasing the intensity temperature of the periodic burning cycle, about (36)% or (33) % , respectively.

For the second group of samples (C_8 and C_9), with concentric pre-load with compared (C_2 and C_4),the stiffness (axial or lateral), increasing about (31and 30)% or (69 and 68)%,respectively.

For the third group samples (C_{11} and C_{12}) with steel ratio (0.014) to, the stiffness(axial or lateral) decreased about (18 and 17)% or (19 and 18)%, for (two cycles and four cycles),respectively. For stiffness compared samples (C_2 and C_4) is less .

For the fourth group(C_{14} and C_{15}) were made from (HSC),the stiffness(axial or lateral) increasing about (30 and 39)% or (32 and 40)%, for displacement, respectively. for stiffness compared samples (C_2 and C_4) is more.

The fifth group for samples (C_{16} and C_{17}), were retrofitted of ((NSC with CFRP) and RPC), receptivity , for (C_{16}) with compared the sample (C_1) ,the stiffness (axial or lateral) decreased about (19 or 13) % , respectively. And with compared the sample (C_4) the stiffness(axial or lateral) increased about (20 or 30)%, respectively ,while sample (C_{17}) with compared the sample (C_1) , the stiffness (axial or lateral) is improvement and increased about (5 or 7)%, respectively. And with compared the sample (C_4) ,the stiffness (axial or lateral) increased about (38)% or (43) % , respectively, as shown in **table (4-5)**, all cyclic burning variables (number of cycles, burning intensity, cycle time, type of reinforcement, and type of concrete) have an effect on the behavior of columns for stiffness.

4.6 Crack Width and Cracking Pattern

During the initial stages of loading the control columns (C_1,C_{10},C_{13}) and repaired columns (C_{16},C_{17}) have no cracks. The first crack was identified by the natural vision ,then the corresponding load was recorded which represent the first cracking load. The flexure cracks were normally started at the tension edge and developed toward the compression edge for eccentricity loaded columns, the shear cracks initiated at the corbels ,as illustrated in **plates (4-1) to(4-17).**

Red cracks were caused by the axially applied load during the periodic burning process, while black cracks were caused by the eccentricity applied load during the post-fire test. **Table (4-6)** includes the maximum crack width measured by the crack meter, due fire exposure and post- fire service load.

Table (4-6): Measured Crack Width of the Tested Columns

Group No.	Specimen Symbol (C_i)	maximum Crack width of fire exposure(mm)	Crack width at service load (mm)	Location of crack
Gruop1	$NC_1S_1E_1$	_____	0.7	Mid height column
	$NC_2S_1E_1F_1$	0.38	1.9	First height column
	$NC_3S_1E_1F_2$	0.32	1.7	First height column
	$NC_4S_1E_1F_3$	0.48	2.7	Last height column
	$NC_5S_1E_1F_4$	0.51	2.3	Mid height column
	$NC_6S_1E_1F_5$	0.62	3.6	last height column
	$NC_7S_1E_1F_6$	0.53	2.9	Mid height column
Gruop2	$NC_8S_1E_2F_1$	0.28	0.87	Top end column
	$NC_9S_1E_2F_3$	0.35	1.23	Top end column
Gruop3	$NC_{10}S_2E_1$	_____	0.57	Last height column
	$NC_{11}S_2E_1F_1$	0.45	1.41	Last height column
	$NC_{12}S_2E_1F_3$	0.56	1.89	Last height column
Gruop4	$HC_{13}S_1E_1$	____	1.95	Last height column
	$HC_{14}S_1E_1F_1$	0.87	2.61	Last height column
	$HC_{15}S_1E_1F_3$	1.24	3.23	Mid height column
Gruop5	$NC_{16}S_1E_1F_3R_1$	0.44	1.34	In the bottom corbel
	$NC_{17}S_1E_1F_3R_2$	0.47	1.16	In the bottom corbel

The crack width for column samples (C_1,$C_{10}$and C_{13}) without fire are about value (0.7 ,0.57 and 1.95 mm). For the column samples with eccentric pre-load with exposure to cyclic fire (C_2 and C_4),(C_3andC_5), the crack widths are increasing about (63% and74%), (59% and 70%),respectively.

For the column samples(C_6 and C_7), the crack widths are increasing about (81% and76%), respectively.

For the column samples (C_8 and C_9)with concentric pre-load with exposure to cyclic fire, the crack widths are decreasing about (54% and 56%),respectively.

For column samples(C_{11} and C_{12}) with low ratio reinforcement the crack widths are decreasing about (60% and 70%),respectively. for crack width then difference between C_1 and C_2, C_4 is larger

For the column samples (C_{14},C_{15}) subjected to cyclic burning , the crack widths were (50% and 59%), respectively

For the strengthening and retrofit with ((NSC with CFRP) and RPC) for columns samples (C_{16},C_{17}), respectively, the crack widths are increasing about (44%and 38%), respectively.

4.7 Concrete Strains

In general, The flexure effect increases the strain value at the column's tension and compression faces, which in turn increases the strain value at the first crack caused by the increased tensile stress of the shell's concrete. The strain esteem increments with an increment the quantity of cyclic fire .

Five pairs of demec discs were used at mid-height of column to monitor the strain concrete at the selected levels of loading for each column specimen. Demec discs were calibrated using an accompanying special ruler. **Figures (C-1 to C-17)** in appendixes **(C)** ,shown the change in strain at mid-height of columns to load increasing presented .

It can be seen that the strains after periodic burning with the load applied to the columns deteriorated significantly, the first group reduced the strains with the increase in the number of cycles for samples (C_2 to C_3) , (C_4 to C_5), that lead to in increase the strains(tension and compression) about (49 and 51)% ,to (45 and 42)%, and (63 and 63)%,(64 and 62)%, respectively.

The strains for sample (C_6) is increasing strains(tension and compression) due to increase intensity of the periodic burning temperature, about (68 and 70)% the strains (tension and compression) also is increasing the periodic burning cycle time (C_7) about (66and 68)%, respectively.

For the second group of samples(C_8 and C_9), with concentric pre-load with have strains less (tension and compression) about (41and 43)% and (42 and 46)%, respectively.

For the third group samples (C_{11} and C_{12}) with low longitudinal steel ratio (0.014), the strains (tension and compression) increased about(51 and 53)% and (59 and 61)% ,respectively.

For the fourth group ($C_{14}$and C_{15}) were made from (HSC), the strains(tension and compression) increasing about (52 and 56)% and (65 and 69)% , respectively.

The fifth group for samples (C_{16} and C_{17}), were retrofitted of ((NSC with CFRP) and RPC), respectively , for sample (C_{16}) the strains (tension and compression) increasing about (14 and 16)%, respectively, ,while sample (C_{17}) the strains (tension and compression) increasing about (6 and 10)%, respectively.

4.8 Effect of Considered Variables

4.8.1 Number of Fire Exposure Cycles

columns samples to exposure fire cyclic with (e=75 mm) (e/h = 0.50) to reduce the cracking load about (51 to 40)% and (51 to 60)% , respectively.

On the other hand, the ultimate load reduction of about (22 to 18)% and (22 to 27)%, respectively. Exposure cyclic fire also, affects the mechanical properties of the column concrete sample. A deterioration in compressive strength was observed about (62 to 56)% and (67 to 71) % , respectively. It also decreased in tensile strength and modulus of elasticity about (55 to 52)% and (59 to 61)% ,and (38 to 34)and (43 to 46 %) respectively.

The ductility (axial or lateral) in column samples with exposure to fire also decreases about (22 to 17)% and (22 to 25)% or (34 to 20)% and (34 to 39)% respectively. The stiffness (axial or lateral) in column samples also decreases with exposure to fire about (25 to17)% and (25 to 35)% or (27 to 19) % and (27 to 37)% ,respectively.

4.8.2 Temperate Target for Each Cycle

for sample with eccentric (e = 75 mm) that higher intensity temperature during exposure to periodic , that cracking load about (74%). The ultimate load was ,also, lower about (37 %) for sample , and the failure mode was the outer shell segmentation of the samples.

The deterioration of the compressive strength was, also observed about (79) % for the sample. It also decreased in tensile strength and modulus of elasticity about (68) % and (55)% ,respectively , for the sample .

Ductility decreases (axial or lateral) with increasing burning intensity

during exposure to fire for column samples about (25 and 32)% or (39 and 48)% , respectively, and the stiffness in displacement (axial or lateral) decreases with increasing burning intensity to about (35 to 58)% or (39 to 59) % ,respectively.

4.8.3 Time Duration of Each Fire Exposure Cycle

For samples with (e=75 mm), with longer period time during exposure to periodic burning , a change in cracking load, about (40 to 64)% and (60 to 66) % ,respectively. Also, the ultimate load was lower about (18 to 28)% and(27 to 29)%, for cyclic burning (one cycle and four cycles), respectively .

A deterioration in compressive strength was observed about (56 to 71)%(67 to 75), respectively. It also decreased in the tensile strength and modulus of elasticity about (52 to 55)%, (59 to 63) %, and (34 to 38)%, (43 to 50) % ,respectively, for cyclic burning (one cycle and four cycles), respectively.

The ductility (axial or lateral) decrease with an increase in the time during exposure to fire for column samples about (17 to 27) % and (25 to 29) %, or (20 to 41)% and (39 to 43)% ,respectively. The stiffness (axial or lateral) decreases with increasing the time during exposure fire to about (17 to 46) % and (35 to 52)% or (19 to 47)% and (37 to 53)% ,respectively. For cyclic burning (one cycle and four cycles), respectively.

4.8.4 Eccentricity of Pre-Load Through Fire Exposure

It was found that samples with concentric loading (e = 0 mm) had a change in cracking load with higher compared to those of eccentric pre-loading (E=75mm) during exposure to cyclic burning, about (80 and 83) % ,

respectively. Also, the ultimate load was greater for samples about (55 % and 56 %), respectively.

The deterioration increasing was also observed, the compressive strength about (47 and 55) % respectively. The tensile strength and modulus of elastic deterioration are less about (49 and 53)% and (30 and 35)% , respectively .

Ductility decreases (axial or lateral) with central loading by less than that of samples with eccentric loading during exposure to fire for column samples about (17 and 19)% or (5 and 6) % .The stiffness decreases in displacement (axial or lateral) with The central loading was less than that of samples with eccentric loading during exposure to fire for column samples to about (31 and 30)% or (69 and 68)%,respectively .

4.8.5 Role of Longitudinal the Steel Reinforcement Steel Ratio

For samples with longitudinal reinforcement ratio (0.014) less than samples with longitudinal reinforcement ratio (0.02) ,have cracking load lesser about (53 and 67) %, respectively .The ultimate load was lower about (22 and 29) % ,respectively.

The deterioration of the compressive strength was also observed by about (64 and 70)%, respectively. It also decreased in tensile strength and modulus of elasticity about (58 and 62)% and (40 and 46) % ,respectively.

Ductility decreased (axial or lateral) with increasing time during exposure to fire about (18 and 23)% or (29 and 36) %,respectively. The stiffness (axial or lateral) decreased with increasing time during exposure to fire about (30 and 39)% or (35 and 43)%,respectively.

4.8.6 Type of Concrete (HSC) for Columns

For samples with (e=75 mm),made of high strength concrete had a change in cracking load about (61 and 72)%,respectively. The ultimate load was also lower about (25 to 31)%,respectively.

The deterioration of the compressive strength was also observed about (64 and 72) % ,respectively ,for the sample periodic burning (two cycles and four cycles), respectively. It also decreased in tensile strength and modulus of elasticity about (59 to 64)% and (32 and 38)% ,respectively, for the samples periodic burning (two cycles and four cycles), respectively.

The ductility decreases (axial or lateral) with the increase in the intensity of combustion during exposure to fire for samples of about (22 and 30)% or (36 and 43)% ,respectively. The stiffness increases (axial or lateral) with the increase in the intensity of combustion about (30 and 39) % or (32 and 40)% , respectively. For samples periodic burning (two cycles and four cycles), respectively.

4.8.7 Evaluation of Adopted Strengthening Techniques

The columns samples(C_{16} and C_{17}) of compensatory outer shell by (NSC with CFRP) laminate or (RPC),respectively.

For (C_{16}) lead to an improvement in the cracking load compared to sample (C_1) and sample (C_4) about(38 and 36)% ,respectively. Also, treatment and repair with hardening led to an improvement and increase in the ultimate load about (3 and 34)% ,respectively.

The ductility ratio improved (axial or lateral) compared for sample (C_1) and sample (C_4) about (12 and 17)% or (22 and 26) ,respectively. The stiffness was increased in displacement (axial or lateral) about (19 and 20)% or (13 and 30)%, respectively.

For (C_{17}) lead to an improvement in the cracking load compared to sample (C_1) and sample (C_4) about (9 and 67)% ,respectively. Also, treatment and repair with hardening led to an improvement and increase in the ultimate load about (46 and 100) %, respectively.

The ductility ratio improved (axial or lateral) compared for sample (C_1) and sample (C_4) about (6 and 25)% or (16 and 36) %, respectively. The stiffness was increased (axial or lateral) about (5 and 38)% or (7 and 43)% , respectively.

Chapter Five

Non-Linear Finite Element Analysis

Chapter Five

Non-Linear Finite Element Analysis

5.1 Introduction

Finite element analysis (FEA) is a cost-effective and efficient method for analyzing the intricate behavior of most member of the construction, particularly those with intricate non-linear structural behavior.For understanding the structural mechanism and carrying out parametric studies, ABAQUS is one of the commercial finite element analysis software programs that is utilized the most frequently.A comparison of the numerical and experimental results is made in this study to demonstrate that modeling of the column is sufficient and contains:Type of elements, properties of materials, real constant, and study of convergence. This section includes the analysis of the columns specimens tested in chapter four and some important parametric studies by using a nonlinear finite element method package ABAQUS/Standard 6.14 (Appendix D).A nonlinear finite element analysis has been carried out to analyze the postfire response of (NSC or HSC) columns, and strengthened columns by (NSC with CPFR laminates or RPC) for external shell

Although the experimental test is the most reliable method for studying the behavior of structures, it is limited, costly, and time-consuming. As a result, FE simulation is an important method for not only performing a parametric study but also cross-checking the experimental results.

5.2 Types of Element

Different type of 3D elements has been offered by nonlinear FE package, ABAQUS, to predict the complicated behavior of the RC structure. However, frequently used 3D elements for modeling of concrete material NSC and RPC are:

- C3D20
- C3D8

The C3D8 element is a straightforward linear solid brick with eight integration points (2*2*2). As depicted in Figure (5-1a), the concrete material of the RC structure, bearing, and loading plate were modeled using the C3D8 element in this study. In contrast, ABAQUS provides a wide range for two-noded link elements like truss element T3D2, and 4-node shell element (S4R) used for the CFRP sheet. As depicted in Figure (5-1b), the T3D2 element was used to model the steel reinforcement of the RC structure in this study.

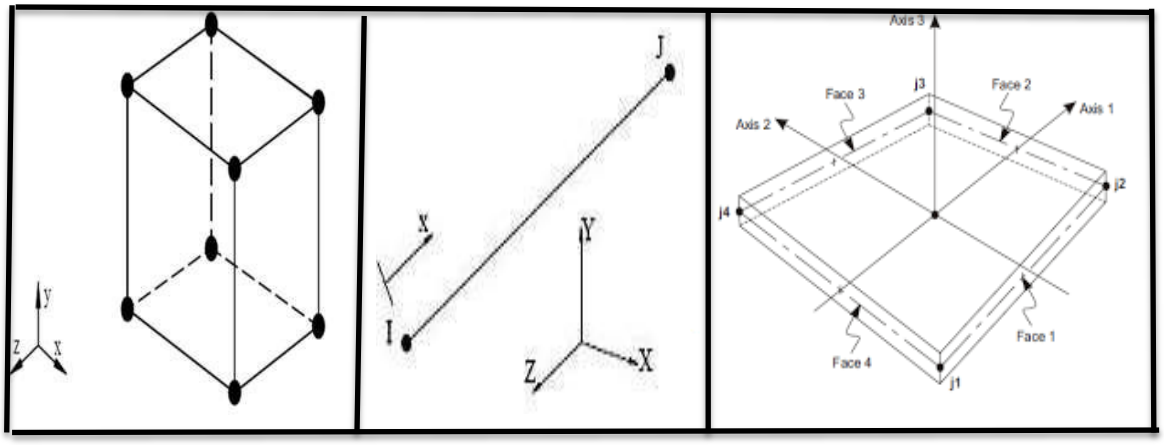

(a) C3D8 element (b) T3D2 truss element (c) S4R shell element

Figure (5-1): C3D8, T3D2 and S4R elements used to model by ABAQUS.

5.3 Material Properties

Concrete can be represented by a number of different material models that have been incorporated into commercial software for the purpose of simulating loads on concrete structures.The most widely used ABAQUS models for modeling concrete are, for instance, the Concrete Damage Plasticity (CDP) model, Concrete Smeared Crack model, and the Modified DruckerPrager/Cap model.Appendix C contains information about the CDP model and the behavior and properties of the concrete and other materials used in this analysis.

5.4 Convergence Study

The primary objective of the convergence study is to select the ideal model mesh size with the fewest possible elements and maximum convergence with the experimental test results.Using control column (C_1) where the same material properties were modeled with a decrease in the element sides(45, 40, 35, 30, 25, and 20)mm,as shown in **Figure (5-2).**

The axial deflection for the column with different mesh sizes was observed at the same load level ,as shown in **Figure (5-3)**. Convergence study, showed that the difference can be ignored when the mesh size decreased from (30 mm to 25 mm), therefore; the 25 mm model is adopted for all tested specimens.

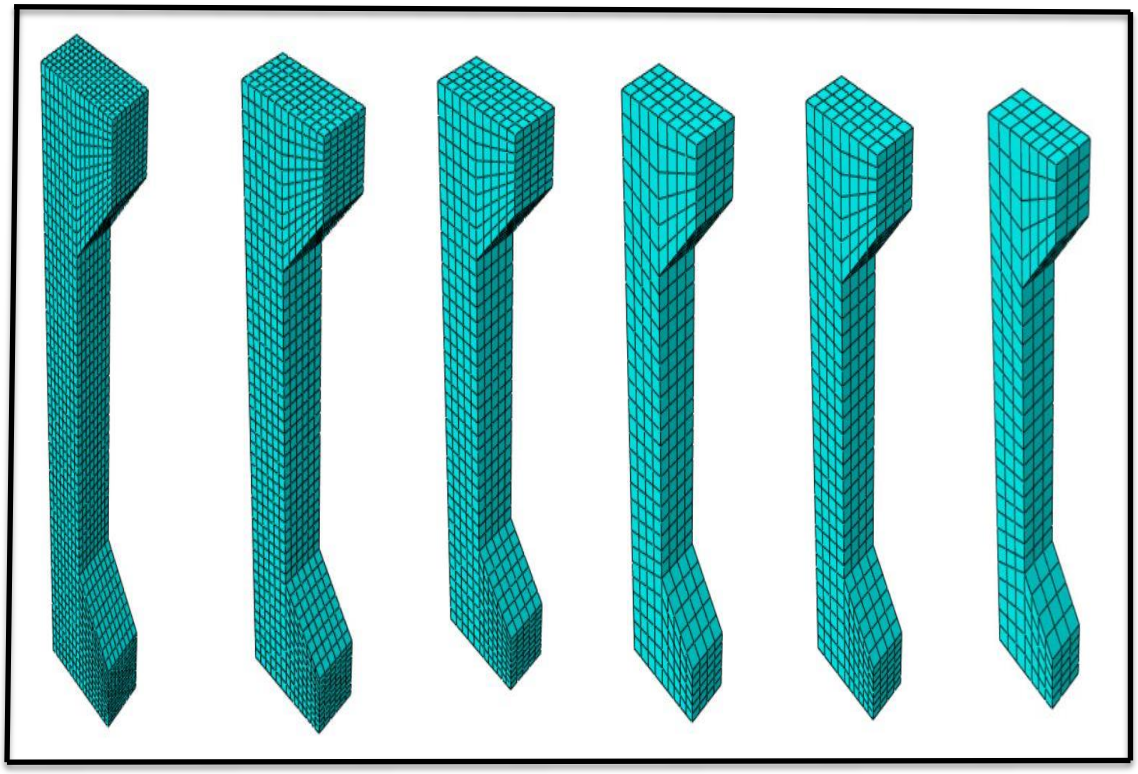

20 mesh 25 mesh 30 mesh 35 mesh 40 mesh 45 mesh

Figure (5-2): The considered meshes for the column specimens.

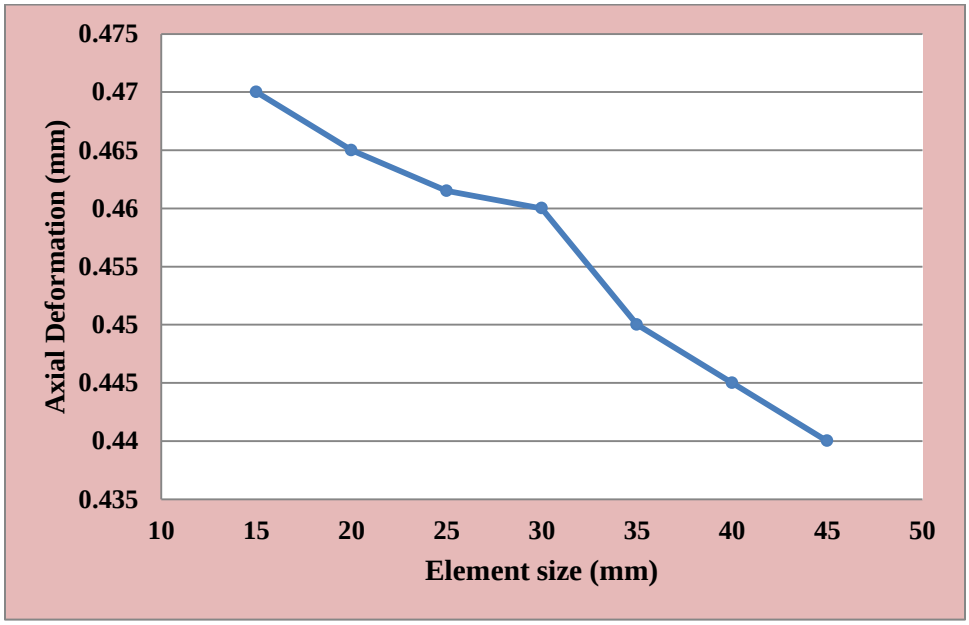

Figure (5-3): The Convergence Study

5.5 Modeling of Column Specimens

The column specimen's components and assembly, as well as the interactions between them, load, and boundary conditions used in this study, are all included in this section.

5.5.1 Elements and Assembly

Each specimen in this study consisted of the following parts: column stem, bracket of column, bearing and loading plates, and different reinforcing steel bar, as well as CFRP laminates The assembly of parts that are used in modeling specimens is shown in **Figure (5-4)**.

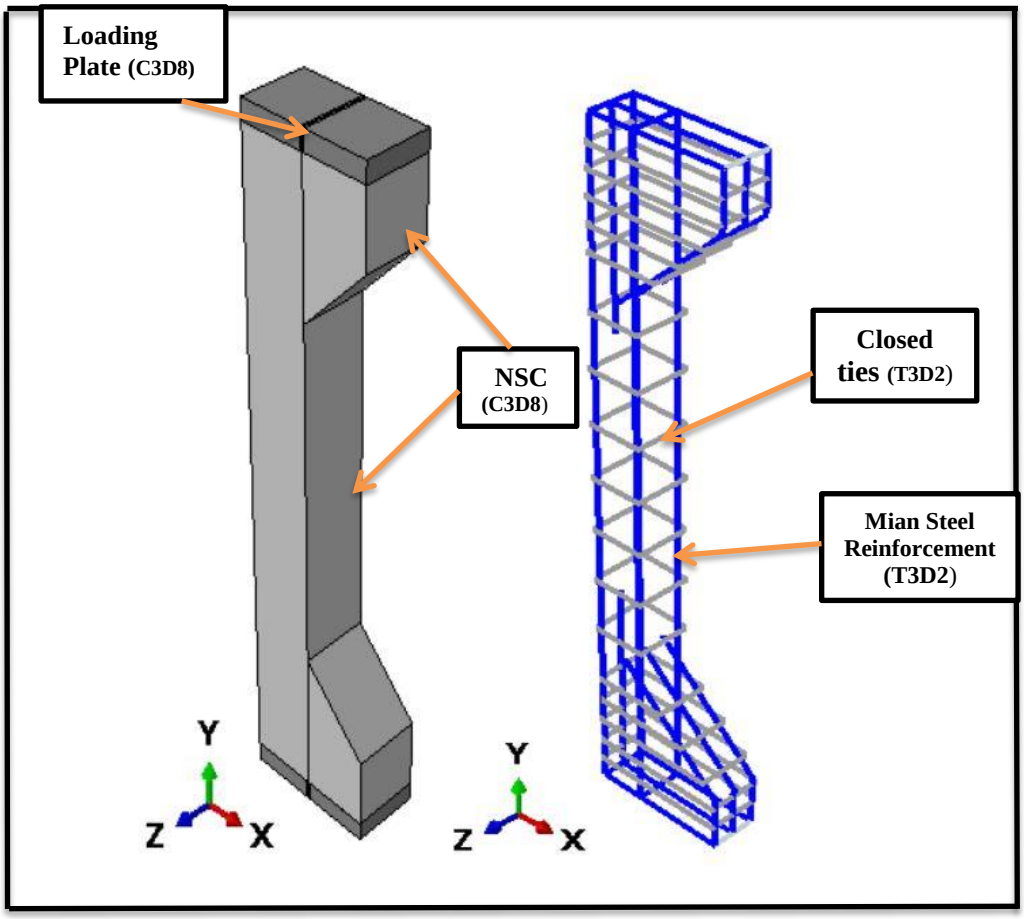

a-specimens without strengthening

Figure (5-4): modeling of column specimes

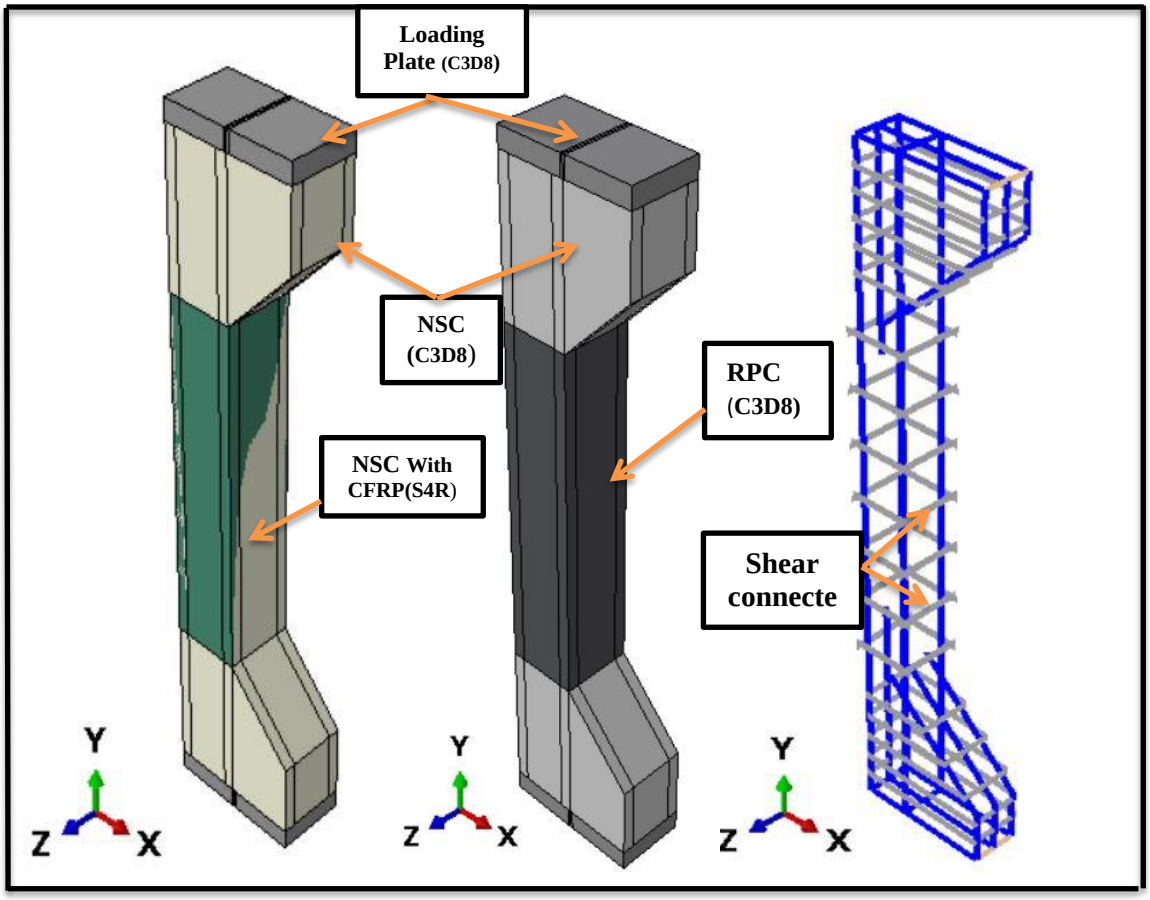

b. specimens with strengthening

Figure (5-4): Continue

5.5.2 Loading and Boundary Conditions

The finite element model is loaded at the same locations of the experimental work for all columns and the load is represented as a uniformly applied pressure by dividing the total applied load on the center line of the bearing plate, as shown in **Figure (5-5).**

The mechanism of representing any column was done by jointing at top and bottom by the hinge, in bottom surface (surface of load) it was restrained in x and z-axis,free displacement are assumed in the direction y-axis (vertical

displacement). At the top support of the column, the top surface was restrained the displacement in the direction x, y and z-axis.

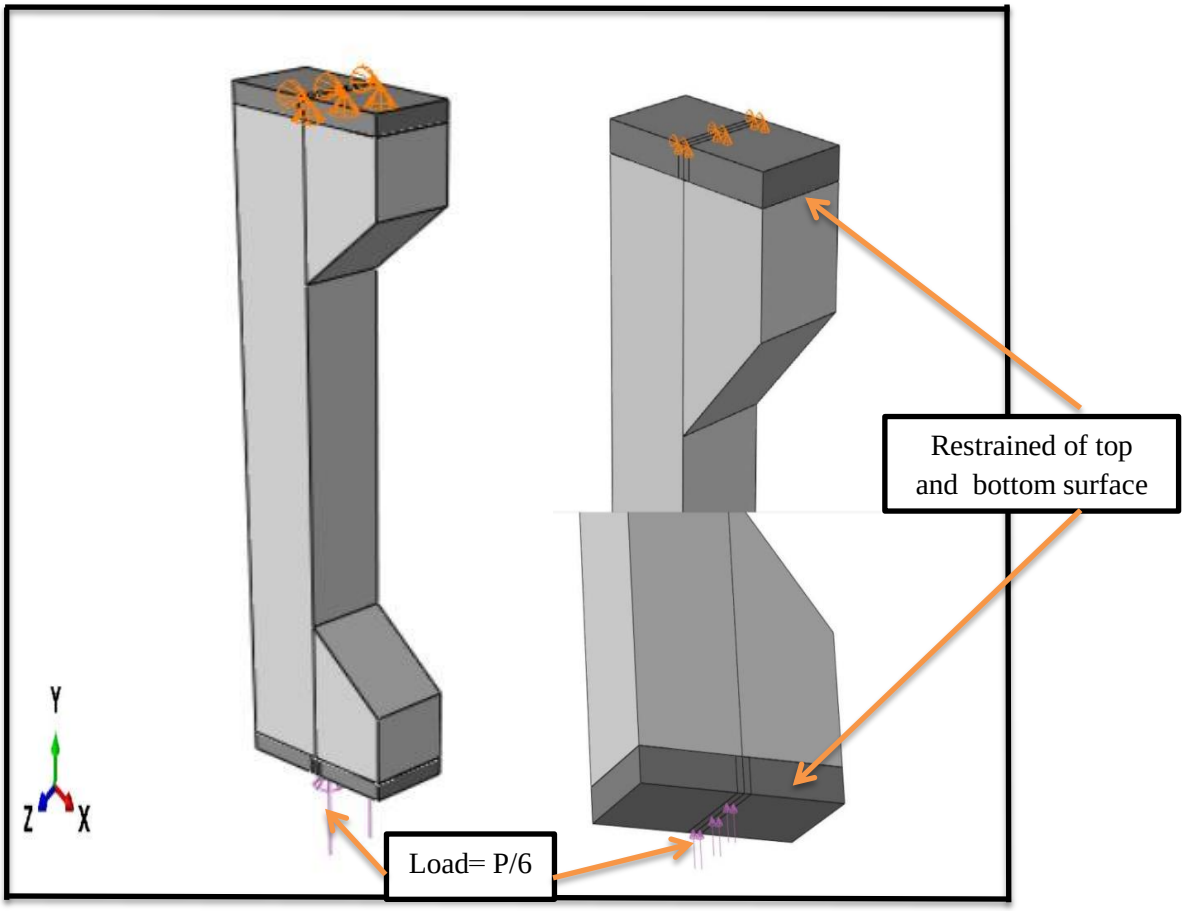

Figure (5-5): Representation (simulation) of applied loads and boundary conditions of modeled column specimen.

5.6 Numerical Analysis Results and Discussion

The results of finite element analysis using the ABAQUS program are compared with the experimental results for all tested columns. The validation of the numerical model is established based on this comparison which includes load-deflection response, ultimate load, service displacement, cracking pattern, plastic strain, and failure modes, **Tables** (5-

1) and **(5-2)** include numerical results, of ultimate load , service deflection , cracking load and ductility index .

Table (5-1): Comparation of Numerical and Experimental Results for ultimate load , cracking load and service displacement.

Specimens		Cracking Loads Pcr (kN)	Percentage difference((*)	Ultimate loads Pu (kN)	Percentage difference (**)	Service axial displacement Δs_v (mm)	Percentage difference (***)	Service lateral displacement Δsh (mm	Percentage difference (***)
$NC_1S_1E_1$	FEM	72	-10.0	265	1.9	4.67	-2.3	3.96	-2.5
	EXP	80		261		4.78		4.06	
$NC_2S_1E_1F_1$	FEM	33	-15.4	210	3.4	4.97	-2.7	5.08	-2.9
	EXP	39		203		5.11		5.23	
$NC_3S_1E_1F_2$	FEM	41	-14.6	221	2.8	4.67	-6.4	4.58	-1.5
	EXP	48		215		4.99		4.65	
$NC_4S_1E_1F_3$	FEM	27	-15.6	199	4.7	5.17	-4.4	5.45	-6.7
	EXP	32		190		5.41		5.84	
$NC_5S_1E_1F_4$	FEM	24	-17.2	189	1.1	6.54	-4.2	6.87	-2.4
	EXP	29		187		6.83		7.04	
$NC_6S_1E_1F_5$	FEM	18	-14.3	172	3.6	7.25	-4.4	8.1	-7.5
	EXP	21		166		7.58		8.76	
$NC_7S_1E_1F_6$	FEM	23	-14.8	188	1.6	6.9	-6.9	8.12	-4.7
	EXP	27		185		7.41		8.52	
$NC_8S_1E_2F_1$	FEM	178	-11.0	458	1.1	7.23	-6.7	3.11	-8.3
	EXP	200		453		7.75		3.39	
$NC_9S_1E_2F_3$	FEM	156	-15.4	441	2.1	8.43	-5.5	3.51	-9.8
	EXP	180		432		8.92		3.89	
$NC_{10}S_2E_1$	FEM	56	-10.7	236	2.6	4.27	-3.6	4.51	-5.1
	EXP	62		230		4.43		4.75	
$NC_{11}S_2E_1F_1$	FEM	26	-15.4	184	2.8	4.97	-4.8	5.73	-3.0
	EXP	30		179		5.22		5.91	
$NC_{12}S_2E_1F_3$	FEM	18	-10.0	168	3.1	5.2	-4.2	5.97	-3.2
	EXP	20		163		5.78		6.17	

Table (5-1):continue									
$HC_{13}S_1E_1$	FEM	93	-9.7	441	3.8	6.38	-2.9	4.92	-6.1
	EXP	103		425		6.57		5.24	
$HC_{14}S_1E_1F_1$	FEM	42	-17.6	337	1.8	6.96	-2.2	6.95	-4.9
	EXP	51		331		7.12		7.31	
$HC_{15}S_1E_1F_3$	FEM	30	-16.7	299	3.1	6.91	-6.4	7.5	-5.4
	EXP	36		290		7.38		7.93	
$NC_{16}S_1E_1F_3R_1$	FEM	43	-14.0	266	8.6	5.96	-5.7	4.93	-3.3
	EXP	50		245		6.32		5.1	
$NC_{17}S_1E_1F_3R_2$	FEM	73	-16.1	401	5.5	6.05	-1.8	6.41	-2.3
	EXP	87		380		6.16		6.56	
Average			**-14.0**		**3.2**		**-4.4**		**-4.7**

* $\frac{Pcr(FE)-Pcr(EXP)}{Pcr(EXP)} \times 100\%$

** $\frac{P_{u(FE)}-P_{u(EXP)}}{P_{u(EXP)}} \times 100\%$

*** $\frac{\Delta s(FE)-\Delta s(EXP)}{\Delta s(EXP)} \times 100\%$

Table (5-2): Numerical and Experimantal results of the Ductility Index.

Specimen		Service displacement Δs (mm)(*)		Ductility index, μ(**)		Percentage difference μ %(***)	
		Axial	Lateral	Axial	Lateral	Axial	Lateral
$NC_1S_1E_1$	FEM	4.67	3.96	1.95	2.83	2.30	4.48
	EXP	4.78	4.06	1.90	2.71		
$NC_2S_1E_1F_1$	FEM	4.97	5.08	1.54	1.90	3.09	3.17
	EXP	5.11	5.23	1.49	1.85		
$NC_3S_1E_1F_2$	FEM	4.67	4.58	1.63	2.23	3.45	2.43
	EXP	4.99	4.65	1.57	2.17		
$NC_4S_1E_1F_3$	FEM	5.17	5.45	1.33	1.74	1.98	4.73
	EXP	5.41	5.84	1.31	1.66		

Table (5-2):continue							
$NC_5S_1E_1F_4$	FEM	6.54	6.87	1.41	1.63	2.22	1.75
	EXP	6.83	7.04	1.38	1.60		
$NC_6S_1E_1F_5$	FEM	7.25	8.1	1.34	1.49	3.39	6.22
	EXP	7.58	8.76	1.30	1.41		
$NC_7S_1E_1F_6$	FEM	6.9	8.12	1.41	1.59	4.80	2.39
	EXP	7.41	8.52	1.34	1.55		
$NC_8S_1E_2F_1$	FEM	7.23	3.11	1.31	1.95	5.63	6.02
	EXP	7.75	3.39	1.24	1.83		
$NC_9S_1E_2F_3$	FEM	8.43	3.51	1.21	1.85	4.58	5.16
	EXP	8.92	3.89	1.16	1.76		
$NC_{10}S_2E_1$	FEM	4.27	4.51	1.84	2.38	4.28	4.35
	EXP	4.43	4.75	1.76	2.28		
$NC_{11}S_2E_1F_1$	FEM	4.97	5.73	1.49	1.62	3.35	1.29
	EXP	5.22	5.91	1.44	1.60		
$NC_{12}S_2E_1F_3$	FEM	5.2	5.97	1.37	1.49	1.99	1.86
	EXP	5.43	6.17	1.35	1.46		
$HC_{13}S_1E_1$	FEM	6.38	4.92	1.65	2.10	3.08	3.01
	EXP	6.57	5.24	1.60	2.04		
$HC_{14}S_1E_1F_1$	FEM	6.8	6.95	1.29	1.34	2.18	2.21
	EXP	7.12	7.31	1.25	1.31		
$HC_{15}S_1E_1F_3$	FEM	6.91	7.5	1.18	1.21	4.75	3.35
	EXP	7.38	7.93	1.13	1.17		
$NC_{16}S_1E_1F_3R_1$	FEM	5.96	4.93	1.69	2.15	2.29	1.72
	EXP	6.32	5.1	1.66	2.11		
$NC_{17}S_1E_1F_3R_2$	FEM	6.05	6.41	1.82	2.31	2.10	2.00
	EXP	6.16	6.56	1.78	2.27		
Average						**3.29**	**3.25**

(*)Δs = displacement at service load (Ps =0.65 Pu) **(Al-Haddad,2016)**.

(**) $\mu = \Delta u / \Delta s$ **(***)$\mu \frac{\text{FEM} - \mu \text{ EXP}}{\mu \text{ EXP}} * 100\%$**

5.6.1 Numerical Results of Control Columns (Without cyclic Fire Exposure)

Comparison of the final load, vertical and lateral service displacement of experimentally tested control column samples with numerical values from finite element analysis are listed in **Table (5-1).** Also, the load displacement finite element results are compared with the experimental data of the control column samples for each group, as shown in **Figures (5-6), (5-7)** and **(5-8),** respectively.

The result of the control column (C_1) for group (I) shows that the ultimate load of (265) kN from the FE model is very close with the ultimate load of (261) kN from the experimental data with a difference of (1.9%). The service axial and service lateral displacements of the model are less than the experimental results by (2.3 and 2.5)%, respectively.

While the result of the control column (C_{10}) for group (III) shows that the ultimate load (236) kN from the FE model is very close to the ultimate load of (230) kN from the experimental data with a difference of (2.6%). The service axial and service lateral displacements of the model are less than the experimental resulte by (3.6 and 5.1)%, respectively.

The result of the control column (C_{13}) of groups (IV) showed that the ultimate load (441) kN from the FE model was only (3.8%) higher than the ultimate load of (425) kN from the experimental data. The service axial and lateral displacement of the model was lower than that of the experimental column by (2.9 and 6.1)%, respectively. It should also be noted that the numerical values of ductility in displacement (axial or lateral) of the control column samples exceed the experimental values by (2.3, 4.28, and 3.08)% or

(4.48, 4.35 and 3.01)% for C_1, C_{10} and C_{13}, respectively, as shown in **Table (5-2).**

These differences between the experimental and FE results can be attributed to many reasons, such as: ***(Memar, 2020)***

- Concrete shrinkage caused by drying results in microscopic cracks.Since the FEM does not account for micro-crack effects, these would make the actual specimen less stiff.
- Concrete is actually a heterogeneous material, despite the FEM's assumption that it is.
- The stiffness of concrete specimens in numerical modeling has been affected by the lack of access to the concrete's actual stress-strain curve.
- A perfect bond was simulated by the embedded region constraint that was used in ABAQUS to model the interaction between concrete and rebars.This idealization may also contribute to the falsely higher initial stiffness in the numerical model because the actual bond is imperfect.

According to the previous,we can assume that the experimental test and the FE analysis are in reasonable agreement. As a result, this demonstrates that the proposed model is reliable and consistent**. Figure (5-9)** depicts the failure modes of all control column specimens from groups (I, III, and V)that were produced by FEA using plastic strain. These failure modes are close to the failure that occurred during the experimental test.

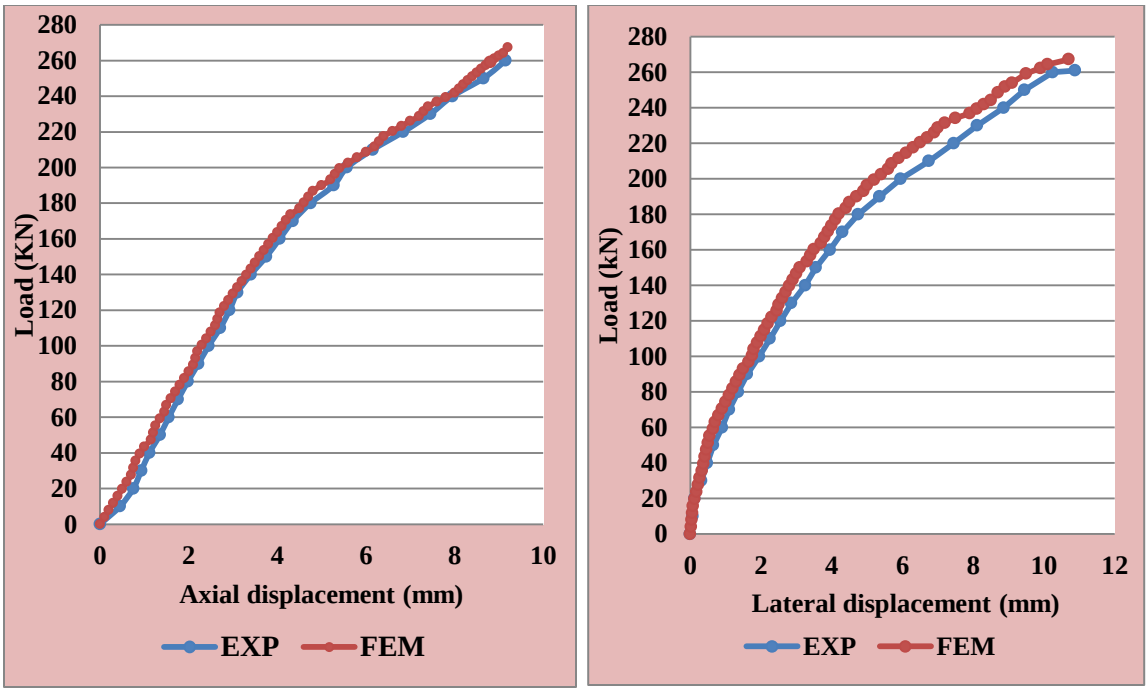

Figure (5-6): The Load- displacement Curves for Specimen (C_1)

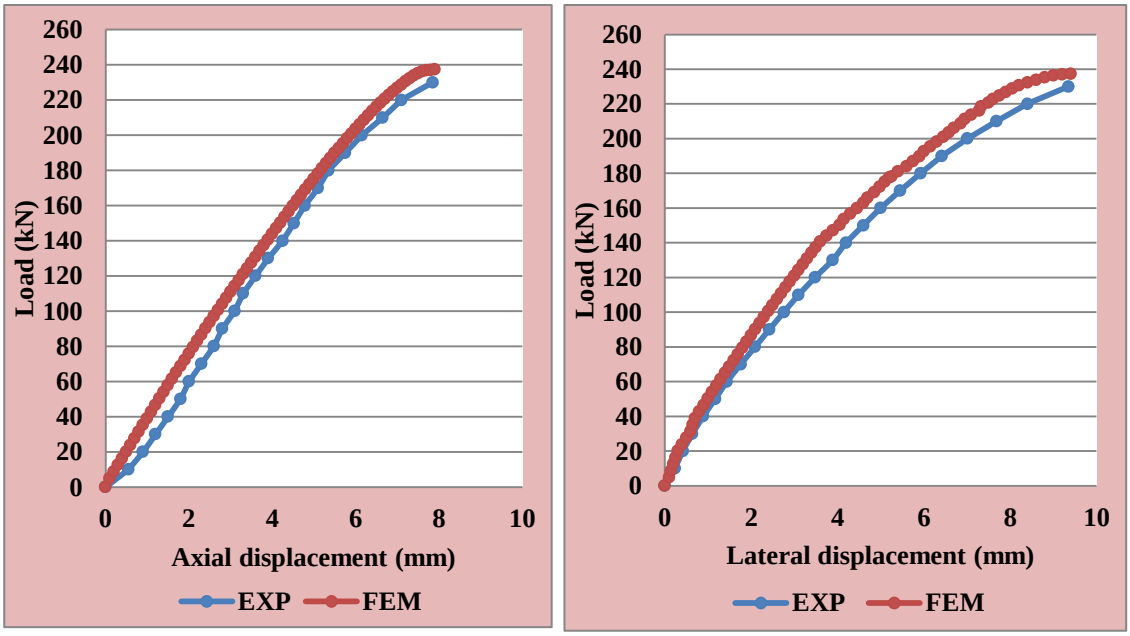

Figure (5-7): The Load- displacement Curves for Specimen (C_{10})

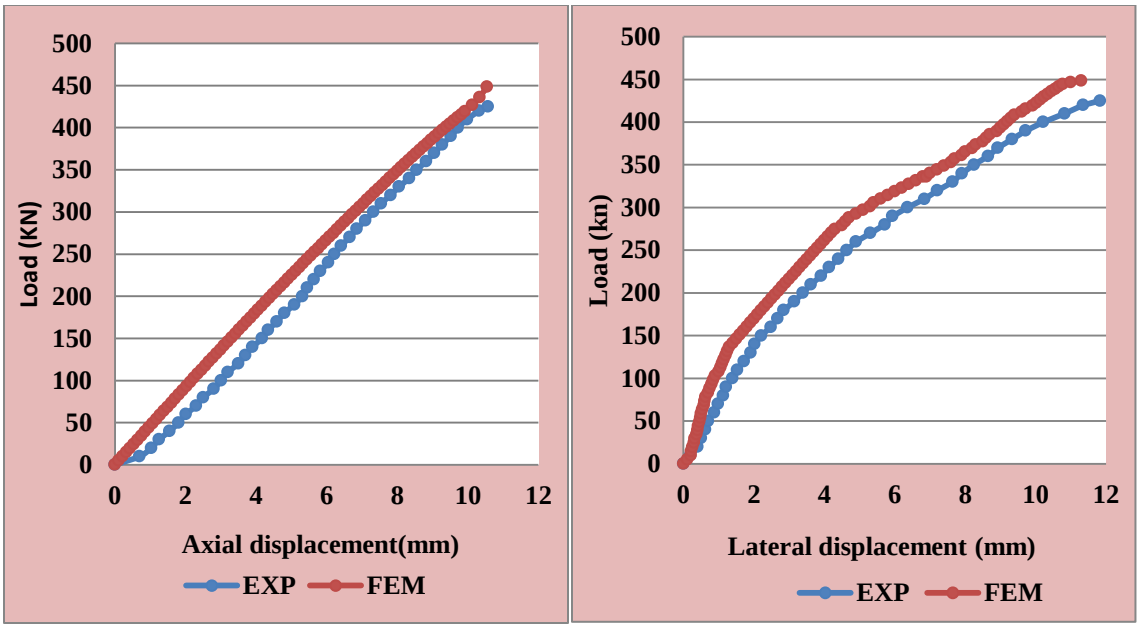

Figure (5-8): The Load- displacement Curves for Specimen (C_{13})

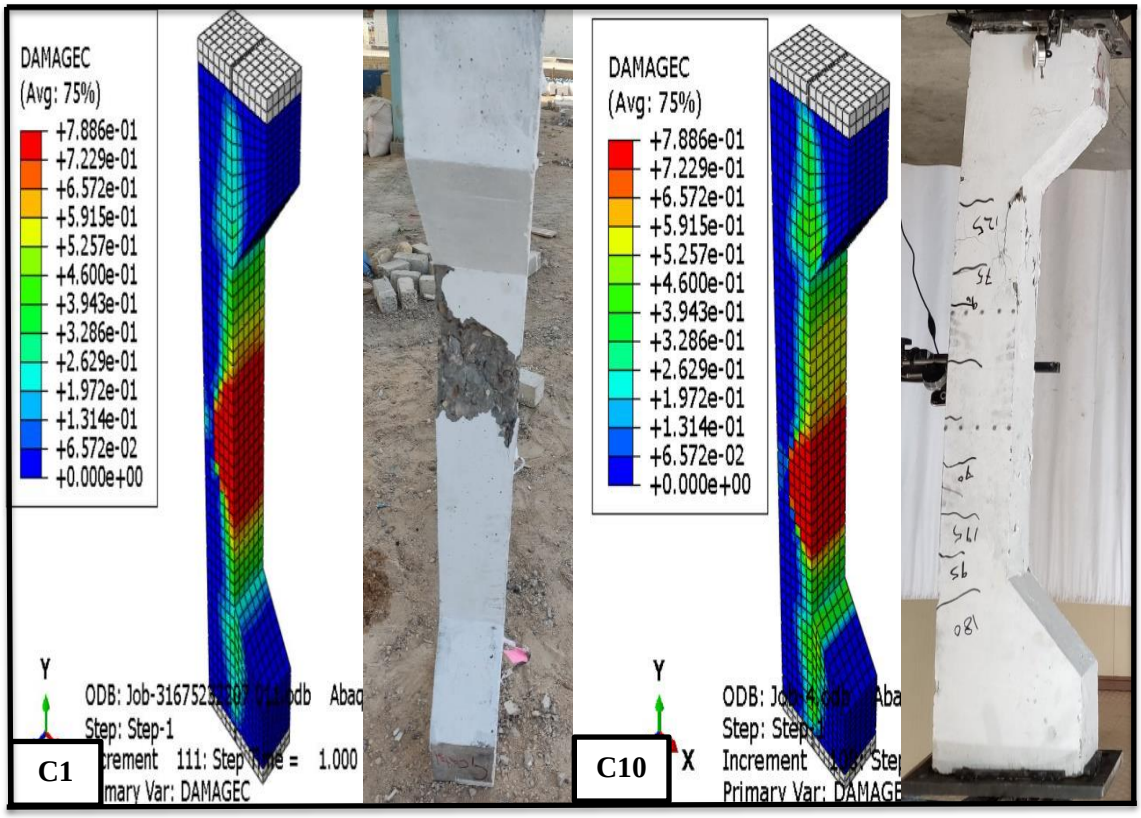

Figure(5-9): Damage Compression and Failure Modes for Control Columns Specimens (C_1,C_{10}, C_{13}).

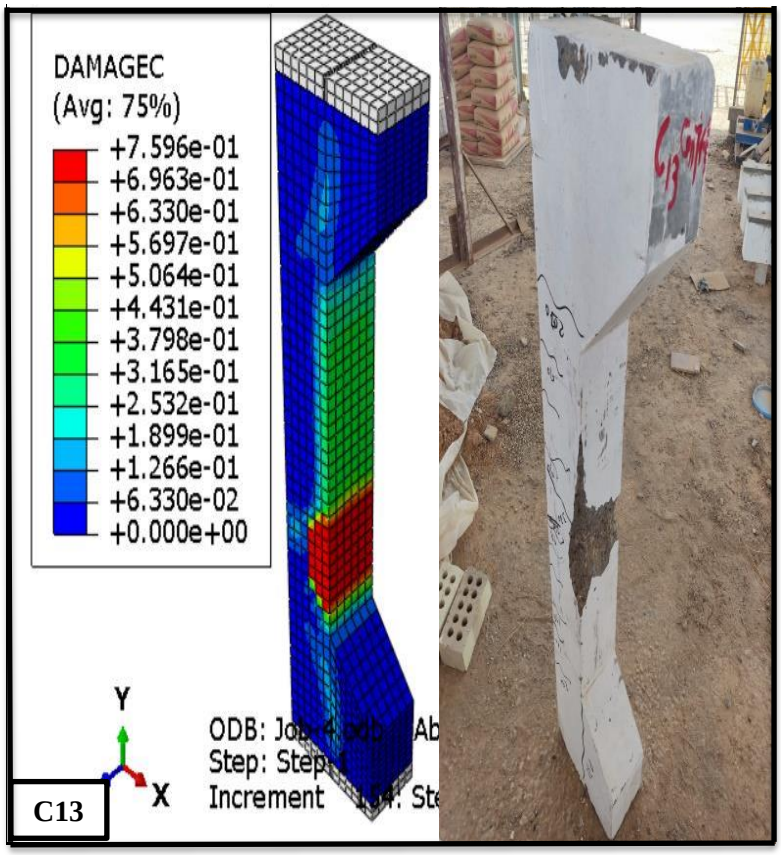

Figure(5-9):contiuse

5.6.2 Numerical Results of Cyclic Fire Exposed Columns

In the experimental test, the column specimens (C_2, C_3, C_4, C_5, C_6, and C_7),(C_8,C_9)(C_{11} and C_{12}),(C_{14} and C_{15}),(C_{16} and C_{17}) of groups (I, II,III,IV and V) ,respectivety were exposed to fire from all sides, to a temperature of level (600°C or 400°C) with eccentric pre – load and through tome burning (45 min or 75 min) . according to the (ASTM- E119) standard fire curve and cooled gradually in the air to room tempreture. The comparison between columns exposed to fire gave the impression that the columns of numerical analysis were stiffer than the experimental columns.

- **Columns Exposed to a Number of Cycles of Fire (GroupI)**

specimens (C_2 and C_4), (C_3 and C_5),for number of fire exposure cycles. the (axial or lateral) displacement that occurs as a result of the ultimate load. **Table (5-1)** provides these details.

The columns (C_2), the ultimate load from the experimental test (203 kN) and the FE model (210 kN), as well as the specimen (C_4), the ultimate load from the experimental test (190 kN) and the FE model (199) kN, about (3.4 and 4.7)%, respectively of one another. The model had service axial and lateral displacements than the experimental column by (2.7 and 4.4) % or (2.9 and 6.7) %, respectively.

The column (C_3), the ultimate load from the experimental test (215 kN) and the FE model (221) kN, as well as the specimen (C_5), the ultimate load from the experimental test (187 kN) and the FE model (189) kN aboute by (2.8 and 1.1) %, respectively. The model had service axial and service lateral displacements than the experimental column by (6.4 and 4.2)% or (1.5 and 2.4)%, respectively.

The plastic strain-based FEA failure modes for both group column specimens ,are depicted in **Figures (5-10)** to **(5-14)**. The tested column failed when spalling occurred in the middle of the RC column's compression face, so the maximum strain is concentric in the middle third of the column. Similar to the tested column, where the failure shape varied from column to column based on exposure case, this strain was distributed on the column in different proportions depending on the exposure case, the numarical values of these column specimens' ductility in the (axial or lateral) displacement are also higher than the experimental values by (3.09 and 3.17) % and (3.45 and 2.22)% or(1.98 and 4.73) %, and (2.43 **and** 1.75)%,respectively,as shown in **Table (5-2).**

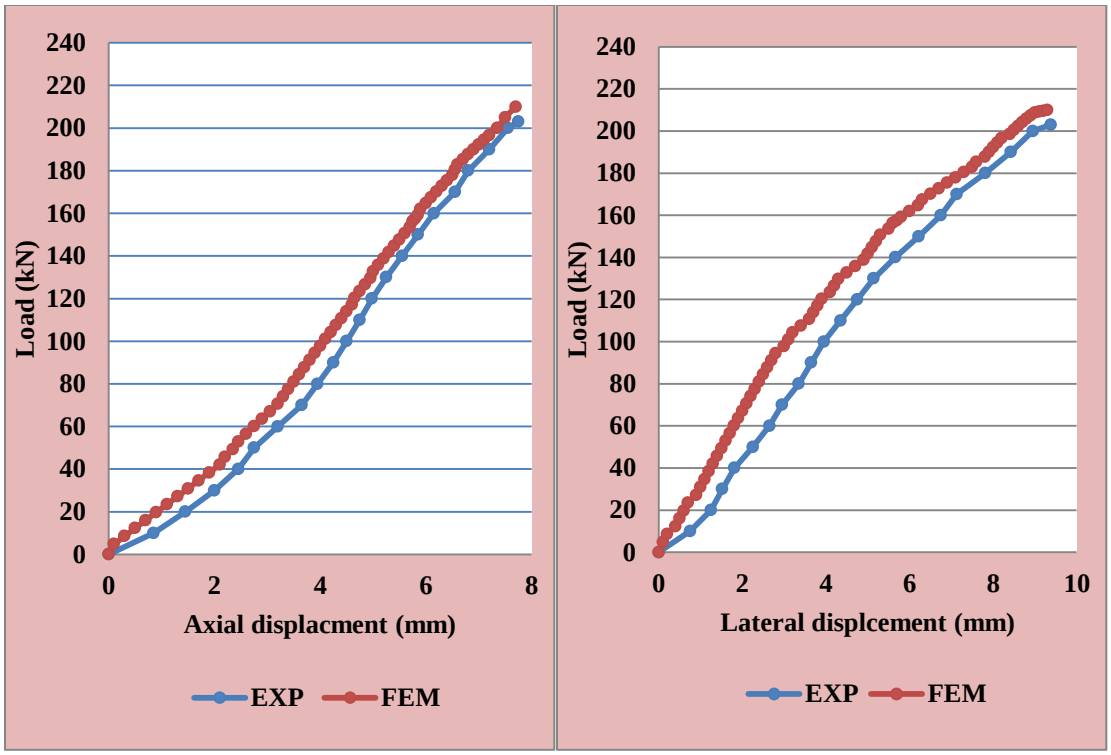

Figure (5-10): The Load- displacement Curves for Specimen (C_2).

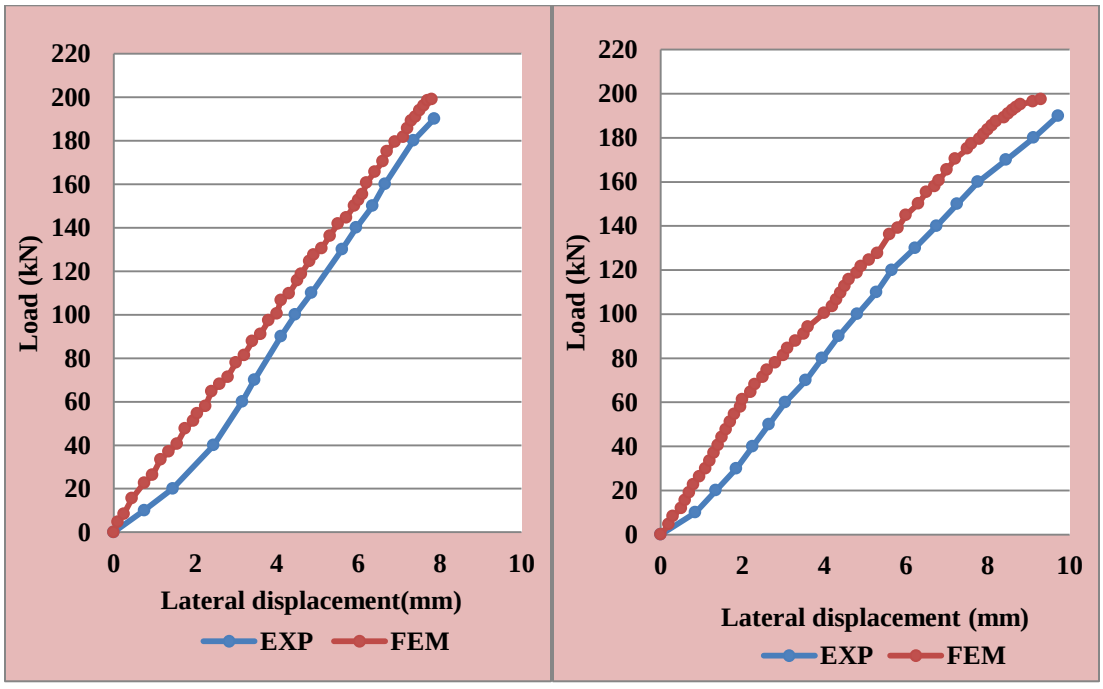

Figure (5-11): The Load- displacement CDurves for Specimen (C_4).

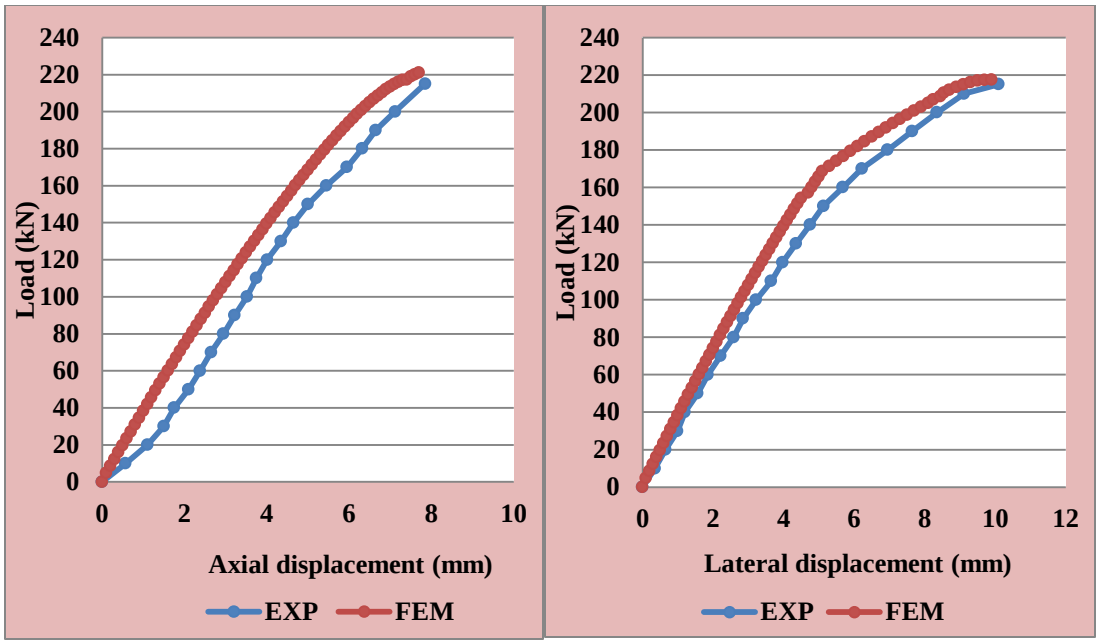

Figure (5-12): The Load- displacement Curves for Specimen (C_3).

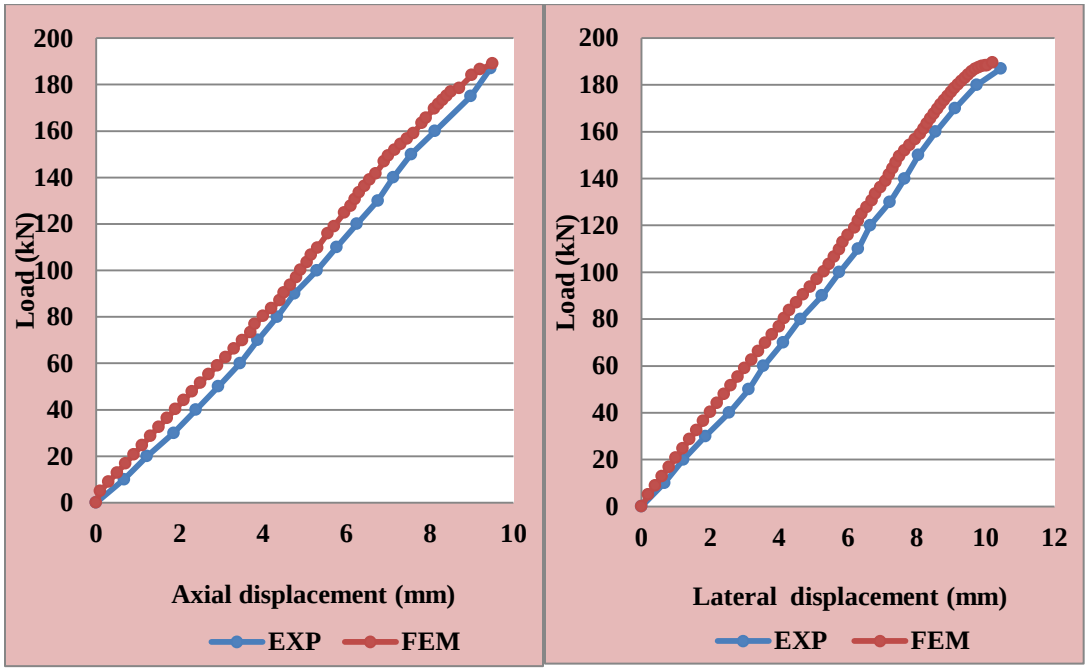

Figure (5-13): The Load- displacement Curves for Specimen (C_5).

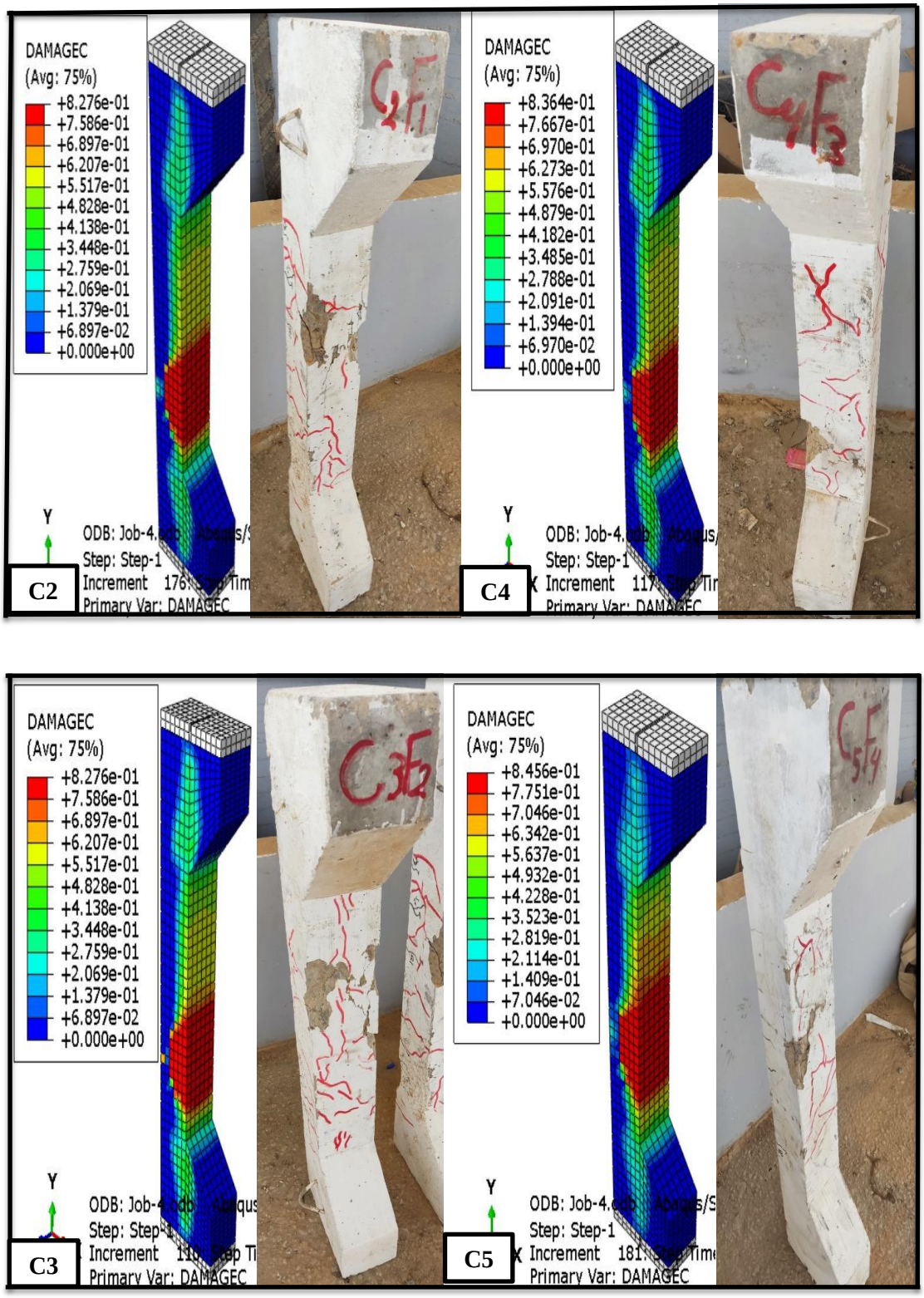

Figure (5-14): Damage Compression and Failure Modes for Columns Specimens (C_2,C_3,C_4, C_5).

- **Target of Temperate of each Cycle(GroupI)**

The column (C6),increases the target of cycles fire exposure at tempreure (600C˚) , The results of the ultimate load, axial and lateral displacement of these column specimens are given in **Table (5-1**).The ultimate load (172)kN from the FE model was higher than the ultimate load of (166)kN from the experimental data by (3.6 %).The service axial and lateral isplacement of the model was lower than the experimental column by (3.2 or 7.5) % respectively, as shown in **Figures (5-15)** and **(5-16)** .

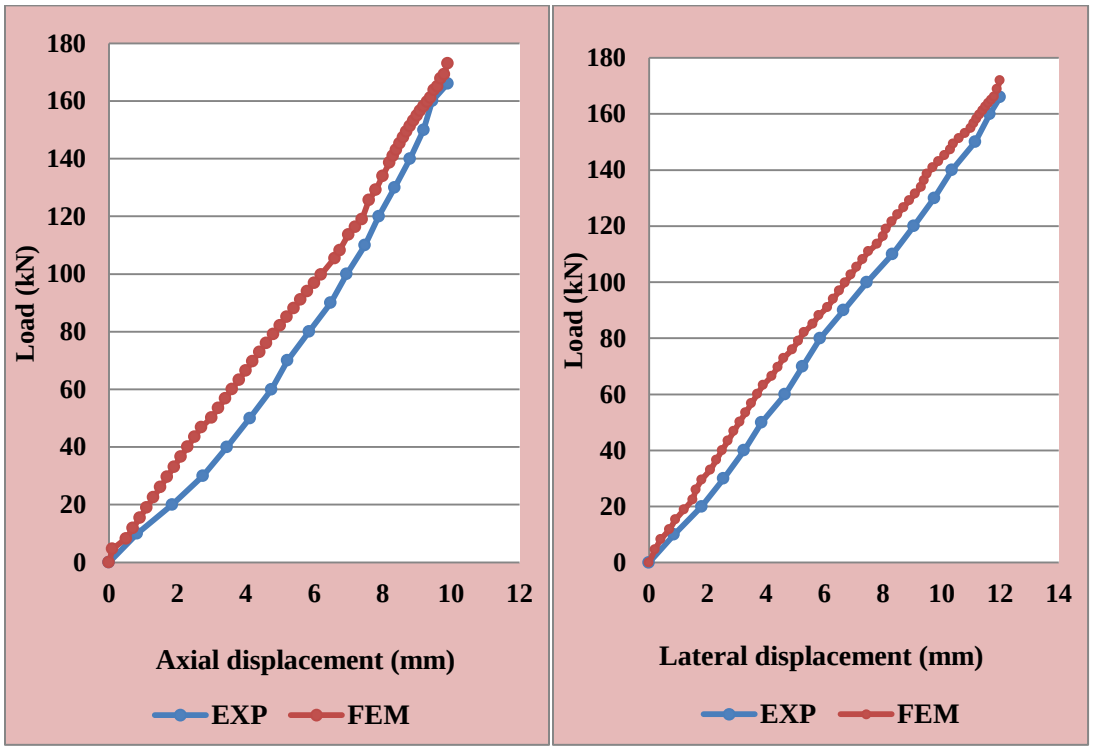

Figure (5-15): The Load- displacement Curves for Specimen (C_6)

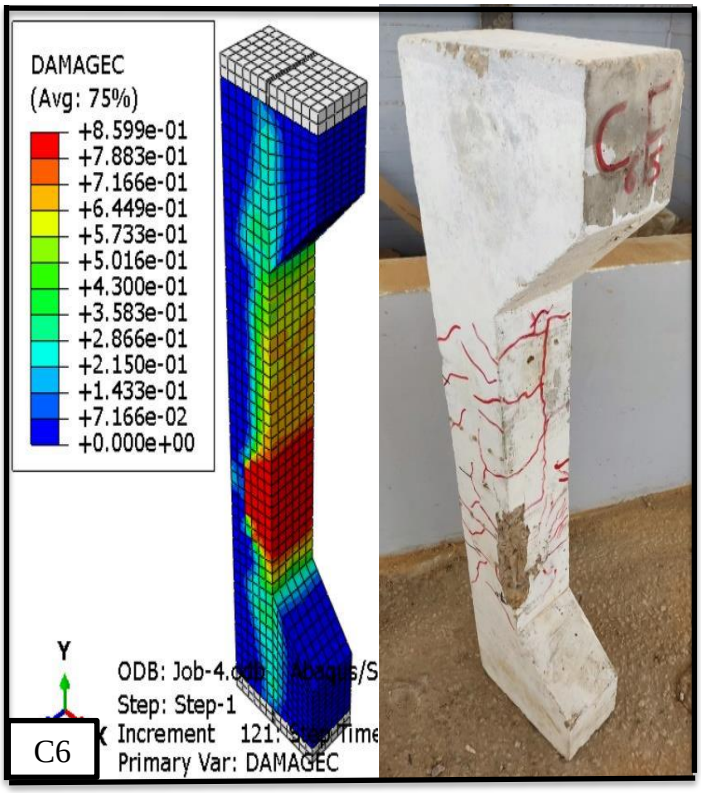

Figure (5-16): Damage Compression and Failure Mode Column Specimen($\mathbf{C_6}$)

- **Time Duration of each Cycle Fire Exposed (GroupI)**

The columns,(C_7) increase time duration cycle fire exposed, The results of the ultimate load, axial and lateral displacement of these column specimens are given in **Table (5-1).** The result ultimate load (188)kN from the FE model was higher than the ultimate load of (185) kN from the experimental data by (1.6 %). The service axial and lateral isplacement of the model was lower than the experimental column by (6.9 and 4.7) % respectively. as shown in **Figures (5-17)** and **(5-18) .**

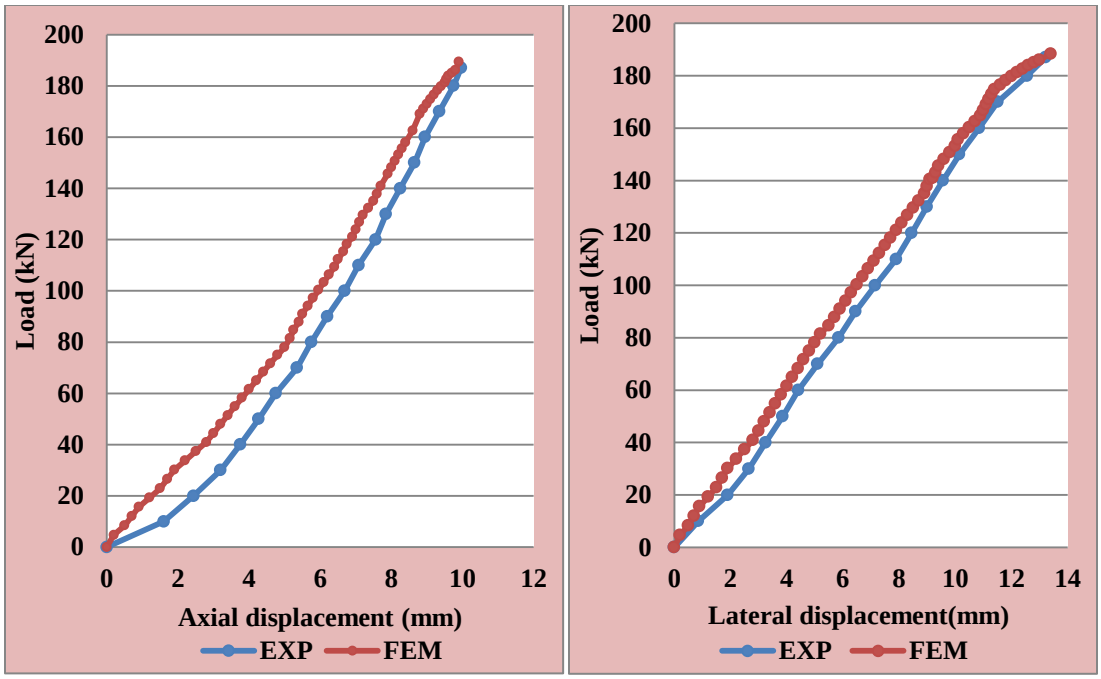

Figure (5-17): The Load- displacement Curves for Specimen (C_7)

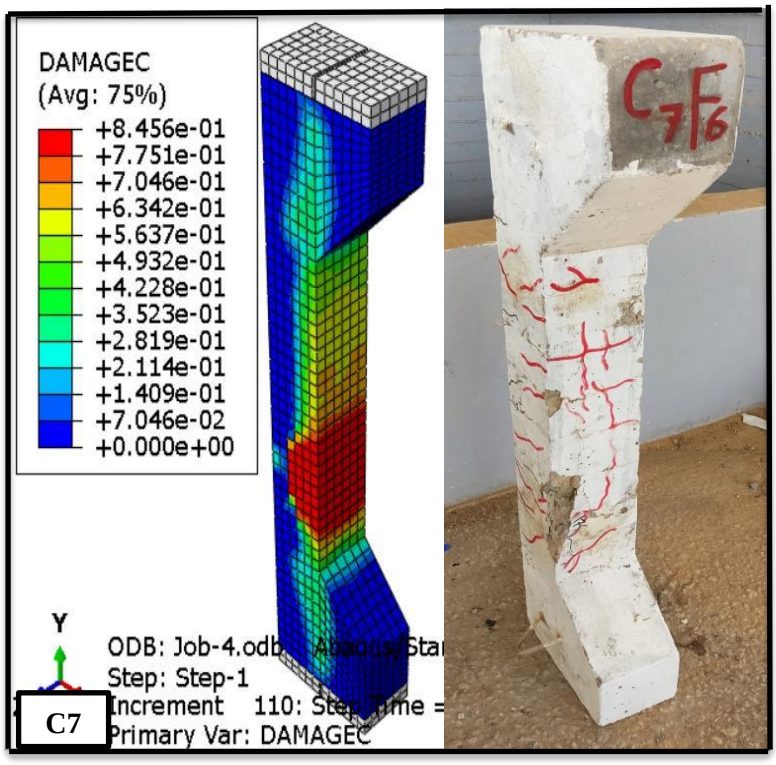

Figure(5-18): Damage Compression and Failure Mode for Columns Specimen(C_7).

➢ **Eccentricity of Pre-load (Ei) of Each Cycle (Group II)**

The samples (C_8 and C_9) with loading concentric pre-load through cyclic fire exposure, the ultimate load (458 and 441) kN from the FE model was higher than the ultimate load (453 and 432) kN from the experimental data by (1.1 and 2.1 %). The service axial and lateral is placement of the model was lower than the experimental column by (6.7 and 5.5) or (8.3 and 9.8)% respectively, as shown in **Table (5-1)** and **Figure (5-19)** to **(5-21)**

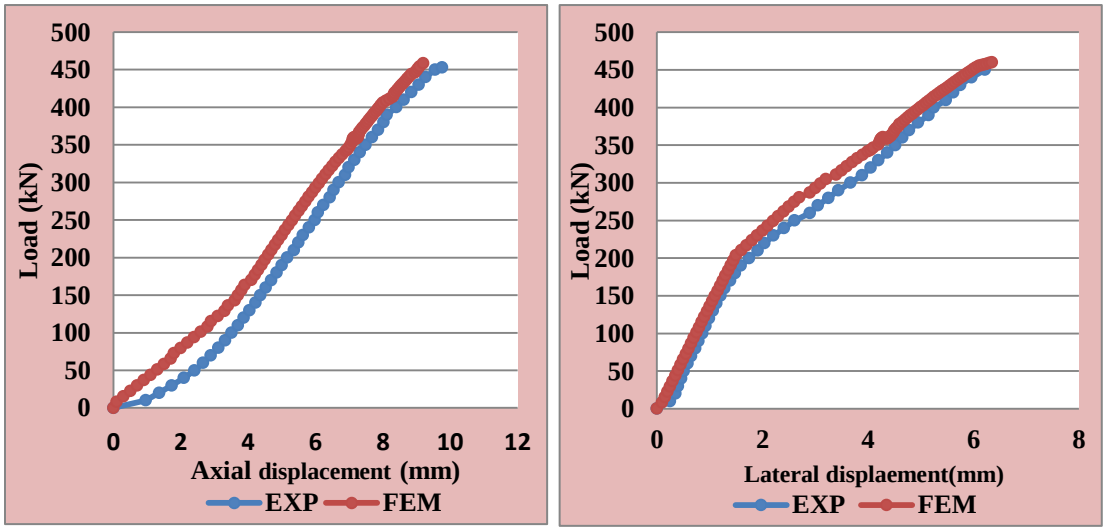

Figure (5-19): The Load- displacement Curves for Specimen (C_8)

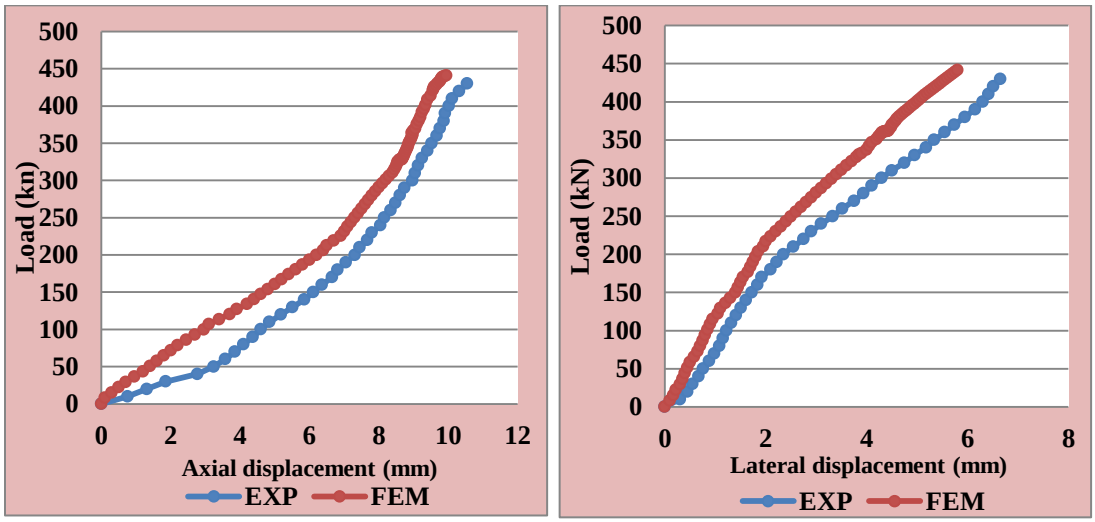

Figure (5-20): The Load- displacement Curves for Specimen (C_9)

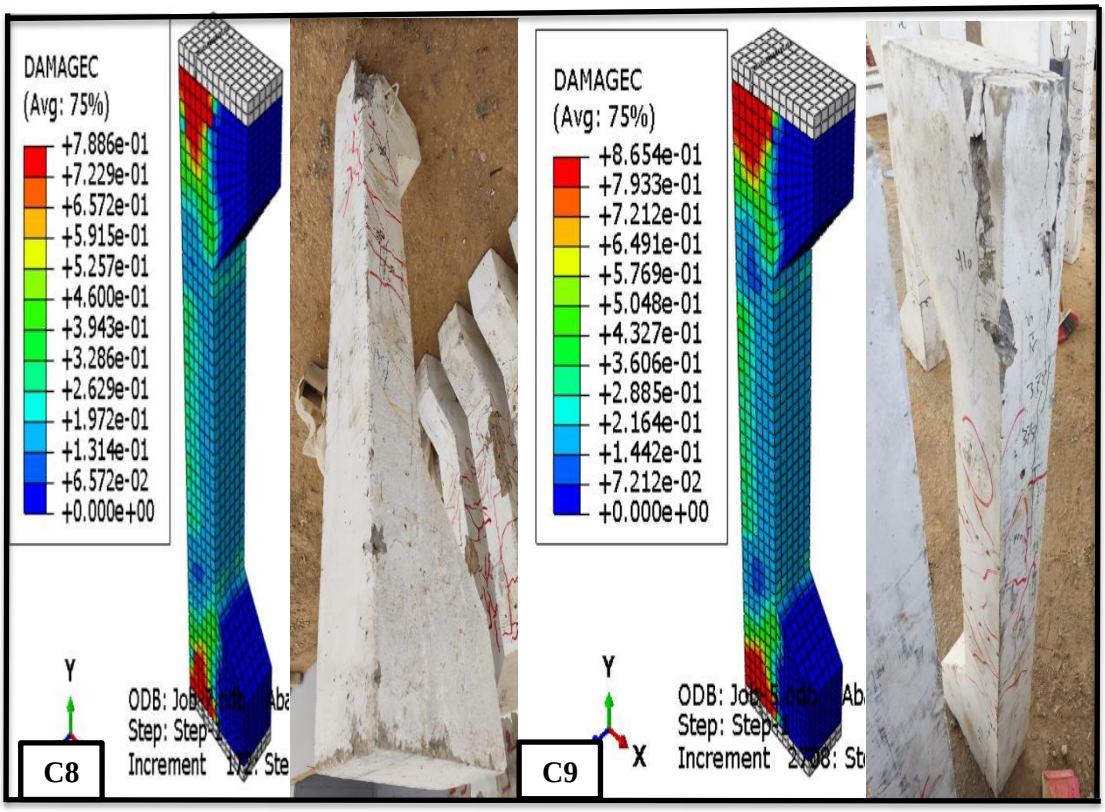

Figure (5-21): Damage Compression and Failure modes for Columns Specimens.

- **Role of Longitudinal the Steel Reinforcement Ratio for Columns(Group III)**

The specimens ($C_{11}$and C_{12}) which have the lowest of longitudinal Steel Reinforcement, are given in **Table (5-1)**. The result of the column for group (III)**,** shows the ultimate load (184 and 168) kN from the FE model was higher than the ultimate load (179 and 163)kN from the experimental data by (2.8 and 3.1 %).The service axial and lateral displacement of the m8odel was lower than the experimental column by (4.8 and 4.2),or (3154 and 3.2) % ,respectively,as shown in **Figure (5-22)** to **(5-24).**

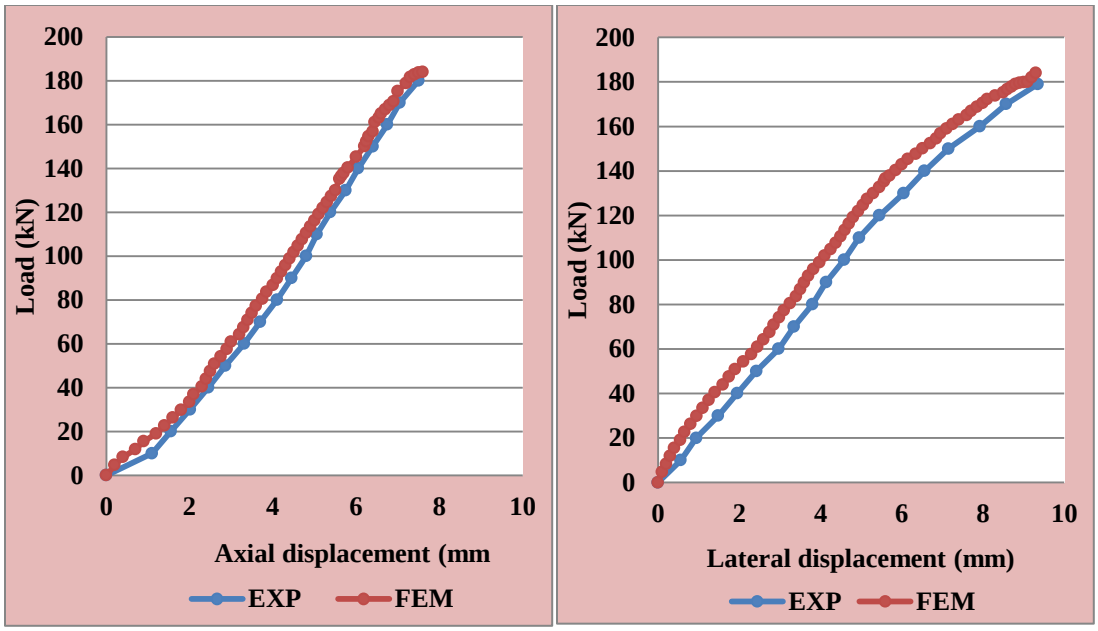

Figure (5-22): The Load- displacement Curves for Specimen (C_{11})

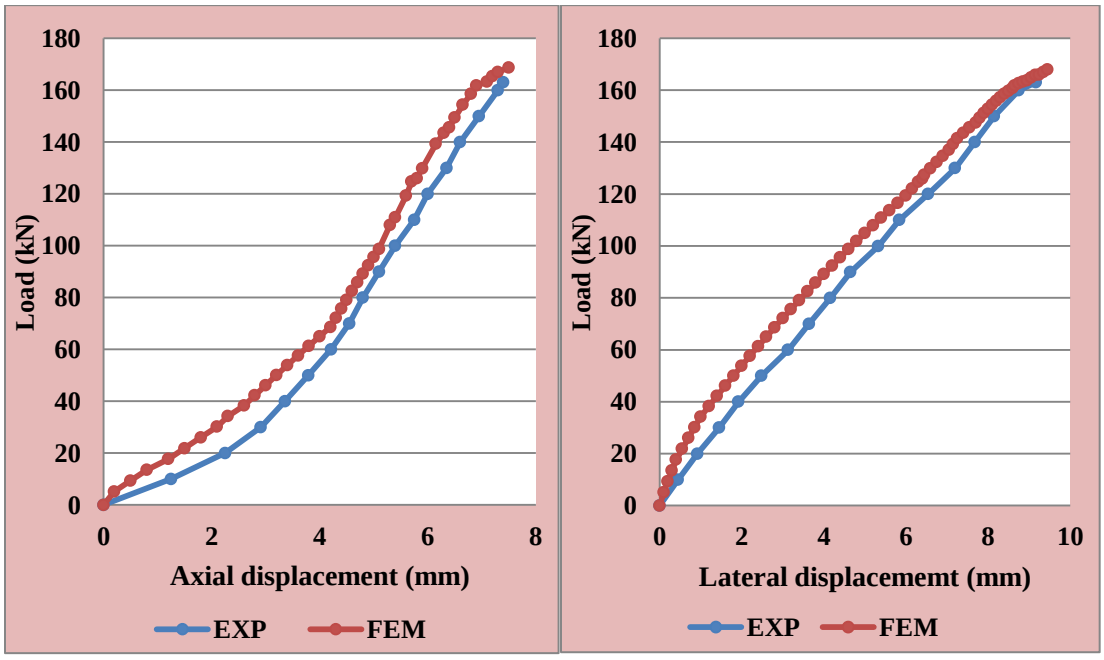

Figure (5-23): The Load- displacement Curves for Specimen (C_{12})

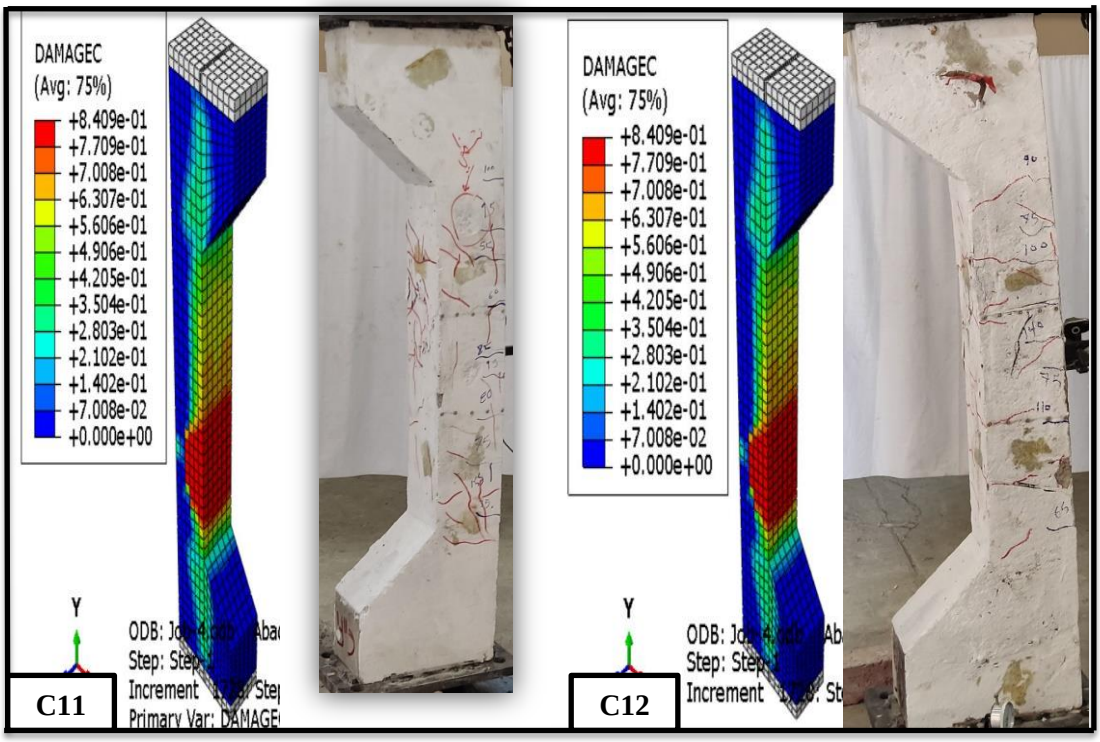

Figure (5-24): Damage Compression and Failure Modes for Columns Specimens ($\mathbf{C_{11}}$,$\mathbf{C_{12}}$).

- **Type of Concrete (HSC) for Columns**(Group IV)

The samples (C_{14} and C_{15}) were made of high-strength concrete, The results of the ultimate load, axial and lateral displacement of these column specimens are given in **Table (5-1).** The result of the column from group (4) shows the ultimate load (337 and 299)kN from the FE model was higher than the ultimate load (331 and 290) kN from the experimental data by (1.8 and 3.1) %.The service axial and lateral displacement of the model was lower than the experimental column by (2.2 and 6.4)% or (4.9 and 5.4)% **,** respectively,as shown in **Figure (5-25)** to **(5-27)**.The ratio ductility values differed by (2.18 and 4.75) % or (2.21 and 3.35) % for (axial or lateral)% displacement, respectively.

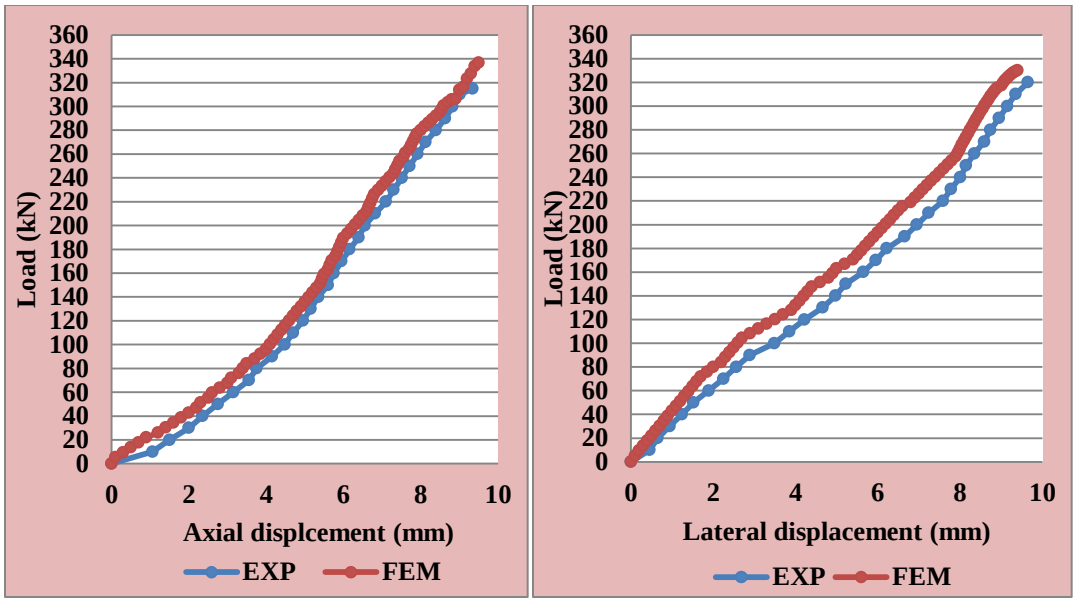

Figure (5-25): The Load- displacement Curves for Specimen (C_{14})

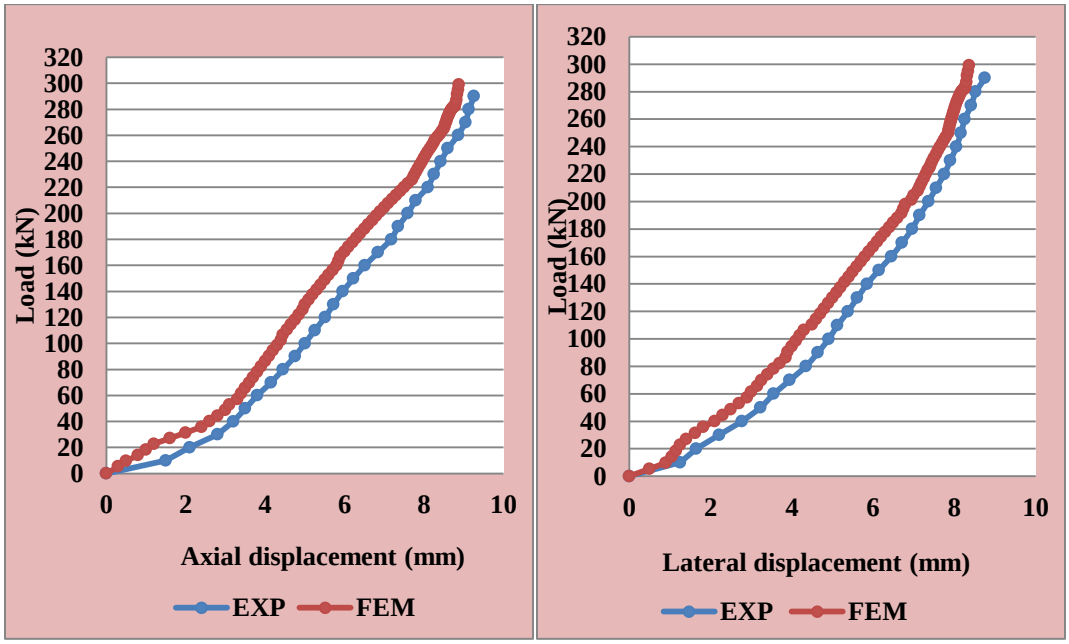

Figure (5-26): The Load- displacement Curves for Specimen (C_{15})

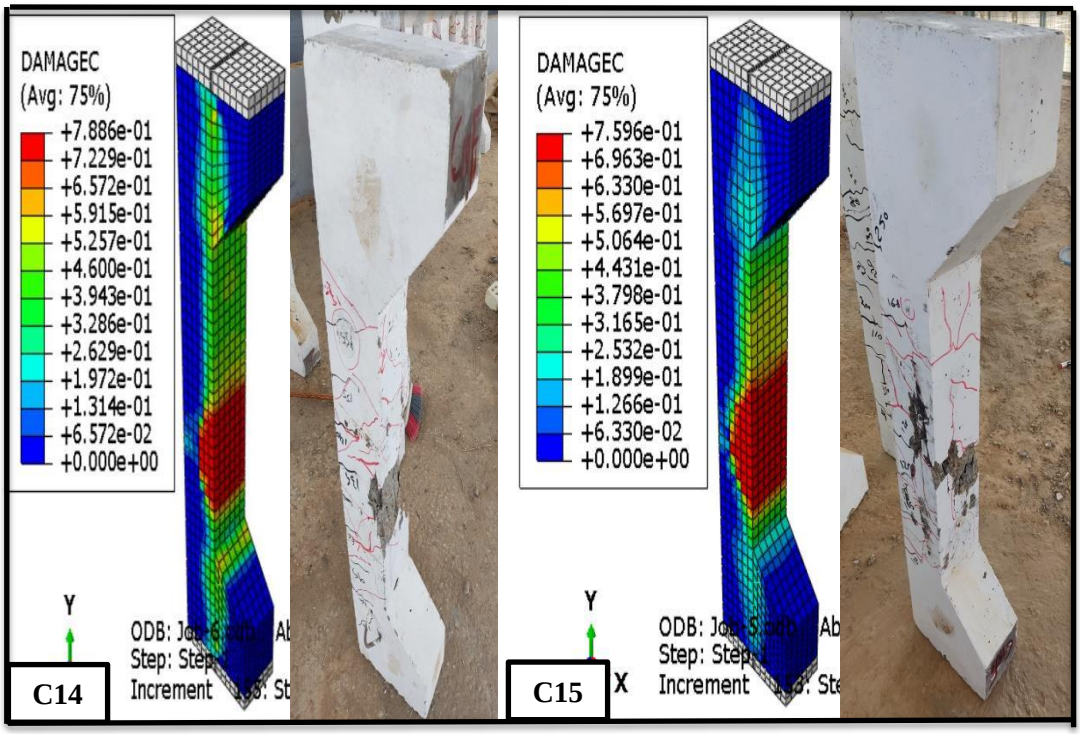

Figure (5-27): Damage Compression and Failure Modes for Columns Specimens (C_{14},C_{15}).

5.6.3 Numerical Results of Strengthened Columns(GroupV)

The analysis of column models that strengthening by an outer shell of (NSC with CFRP)(C_{16}) and (RPC)(C_{17}), the results obtained by Finite elemente with those of experimente are listed in **Tables (5-1)** and **(5-2)**. **Figures (5-28)** to **(5-30)** show the comparison of the load-displacement (lateral and axial).

The results of the numerical analysis agree reasonably well with those of the laboratory. All models show that it causes a large displacement in the last quarter of the load. The theoretical models and the results from the experiments were in good agreement with respect to the ultimate load as well as the lateral and axial displacements. When it comes to load failure, simulation models offer approximately (8.6 and 5.5)% , respectively , more capacity than experimental columns.

The difference between the numerical and experimental specimens for (axial and lateral) displacement by (5.7 and 1.8) % or (3.3 and 2.3)% , respectively. Between experimental and numerical specimens, the theoretical ductility values differed by (2.29 and 2.10) % or (1.72 and 2) % for (axial or lateral)% displacement, respectively.

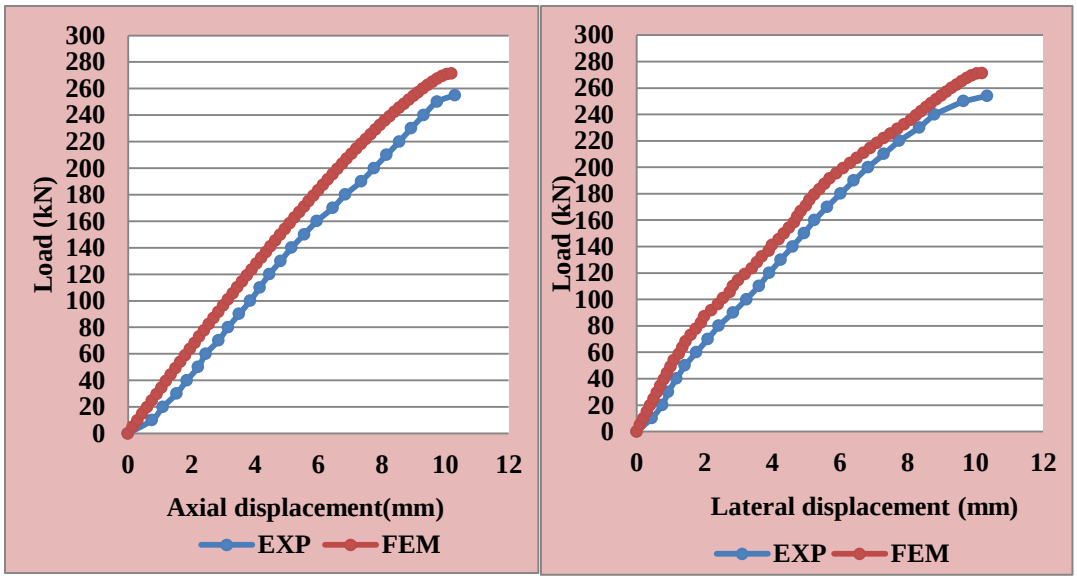

Figure (5-28): The Load- displacement Curves for Specimen (C_{16}).

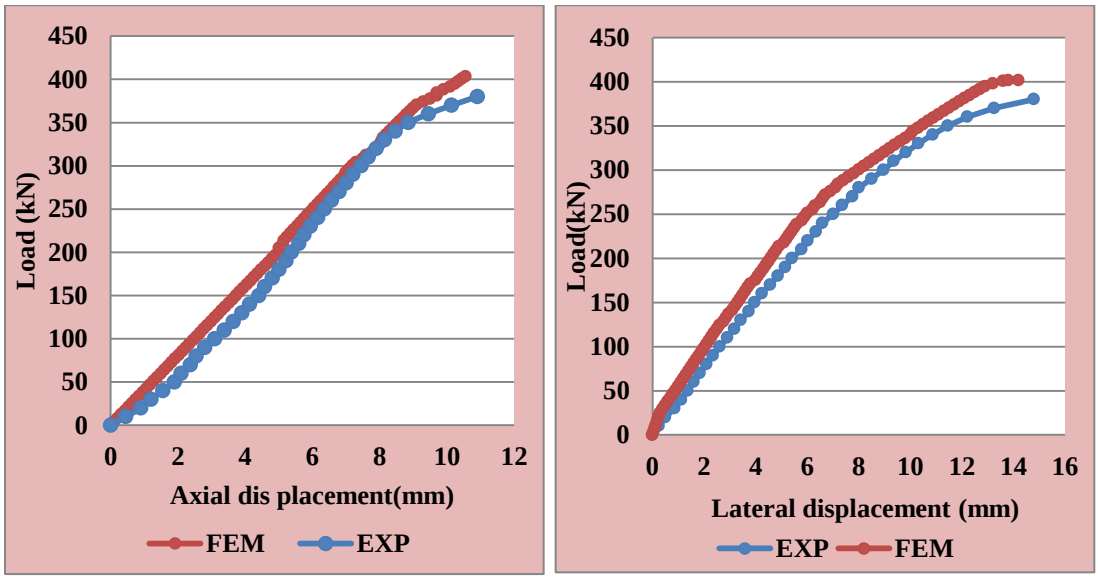

Figure (5-29): The Load- displacement Curves for Specimen (C_{17}).

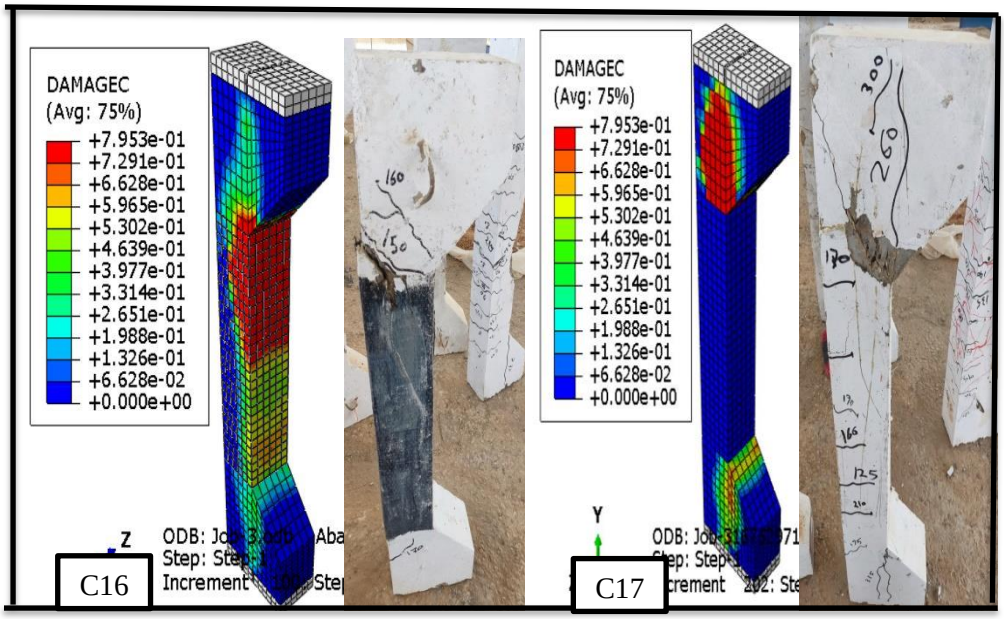

Figure (5-30): Damage Compression and Failure Modes for Columns Specimens (C_{16},C_{17})

5.7 Parametric Study

The nonlinear solution carried out by using the FE computer ABAQUS program with the adopted models showed a reasonable correlation with results obtained from experimental tests. Therefore, the effect of some parameters that were not executed in the experimental program was studied. These parameters are as follows:-

1. **Compressive Strength of the External RPC shell.**
2. **Eccentricity of Post-fire Load.**
3. **Length of Column (Slenderness Ratio).**

5.7.1 Compressive Strength of External RPC Shell

The specimens (C_4) with compressive strengths of (30 MPa) for the core and 200 MPa for the shell were taken for the purpose of examining the effect of increasing the compressive strength of the column shell. The numerical results are presented in **Table (5-3)** and **Figure (5-31)**. The results showed that the unloaded column specimen (C_4) experienced the

axial and lateral displacement about (4.69 and 18.59) %, respectively, as a result of the increase in the compressive strength of the column shell from (110 to 200) MPa to load failure (412KN). the numerical results showed an obvious change in the performance where failure mode out the repaired region the cracking load and ultimate load about (1.75)%.

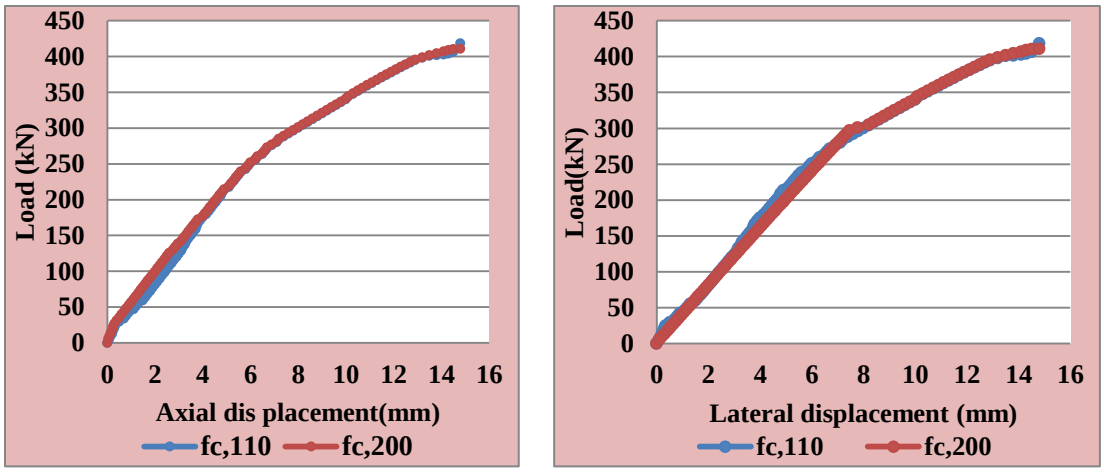

Figure (5-31): The Load- displacement Curves for Specimen (C_{17})with different strength of RPC shell

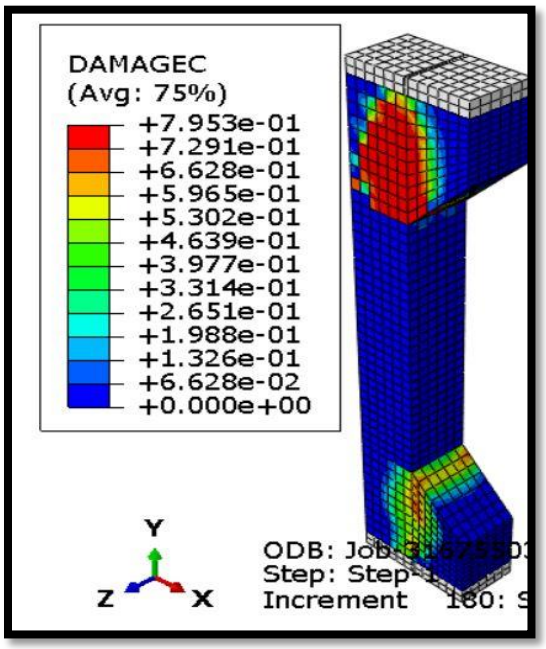

Figure (5-32): Damage Compression and Failure Mode for Column Specimen (C_{17})with RPC 200

5.7.2 Eccentricity of Post-Fire Load

The amount of eccentricity of load that is applied to the column is important in studying the behavior of columns.Two eccentricities were studied in this part of the study less and more than the distance studied in the experimental models to show their effect, the eccentricities were applied (37.5 mm and 112.5 mm) ,respectively,for specimen (C_4),are shown in **Figures (5-33)** and **(5-34).**

The following were the outcomes of increasing the column's (e/h) ratio from (0.25 to 0.75) increasing the load by approximately (295) kN for (e/h= 0.25) and decreasing it by approximately (143) kN for (e/h= 0.75); the change in the ductility ratio; the (axial or lateral) service load displacement by approximately (11.02 and 16.23)%, or (29.18 and 24.03) % for, respectively.

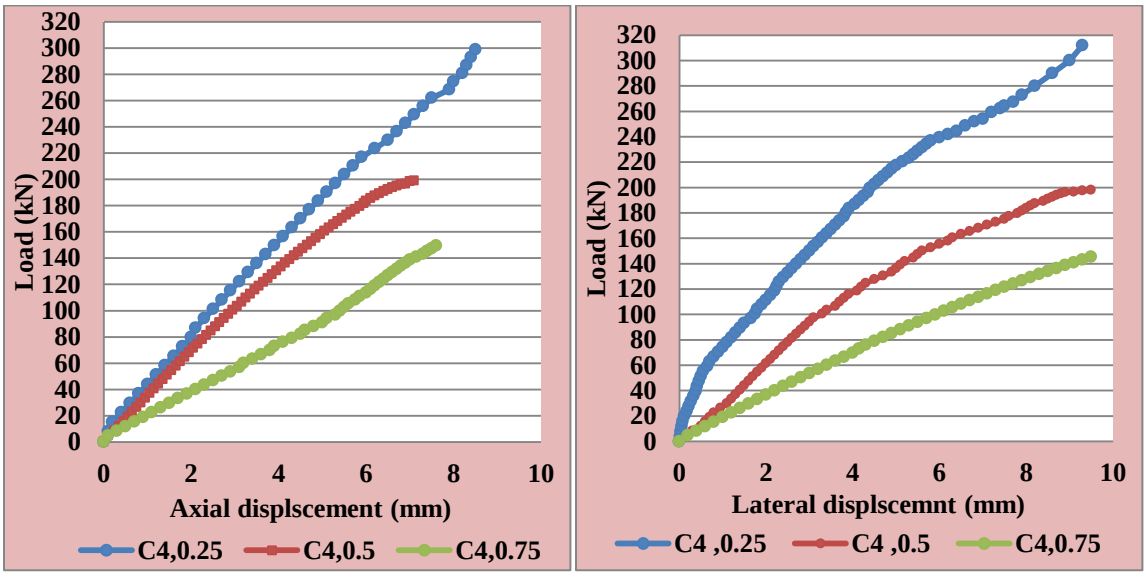

Figure (5-33): The Load- displacement Curves Different Eccentricity Ratio for C_4

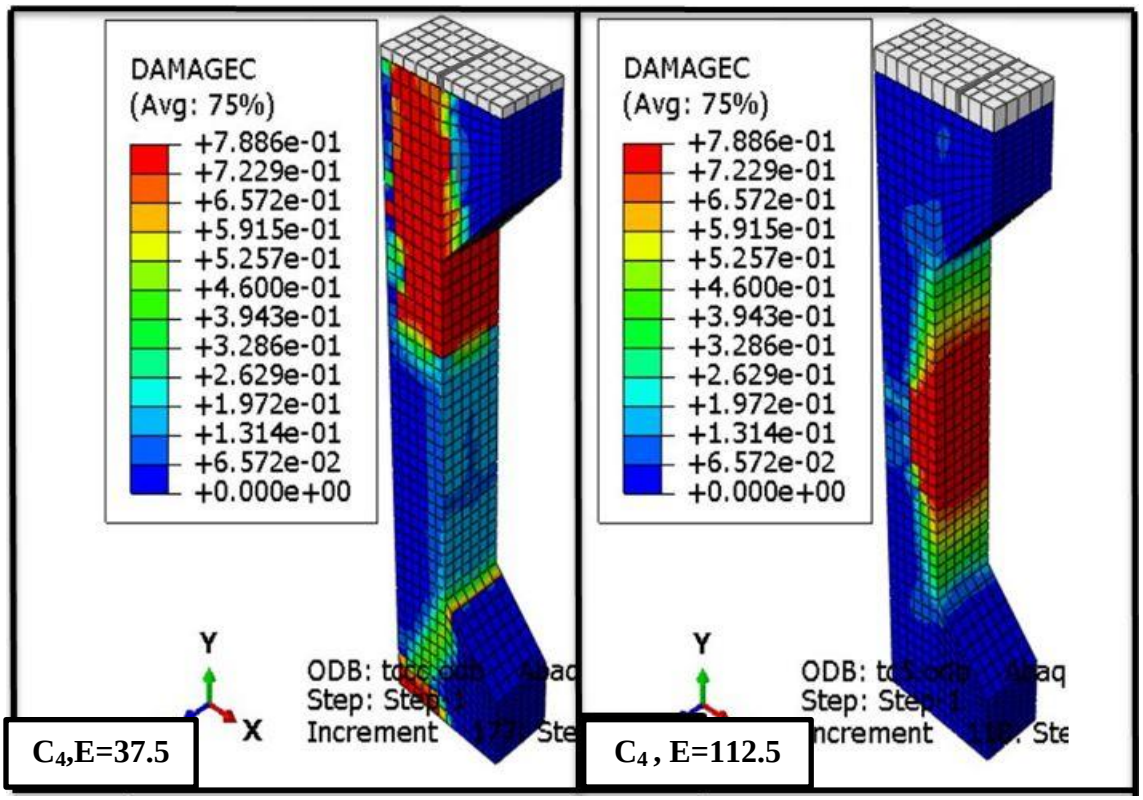

Figure (5-34): Damage Compression and Failure Modes Different Eccentricity Ratio for C_4

5.7.3 Length of Column (Slenderness Ratio)

To investigate the slenderness ratio effect on a column response, specimen (**C_4**) was taken with a different slenderness ratio (different height of the column), (1000 mm and 1250 mm) , as shown in **Figure (5-35) and (5-36).**

When as in an increase in the slenderness ratio of the column the ultimate load was decreased about (10 and 19) % when the slenderness ratio change from (23 and 29)% respectively.The ultimate load for speicmen C4 changing slenderness ratio is (174 and 157) kN for (L=1000mm and L=1250 mm) , respectively.

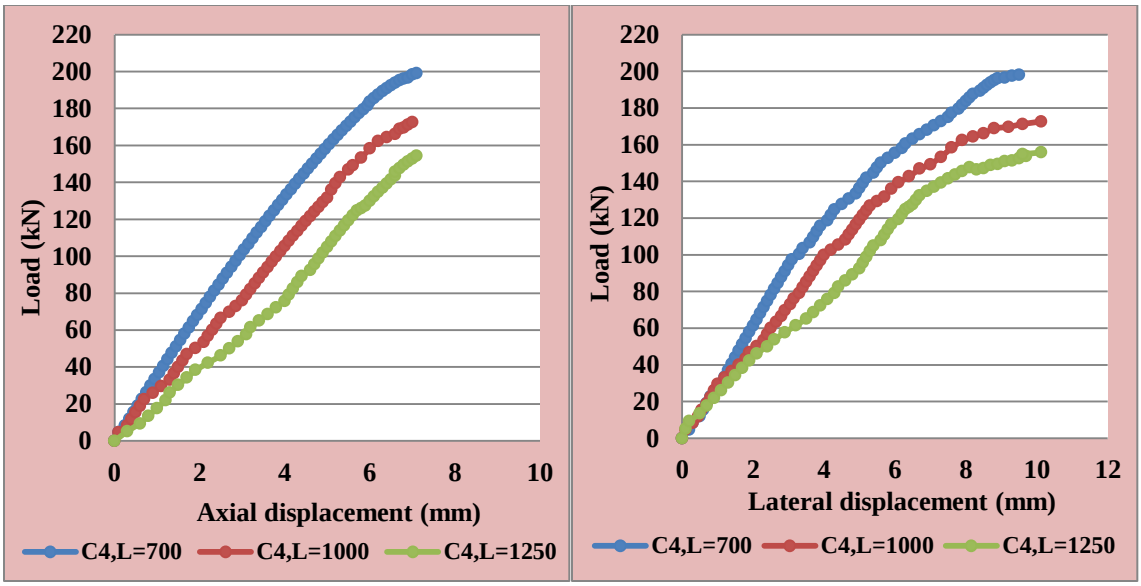

Figure (5-35): The Load- displacement Curves different Slenderness Ratio for C_4.

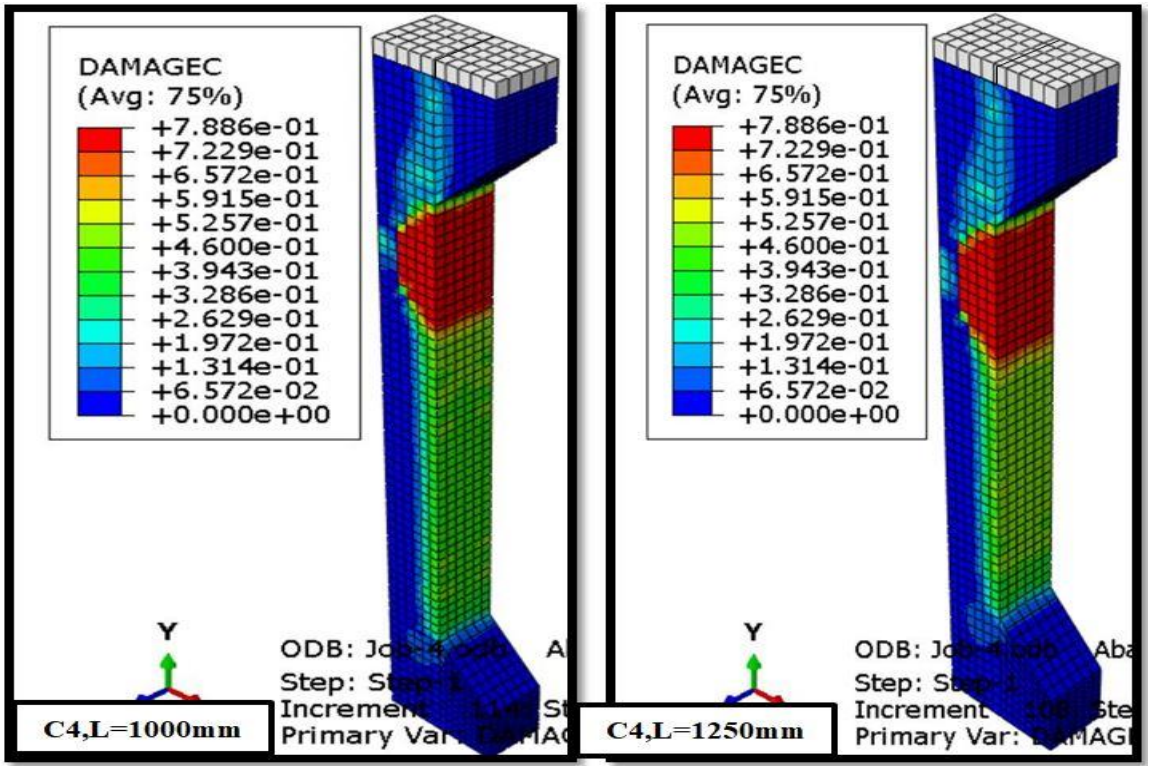

Figure (5-36): Damage Compression and Failure Modes for Different Slenderness Ratio for C_4

Chapter Six
Conclusions and Recommendations for Future Work

Chapter Six

Conclusion and Recommendation for Future Work

6.1 Introduction

An experimental work together with finite element analysis and parametric study for the reinforced concrete columns, exposed to cyclic burning with eccentric pre-loading (30 %Pu) had been performed in this study. The main objective of this research was to explore structural response through and after fire exposure and study .The effect of many variables such as a number of fire cycles ,duration of fire cycles, temperature target , type of concrete, steel ratio and pre- load eccentricity ,as well as repair techniques for damaged columns. From the experimental and numerical results, conclusions can be drawn in this field as well as some suggestions for future works are presented below.

6.2 Conclusions From Experimental Work

The following conclusions can be drawn from considered the experimental investigation:

1- Increasing number of fire exposure cycles for column samples , lead to reduction in the cracking load about (51)% and(60)%, and reduction of ultimate load of about (22)%and (27)% ,respectively. for (two cycles and four cycles),respectively,

2-Increasing of the temperate target for each fire cycle for sample with eccentric (30% Pu) , lead to reduction cracking load about (74%) ,and ultimate load about (37 %), respectively, for four cycles of burning .

3- Increasing the time duration of each fire exposure cycles, lead to reduce cracking load about (64) %and (66%),respectively. Also, the ultimate load was lower about (28)% and (29)% ,respectively, as well as. for (one cycle and four cycles),respectively, .

4-Samples with concentric loading (E = 0 mm) ,lead to increasing in cracking load about (80 and 83) % ,and the ultimate load increasing about by (55 % and 56 %),respectively. for (two cycles and four cycles),respectively.

5- Samples with less longitudinal reinforcement (0.014),with eccentric pre-loading (30% pu) (E=75 mm) , lead to reduce in cracking load (53 and 67)%,and ultimate load was lower for samples about (22 and 29) %,for two cycles and four cycles, respectively,

6- Samples made of high strength concrete with eccentric pre-loading (30% pu) (E=75 mm), cracking load about (61 and 72)% ,and the ultimate load about (25 to 31)% ,for two cycles and four cycles, respectively, which are more than NSC columns.

7-The columns samples with the alternate outer shell by (NSC with CFRP) or RPC) leads to an improvement in the cracking load about(36 and 67)% ,and the ultimate load of the samples, about (34 and 100) %, respectively. this means that second technique was more challenge.

8-By tracking the crack width versus the applied load, crack width increasing values of column specimens with applied load eccentric (E=75)during cyclic fire exposure.

9-When increasing number of fire exposure cycles for columns samples, each of compressive strength, splitting strength and modulus of elasticity

was decreased about (62)% and (67) % , (55)% and (58)%, and (38 and 43) %,respectively, for two cycles and four cycles, respectively,

10-Increasing of the temperate target for each cycles, lead to decreased in compressive strength, tensile strength and modulus of elasticity about (79)% ,(68) and (55)% ,respectively, for four cycles of burning .

11-Increasing the time duration for each fire exposure cycles, caused decrease in the compressive strength, splitting strength and modulus of elasticity about (71)% and (75%), (55 and 63)% and (38 and 50)% ,respectively ,for one cycle and four cycles, respectively,

12- For column samples with concentric loading (E = 0 mm),reduction in compressive strength, splitting strength and modulus of elasticity about (47 and 55)%, (49 and 53) % and (30 and 35 %) ,respectively, for two cycles and four cycles, respectively,

13-Steel ratio of (0.014) lead to ,decrease in compressive strength, splitting strength and modulus of elasticity of elasticity about (64 and 70)%, (58 and 62 %) and (40 and 46 %) , respectively, for two cycles and four cycles of burning ,respectively.

14-For column samples made of , high strength concrete ,reduction in compressive strength, splitting strength and modulus of elasticity about (64 and 72)% , (59 and 64)% ,and(32 and 38)%, for two cycles and four cycles ,respectively , which are more than in case of NSC.

15-When increasing number of fire exposure cycles ,the ductility in displacement (axial or lateral) of column samples with exposure to fire also

decreases about (22)% and (25)% or (34)% and (39)% ,respectively, for two cycles and four cycles.

16-For increasing of the temperate target of each cycles, ductility decreased in displacement (axial or lateral) about (32)% or (48)% ,respectively, for four cycles of burning.

17-For increasing time duration of each fire exposure cycle, the ductility in displacement (axial or lateral) decreased about (27)%and (29%),or(41)%and (43) % ,respectively, for one cycle and four cycles.

18-For column samples with concentric loading (E = 0 mm),ductility decreased in displacement (axial or lateral) with central loading by less than that of samples with eccentric loading during fire exposure about (17 to 19)% or (5 to 6 %) ,respectively , for two cycles and four cycles.

19-For column samples with eccentric (E=75 mm) and longitudinal reinforcement (0.014) ,ductility decreased in displacement (axial or lateral) about (12 and 18)% or (27 and 33) %,respectively, for two cycles and four cycles .

20-For column samples with eccentric (E=75 mm) and high strength concrete ,ductility decreased in displacement (axial or lateral) about (22 and 30)% or (36 and 43)%, ,respectively, for two cycles and four cycles ,respectively, which are more than in case of NSC columns.

21-The columns samples with the replacing outer shell by (NSC with CFRP) or RPC),ductility ratio improved in the displacement (axial or lateral) about(17 and 25)% or (22 or 36) %, respectively. This means that second technique is more active .

22-For increasing number of fire exposure cycles ,the stiffness in displacement (axial or lateral) decreased about (25 and 35)% or (27 and 37)% ,respectively, for two cycles and four cycles, respectively,

23-For increasing of the temperate target for each cycle, stiffness in displacement (axial or lateral) decreased with increasing burning intensity to about (58)% or (59)%,respectively ,for four cycles of burning.

24-For increasing the time duration of each fire exposure cycles, The stiffness in displacement (axial or lateral) decreased with increasing the time during exposure fire to about (46) % and (52)% or (47) %and (53)%, ,respectively ,for one cycle and four cycles, respectively.

25-For column samples with concentric loading (E = 0 mm),the stiffness increased in displacement (axial or lateral) about (31 and 30)% or (69 and 68)%, respectively, for two cycles and four cycles, respectively,

26-For samples with eccentric (E=75 mm) and longitudinal reinforcement (0.014) , stiffness (axial or lateral) decreased with increasing time during of fire exposure about (30 and 39)% or (35 and 43)%,respectively. For periodic burning (one cycle and four cycles) respectively.

27-For column samples made of high strength concrete with eccentric (E=75 mm), ,stiffness increased (axial or lateral) about (30 and 39) % or (32 and 40)% , respectively ,for two cycles and four cycles, respectively.

28- The columns samples with the alternate outer shell by (NSC with CFRP) or RPC),the stiffness was increased in displacement (axial or lateral) about (20)% and (25)% or (30)% and (36)% , respectively. This means that second technique was more active.

6.3 Conclusions from Analytical Study

1-Non-Linear three-dimensional finite element analysis (FEA) by using computer program ABAQUS / Standard (6.14) was capable to simulate the general post-cyclic fire exposure response behavior of column specimens with eccentric load. Where the comparison between the analytical and experimental results exhibited reasonable agreement for load –deflection response with maximum difference as average about (14%) and (3)% for cracking load and ultimate load, respectively.

2-Non-Linear three-dimensional finite element analysis (FEA) by using computer program ABAQUS / Standard (6.14) was capable to simulate behavior of columns strengthened by outer shell of RPC or NSC with CFRP laminates. Where the comparison between the analytical and experimental results exhibited reasonable agreement with maximum difference about (15%) and (7)% as average for cracking load and ultimate load, respectively.

3- For the majority of the selected column specimens, the numerical failure modes derived from plastic strain in FE analysis were comparable to the failure modes in the experimental test, with acceptable differences.

4- Measurements of concrete mechanical properties using non-destruction tests and the ABAQUS program provided a reasonable estimate for the load-displacement response, ultimate load, and service deflection of the exposed cyclic fire column with preloading.

5- When the compressive strength of the RPC outer shell changes from to (110 and 200) MPa, that not give any clear change.

6- For the loading RC columns, with eccentricity ratio , (e/h) ratio from (0.25 to 0.75) loads to decrease the ultimate load by approximately (52) %.

7- When the column slenderness ratio (l/r) increased by (23 and 29)%, the ultimate load decreased about (10 and 19) %, respectively, for specimen during cyclic fire exposure (four cycles).

6.4 Recommendations for Future Researches

A number of suggestions for future research are listed below. These suggestions may lead to more understanding of the performance of columns through and after exposure cyclic fire with pre-loading and repair by different techniques:

1-Further tests need to be conducted on hollow column specimens with fire exposure .

2-Further tests need to be conducted on column specimens with large scale dimensions .

3.Further tests need to be conducted on the outer shell of RPC with different volumetric percentages of steel fibers to further evaluate the ability of steel fibers to prevent concrete cover spalling

4-Further tests need to be conducted on column specimens with loading that , electronic for loads must be controlled in order for the load amount to remain constant loading during the periodic burning

5. For strengthened columns with RPC, tests should be conducted with higher compressive strength of RPC (200 Map and 800 Map).

6.The effect of biaxial pre-applied load through fire exposure on the column behavior.

7.For future use cyclic loading through and after fire exposure.

8-Various supporting conditions may be considered on the performance through and after cyclic fire exposure.

References

Reference

- Aba wihed , Ahmed ,book ,2019.
- Abdel-Hafez, L.M., Alaa E. Y. Abouelezz, and Ahmed M. H. **"Behavior of RC columns retrofitted with CFRP exposed to fire under axial load."** HBRC Journal 11.1, (2015).
- Abdulraheem, Mustafa S., and Mohammed M. Kadhum. **"Experimental and numerical study on post-fire behaviour of concentrically loaded reinforced reactive powder concrete columns."** Construction and Building Materials , 2017.
- ACI 216.1, "**Code requirements for determining fire resistance of concrete and masonry construction assemblies**" ACI 216.1- 07/TMS-0216-07, American Concrete Institute, Farmington Hills, Mich, USA, 2007.
- ACI Committee 211.1-91, **"Standard Practice for Selecting Proportions for Normal Heavyweight, and Mass Concrete"** (ACI 211.1 - 91)
- ACI Committee. **"Guide to Quality Control and Assurance of High-Strength Concrete (363.2 R-11)."** In American Concrete Institute. 2011.
- ACI-318, **"Building Code Requirements For Reinforced Concrete and Commentary",** American Concrete Institute, Farmington Hills,Mich,USA,2019.
- Ada, M., Sevim, B., Yüzer, N., & Ayvaz, Y.**. "Assessment of damages on a RC building after a big fire."** Advances in concrete construction , (2018).
- Al-Ameeri, A.S., AL-Hussain, K. and Essa, M., **"Predicting a mathematical models of some mechanical properties of concrete from non-destructive testing."** Civil and Environmental Research ,(2013).
- Al-Gasham, Thaar S. S. **" Experimental performance of reinforced concrete hollow columns exposed to fire."** Al-Qadisiyah Journal For Engineering Sciences ,(2016).
- Ali, A, Y **"Constructional Repair for a Concrete Building Adversed by Fire",** 1992.
- Ali, A. Y., and Jawad S.A. **"Restoration of Environmental and Structural Characteristics of Reinforced Concrete Column Damaged By Fire."** Journal of Green Engineering , (2020).
- Ali, F., Nadjai, A., & Choi, S.. **"Numerical and experimental investigation of the behavior of high strength concrete columns in fire".** Engineering structures, (2010).

Reference

- Al-Kamaki, Y. S. S., Al-Mahaidi, R., & Bennetts, I. D**."Confinement of heat-damaged RC circular columns using CFRP fabrics".** 23rd Australasian Conference on the Mechanics of Structures and Materials (ACMSM23), I, 2014.
- Al-Mashhadany, S. Abd al-Amir i **"High Strength Concrete"** Al-Qithara Center for Printing and Design, Babylon - Street 40 , (2009).
- Alogla, S., and V. K. R. Kodur. **"Quantifying transient creep effects on fire response of reinforced concrete columns."** Engineering Structures , (2018).
- Arna'ot, Farid H., Ahmmad A. Abbass, Ahmed Abbas Abualtemen, Sallal R. Abid, and Mustafa Özakça. "**Residual strength of high strength concentric column-SFRC flat plate exposed to high temperatures."** Construction and Building Materials , (2017).
- ASTM A615-16, **"Standard Specification for Deformed and Plain Carbon Structural Steel Bars for Concrete Reinforcement"**, Annual Book of ASTM Standards, 2016
- ASTM C 192-88, **"Standard Practice for making and Curing Concrete Test Specimens in Laboratory",** Annual Book of ASTM Standard, Vol. 4. 2, 2003.
- ASTM C 494 /C 494M-05a, **"Standard Specification for Chemical Admixtures for Concrete",** Vol. 04.02, 2005.
- ASTM C 496/C 496M-11, "**Standard Test Method for Splitting Tensile Strength of Cylinder Concrete Specimens",** Annual Book of ASTM Standards, American Society for Testing and Materials, 2011
- ASTM C 78-15a, "**Standard Test Method for Flexural Strength of Concrete (Using Simple Beam with Third-Point Loading)"**, Annual Book of ASTM Standards, American Society for Testing and Materials, 2010
- ASTM C1240-04, **"Standard Specification for the Use of Silica Fume as a Mineral Admixture in Hydraulic Cement Concrete, Mortar and Grout"** , Vol. 4.2, 2004.
- ASTM C597 − 09, **"Standard Test Method for Pulse Velocity through Concrete"**, Annual Book of ASTM Standards, American Society for Testing and Materials, 2009.
- Balaji, A., Nagarajan, P., & Pillai, T. M. **"Studies on the behavior of Reinforced Concrete Short Column subjected to fire".** Alexandria Engineering Journal, 2015.

Reference

- Bamonte, Patrick, and F. Lo Monte. **"Reinforced concrete columns exposed to standard fire: Comparison among different constitutive models for concrete at high temperature."** Fire safety journal ,(2015).
- Bikhiet, M., F. Nasser El-Shafey and M.H. El-Hashimy, "Behavior of reinforced concrete short columns exposed to fire", 2014.
- Bissonnette, R., T. Luger, D. Thaçi, D. Toth, A. Lacombe, S. Xia, R. Mazur et al. **"Secukinumab demonstrates high sustained efficacy and a favourable safety profile in patients with moderate-to-severe psoriasis through 5 years of treatment (SCULPTURE Extension Study)."** Journal of the European Academy of Dermatology and Venereology , (2018).
- Britez, C., M. Carvalho, and P. Helene. **"Fire impacts on concrete structures. A brief review."** Revista ALCONPAT , (2020).
- Brushlinsky, N. N., M. Ahrens, S. V. Sokolov, and P. Wagner. **"World fire statistics. International Association of Fire and Rescue Services."** Center for Fire Statistics, (2017).
- BS 1881: Part 116, **''Method for Determination of Compressive Strength of Concrete Cubes''**, British Standards Institution, 1989.
- BS8110-1: 1997, "**Structural Use of Concrete"** , British Standard, 1997.
- Buch, Sh.H., and Umesh K. Sh. **"Fire resistance of eccentrically loaded reinforced concrete columns."** Fire technology , (2019).
- Buch, Shujaat H., and Umesh K. Sharma. **"Empirical model for determining fire resistance of Reinforced Concrete columns."** Construction and Building Materials , (2019).
- Camara, L. A., Wons, M., Esteves, I. C., & Medeiros-Junior, R. A. **"Monitoring the Self-healing of Concrete from the Ultrasonic Pulse Velocity".** Journal of Composites Science, 2019.
- Chan, Sammy YN, Gai-fei Peng, and John KW Chan. **"Comparison between high strength concrete and normal strength concrete subjected to high temperature."** Materials and Structures , (1996).
- Chen, Yih-Houng, Yun-Fei Chang, George C. Yao, and Maw-Shyong Sheu. **"Experimental research on post-fire behavior of reinforced concrete columns."** Fire safety journal , (2009).
- Chowdhury, E. U. **"Behaviour of fibre reinforced polymer confined reinforced concrete columns under fire condition "(**Doctoral dissertation, Queen's University). (2009).
- Chowdhury, E., Bisby, L., Green, M., Bénichou, N., & Kodur, V. **"Heat**

transfer and structural response modelling of FRP confined rectangular concrete columns in fire". Construction and Building Materials, 2012.

- Deglandon, Kathy. **"Selectring the Best Hydraulic Pressure Sensor".** Drilling Instruments. Drilling Instruments. , 2016.
- El-Shaer, M. A. **"Structural Analysis for Concrete Columns Subjected to Temperture"**. Acta Technica Corvininesis-Bulletin of Engineering, 2014.
- Elshamandy, M. G., Farghaly A. S., and Benmokrane B. "**Experimental behavior of glass fiber-reinforced polymer-reinforced concrete columns under lateral cyclic load."** ACI Struct. J , (2018).
- Ghimire, A. **"Basic Principles of Engineering".** Lulu. Com, 2017.
- Gil, A. M., Fernandes, B., Bolina, F. L., & Tutikian, B. F. **"Experimental analysis of the spalling phenomenon in precast reinforced concrete columns exposed to high temperatures"** Revista IBRACON de Estruturas e Materiais ,2018
- Hamakareem, **"Explosive Spalling of Concrete Structural Elements during Fire",** 2009.
- Han, L.H., Yang, Y.F. and Xu, L. **"An experimental study and calculation on the fire resistance of concrete-filled SHS and RHS columns."** Journal of constructional steel research, (2003).
- Han, Lin-Hai, and Wei Li. **"Seismic Performance of Concrete-Filled Steel Tubular (CFST) Structures."** In Seismic Design of Industrial Facilities, . Springer Vieweg, Wiesbaden, 2014.
- Hassan, M. K. M. Abdul. "**Utilizing of Carbon Fiber Reinforced Polymer Sheets for Strengthening of Fire Exposed Reinforced Concrete Columns".** Diss. University of Babylon, (2019).
- Hu,Y., Zhao, P., Yang, B. and Dai, G., **"Numerical study on temperature distribution of high-strength concrete-filled steel tubes subjected to a fire**." International Journal of Steel Structures, (2016).
- Iraqi Specification, No. 5/1984, **"Portland Cement**" , Ministry, Organ Central planning for standardization and quality control
- Iraqi Standard Specification, No.45/1984**," Aggregate from Natural Sources for Concrete and Construction**", Central Organ, Planning Ministry for standardization and quality control
- Jau, W.C. and Huang, K.L**.,"A study of reinforced concrete corner columns after fire."** Cement and concrete Composites , (2008).

Reference

- Jawad, S.A., and Ammar Y. A. **"Structural Response of Post-Fire Exposed Reinforced Concrete Column with Pre-Load."** In IOP Conference Series: Materials Science and Engineering, , 2020.
- Kadhim, A. H., M. M. Rasheed, and H. K. Jarallah. **"Structural behavior of eccentrically loaded RC columns under fire temperature loading."** In IOP Conference Series: Materials Science and Engineering, (2019).
- Kadhum, M., Mahdi, Z., Funfakh, Y., Mohammed, Z., Abdulraheem, M. and Gkantou, M.,**"Experimental investigation on the post-fire performance of reactive powder concrete columns."** Przegląd Naukowy. Inżynieria i Kształtowanie Środowiska ,(2021).
- Kanaka Lakshmi, L.Lanish Jafrin, B.Hari Prasanth, A.Santhosh Kumar, P.prashanth kumar,**"Strengthening of fire damaged concrete column using glass fibres".** Panimalar Engineering College,India, 2016.
- Khaliq, W. and Kodur, V. **"Behavior of high strength fly ash concrete columns under fire conditions."** Materials and structures ,(2013).
- Kodur, V. and Mcgrath, R. **"Fire endurance of high strength concrete columns."** Fire technology , (2003).
- Kodur, V. K. R., Bisby, L. A., Green, M. F., & Chowdhury, E. **"Fire endurance of insulated FRP-strengthened square concrete columns",** (2005).
- Kodur, V. K. R., Cheng, F.-P., Wang, T.-C., & Sultan, M. A. **"Effect of Strength and Fiber Reinforcement on Fire Resistance of High-Strength Concrete Columns".** Journal of Structural Engineering, 2003
- Kodur, V. K. R., Fu-Ping Cheng, Tien-Chih Wang, and M. A. Sultan. **"Effect of strength and fiber reinforcement on fire resistance of high-strength concrete columns."** Journal of Structural Engineering (2003).
- Kodur, V. K. R., T. C. Wang, and F. P. Cheng. **"Predicting the fire resistance behaviour of high strength concrete columns."** Cement and Concrete Composites (2004).
- Kodur, V., Hibner, D., & Agrawal, A. **"Residual response of reinforced concrete columns exposed to design fires"**. Procedia engineering, (2017).
- Kodur, Venkatesh, and Nikhil Raut. **"A simplified approach for predicting fire resistance of reinforced concrete columns under biaxial bending."** Engineering structures , (2012).
- Li, J.H., Tang, Y.F. and Liu, M.Z. "**Experimental Study on Residual Load Bearing Capacity of SRC Eccentric Columns after Exposure to Fire."** In Advanced Materials Research,. Trans Tech Publications Ltd,(

2011).

- Li, L.Z., Liu, X., Yu, J.T., Lu, Z.D., Su, M.N., Liao, J.H. and Xia, M., **"Experimental study on seismic performance of post-fire reinforced concrete frames."** Engineering Structures ,(2019).
- Li, X., Zhang, R., Jin, L. and Du, X**."Numerical analysis of axial compressive behavior of RC short columns subjected to non-uniform fire: A meso-scale study."** In E3S Web of Conferences, EDP Sciences, (2021).
- Liu, L., George A. Kardomateas, Victor Birman, J. W. Holmes, and George J. Simitses. **"Thermal buckling of a heat-exposed, axially restrained composite column."** Composites Part A: Applied Science and Manufacturing , (2006).
- Lixian, L., Reddy, D. V., & Sobhan, K. **"Strengthening of Fire- damaged Columns by Cross-sectional Enlargement:** A Computational Evaluation", (2009).
- M. Yaqub, C. Bailey, "**Repair of fire damaged circular reinforced concrete columns with FRP composites,"** Construction and Building Materials 2011.
- Malhotra, V.M., **"Testing Hardened Concrete : Nondestructive Methods",** American Concrete Institutes Monograph, 1976.
- Mao, Xiaoyong, and V. K. R. Kodur. **"Fire resistance of concrete encased steel columns under 3-and 4-side standard heating."** Journal of constructional steel Research , (2011),
- Martins, A.M. and Rodrigues, J.P.C. **"Fire resistance of reinforced concrete columns with elastically restrained thermal elongation."** Engineering Structures , (2010).
- Memar, M.J., Kheyroddin, A. and Hemmati, A., **"Finite Element Analysis on Reinforced Concrete Columns Strengthened by ECC Jacketing under Eccentric Compressive Load."** Engineering Journal , (2020).
- Mohana, M.H., "**Assessment of concrete compressive strength by ultrasonic pulse velocity test."** Iraqi Journal of Civil Engineering ,(2020).
- Muller, I., de Brito, R.M., Pereira, C.E. and Brusamarello, V**., "Load cells in force sensing analysis--theory and a novel application."** IEEE Instrumentation & Measurement Magazine , (2010).
- Muslim Y.T.**" Residual Bearing Capabilities of Fire Exposed Reactive Powder Concrete Columns",** University of Babylon,2018.
- Muthuswamy, K.R., and Thirugnanam G.S. **"Structural Behavior of**

Hybrid Fiber Reinforced Concrete Exterior Beam-Column Joint Subjected to Cyclic Loading".International Journal of Civil and Structural Engineering, 2014.

- Navrátil, J. **"Nonlinear analysis of reinforced and composite columns in fire".** Frattura ed Integrità Strutturale, (2017).
- Nguyen, D.L., Ryu, G.S., Koh, K.T. and Kim, D.J.,"**Size and geometry dependent tensile behavior of ultra-high-performance fiber-reinforced concrete."** Composites Part B: Engineering , (2014).
- Qiu, J., Jiang, L. and Usmani, A., **"Post-fire Repair of Concrete Structural Members: A Review on Fire Conditions and Recovered Performance."** International Journal of High-Rise Buildings , (2021).
- Sadaoui, A., S. Illouli, and A. Khennane. **"Effect of restraints on the response of RC columns in a parametric fire."** In 8th International conference on fracture mechanics of concrete and concrete structures, (2013).
- Shubbar, H. A., and Nameer ,A. A. "**The fire exposure effect on hybrid reinforced reactive powder concrete columns."** Civil Engineering Journal , (2020).
- Talebi, E., Korzen, M., Espinós, A., & Hothan, S. **"The effect of damage location on the performance of seismically damaged concrete filled steel tube columns at fire"**. In Proceedings of the 12th International Conference on Advances in Steel-Concrete Composite Structures). Editorial Universitat Politècnica de València. (2018).
- Tan, K. H., and Y. Yao. **"Fire resistance of reinforced concrete columns subjected to 1-, 2-, and 3-face heating."** Journal of Structural Engineering, (2004).
- Trtnik, G., Kavčič, F. in Turk, G. **"Prediction of concrete strength using ultrasonic pulse velocity and artificial neural networks",** Ultrasonics 49, (2009).
- Wang, L., Caspeele, R. and Taerwe, L**.,"Study on the fire resistance of rectangular concrete columns exposed to natural fires."** 8th International Conference on Structures in Fire ,(2014).
- Waryosh, W.A., Rasheed, M.M. and AL-musawi, A.H**.,"Experimental study of reinforced concrete columns strengthened with CFRP under eccentric loading."** Journal of Engineering and Development , (2012).
- Waseem H. M. Al-Haddad **"Experimental and Theoretical Investigations for Behavior of Hybrid Reinforced Concrete Corbel-Column Connections**" University of Babylon,2016

Reference

- Wu, B., Li, Y.H. and Chen, S.L.,"**Fire resistance of reinforced concrete columns with square cross section."** Advances in Structural Engineering , (2007).
- Wu, Bo, Yi-Hai Li, and Shu-Liang Chen. "**Effect of heating and cooling on axially restrained RC columns with special-shaped cross section."** Fire technology , (2010).
- Xu, J., C. Tan, and R. Aboutaha. **"Experimental investigation of high strength reinforced concrete columns damaged by fire and retrofitted with CFRP jackets."** In IOP Conference Series: Earth and Environmental Science, , (2019).
- Yadav, R., Chen, B., Huihui, Y. and Lian, Z. **"Numerical study on the seismic behavior of CFST columns."** In 11th Pacific Structural Steel Conference, Shanghai, China,(2016).
- Yousif, S. T., Omar M. Abdul-Kareem, and Kaythar A. I**. "Artificial neural network model for predicting the compressive strength of concrete using ultrasonic pulse velocity."** Muthanna J. Eng. Technol , (2017).
- Zhang, C., Wang, G.Y., Xue, S.D. and Yu, H.X.,. **"Experimental research on the behavior of eccentrically loaded SRC columns subjected to the ISO-834 standard fire including a cooling phase."** International journal of steel structures , (2016).
- Zhao, H., Yu, H., Yuan, Y., Li, P., & Chen, J. **"Cyclic loading behavior of a repaired subway station after fire exposure."** Tunnelling and Underground Space Technology,2019
- Zhou, J., and Lu W.**"Repair of fire-damaged reinforced concrete members with axial load: a review."** Sustainability , (2019).

Appendices

Appendix A

Design of Control Columns

A-1 Design of Concrete Columns (4 ϕ 12) , f_C=30 Mpa

According to the ACI 318M-19, the design calculation is induced, as follows:

(k/r) for (L=700mm) =16.17 (short column)

● Longitudinal Reinforcement

A_g =150*150=22500 mm^2

A_{st} = 4* π/4*$(12)^2$ =452.389 mm^2

ρ = A_{st}/ A_g =452.389 / 22500 =0.02

0.01 ≤ ρ ≤ 0.08 (Ok)

● Clear Spacing of Longitsudinal Reinforcement

The greatest of { 16 d_b ; 48 d_{tie} ; Least dimension } **=150 mm** = 100 mm

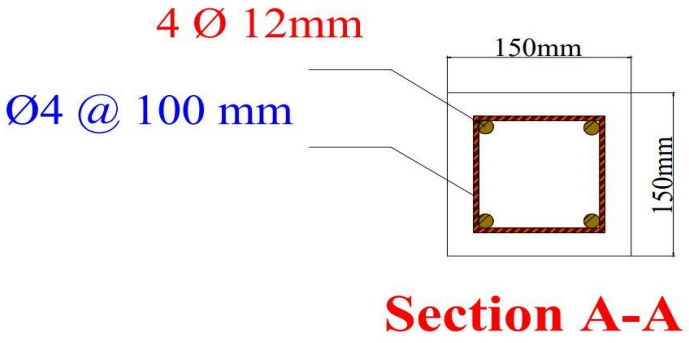

Figure (A-1): Cross-Section of Column (G1,G2,G4 ,G5)

A-2 Ultimate Strength Calculation

***For e=0**

h=150 mm

$P_o = 0.85 * f_C' * (A_g - A_{st}) + A_{st} * f_y$

$P_o = (0.85 * 30 * (0.15*0.15 - 452.389 * 10^{-6}) + 452.389 * 600 * 10^{-6}) * 10^3$

$= 833.65 \ KN$

$p_u = 0.65 * 833.96 = 542$ KN

***For e=75**

h=150 mm

$\sum$ Force =0 ,$Pu' = 0.85 * f_C' * b * a + A_S' * f_y - A_S * f_S$ ……①

$Pu' = 0.85 * 30 * a * 0.15 + 226.195 * 10^{-6} * 600 - 226.195 * 10^{-6} * F_S$ ….. ①

$e' = e + h/2 - d'$

$e' = 75 + 150/2 - 35$

$e' = 115$ mm

$\sum M_{AS} = 0$

$Pu' * e' = 0.85 * f_C' * b * a * (d - a/2) + A_S' * f_y * (d - d')$ …… ②

$Pu' * 0.115 = 0.85 * 30 * 0.15 * a * (0.115 - a/2) + 226.195 * 10^{-6} * 600 * (0.115 - 0.035)$ …… ②

From strain diagram :

$\varepsilon_s /(d-c) = \varepsilon_s/c$

$f_S = \varepsilon s * ES = 600 (B_1 * d/a - 1) = 600(0.85 * 0.115/a - 1)$ …….③

Solution of eq ①, ② and ③

a =0.057

$f_S = 600(0.85 * 0.115/0.057 - 1) = 429$ Mpa

$Pu' = (0.85 * 30 * 0.057 * 0.15 + 226.195 * 10^{-6} * 600 - 226.195 * 10^{-6} * 429) * 10^3$

Pu′ = 256.7 KN

B-1 Design of Concrete Columns (4 Φ 10) , f'_C=30 Mpa

According to the ACI 318M-19, the design calculation is induced, as follows:

● Longitudinal Reinforcement

A_g =150*150=22500 mm^2

A_{st} = 4* π/4*$(10)^2$ =314.16 mm^2

ρ= A_{st}/ A_g =314.16 / 22500 =0.014

$0.01 \leq \rho \leq 0.08$ (Ok)

● Clear Spacing of Longitudinal Reinforcement

The greatest of { 16 d_b ; 48 d_{tie} ; Least dimension } **=150 mm**

use = 100 mm

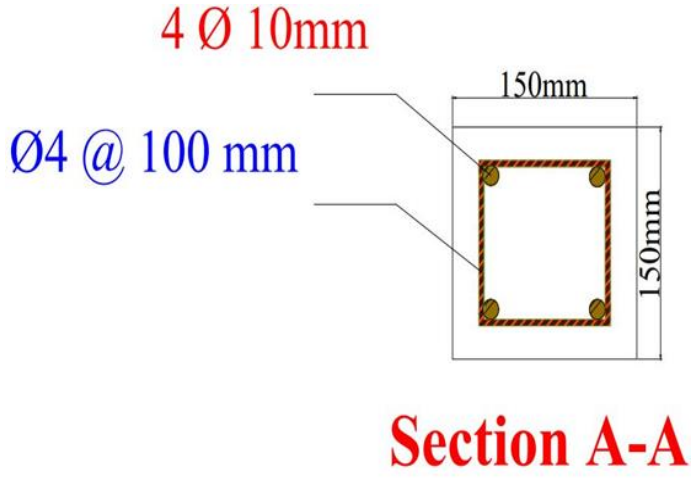

Figure (A-2): Cross-Section of Column (G3)

B-2 Ultimate Strength Calculation

*For e=0

h=150 mm

P_o =0.85 * f_C' *(A_g-A_{st}) + A_{st} * f_y

P_o =(0.85 * 30 * (0.15*0.15 – 314.16 * 10^{-6}) + 314.16 *613 *10^{-6}) *10^3

=758.3 *KN*

p_u =0.65 *758.3 =493 KN

*For e=75

h=150 mm

∑ Force =0 ,Pu′= 0.85 * f_C *b * a +A_S' * f_y - A_S *f_S ……①

Pu′= 0.85 *30*a *0.15 + 157.1 *10^{-6} * 613 - 157.1 *10^{-6} *F_S …….. ①

e′ = e + h/2 -d′

e′= 75 + 150/2 – 34

e′ = 116 mm

∑ M_{AS} =0

Pu′ * e′ = 0.85 * f_C *b * a * (d - a/2) +A_S' * f_y *(d -d′) …… ②

Pu′ * 0.116= 0.85 *30* 0.15*a (0.116 – a/2) + *10^{-6} * 613 *(0.116 – 0.034) ……②

From strain diagram :

Ɛs /(d-c)= Ɛs/c

f_s = Ɛs*E_s =600 (B_1*d/a -1) = 600(0.85* 0.115/a-1) …….③

Solution of eq ①, ② and ③

a =0.054 m

f_s = 600(0.85* 0.116/0.054 -1) = 495.6 Mpa

Pu′= (0.85 *30*0.054*0.15 +157.1 *10^{-6} * 613 - 157.1 *10^{-6} *495.6) *10^3

Pu′ = 225 KN

C-1 Design of Concrete Columns (4 Φ 12) , f_C=55 Mpa

According to the ACI 318M-19, the design calculation is induced, as follows:

● Longitudinal Reinforcement

A_g =150*150=22500 mm^2

A_{st} = 4* π/4*$(12)^2$ =452.389 mm^2

$\varrho = A_{st}/ A_g$ =452.389 / 22500 =0.02

$0.01 \leq \varrho \leq 0.08$ (Ok)

● Clear Spacing of Longitudinal Reinforcement

The greatest of { 16 d_b ; 48 d_{tie} ; Least dimension } **=150 mm** = 100 mm

C-2 Ultimate Strength Calculation

***For e=0**

h=150 mm

$P_o = 0.85 * f_C' * (A_g - A_{st}) + A_{st} * f_y$

$P_o = (0.85 * 55 * (0.15*0.15 - 452.389 * 10^{-6}) + 452.389 * 600 * 10^{-6}) * 10^3$

$= 1302\ KN$

$p_u = 0.65 * 1302 = 846.4\ KN$

***For e=75**

h=150 mm

$\sum$ Force =0 ,$Pu' = 0.85 * f_C * b * a + A_S' * f_y - A_S * f_S$ ……①

$Pu' = 0.85 * 55 * a * 0.15 + 226.195 * 10^{-6} * 600 - 226.195 * 10^{-6} * F_S$ ……..①

$e' = e + h/2 - d'$

$e' = 75 + 150/2 - 35$

$e' = 115$ mm

$\sum M_{AS} = 0$

$Pu' * e' = 0.85 * f_C * b * a * (d - a/2) + A_S' * f_y * (d - d')$ …… ②

$Pu' * 0.115 = 0.85 * 55 * 0.15 * a\ (0.115 - a/2) + 226.195 * 10^{-6} * 520 * (0.115 - 0.035)$ **……**②

From strain diagram :-

Ɛs /(d-c)= Ɛs/c

f_S = Ɛs*ES =600 (B_1*d/a -1) = 600(0.85* 0.115/a-1) …….③

Solution of eq ①, ② and ③

a =0.051

f_S = 600 (0.85* 0.115/0.051 -1) = 550 Mpa

Pu′= (0.85 *55*0.051*0.15 + 226.195 *10^{-6} * 600 - 226.195 *10^{-6} *550) *10^{3}

Pu′ = 369 KN

Design of corbel:-

A-When (f_C' =30)

Pu= 270 KN / 2 =135 KN = Vu

Mu =Vu *a + Nu * (h-d)

Mu= 135 * 0.075 + 0.2 * 135 * (0.3- 0.275)

=10.125 +0.675 =10.8 KN.m

A_f =Mu/ Φ* f_y *la =10.8 *10^6/(0.75*520*0.9*275) =112 mm^2

A_n =Nu/ Φ* f_y =0.2 *135 *10^3/(0.75*520) =78 mm^2

A_{vf} =Vu/ Φ* f_y *μ =135 *10^3/(0.75*520* 1.4)= 248 mm^2

$A_s = A_f + A_n$

=112 + 78 = 182 mm^2

A_s = ⅔ A_{vf} + A_n

=⅔* 248 +78 = 236 mm^2

} use A_S= 236 mm^2

Use 3 Φ12 = 339 .29 > 236 mm^2 (ok)

Ah = 0.5 (A_s- A_n)

0.5 (236 -78) = 83 mm^2

Use 4 Φ 4 =101 mm^2 > 83 mm^2 (ok) (Closed)

B-When (f_C' =55):-

Pu= 380 KN / 2 =190 Vu

Mu =Vu *a + Nu * (h-d)

Mu= 190 * 0.075 + 0.2 * 190 * (0.3- 0.275)

=14.25 +0.95 =15.2 KN.m

A_f =Mu/ Φ* f_y *la =15.2*10^6/(0.75*520*0.9*275) =158 mm^2

A_n =Nu/ Φ* f_y =0.2 *190 *10^3/(0.75*520) =98 mm^2

A_{vf} =Vu/ Φ* f_y*μ =190 *10^3/(0.75*520* 1.4)= 348 mm^2

$A_s = A_f + A_n$

$=158 + 98 = 256\ mm^2$

$A_s = ⅔\ A_{vf} + A_n$

$=⅔ * 348 + 98 = 330\ mm^2$

use A_S= 330 mm^2

Use 3 Φ12 = 339 .29 > 330 mm^2 (ok)

Ah = 0.5 (A_s- A_n)

0.5 (330 -98) = 116 mm^2

Use 5 Φ 4 =126 mm^2 > 116 mm^2 (ok) (Closed)

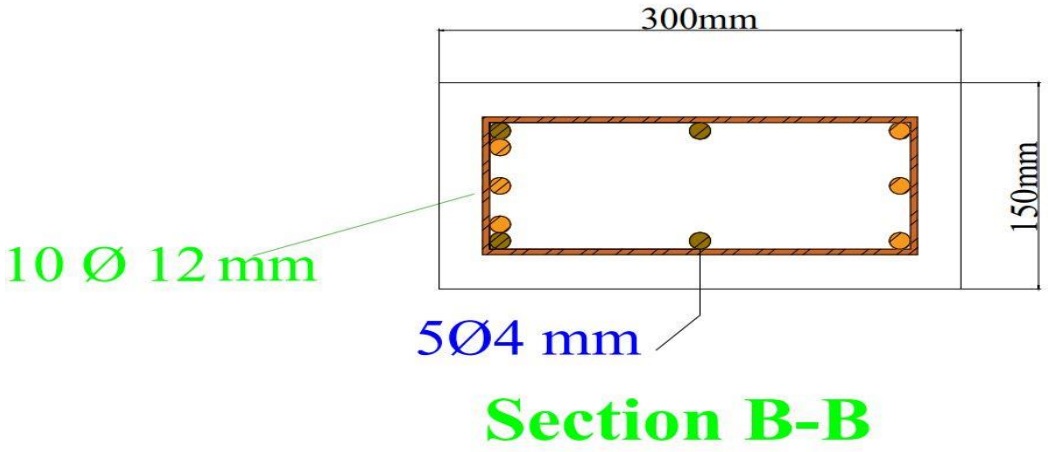

Figure (A-3): Cross-Section of Corbel for Column

Appendix B

Material Safety Datasheets

B.1 Data sheet of steel fibers provided by the manufacturer

赣州大业金属纤维有限公司

Ganzhou Daye Metallic Fibres Co., Ltd

Steel fiber for concrete reinforcement

http//: www.gzdymf.com • Email: may @ gzdymf.com • Tel: +86-797-8259566 • Fax:+86-797-8259568



Product Description

Micro Steel Fiber	
Type	WSF 0213
Surface	Brass coated

Chemical Composition

C:	MN:	P:	S:	Si:
=0.80%	=0.75%	=0.035%	=0.035%	=0.30%

Tensile Strength	Minimum 2300Mpa
Melting Point	1500°C
Length	13mm±1mm
Diameter	=0.2mm±0.05mm
Form	Straight

This steel fibers can be produced with different length and diameters

Package: By damp-proof poly bag, 25Kg/bag,1800Kg/pallet, 18000Kg/20ft container.

Application: Micro steel fiber is the material of ultra high performance concrete (UHPC), Reactive powder concrete (RPC) and slurry infiltrated concrete(SIFCON) , is well used in the project such as bank cash-box, strong-box, plant , water conservancy, foundation grouting, military project and blast protect panel and etc.


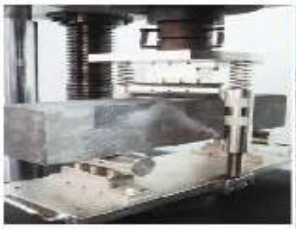


B.2 Data sheet of silica fume provided by the manufacturer

- Ferrosilicon
- Silica
- Power

SILICA

We offer both densed (500 - 700 Kg/m3) and undensed (200 - 350 Kg/m3) material. Due to a strong commitment to quality, the plant has strikt process control during the production process. Each lot leaving the plant has its own certicicate of analysis. The company is certified in accordance with EN 13263-1:2009 by Kontrollrådet, and is certified according to ISO 9001:2008 and ISO 14001:2004 by Det Norske Veritas.

The annual production of silica is 18.000 metric tons.

What is Silica?

The silica dust is initially a waste product from the production of FeSi. However, with today's cleaning technology, it has become a resource. New areas of application are constantly found, e.g. as an additive in concrete (increases the strength, prevents chlorine penetration and hence the corrotion of the reinforcing rods), and as a substitute for asbestos in wallboards. It is also used in cosmetics and contact lences. To strengthen and seal the concrete in the world's largest building, The Petronas Twin Towers in Kuala Lumpur, 4800 tons of silica was used, all delivered by Finnfjord AS. Silica has been named the most important new concrete product of the nineties, even though it has been in commercial use since the end of the seventies.

Chemical Properties

Silica is an ultra fine powder made up of nearly completely round particles with an average sice of 0,15 micrometer. The particles are approximately 100 times smaller than cement granes, and fill the gaps that arise in ordinary concrete mixtures.

Advantages

- improves longevity in general
- increases resistance against sulfates and chlorides
- contibutes to increased compressive, flexural and tensile strength
- reduces permeability and water break-through
- increases abrasion resistance
- eliminates bleeding

Chemical properties of silica manufactured by Finnfjord

Element	Limit	Typical values
SiO2	>85	90-93
CaO	<2,5	0,2-0,7
Na2O	<1.8	0,2-0,6
K2O	<2,5	1,0-1,3
Cl	<0,3	0,05-0,15
SO3	<1,5	0,25-0,35
MgO	<3,5	0,9-1,3
Fe2O3	<3,5	1,0-2,0
Al2O3	<2,2	0,4-0,9
Screen analysis, particles > 0,45µm	<40	0,8-2,2
Loss of ignition, (LOI)	<5	1,0-2,5
Free silicon <0,4	<0,4	0,04-0,15
Specific surface, BET	>15	20-24
Accelerated pozzolanic index	>95	120-135
Carbon is normally 0-0,2 % lower than LOI.		

B.3 Data sheet of superplasticizer provided by the manufacturer

Construction

Product Data Sheet
Edition 02, 2014
Version no. 01.20
Sika® ViscoCrete® -5930

Sika® ViscoCrete® -5930

Ultra High Performance Superplasticiser for Concrete

Product Description	**Sika® ViscoCrete® -5930** is a superplasticiser for concrete meeting the standard requirements of EN934-2 and ASTM C494/C494M type F & G. It is designed for use in hot climatic conditions.
Uses	**Sika® ViscoCrete® -5930** is suitable for the production of high performance and self-compacting concrete. **Sika® ViscoCrete® -5930** combines very high water reduction, with high workability retention and high strength development. **Sika® ViscoCrete® -5930** is used for the following types of concrete: ■ Ready Mix Concrete ■ High strength concrete ■ High durability concrete ■ Self-compacting concrete
Advantages	**Sika® ViscoCrete® -5930** is a multi-function product enabling the efficient dispersion of cementitious materials and control of the hydration process. Concrete properties are significantly enhanced with the use of Sika ViscoCrete® -5930: ■ Water reduction ■ Workability ■ Higher early and ultimate strength development ■ Better shrinkage and creep behaviour. ■ Significantly better durability characteristics **Sika® ViscoCrete® -5930** does not contain chloride or other, steel corrosion promoting ingredients, It may therefore be used without any restrictions for reinforced and prestressed concrete construction.
Product Data	
Form	
Appearance / Colour	Turbid liquid
Packaging	5 and 20 kg pails 200 kg drums Bulk Tanks packing available upon request
Storage	
Storage / Shelf Life	12 months from date of production if stored properly in unopened and undamaged, original sealed packaging, in dry temperatures between +5°C and +35°C. Protected from direct sunlight and frost.
Technical Data	
Basis	Aqueous solution of modified polycarboxylate
Density	Approximately 1.080 kg / litre
pH	8.0 ± 1.0
Chloride Content	Nil (EN934-2)

Construction

Application Details

Dosage / consumption	0.2 – 1.5% by weight of cement, depending on the concrete type
Addition	**Sika® ViscoCrete®-5930** can be added to the gauging water or simultaneously into the concrete mixer. To achieve maximum workability, mix for a minimum of 60 seconds. To avoid excess workability or potential segregation, add the remaining mix water as late in the mix cycle as possible.
Concrete Placing	The standard rules of good concrete practice (production, placing, curing) must be observed with **Sika® ViscoCrete® -5930** concrete in order to maximise production advantages.
Compatibility	**Sika® ViscoCrete® -5930** may be combined with many other Sika products to enhance a specific precast concrete application. Always conduct trial mixes to prove the performance of the precast concrete containing the combined products and contact Sika technical services department for assistance.

Safety Instructions

Safety Precautions	In contact with skin, wash off with soap & water. In contact with eyes or mucous membrane, rinse immediately with clean warm water and seek medical attention without delay.
Ecology	Residues of material must be removed according to local regulations. Fully cured material can be disposed of as household waste under agreement with the responsible local authorities.
Transport	Non-hazardous.
Toxicity	Non-Toxic under relevant health and safety codes.

Legal notes

Sika Egypt for Construction Chemicals
El Abour City
1st industrial zone (A)
Section # 5930 Block 13035,
Egypt

Tel:+202- 46100714/15/16/17/18
Fax :+202- 659300759
Mob :+2012- 3908822/55
www.sika.com.eg

B.4 Data sheet of epoxy provided by the manufacturer

Quickmast 108

Epoxy bonding agent for concrete

Description

Quickmast 108 is a slow cure, solvent-free epoxy resin bonding agent that is supplied in pre-weighted two component packs which when mixed together produce a medium viscosity epoxy adhesive.

Quickmast 108 can be easily spread over old concrete or cementitious substrates to permanently bond freshly casted concrete or new mortars.

Applications

Quickmast 108 is a permanent epoxy adhesive for bonding fresh wet concrete/cementitious material to old concrete/cementitious surfaces, which is suitable for internal and external application.

Advantages

- High bond strength.
- Moisture tolerant; can be applied to damp surfaces.
- Slow cure, allows more time for subsequent works such as fixing steel reinforcements and erecting shutter.
- High strength.

Standards

Quickmast 108 complies with ASTM C881, Type II, Grade 2, Class C.

Method of Use

Substrate Preparation

The Substrate should be sound, clean and free from contamination. Surface Laitance should be removed by acid etching or light grit blasting.

Oil, grease, and fat deposit should be removed by using either appropriate degreaser or steam cleaning. Weak or deteriorated concrete should be removed by scabbling, chipping or grit blasting.

Mixing

The base and the hardener should be mixed separately before mixing together to disperse any settlement.

Technical Properties:

Colour:	Green for mixed material
Mixed density:	1.2 ± 0.1 g/cm³
Compressive yield strength: ASTM D695	≥ 50 MPa @ 7 days
Bond strength by slant shear: (old/new concrete) ASTM C882	≥ 10 MPa @ 14 days moist cure
Water absorption: ASTM D570	≤ 0.2%
Full cure:	7 days @ 25°C 5 days @ 40°C
Typical minimum overlay time*:	2 hr @ 25°C 1 hr @ 40°C
Typical maximum overlay time*:	9 hr @ 25°C 5 hr @ 40°C
Gel time: ASTM C881	6 hr @25°C
Viscosity: ASTM D2393	40 ± 10 poise @ 25°C (medium viscosity)
VOC: ASTM D2369	≤ 10 g/ltr

**Minimum and maximum overlaying times depend on the ambient weathering conditions. In general the new concrete/cementitious material should be only applied over tacky layer of Quickmast 108.*

Carefully transfer the entire contents of the hardener container into the base component container and thoroughly mix using slow speed drill with appropriate mixing paddle for 3 minutes until uniformity is obtained. Do not attempt to mix partially nor add any thinning materials.

Quickmast 108 is designed to have an overlaying time of 9 hours at 25˚C and 5 hours at 40˚C. This should allow for subsequent works such as steel reinforcement fixation and shutter erection.

Quickmast 108

Application

Quickmast 108 should be applied immediately after mixing using a short haired paint brush.

The material should be painted evenly across the whole surface and left until it becomes tacky (typically 2 hours at 25˚C and 1 hour at 40˚C) before the new concrete, screed or mortar is placed.

Care should be taken to apply the new concrete, screed or mortar within the overlay time specified in Technical Properties.

Failure to do so will have an adverse result and the material will form a de-bonding plane rather than a bonding coat.

Minimum application temperature is 5°C while temperatures exceeding 35°C will decrease pot life and setting time.

Notes:

- If temperature of the material is less than 12°C, it is needed to elevate their temperature to 25°C before the application.
- And if the ambient and the substrate temperature is less than 5°C, don't use the material.
- Also, at high temperatures (35°C and above), cooling the material is needed before the application. And try not to make the application in the middle of the day or under direct sunlight.

Cleaning

All tools should be cleaned immediately after finishing by DCP solvent. Hardened materials should be cleaned mechanically.

Packaging

Quickmast 108 is available in 1 and 5 kg packs.

Coverage

3.0 – 3.5 m^2/kg.

Storage

Quickmast 108 has a shelf life of 12 months from date of manufacture if stored at temperatures between 5°C and 35°C.

If these conditions are exceeded, DCP Technical Department should be contacted for advice.

Cautions

Health and Safety

Quickmast 108 should not come in contact with skin or eyes.

Rubber gloves and eye protection should be worn all the time. The use of barrier cream is recommended on exposed areas of the skin.

In case of contact with eye, rinse with clean water and seek medical consultation.

For further information refer to the Material Safety Data Sheet.

Fire

Quickmast 108 is nonflammable.

More from Don Construction Products

A wide range of construction chemical products are manufactured by DCP which include:

- Concrete admixtures.
- Surface treatments
- Grouts and anchors.
- Concrete repair.
- Flooring systems.
- Protective coatings.
- Sealants.
- Waterproofing.
- Adhesives.
- Tile adhesives and grouts.
- Building products.
- Structural strengthening.

B.5 Properties of CFRP sheet and Epoxy

BUILDING TRUST

PRODUCT DATA SHEET

SikaWrap®-300 C

WOVEN UNIDIRECTIONAL CARBON FIBRE FABRIC, DESIGNED FOR STRUCTURAL STRENGTHENING APPLICATIONS AS PART OF THE SIKA® STRENGTHENING SYSTEM

DESCRIPTION

SikaWrap®-300 C is a unidirectional woven carbon fibre fabric with mid-range strengths, designed for installation using the dry or wet application process. Suitable for use in hot and tropical climatic conditions.

USES

SikaWrap®-300 C may only be used by experienced professionals.
Structural strengthening of reinforced concrete, masonry, brickwork and timber elements or structures, to increase flexural and shear loading capacity for:

- Improved seismic performance of masonry walls
- Replacing missing steel reinforcement
- Increasing the strength and ductility of columns
- Increasing the loading capacity of structural elements
- Enabling changes in use / alterations and refurbishment
- Correcting structural design and / or construction defects
- Increasing resistance to seismic movement
- Improving service life and durability
- Structural upgrading to comply with current standards

CHARACTERISTICS / ADVANTAGES

- Multifunctional fabric for use in many different strengthening applications
- Flexible and accommodating of different surface planes and geometry (beams, columns, chimneys, piles, walls, soffits, silos etc.)
- Low density for minimal additional weight
- Extremely cost effective in comparison to traditional strengthening techniques

APPROVALS / STANDARDS

- Poland: Technical Approval ITB AT-15-5604/2011: Zestaw wyrobów Sika CarboDur do wzmacniania i napraw konstrukcji betonowych.
- Poland: Technical Approval IBDiM Nr AT/2008-03-0336/1, Płaskowniki. pręty, kształtki i maty kompozytowe do wzmacniania betonu o nazwie handlowej: Zestaw materiałów Sika CarboDur® do wzmacniania konstrukcji obiektów mostowych.
- USA: ACI 440.2R-08, Guide for the Design and construction of Externally Bonded FRP Systems for strengthening concrete structures, July 2008.
- UK: Concrete Society Technical Report No. 55, Design guidance for strengthening concrete structures using fibre composite material, 2012.

PRODUCT INFORMATION

Construction	Fibre orientation	0° (unidirectional)
	Warp	Black carbon fibres 99 %
	Weft	White thermoplastic heat-set fibres 1 %
Fibre Type	Selected mid-range strength carbon fibres	
Packaging	**Fabric length per roll**	**Fabric width**
	≥ 100 m	500 mm
Shelf life	24 months from date of production	

Storage conditions	Store in undamaged, original sealed packaging, in dry conditions at temperatures between +5 °C and +35 °C. Protect from direct sunlight.	
Dry Fibre Density	1.82 g/cm³	
Dry Fibre Thickness	0.167 mm (based on fibre content)	
Area Density	304 g/m² ± 10 g/m² (carbon fibres only)	
Dry Fibre Tensile Strength	4 000 N/mm²	(ISO 10618)
Dry Fibre Modulus of Elasticity in Tension	230 000 N/mm²	(ISO 10618)
Dry Fibre Elongation at Break	1.7 %	(ISO 10618)

TECHNICAL INFORMATION

Laminate Nominal Thickness	0.167 mm		
Laminate Nominal Cross Section	167 mm² per m width		
Laminate Tensile Strength	**Average** 3 500 N/mm²	**Characteristic** 3 200 kN/mm²	(EN 2561*) (ASTM D 3039*)
Laminate Modulus of Elasticity in Tension	**Average** 225 kN/mm² **Average** 220 kN/mm²	**Characteristic** 220 kN/mm² **Characteristic** 210 kN/mm²	(EN 2561*) (ASTM D 3039*)
	* modification: sample with 50 mm Values in the longitudinal direction of the fibres Single layer, minimum 27 samples per test series		
Laminate Elongation at Break in Tension	1.56 % 1.59 %		(EN 2561) (ASTM D 3039)
Tensile Resistance	**Average** 585 N/mm	**Characterstic** 534 N/mm	(EN 2561) (ASTM D 3039)
Tensile Stiffness	**Average** 37.6 MN/m 37.6 kN/m per ‰ elongation **Average** 36.7 MN/m 36.7 kN/m per ‰ elongation	**Characteristic** 36.7 MN/m 36.7 kN/m per ‰ elongation **Characteristic** 35.1 MN/m 35.1 kN/m per ‰ elongation	(EN 2561) (ASTM D 3039)

SYSTEMS

System Structure

The system build-up and configuration as described must be fully complied with and may not be changed.

Concrete substrate adhesive primer	Sikadur®-330
Impregnating / laminating resin	Sikadur®-330 or Sikadur®-300
Structural strengthening fabric	SikaWrap®-300 C

For detailed information on Sikadur®-330 or Sikadur®-300, together with the resin and fabric application details, please refer to the Sikadur®-330 or Sikadur®-300 Product Data Sheet and the relevant Method Statement.

APPLICATION INFORMATION

Consumption

Dry application with Sikadur®-330	
First layer including primer layer	1.0 - 1.5 kg/m²
Following layers	0.8 kg/m²
Wet application with Sikadur®-300	
Primer layer	0.4 - 0.6 kg/m²
Fabric layers	0.6 kg/m²

Please also refer to the relevant Method Statement for further information.

APPLICATION INSTRUCTIONS

SUBSTRATE QUALITY

Minimal substrate tensile strength: 1.0 N/mm² or as specified in the strengthening design.
Please also refer to the relevant Method Statement or further information.

SUBSTRATE PREPARATION

Concrete must be cleaned and prepared to achieve a laitance and contaminant free, open textured surface.
Please also refer to the relevant Method Statement for further information.

APPLICATION METHOD / TOOLS

The fabric can be cut with special scissors or a Stanley knife (razor knife / box-cutter knife). Never fold the fabric.
SikaWrap®-300 C is applied using the dry or wet application process.
Please refer to the relevant Method Statement for details on the impregnating / laminating procedure

LIMITATIONS

- SikaWrap®-300 C shall only be applied by trained and experienced professionals.
- A specialist structural engineer must be consulted for any structural strengthening design calculation.
- SikaWrap®-300 C fabric is coated to ensure maximum bond and durability with the Sikadur® adhesives / impregnating / laminating resins. To maintain and ensure full system compatibility, do not interchange different system components.
- SikaWrap®-300 C can be over coated with a cementitious overlay or other coatings for aesthetic and / or protective purposes. The over coating system selection is dependent on the exposure and the project specific requirements. For additional UV light protection in exposed areas use Sikagard®-550 W Elastic (G) or Sikagard®-680 SG.
- Please refer to the Method Statement of SikaWrap® manual dry application, SikaWrap® manual wet application or SikaWrap® machine wet application for further information, guidelines and limitations.

BASIS OF PRODUCT DATA

All technical data stated in this Data Sheet are based on laboratory tests. Actual measured data may vary due to circumstances beyond our control.

LOCAL RESTRICTIONS

Please note that as a result of specific local regulations the declared data and recommended uses for this product may vary from country to country. Please consult the local Product Data Sheet for the exact product data and uses.

ECOLOGY, HEALTH AND SAFETY

This product is an article as defined in article 3 of regulation (EC) No 1907/2006 (REACH). It contains no substances which are intended to be released from the article under normal or reasonably foreseeable conditions of use. A safety data sheet following article 31 of the same regulation is not needed to bring the product to the market, to transport or to use it. For safe use follow the instructions given in this product data sheet. Based on our current knowledge, this product does not contain SVHC (substances of very high concern) as listed in Annex XIV of the REACH regulation or on the candidate list published by the European Chemicals Agency in concentrations above 0.1 % (w/w)

LEGAL NOTES

The information, and, in particular, the recommendations relating to the application and end-use of Sika products, are given in good faith based on Sika's current knowledge and experience of the products when properly stored, handled and applied under normal conditions in accordance with Sika's recommendations. In practice, the differences in materials, substrates and actual site conditions are such that no warranty in respect of merchantability or of fitness for a particular purpose, nor any liability arising out of any legal relationship whatsoever, can be inferred either from this information, or from any written recommendations, or from any other advice offered. The user of the product must test the product's suitability for the intended application and purpose. Sika reserves the right to change the properties of its products. The proprietary rights of third parties must be observed. All orders are accepted subject to our current terms of sale and delivery. Users must always refer to the most recent issue of the local Product Data Sheet for the product concerned, copies of which will be supplied on request.

SIKA NORTHERN GULF
Bahrain / Qatar / Kuwait
Tel: +973 177 38188
sika.gulf@bh.sika.com
gcc.sika.com

SIKA SOUTHERN GULF
UAE / Oman / SIC
Tel: +971 4 439 8200
info@ae.sika.com
gcc.sika.com

SIKA SAUDI ARABIA
Riyadh / Jeddah / Dammam
Tel: +966 11 217 6532
info@sa.sika.com
gcc.sika.com

Appendix C

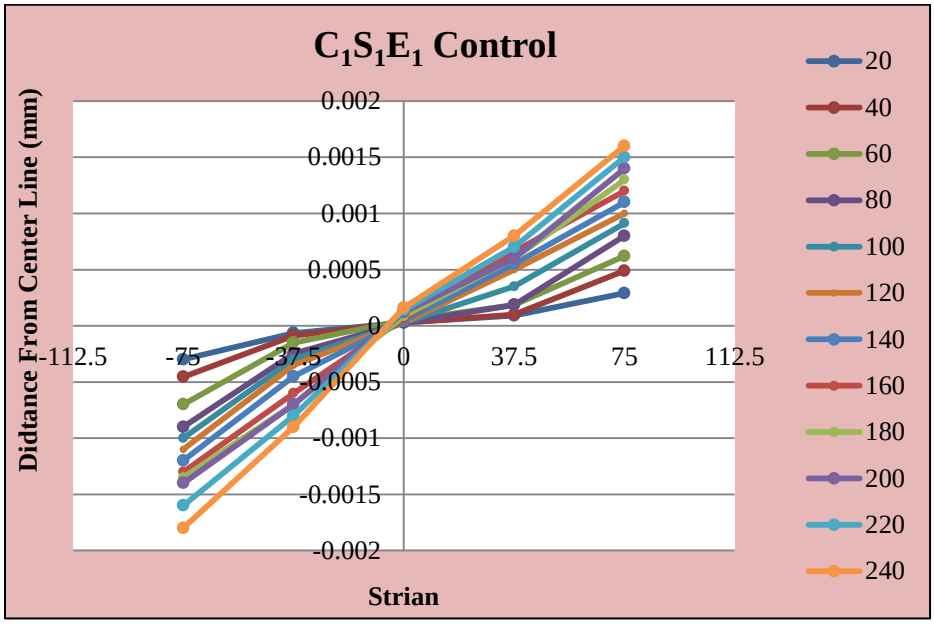

Figure (C-1): Concrete Strain Distribution for Columns

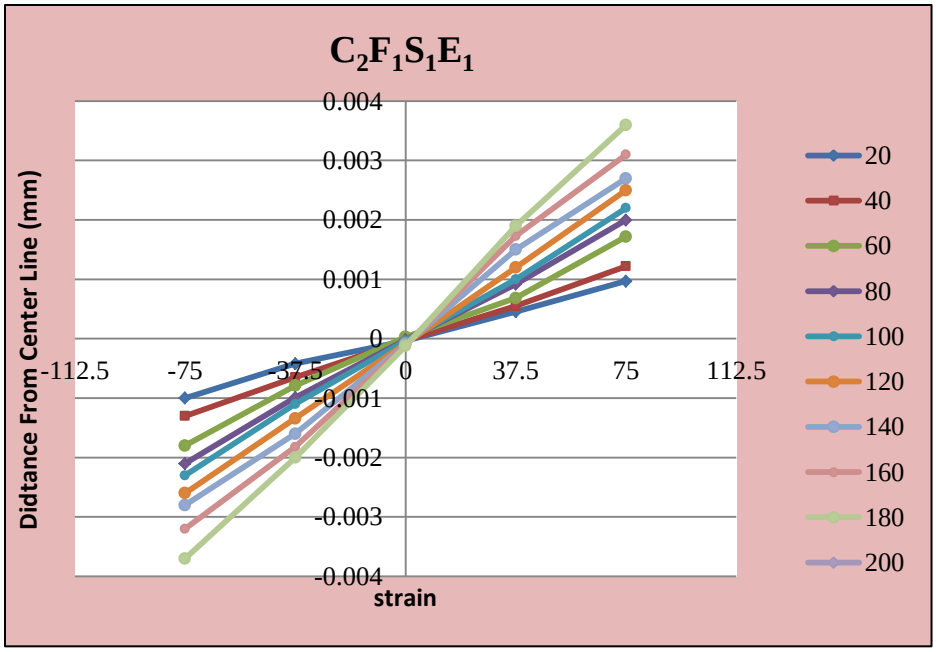

Figure (C-2): Concrete Strain Distribution for Columns

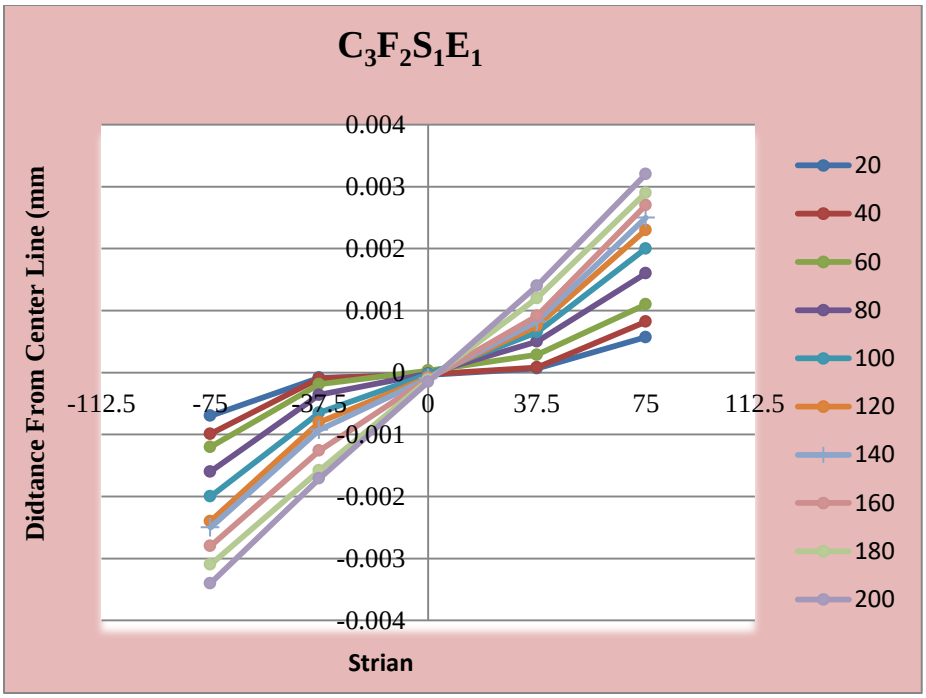

Figure (C-3): Concrete Strain Distribution for Columns

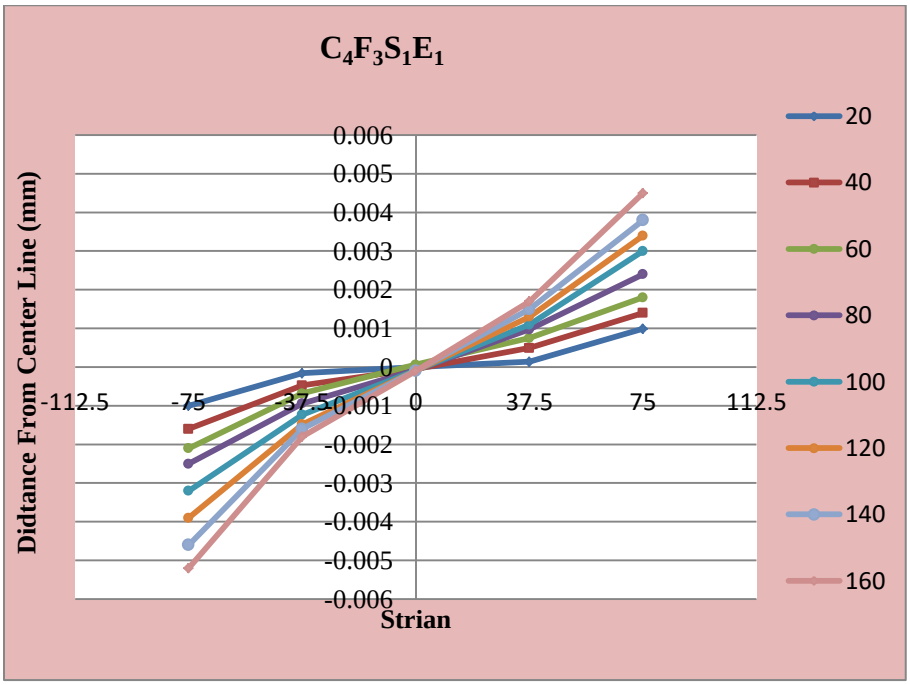

Figure (C-4): Concrete Strain Distribution for Columns

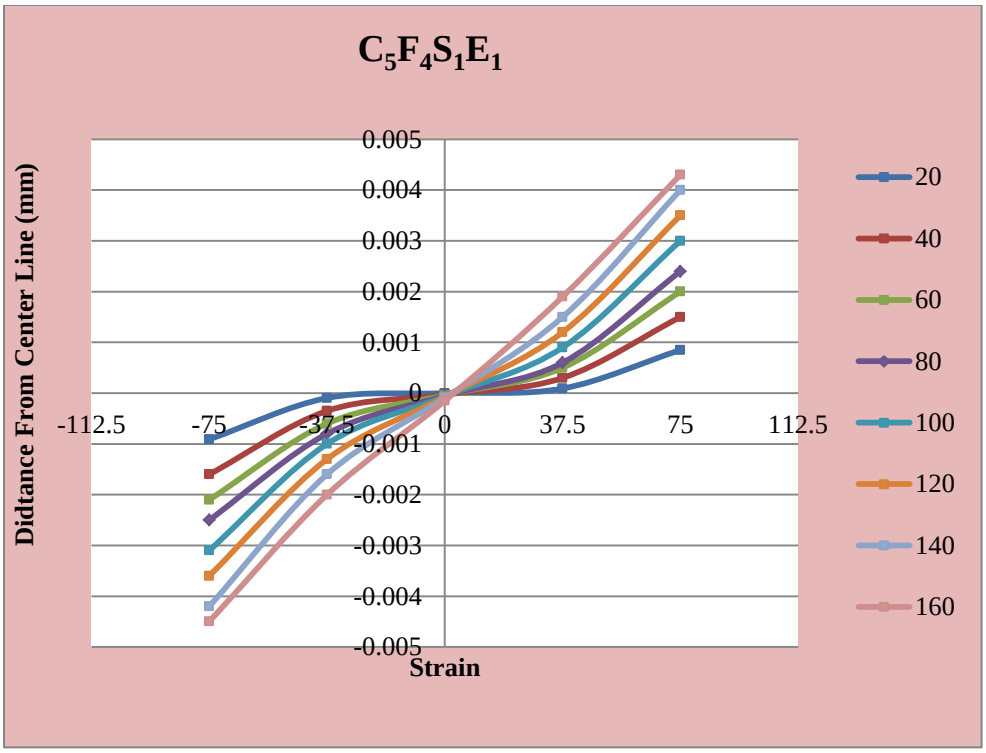

Figure (C-5): Concrete Strain Distribution for Column

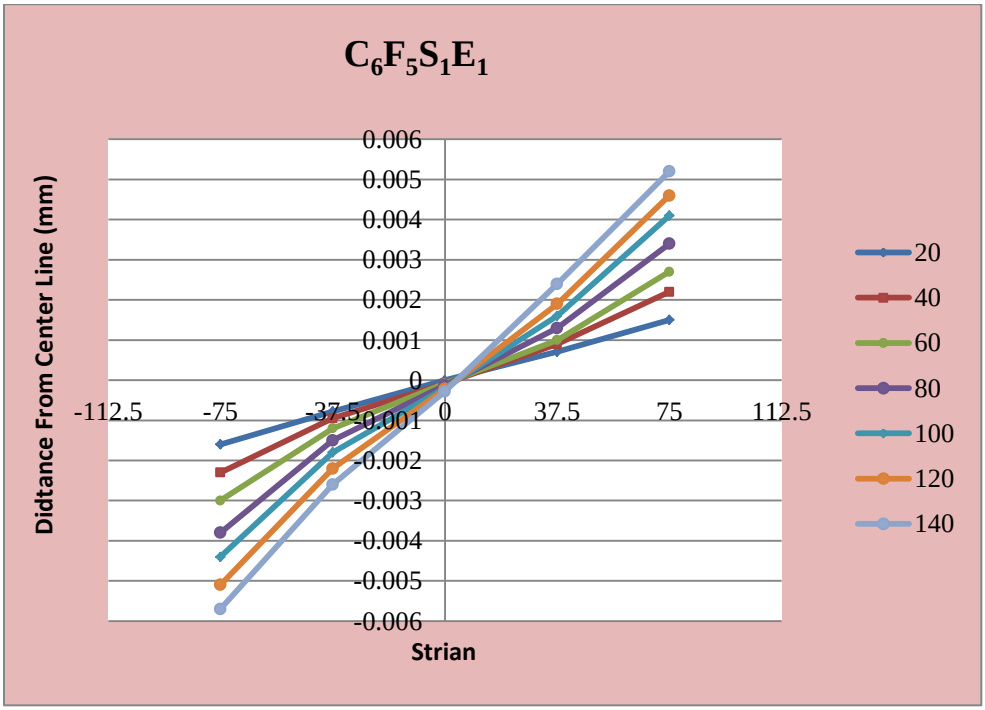

Figure (C-6): Concrete Strain Distribution for Column

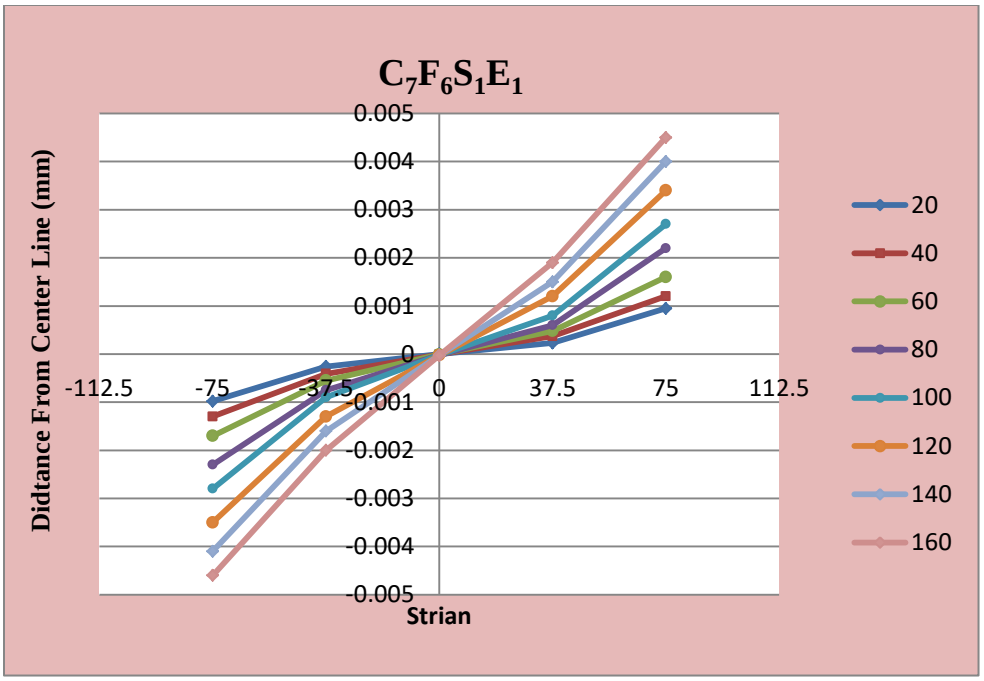

Figure (C-7): Concrete Strain Distribution for Column

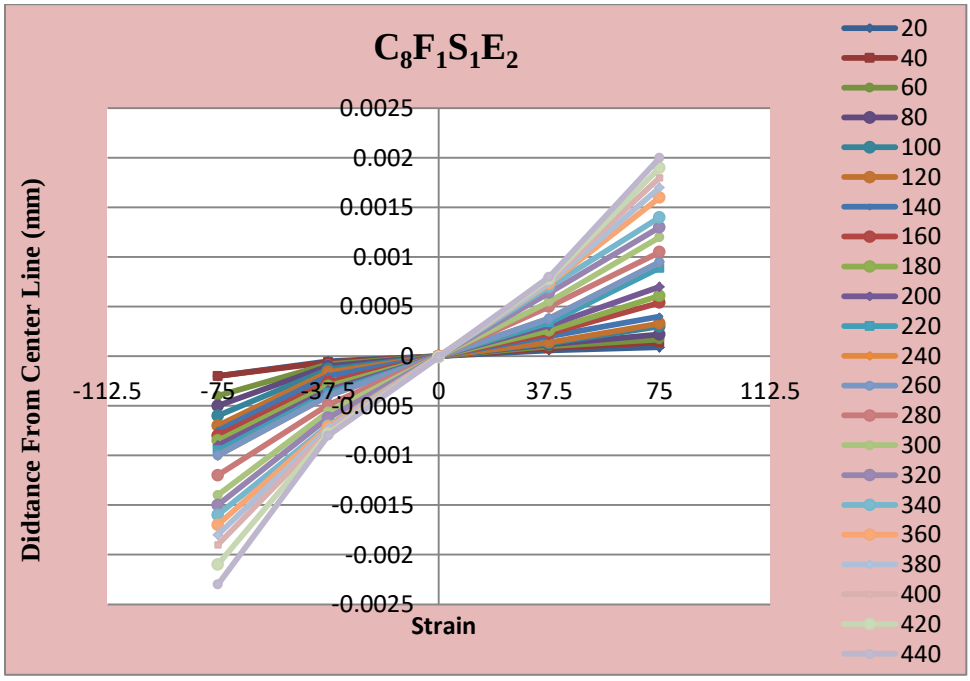

Figure (C-8): Concrete Strain Distribution for Column

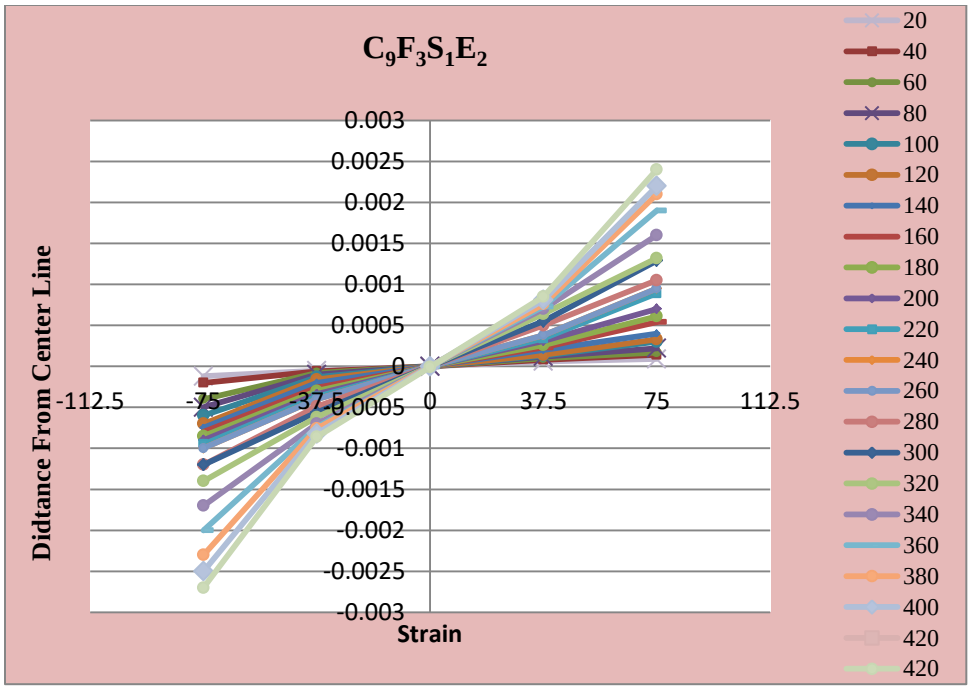

Figure (C-9): Concrete Strain Distribution for Column

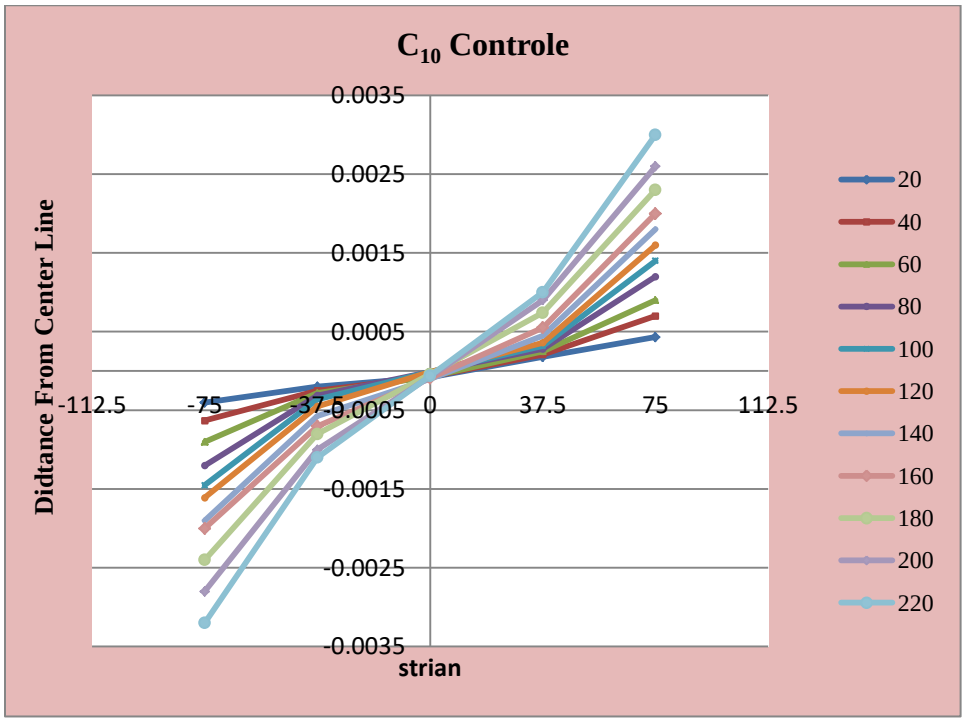

Figure (C-10): Concrete Strain Distribution for Column

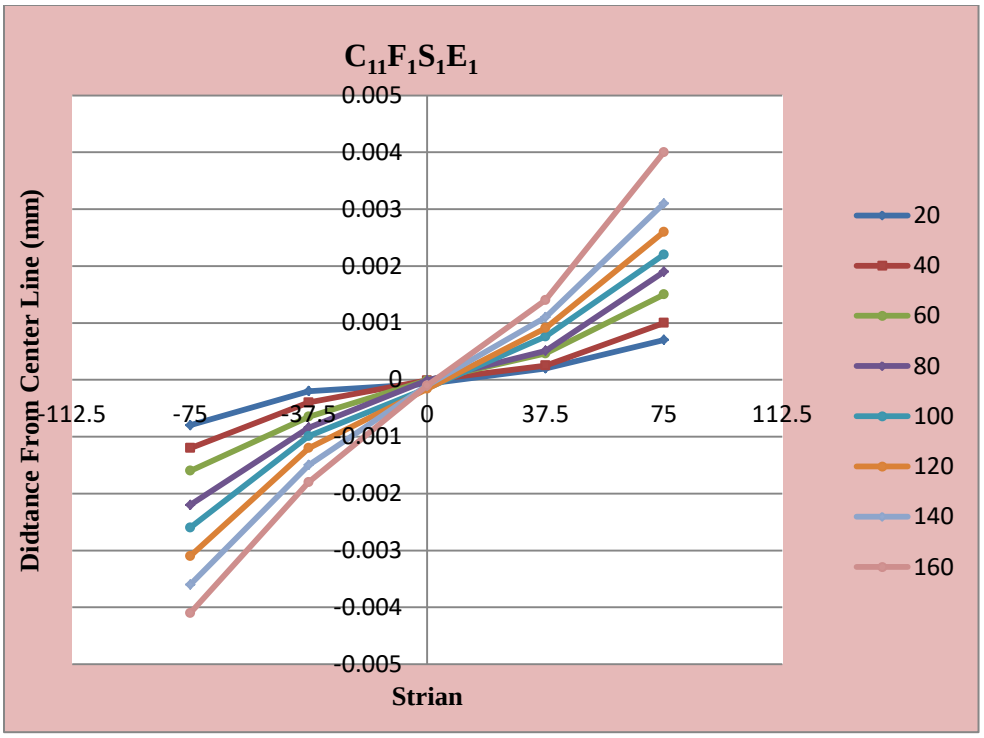

Figure (C-11): Concrete Strain Distribution for Column

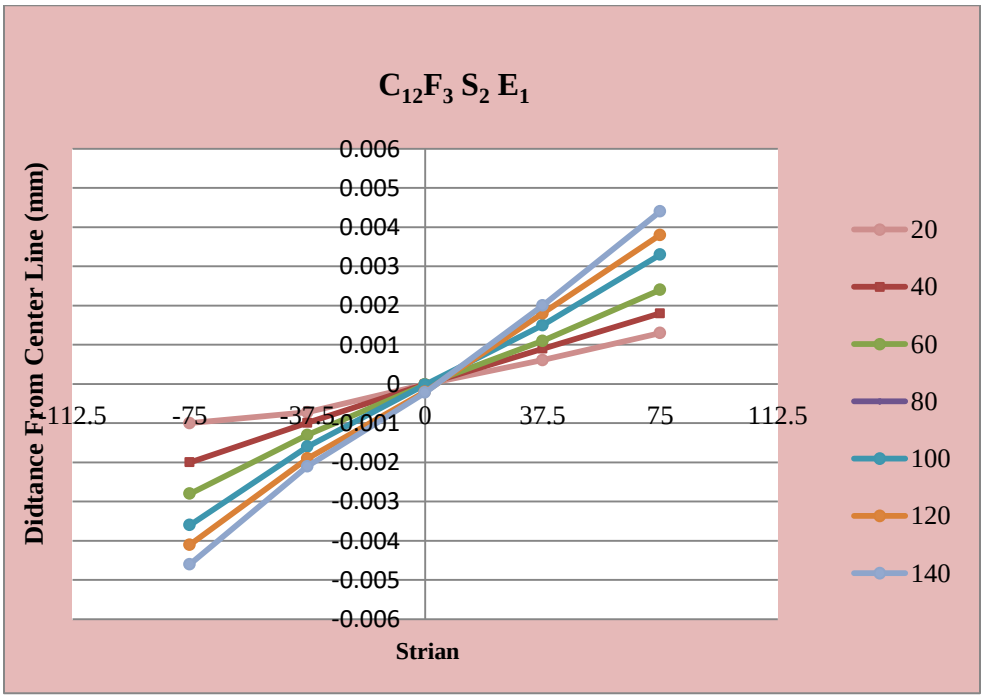

Figure (C-12): Concrete Strain Distribution for Column

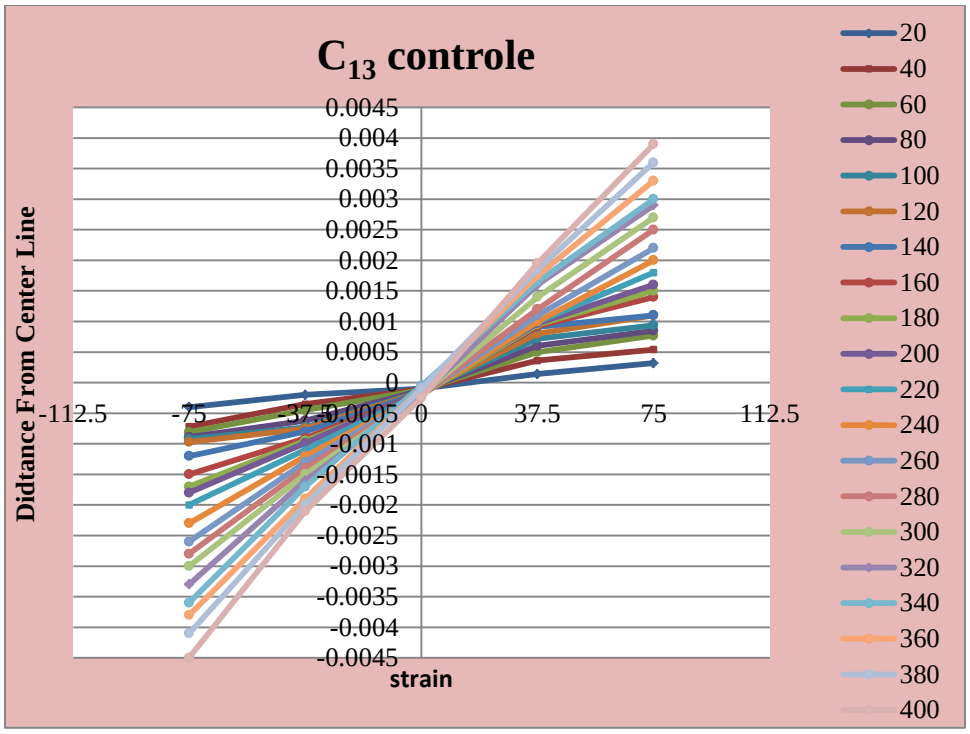

Figure (C-13): Concrete Strain Distribution for Column

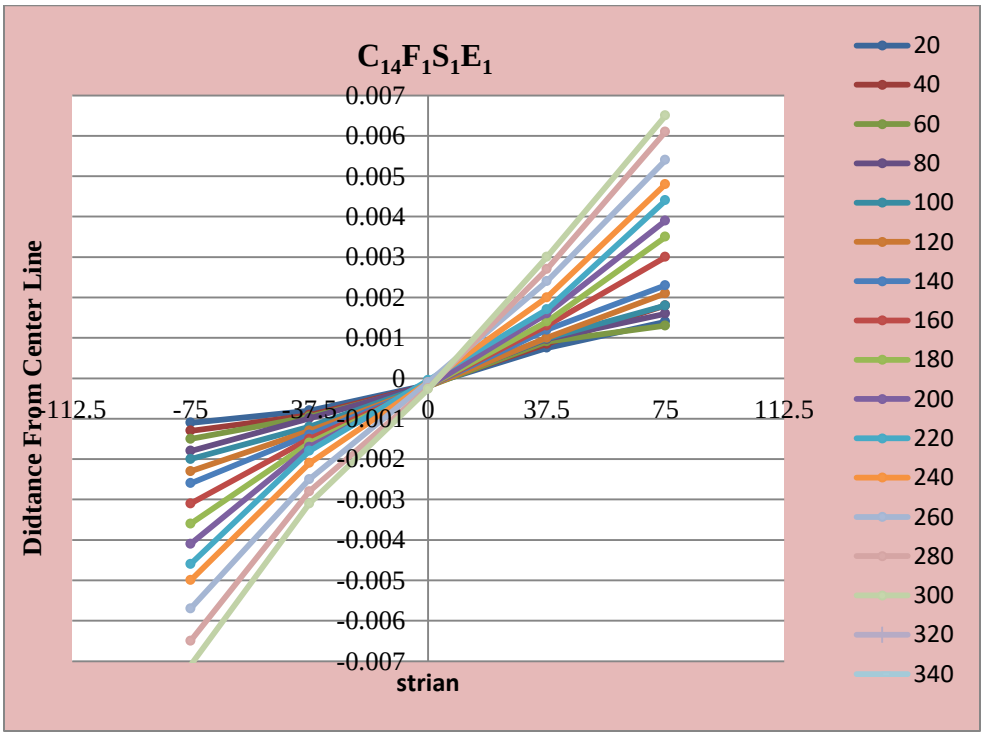

Figure (C-14): Concrete Strain Distribution for Column

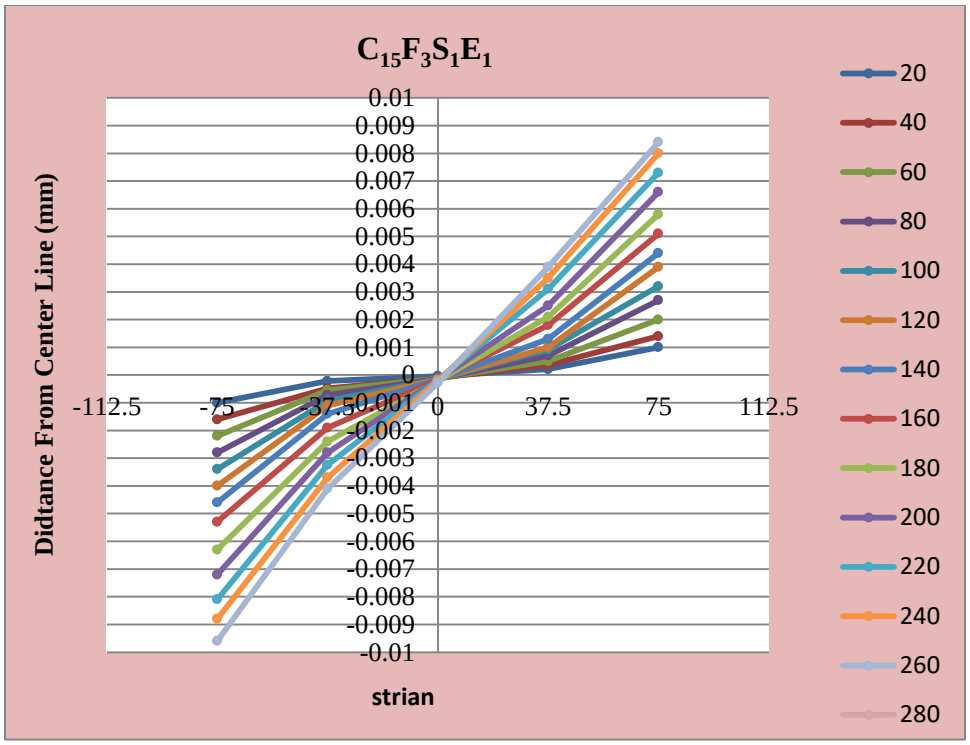

Figure (C-15): Concrete Strain Distribution for Column

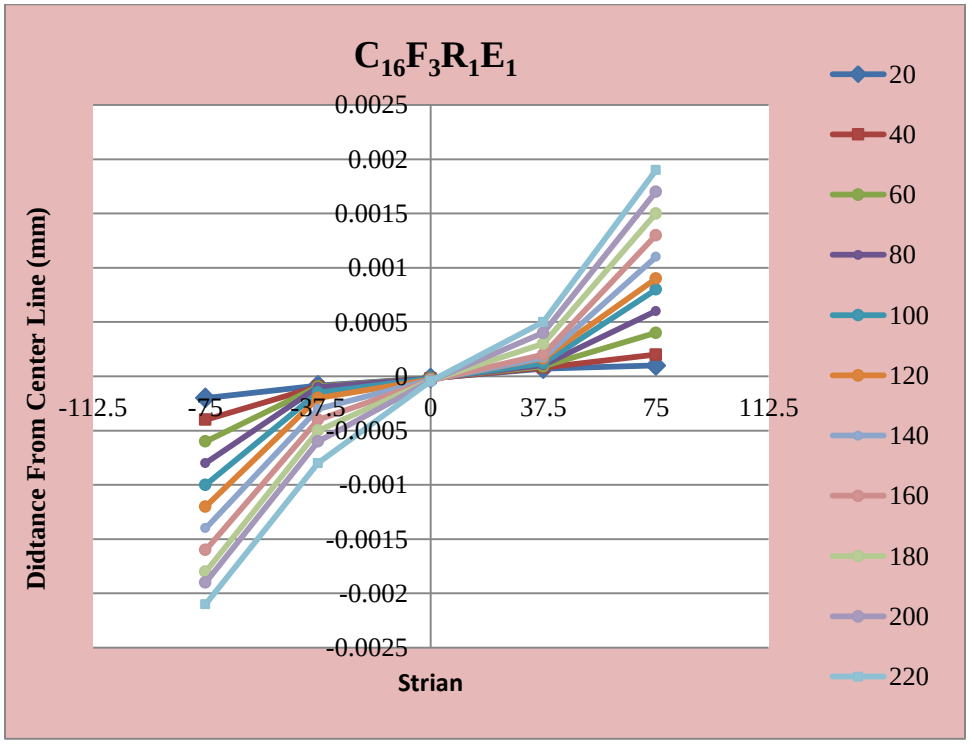

Figure (C-16): Concrete Strain Distribution for Column

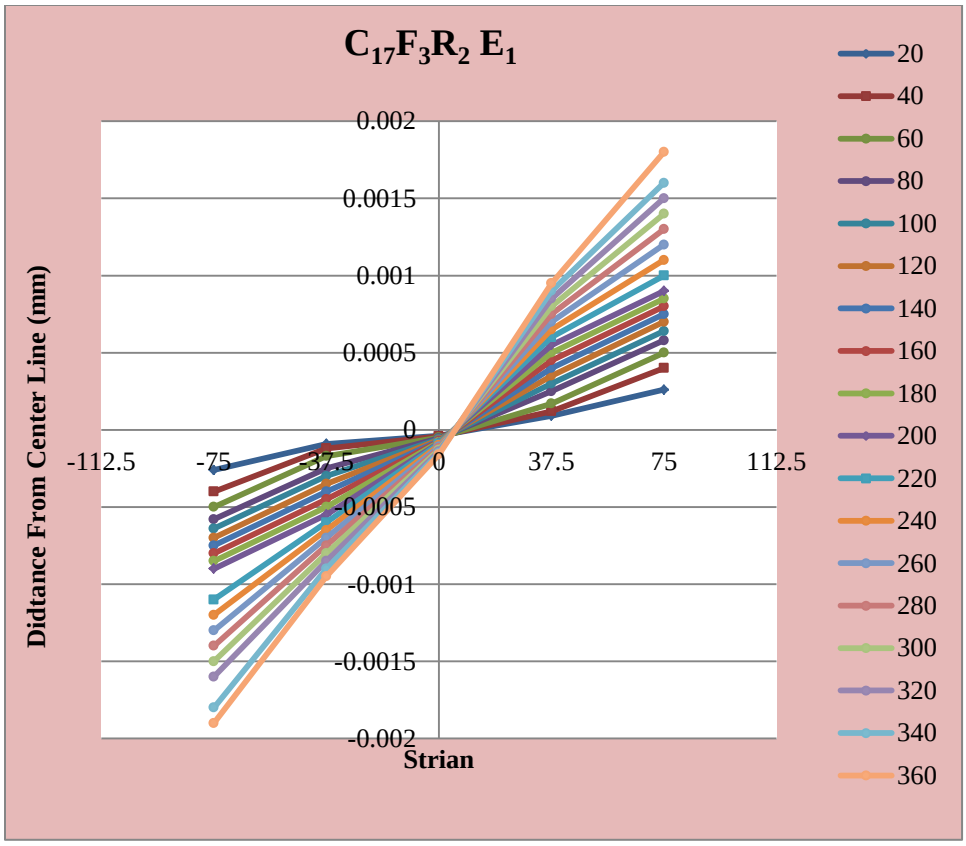

Figure (C-17): Concrete Strain Distribution for Column

Appendix D

Modelling of Material Properties in FEA

D.1Introduction

ABAQUS is a popular civil engineering practice's complex finite element (FE) package. It is specifically used to model reinforced concrete structures.

The Concrete Damaged Plasticity (CDP) model is one of the concrete models included in ABAQUS. This model takes into account both tensile cracking and compressive crushing as possible failure modes for concrete. All of the modeling assumptions and definitions of element properties are outlined below, along with a brief description of concrete and steel reinforcement modeling.

D.2 Material Model Properties

D.2.1 Plasticity of concrete damage (CDP)

All structural types of reinforced or unreinforced concrete as well as other quasi-brittle materials subjected to monotonic or cyclic stresses can be modeled using concrete damaged plasticity (CDP). The multi-axial behavior of concrete in the damaged plasticity model is governed by a yield surface, and this model is based on a coupled damage plasticity theory, which proposed **(Lubliner et. al., 1989*)***, as shown in **Figure (D-1).** This model assumes that concrete's tensile cracking and compressive crushing are the two primary failure mechanisms. This model also takes into account material degradation for both tension and compression behavior.

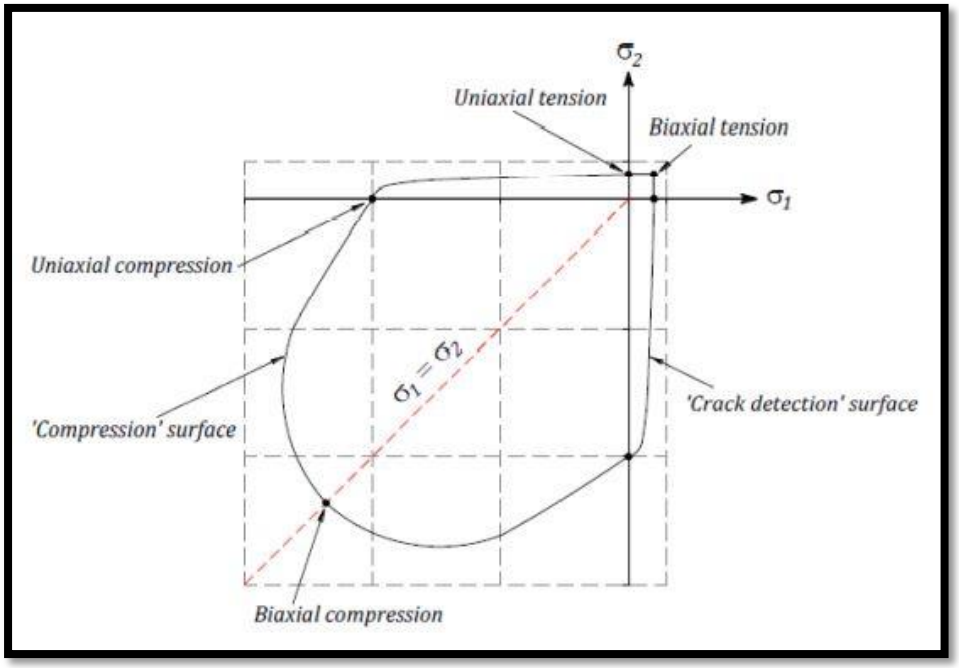

Figure (D-1): Yield surface in plane stress reproduced from ***(Lubliner et. al., 1989)***.

D.2.2 Uniaxial and Multi-axial Behavior

Under uniaxial tension, as can be seen in **Figure (D-2)**, the stress increases with a linear elastic relationship with strain up to the ultimate tensile strength (f_t), and then micro-cracks from microscopically with a tension softening response. There are three different methods to define tension softening response in ABAQUS: stress-strain, stress-displacement, or by use of fracture energy **(Hibbitt, et.al, 2010).**

Additionally, stress-strain has a linear elastic relationship until initial yield (f_{co}) under uniaxial compression. The behavior becomes nonlinear after losing stiffness due to bond failure between the aggregates and the cement paste. The plastic response is characterized by stress hardening and strain softening at stresses greater than ultimate strength. To put it another way, compressive strain rises while compressive stress decreases. **Figure (D-3)** shows how concrete compresses in one direction.

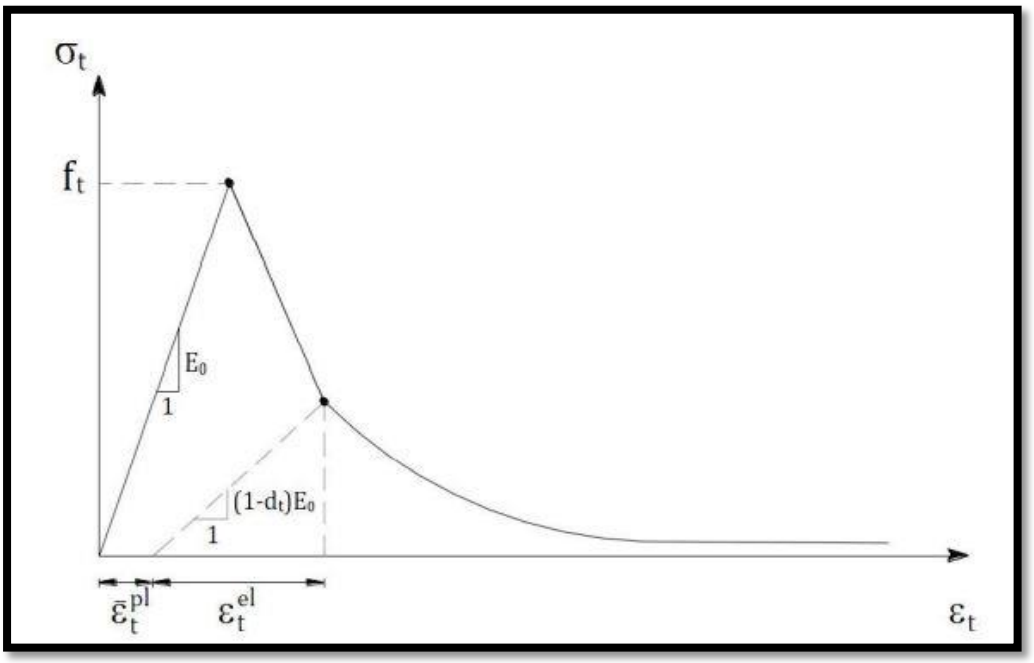

Figure (D-2) Uniaxial tensile behavior of concrete ***(Hibbitt, et.al, 2010).***

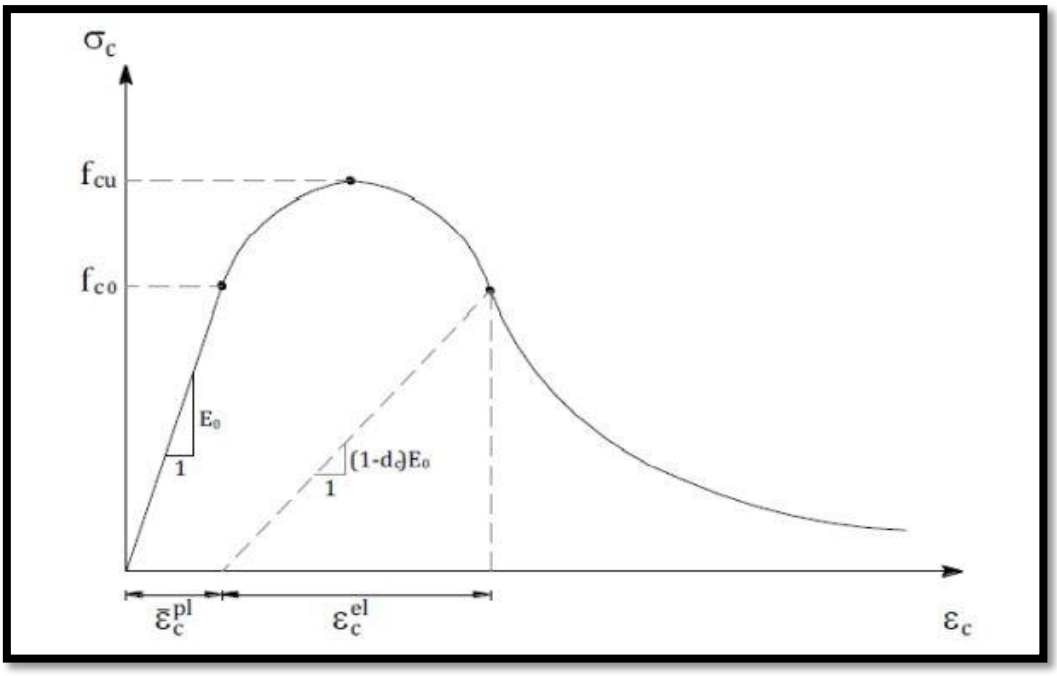

Figure (D-3): Uniaxial compressive behavior of concrete reproduced from **(Hibbitt, et.al, 2010).**

D.3 Concrete Damaged Plasticity Definitions

Different input data, which should be defined in concrete damaged plasticity, are:

Ψ: is the dilation angle, which should be defined in the (p-q) plane in order to

calculate the plastic flow potential's inclination at high confining pressures, as depicted in Figure C-4. The dilation angle decreases at higher levels of confinement stress and plastic strain. It has a value of equal magnitude (56,3o) and a value close to zero. Lower values indicate a more brittle behavior, while higher values indicate a more ductile behavior***(Malm ,2006)*** says that the effect of the dilation angle is between $30^o \leq \psi \leq 40^o$.

ϵ: is the potential eccentricity of the flow. The range within which the plastic potential function approaches the asymptote is represented in Figure (C-4) by a small positive number. The dilation angle is nearly constant over a wide range of confining pressure when the default value in ABAQUS is (0.1). With a lower confining pressure at a higher value of (), the dilation angle grows more quickly. Due to the extremely tight flow potential curvature at the point of intersection with the (p-axis), very small values of in comparison to the default value may result in convergence issues in situations with low confining pressure (***Malm, 2006***).

F_{b0}/f_{c0}: is the proportion of initial equibiaxial compressive yield stress and initial uniaxial compressive yield stress. The default value in ABAQUS is (1.16).

K: is the ratio of the second stress invariant in the tensile meridian to compressive meridian for any defined value of the pressure invariant at initial yield. It is used to define the multi-axial behavior of concrete and is ($0.5<Kc\leq1$). The default value in ABAQUS is (0.667).

μ: is the viscosity parameter. According to ***(Malm, 2006)*** $\mu=10^{-7}$ is recommended because in comparison with characteristic time increment it should be small.

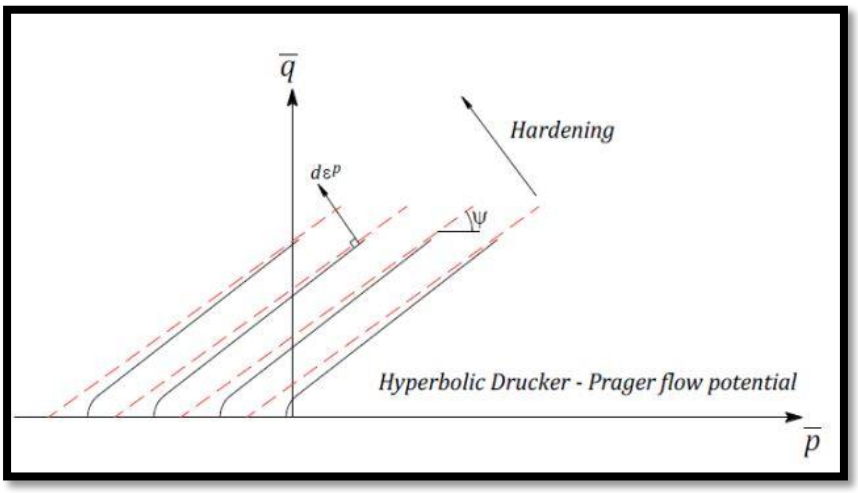

Figure (D-4): Hyperbolic plastic flow rule reproduced from ***(Malm, 2006)***.

D.4 Concrete Model Properties

D.4.1Uniaxial Compressive behavior

- **Normal Concreter**

After the elastic regime, the uniaxial compressive stress-strain relationship for plain concrete must be defined. Both hardening and strain softening ranges, according to ABAQUS, are described in terms of compressive stress, σc, and elastic strain, $\epsilon\sim$in, which is provided as follows:

$$\epsilon_c^{\sim in} = \epsilon_c - \epsilon_{0c}^{el} \qquad \text{D.1}$$

where $\epsilon el = \sigma c/Ecm$, Ecm is the initial modulus of elasticity, and εc = total compression strain.

$$\sigma c / \ fcm = (kn - n\ 2)/\ (1 + (k - 2)) \qquad \text{D.2}$$

Where:

$$n = ec\ /ec1 \qquad \text{D.3}$$

$$k = 1.05\ Ecm \times |ec1|/fcm \qquad \text{D.4}$$

It is important to point out that Equation D.6 holds true for $0 < |\epsilon c1| < |\epsilon cu1|$, where $\epsilon cu1$ is the nominal ultimate strain (0.0035), $\epsilon c1$ is the strain at peak stress and fcm is the mean compressive strength.

- **Reactive powder concrete**

Mechanical characteristics of RPC are different from the normal concrete and high compressive strength concrete under loads due to very high strength in compressive load as well as tensile load of RPC. Many studies were carried out to predict the behavior of RPC, but very few researches described the uniaxial behavior of RPC. (**Schmidt & Fehling, 2005**).

RPC under uniaxial compression was modeled in form of elastic–plastic model as illustrated in figure D.5. The input data includes: the concrete compressive strength; fcu, modulus of elasticity; Ec, Poisson's ratio; vc, stress-plastic strain relationship.

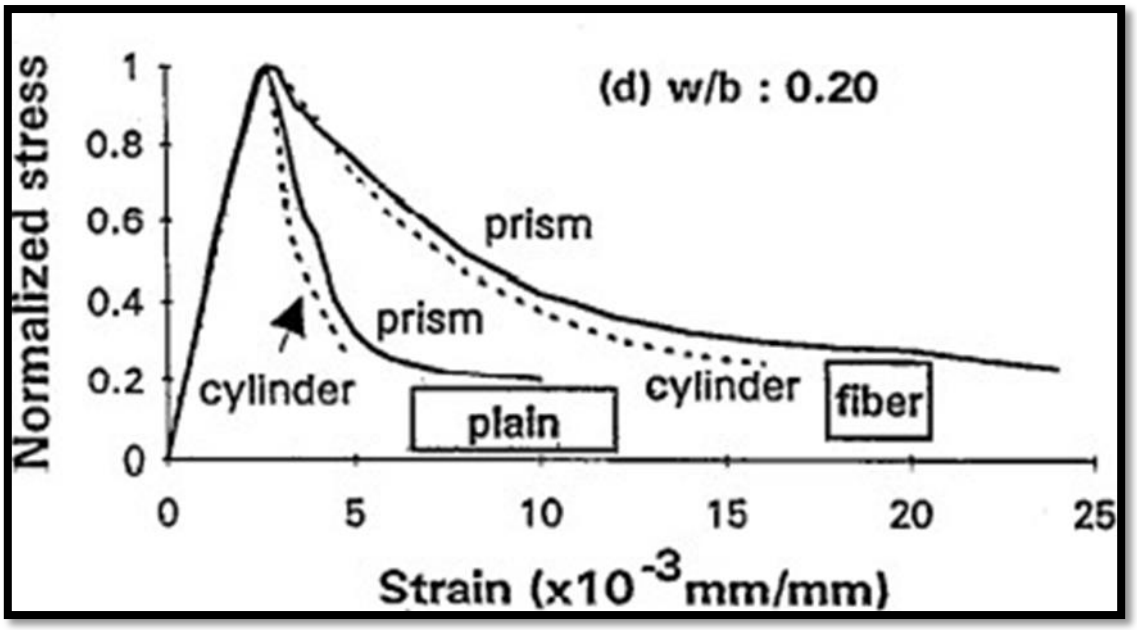

*

Figure D.5 :+Stress-Strain Curves for Both Horizontally and Vertically Cast Prisms with and without Fiber Under Uniaxial Compression (**Prem et.al.,2012**)

D.5 Reinforcement Model Properties

D.5.1 Steel Reinforcement

The required input parameters for material definition of steel bars, includes density, elastic and plastic behavior. Elastic behavior of steel material is defined by specifying Young's modulus (Es) and Poisson's ratio (v) of which typical values are 200000 MPa and 0.3, respectively. Plastic behavior is defined in a tabular form, included yield stress and corresponding plastic strain.

D.5.2 CFRT

The CFRP composite sheet was modeled as an orthotropic material and laminates method , **Table (D-1**) the input data for concrete plasticity properties and CFRP material properties. It has linear behavior to the end of failure. The expression below represents the stress-strain of CFRP.

$$\begin{bmatrix}\sigma_1\\ \sigma_2\\ \sigma_3\\ \tau_{12}\\ \tau_{13}\\ \tau_{23}\end{bmatrix} = \begin{bmatrix} D_{1111} & D_{1122} & D_{1133} & 0 & 0 & 0 \\ & D_{2222} & D_{1212} & 0 & 0 & 0 \\ & & D_{3333} & 0 & 0 & 0 \\ & & & D_{1212} & 0 & 0 \\ & Sym. & & & D_{1313} & 0 \\ & & & & & D_{2323} \end{bmatrix} \begin{bmatrix}\varepsilon_{11}\\ \varepsilon_{22}\\ \varepsilon_{33}\\ \gamma_{12}\\ \gamma_{13}\\ \gamma_{23}\end{bmatrix}$$

Equations below defined the nine independent elastic stiffness parameters (Dijkl) **(J. Lubliner, 1989)**

$$D_{1111} = E_1(1 - \nu_{23}\nu_{32})\gamma,$$

$$D_{2222} = E_2(1 - \nu_{13}\nu_{31})\gamma,$$

$$D_{3333} = E_3(1 - \nu_{12}\nu_{21})\gamma,$$

$$D_{1122} = E_1(\nu_{21} - \nu_{31}\nu_{23})\gamma = E_2(\nu_{12} - \nu_{32}\nu_{13})\gamma,$$

$$D_{1133} = E_1(\nu_{31} - \nu_{21}\nu_{32})\gamma = E_3(\nu_{13} - \nu_{12}\nu_{23})\gamma,$$

$$D_{2233} = E_2(\nu_{32} - \nu_{12}\nu_{31})\gamma = E_3(\nu_{23} - \nu_{21}\nu_{13})\gamma,$$

$$D_{1212} = G_{12}, \quad D_{1313} = G_{13}, \quad D_{2323} = G_{23}$$

$$\gamma = \frac{1}{1-\nu_{12}\nu_{21}-\nu_{23}\nu_{32}-\nu_{31}\nu_{13}-2\nu_{21}\nu_{32}\nu_{13}}$$

Table (D-1): the input data for concrete plasticity properties and CFRP material properties(**Herrmann and Bucksch,2014**)

Material	Description	CFRP plate
CFRP plate	Longitudinal modulus (E1), Gpa	165
	Transverse in-plane modulus(E2), GPa	16.5
	Transverse out-plane modulus(E3), GPa	16.5
	In- plane shear modulus (G12), GPa	6.894
	out- of-plane shear modulus (G23), GPa	4.136
	out- of-plane shear modulus(G13),GPa	6.894
	Major in -plane Passion's ratio, ν12	0.3
	Out-of-plane Passion's ratio, ν23	0.25
	Out-of-plane Passion's ratio, ν13	0.25

الخلاصة

الغرض من هذه الرسالة هو الدراسة السلوك الإنشائي للأعمدة الخرسانية المسلحة المحملة مسبقًا غير المركزي تحت التعرض لدورات الاحتراق ، من خلال تقييم استجابة الحمل والإزاحة ، والحمل النهائي ، وحمل التكسير ، وكذلك نمط التكسير وأنماط الفشل.

تضمن البرنامج التجريبي اختبار ثمانية عشر عينة عمود ، وخمسة عشر عمودًا مصنوعة من الخرسانة ذات القوة العادية ، وثلاثة أعمدة مصنوعة من الخرسانة عالية المقاومة. تم اختيار إحدى هذه عينات العمود كعمود تجريبي وتم تقسيم سبع عشره عمودًا الاخرى إلى خمس مجموعات لدراسة تأثيرات: (عدد دورات التعرض للحريق ، شدة الحرارة المستهدفة لكل دورة ، المدة الزمنية لكل دورة تعرض للحريق ،نسبة ، ، الانحراف الحمل نسبة التعزيز الطولي, نوع الخرسانة ، بالإضافة إلى تقييم تقنيات التقوية المعتمدة عن جميع عينات العمود لها نفس أبعاد المقطع .أو استخدام بشرائح طريق استبدال الغلاف الخارجي التالف من العرضي (150) * 150) ملم وطول فعال (700) ملم ، وتم اختباره تحت الحمل اللامركزي مع نسبة الانحراف ، (e / h = 0.5) ،

من النتائج التجريبية تقل سعة التكسير والحمل النهائي مع زيادة عدد الدورات حوالي (41)٪ ، (66)٪ و (22)٪ ، (28)٪ على التوالي لـ (دورتين وأربع دورات). تنخفض سعة التكسير والحمل النهائي مع زيادة درجة الحرارة المستهدفة من (400 درجة مئوية إلى 600 درجة مئوية) للدورة حوالي (74) ٪ و (36) ٪ على التوالي لـ (أربع دورات) ، وكذلك التكسير وسعة الحمل النهائية تنخفض مع الزيادة المدة الزمنية لكل دورة تعرض للحريق (45)٪ ، (23)٪ و (23)٪ ، (28)٪ ، على التوالي (دورة واحدة وأربع دورات). من (0.5 إلى 0) ، زاد الحمل النهائي حوالي (83 إلى 86) ٪ و (e / h) بينما مع انخفاض نسبة الانحراف ((55 إلى 65) ٪ على التوالي لـ (دورتين وأربع دورات).

كما أن تقليل نسبة الفولاذ الطولي يؤدي إلى إنقاص قدرة التكسير والحمل النهائي حوالي (46 إلى 64)٪ و HSC ، (22 إلى 29)٪ على التوالي لـ (دورتين وأربع دورات). بالنسبة لعينات الأعمدة المصنوعة من تنخفض سعة التكسير والحمل النهائي بحوالي (61 إلى 72)٪ و (25 إلى 31)٪ على التوالي لمدة (دورتين وأربع دورات).

مع صفائح NSC) لتقوية عينات الأعمدة المعرضة للحريق عن طريق استبدال الغلاف الخارجي التالف لـ يؤدي إلى تحسين في التكسير وقدرة التحميل النهائية ، حوالي (3 و 46) ٪ ، و (38 و9) (RPC أو CRFP ٪ ، على التوالي عند مقارنتها بعينة التحكم. هذا يعني أن الطريقة الثانية أكثر نشاطًا وتفوقًا.

تمت مقارنة النتائج العددية مع النتائج التجريبية التي تم الحصول عليها من حيث استجابة الحمل والتشوه والحمل النهائي وانتشار التكسير. دلت نتائج نموذج العناصر المحدودة على توافق معقول مع النتائج التجريبية والاختلاف في التكسير والحمل النهائي بحوالي (14.4)٪ و (3.2٪) كمتوسط على التوالي.

الخارجية ، ونسبة RPC تضمنت دراسة بارامترية تأثيرات العوامل المختلفة: قوة الانضغاط لقذيفة الخارجية البالغة (200) RPC الانحراف في حمل ما بعد الحريق. فيما يتعلق بمقاومة الانضغاط لقذيفة

ميجاباسكال ، فقد أظهرت النتائج العددية تغيراً واضحاً في الأداء حيث تم وضع العطل خارج المنطقة التي تم من (0.25 إلى (e / h إصلاحها ، وكذلك الحمل النهائي بحوالي (1.75)٪. كما أدت زيادة نسبة الانحراف 0.75) إلى إنقاص الحمل النهائي بحوالي (55، 25)٪ على التوالي.

جمهوريـــــــــة العراق

وزارة التعليم العالي والبحث العلمي

جامـــعة بابـل كـلية الهندســـــــــة

قسم الهـندسة المدنيـــــة

السلوك الإنشائي للأعمدة الخرسانة المسلحة المحملة مسبقًا تحت تأثير التعرض للحريق الدوري

رسالة

مقدمة الى كلية الهندسة – جامعة بابل

جزء من متطلبات نيل درجة الماجستير في علوم الهندسة/ الهندسة المدنية/ إنشاءات

اعداد

نهى شاكر كاظم العويدي

اشراف

أ.د عمار ياسر علي الجنابي

2023 ميلادي

1444 هجري